BIOGEOCHEMISTRY OF BASEMENT FLUIDS FROM THE SEDIMENT-BURIED JUAN de FUCA RIDGE FLANKS

A DISSERTATION SUBMITTED TO THE GRADUATE DIVISION OF THE UNIVERSITY OF HAWAI'I AT MĀNOA IN PARTIAL FULFILLMENT OF THE REQUIREMENTS FOR THE DEGREE OF

DOCTOR OF PHILOSOPHY

IN

OCEANOGRAPHY

AUGUST 2013

By

Huei-Ting Lin

Dissertation Committee:

James P. Cowen, Chairperson
Michael J. Mottl
Telu Yuan-Hui Li
Brian N. Popp
Jan P. Amend
Stephen Freeland

ACKNOWLEDGEMENTS

This dissertation could not have been completed without the help of many people. Most importantly, I must express sincere gratitude to my research advisor, Dr. Jim Cowen. He was brave enough to take me into an outstanding Ph.D. program and invest a tremendous amount of time and money in me. He was extremely supportive of my research over the years. The most valuable words of advice he gave me was, "NEVER LIMIT YOURSELF." Whenever I feel low on confidence, this phrase always pops up in my mind and encourages me to keep trying. His dedication to science has inspired me greatly; he showed me again and again to never give up when performing high integrity research. He was extremely patient in reviewing my manuscripts and the advice I received from him have made me a better scientist and person. Dr. Cowen passed away not long after the completion of this dissertation; he will always be remembered.

I would like to thank my husband and long-term work partner, Oliver Hsieh. Working with him was an awesome experience. It is hard to understand how someone can come up with ideas and solutions to technical problems so fast, but he always did. The amount of time and effort he invests in his work has allowed us to obtain a large volume of high quality basement fluid samples. This research would not have been possible without those samples. I also thank him for tolerating my nonstop talk about my research. Much of the time, I knew he had no clue what I was talking about, but he listened anyways and encouraged me to keep thinking and talking about it. I also want to thank him for feeding me well so that I had the energy to work on this dissertation.

I also appreciate the guidance of my dissertation committee. Two important classes, Isotopic Marine Geochemistry and Elemental Composition Changes taught by Telu Li, instilled me with ideas for my research. Telu taught me how to interpret geochemical data sets. Mike Mottl broadened my knowledge of seawater-basaltic rock interactions and crustal hydrogeology. I especially appreciate him being tough on me because I did not prepare well for those parts of my research. His editorial assistance made this dissertation much easier to read. Jan Amen taught me to use thermodynamic modeling as a powerful tool to exploit the biogeochemical data generated by this research. Brian Popp helped me interpret the isotopic composition of my samples. He spent an enormous amount of effort giving me detailed comments to improve this dissertation. Steve Freeland, as a UH representative, helped pull me out of the geochemical jargon and to see this research from a completely different angle. He sparked my interest in applying this study to other fields, including astrobiology.

I need to thank my awesome student assistants: Natalie Hamada, Kathryn Hu, and Ryan Matsumoto. Not only did they assist me in field and laboratory work, they also showed me the meaning of aloha. This research would not have been possible without Kathy Kozuma's assistance in dealing with logistics and purchase orders. I am glad to have had Kristin Uyemura remind me about the forms that needed to be signed and the deadlines that needed to be met so that I was always on track.

I want to thank my best friend, Mariko Kershaw, for spending so much time studying with me. Her calmness helped me focus on my writing and her company made studying so much more joyful. Finally, I want to thank my family--especially my four-month-old son, little Kainoa. He motivated me to push myself hard to complete this dissertation. I

also want to thank my parents; since they do not read English, I have written to them in Chinese: 親愛的老爸跟老媽，謝謝你們的栽培與鼓勵，讓我有機會到美國闖蕩，完成這個論文，謝謝老弟跟老妹，在我不在台灣的日子，陪伴老爸老媽，讓我沒有後顧之憂地攻讀這個學位。

ABSTRACT

The most in depth examination to date of the biogeochemistry of oceanic basement fluids is provided for the sediment-buried Juan de Fuca Ridge flank with a crustal age of 3.5 Ma. The overall goals of this study are to understand the available nutrients, substrates and geochemical energy for the sediment-buried ridge-flank basement biosphere and to evaluate the impact that the ridge-flank hydrothermal system may have on the global ocean organic carbon cycle. Tremendous efforts were made to obtain high quality ridge-flank basement fluid samples by developing a novel clean sampling system to obtain fluids via delivery lines associated with Circulation Obviation Retrofit Kit (CORK) observatories installed in Integrated Ocean Drilling Program (IODP) boreholes 1301A, 1362A and 1362B.

The low phosphate concentrations (0.06-0.1 μM) in ridge-flank basement fluids, relative to dissolved inorganic carbon (0.46-0.59 mM) and ammonium (99-102 μM) suggest that phosphate could be a limiting major nutrient in the basement biosphere. Both methane (1.5-13μM) and hydrogen (0.05-2 μM) are present at significantly higher concentrations in ridge-flank basement fluids than in background seawater (0.0002 and 0.0004 μM, respectively), providing energy for methanotrophs and hydrogenotrophic microorganisms. The $\delta^{13}C\text{-}CH_4$ values for CORK 1301A fluids (-42±2 ‰, n=4) fall within the range of isotopic values for thermogenic (-20‰ to -62‰) and near the ^{13}C enriched compositions of biogenic (-110‰ to -45‰) methane. The low dissolved organic carbon (DOC) concentrations in the ridge-flank basement fluids (11-16 μM) confirm that the basement is a net sink for deep seawater DOC (~40 μM). However, the elevated dissolved amino acids concentrations (53-89 nM) suggest that ridge-flank basement fluid is a net source

for deep seawater amino acids (~50 nM) and that amino acids may be utilized by heterotrophic microorganisms in the basement environment. In addition, significant differences in concentrations of dissolved methane, hydrogen and amino acids in basement fluids collected from the three study sites indicate that the aquifer is heterogeneous on at the scale of hundreds of meters, suggesting that variable microbial community compositions and/or different microbial activities may be found at the three sites.

TABLE OF CONTENTS

LIST OF TABLES

LIST OF FIGURES

LIST OF ABBREVIATIONS-General terms

ABBREVIATIONS	DEFINITIONS
CORK	Circulation Obviation Retrofit Kit
DCAA	Dissolved combined amino acids
DFAA	Dissolved free amino acids
DHAA	Dissovled hydrolyzable amino acids; same as total dissolved amino acids (TDAA); the sum of DFAA and DCAA
DIC	Dissolved inorganic carbon
DIN	Dissolved inorganic nitrogen
DIP	Dissolved inorganic phosphate
DOC	Dissolved organic carbon
DON	Dissolved organic nitrogen
DOP	Dissolved organic phosphate
ESI FT-ICR-MS	Electrospray ionization coupled with Fourier-transform ion cyclotron resonance mass spectrometry
FDL	Fluid delivery line
GF/F filters	Glass fiber filters; poresize 0.7 μm
HDPE	High density polyethylene
HEPA filter	High-efficiency particulate air (HEPA) filter; an air filter must remove 99.97% of all particles greater than 0.3 micrometre from the air that passes through.

HFPS	Hydrothermal Fluid and Particulate Sampler
HMW-DOC	High-molecular-weight dissolved organic carbon; same as DOC
HMW-DON	High-molecular-weight dissolved organic nitrogen
HOV	Human-occupied vehicle
IODP	Integrated Ocean Drilling Program
Kyr	Thousand years before present
LMW-OAs	Low-molecular-weight organic acids (monocarboxylic acids with 1-5 carbon atoms per molecule)
LVBS	Large volume bag sampler
Ma	Millions of years before present
mbs	Meters below sediment-basement interface
mbsf	Meters below seafloor
MPS	Mobile pump system
MVBS	Medium volume bag sampler
Myr	Million year ago
NMR	Nuclear magnetic resonance spectroscopy
ODP	Ocean Drilling Program
OSMO	Osmotic-pump fluid sampler

PN	Particulate nitrogen
POC	Particulate organic carbon
PVDF	Polyvinylidene fluoride; a material similar to ETFE and Teflon
ROV	Remotely operated vehicle
TDAA	Total dissolved amino acids; same as DHAA
TDN	Total dissolved nitrogen
Tefzel™	Ethylene-tetrafluoroethylene fluoropolymer (ETFE); a material similar to Teflon
TOC	Total organic carbon
UDOC	Ultrafiltration DOC; same as HMW-DOC
dNTU	Anomaly in nephelometric turbidity units

LIST OF ABBREVIATIONS-Amino acids

ABBREVIATIONS	DEFINITIONS
ALA	Alanine
ARG	Arginine
ASN	Asparagine
ASP	Aspartic acid
BALA	β-alanine
GABA	ϒ-aminobutyric acid
GLN	Glutamine
GLU	Glutamic acid
GLY	Glycine
HIS	Histidine
ILE	Isoleucine
LEU	Leucine
LYS	Lysine
MET	Methionine
OPA	o-phthalaldehyde
SER	Serine
THR	Threonine
TRY	Tryptophan
TYR	Tyrosine

CHAPTER 1

An Introduction

1.1 Introduction

Ocean crust consists of ocean basement and the overlying sediment. Heat flow anomalies (Lister, 1972; Anderson et al., 1977; Davis and Lister, 1977), alteration of basaltic basement (Alt et al., 1986; Alt et al., 1996), high basement permeability (Anderson et al., 1985; Becker et al., 1989; Becker and Fisher, 2000) and the discovery of hydrothermal plumes (Weiss et al., 1977) have all indicated pervasive hydrothermal circulation within the upper part of the basement. Based on a global seafloor heat flow data set, Stein et al. (1995) suggest that most of the advective heat loss from the ocean crust occurs via hydrothermal circulation on ridge flanks with crustal ages greater than 1 Ma; and hydrothermal circulation continues past an average crustal age of about 65 Ma. Permeability data suggest that hydrothermal circulation extends to a thickness of ~600m in the upper basement (Anderson et al., 1985; Johnson and Pruis, 2003), consistent with evidence for crustal alteration (Alt et al., 1996). The circulating hydrothermal fluids within the basement are referred to as "basement fluids" (Elderfield et al., 1999) throughout this dissertation.

Basement fluids originate from bottom seawater entering the basement at highly permeable unsedimented mid-ocean ridges, young poorly-sedimented ridge flank areas and unsedimented recharge seamounts (Davis et al., 1999; Fisher and Becker, 2000; Fisher et al., 2003; Fisher, 2005b). The upper ocean basement (~600 m thick) comprises the largest aquifer on earth, holding hydrothermal fluids equivalent to an estimated 2% of the ocean volume (Johnson and Pruis, 2003), and may harbor a substantial biosphere (Cowen, 2004). The total hydrothermal fluid flux from the basement into the ocean is estimated to be 20% of global riverine input (Johnson and Pruis, 2003) and the

hydrothermal fluid flux from ridge-flanks (crustal age >1Ma) alone is about 5-60% of the total hydrothermal fluid flux (Mottl, 2003; Wheat et al., 2003). Despite the immense volume of this aquifer and its potential to support a large biosphere, only a few studies of this difficult-to-access environment have been completed (e.g. Mottl et al., 1998; Elderfield et al., 1999; Wheat et al., 2000; Cowen et al., 2003; Cowen, 2004; Wheat et al., 2004a; Huber et al., 2006; Lang et al., 2006; McCarthy et al., 2010; Wheat et al., 2010). These are briefly summarized below.

On the eastern flank of Juan de Fuca Ridge (Fig. 1), access to basement fluids is provided by natural spring waters discharging from unsedimented outcrops (Mottl et al., 1998; Wheat and Mottl, 2000; Huber et al., 2006; Lang et al., 2006) and by the circulation obviation retrofit kits (CORKs) installed in Ocean Drilling Program (ODP) and Integrated Ocean Drilling Program (IODP) boreholes (Elderfield et al., 1999; Cowen et al., 2003; Cowen, 2004; Wheat et al., 2004a; Huber et al., 2006; Lang et al., 2006; McCarthy et al., 2010; Wheat et al., 2010). These early studies document the alteration of inorganic chemical compositions of the basement fluid, the high diversity of microbial community and evidence for the removal and production of dissolved organic carbon (DOC).

Mottl et al. (1998) and Wheat and Mottl (2000) reported that relative to bottom seawater, basement fluids venting from the exposed rocky seamount called Baby Bare (Fig. 1) are heavily depleted in magnesium, alkalinity, dissolved carbon dioxide, sulfate, potassium, lithium, uranium, oxygen, nitrate and phosphate, and enriched in calcium, chlorinity, ammonia, iron, manganese, hydrogen sulfide, hydrogen and methane. Based on deep sediment porewater profiles and basement fluid samples (CORK 1026B), Elderfield et al.

(1999) observed that seawater-basement rock interaction leads to gradual increases in calcium and decreases in alkalinity, magnesium, sodium, potassium and sulfate in basement fluids along a 80-km transect of boreholes drilled across the eastern flanks of the Juan de Fuca Ridge during ODP expedition 168 (Shipboard Scientific Party, 1997a), an observation consistent with that made by using spring waters from unsedimented outcrops (Mottl et al., 1998; Wheat et al., 2000). Analyses of basement fluids venting from ODP CORK 1025C and 1026B also verified the degree of geochemical alteration of circulating basement fluids inferred from deep sediment porewater profiles (Wheat et al., 2004a). The consistency in the inorganic geochemical compositions of basement fluids in previous studies provides a foundation for sample quality control for this study.

The diversity of the microbial community residing within the subseafloor basement was explored using ribosomal RNA gene sequencing of materials collected from basement fluids discharged from CORK 1026B (Cowen et al., 2003) and Baby Bare spring (Huber et al., 2006). Cowen et al. (2003) suggested that fluids from CORK 1026B nourish a diverse assemblage of bacteria and archaea with phylogenetic groups that are closely related to known nitrate reducers, thermophilic sulfate reducers and thermophilic fermentative heterotrophs. Huber et al. (2006) found even more diverse groups of bacteria and archaea in Baby Bare and CORK 1026B basement fluids and that the clones of these groups are closely related to known cultured anaerobic thermophiles. While both studies suggest the presence of a subseafloor biosphere within the basement environment, little is known about the available inorganic nutrients, organic substrates and geochemical energy potential for chemoautotrophs or heterotrophs that may thrive in this environment. A goal of this dissertation was to fill these gaps in knowledge.

Dissolved organic carbon (DOC) is the product of vigorous biological activity and is an important measure of the organic fuels available for subseafloor heterotrophic activities (e.g. Williams, 1970; Azam et al., 1983; Ducklow and Carlson, 1992; Carlson, 2002). Lang et al. (2006) reported that DOC concentrations in basement fluids from Baby Bare and CORK 1026B are much lower than that in bottom seawater and suggested that the biotic and abiotic reactions within this environment make the basement a net sink for deep ocean DOC. In contrast, high-molecular-weight (HMW) DOC in basement fluids from Baby Bare and CORK 1026B ($\delta^{13}C$=-26.1 to -34.5‰) is highly depleted in ^{13}C relative to deep ocean DOC ($\delta^{13}C$=-21.1‰), which is consistent with a chemoautotrophic origin (McCarthy et al., 2010). The radiocarbon ages of the HMW-DOC (11,800-14,400 years before present) are also similar to the radiocarbon ages of the dissolved inorganic carbon in ridge-flank fluids, suggesting that the HMW-DOC of basement fluids was synthesized by chemoautotrophic microbial communities in ridge-flank fluids (McCarthy et al., 2010). McCarthy et al. (2010) further suggested that organisms residing within the ridge-flank basement biosphere may synthesize organic carbon extensive enough to export to the overlying ocean. Data presented by this dissertation will help to clarify these issues further.

The research presented in this dissertation focuses on basement fluids collected via IODP-CORKs 1301A, 1362A and 1362B. The three sites were selected because the three CORKs are equipped with fluid delivery lines (FDLs) that extend from the basement to seafloor sampling ports. The FDLs are made of stainless steel for CORK 1301A and Tefzel (ethylene-tetrafluoroethylene fluoropolymer) for CORKs 1362A and 1362B. One advantage of using FDLs is that sampled basement fluids do not flow in direct contact

with the CORKs' lengthy and reactive steel casings, a disadvantage of collecting samples from old-style CORKs, as pointed out by Cowen et al. (2003). Another advantage of using FDLs is that flushing of stagnant fluids residing within the FDL can be quickly performed using a seafloor pumping system (Cowen et al. 2012). Flushing of venting fluids via a stainless steel sampling device at Baby Bare outcrop significantly reduced the sediment influence, as indicated by Huber et al.(2006) and Lang et al. (2006). The locations and penetration depths of CORKs 1301A, 1362A and 1362B also permit the examination of spatial variations in basement fluid compositions at a scale of 300-800 m horizontally and ~150m vertically. CORK 1362B is located ~550 m north-northwest (NNW) of CORK 1301A; CORK 1362A is ~311 m further NNW of 1362B. The fluid intake is ~30 m below the sediment-basement interface (mbs) at CORK 1301A, 200 mbs at CORK 1362A and ~50 mbs at CORK 1362B (Fig. 1).

In this dissertation we provide the most detailed examination of the biogeochemistry of basement fluids to date. The data set includes major ions, nutrients, DOC, dissolved methane and hydrogen, dissolved iron, and dissolved amino acids in basement fluids from CORKs 1301A, 1362A and 1362B (Appendix A). A four-year time series data set for many key biogeochemical parameters in basement fluids collected from CORK 1301A is also discussed (Chapter 2). These biogeochemical data provide evidence for available nutrients, substrates and geochemical energy within the subseafloor basement biosphere and the dissolve organic carbon data allow us to evaluate the extent to which the ridge-flank hydrothermal system impacts the global ocean organic carbon cycle.

This dissertation is comprised of six chapters. Chapter 1 is the introduction. Chapter 2 discusses inorganic nutrients, dissolved methane and hydrogen and DOC in basement

fluids collected from CORK 1301A and the implications of these data. Concentrations of inorganic major ions, nutrients, DOC and dissolved iron for fluids from CORKs 1362A and 1362B are similar to those from CORK 1301A (Table 3.1); thus the conclusions drawn in Chapter 2 from the composition of fluids from CORK 1301A can also be made for fluids from CORKs 1362A and 1362B. In contrast, basement fluids from CORKs 1301A, 1362A and 1362B show larger variations in their dissolved methane, hydrogen and amino acid compositions and thus are discussed in greater detail in the following two chapters. Chapter 3 presents the data on dissolved methane and hydrogen in basement fluids collected from CORKs 1301A, 1362A and 1362B. Chapter 4 discusses amino acids in basement fluids from CORKs 1301A, 1362A and 1362B. Chapter 5 represents a departure from the ridge flank environments of the previous chapters and instead examines dissolved and particulate organic carbon data from back-arc spreading/eruption vent fields, allowing a comparison with ridge-flank basement fluids. Chapter 6 summarizes the previous chapters and includes directions for future research.

Specific objectives, together with related hypothesis and approaches, which guided the research presented in this dissertation, are as follows:

(1) To obtain high quality ridge-flank basement fluid samples.

Obtaining high quality basement fluid samples with little or no bottom seawater contamination and minimum or no influence by CORK materials was a critical step for the entire research program. Although CORK observatories provide unprecedented opportunities for basement fluid collection, possible influences by CORK casing materials have been pointed out (Cowen et al., 2003; Nakagawa et al., 2006);

contamination of ammonium and iron in basement fluids collected using samplers installed inside a CORK's casing are identified by this study and discussed in Chapter 2. Thus, extreme efforts and improvements in instrumentation and methods were made progressively through the four sampling cruises (every summer from 2008 to 2011) in order to obtain high quality samples for this research. The details of the sampling methods and the sample quality are described in Chapter 2.

(2) To assess the levels of essential bioelements within the ridge-flank.

Mottl et al. (1998) reported nitrate and phosphate concentrations in Baby Bare spring water to be 0.8±0.7 µM and 0.4±0.1 µM, respectively. Similarly, Wheat et al. (2000) reported nitrate and phosphate concentrations in Baby Bare spring water to be 0.8±0.7 µM and 0.3±0.1 µM, respectively. The sub-micromolar concentrations of nitrate in Baby Bare spring water indicates that nitrate (~40µM) in recharged seawater has been consumed either by reactions within basement and/or by diffusional transport of nitrate from basement into the sediments (Wheat et al., 2000). Depletion in nitrate also indicates that the basement fluids discharged from Baby Bare are reducing (Wheat et al., 2000). However, sampling of basement fluids discharged from Baby Bare without bottom seawater entrainment has been challenging and the sub-micromolar concentrations of nitrate reported were calculated from a regression of magnesium versus nitrate for all samples collected (Wheat et al., 2000), resulting in a large uncertainty. The presence of nitrate has significant impact on the basement biosphere not only because it is a major nutrient but, more importantly, because it can provide a significant amount of energy to microorganisms via nitrate reduction (e.g. Nealson, 1997; Amend and Shock, 2001).

Thus, it is important to understand whether nitrate is present in a sub-micromolar level or is completely exhausted (zero nitrate) in the ridge-flank basement fluids.

The depletion in phosphate in Baby Bare spring fluids is likely related to phosphate adsorption onto iron oxyhydroxide and to biological uptake (Wheat et al., 1996). Iron oxyhydroxide is one of the most abundant secondary minerals present in 3.5 Myr-old rock cores from this study site (Marescotti et al., 2000). Sorption of phosphate onto iron oxyhydroxide surfaces lowers the dissolved inorganic phosphate concentrations in the fluid and renders phosphate unavailable for biological uptake (Reynolds and Davies, 2001; Ruttenberg and Sulak, 2011). As noted above, collecting basement fluids from an outcrop without contamination by bottom seawater has been challenging. Additional analysis of phosphate concentrations in basement fluids collected using more advanced sampling methods would help to constrain the level of phosphate that is available for microorganisms residing in the basement environment.

Hypothesis 1: Phosphate is the limiting nutrient for basement biosphere.

Despite low nitrate, elevated ammonium concentrations are expected as a result of downward diffusional transport from the overlying sediment porewater (Wheat et al., 2000). In contrast, low phosphate concentrations are expected in basement fluids for reasons stated above, making phosphate a potential candidate as a limiting nutrient in this environment. As a partial test of this hypothesis, basement fluid samples from CORKs at boreholes 1301A, 1362A and 1362B were analyzed for major nutrients including ammonium, nitrate, nitrite, phosphate and alkalinity. These results will guide future

nutrient-addition experiments (which are outside the scope of this dissertation), to test whether the nutrient(s) with low dissolved concentrations actually limit life in the basement environment. The results and detailed discussion regarding this objective are presented in Chapter 2.

(3) To determine the hydrogen and methane levels in the ridge-flank basement fluids.

Hydrogen and methane are important sources of energy, and methane can also serve as a source of carbon source for microorganisms (e.g. Lovley and Goodwin, 1988; Nealson, 1997; Hinrichs et al., 1999; Boetius et al., 2000; Amend and Shock, 2001; Orphan et al., 2001; Chapelle et al., 2002). The concentrations of hydrogen have been proposed to be an indicator of the predominant terminal electron-accepting reactions in anoxic groundwater systems and in aquatic sediments, provided that hydrogen concentrations in these systems are near thermodynamic equilibrium (Lovley and Goodwin, 1988; Lovley et al., 1994; Hoehler et al., 1998). The highest H_2 concentrations (30-1000 nM) result from acetogenesis, followed by methanogenesis (1-10nM), sulfate reduction (0.02-2nM), iron reduction (0.2nM), manganese reduction (<0.05 nM) and nitrate reduction (<0.05). Microbial metabolism controlled hydrogen concentrations are predicted and/or observed in anoxic groundwater systems and in aquatic sediments (Lovley et al., 1994; Hoehler et al., 1998; Lever et al., 2010). Thus, hydrogen levels in basement fluids could help to predict the dominant microbial-mediated terminal electron-accepting reactions. These data will also help to constrain whether the basement environment is a net source or a net sink for hydrogen. Basalt-hosted high temperature hydrothermal vents contain 0.04-1.7mM of H_2 (summarized in Amend et al., 2011). Abiotic production of H_2 from seawater-basalt reactions in aqueous solutions at neutral pH and 60°C has been observed

in laboratory experiments (Stevens and McKinley, 2000) and in terrestrial subsurface environments (Stevens and McKinley, 1995).

As previously stated, the presence of hydrogen may promote methanogenesis, as the production of methane from hydrogen oxidation coupled with carbon-dioxide reduction becomes thermodynamically favorable when hydrogen is present at high concentrations (Lovley and Goodwin, 1988; Lovley et al., 1994; Hoehler et al., 1998; Lever et al., 2010). A hydrogen-based terrestrial subsurface microbial community that is dominated by methanogens has been observed (Chapelle et al., 2002). The presence of hydrogen may not only promote microbial methanogenesis, but abiotic methane production may also be plausible (Sherwood Lollar et al., 1993b; Sherwood Lollar et al., 2002; Sherwood Lollar et al., 2006; Sherwood Lollar et al., 2008). The presence of methane would suggest that the environment can provide substrates for methanotrophs to thrive, as depicted in a Guaymas Basin hydrothermal system (Teske et al., 2003). Whether the ridge-flank basement environment can support methanogens and anaerobic methanotrophs is of great interest.

Hypothesis 2: The ocean basement is a source for hydrogen and methane.

To test the hypothesis, basement fluid samples from CORK 1301A, 1362A and 1362B were analyzed for their methane and hydrogen concentrations and compared with similar analyses of bottom seawater and overlying sediment porewater, especially those near the sediment-basement interface. Methane isotope analyses were also performed to provide information on the potential sources for methane observed in the basement fluids. The results and their implications are discussed in Chapter 3.

Hypothesis 3: The presence of hydrogen and methane provide energy for various thermodynamically favorable metabolic reactions including hydrogenotrophic methanogenesis, hydrogenotrophic sulfate reduction, hydrogenotrophic iron reduction and anaerobic methane oxidation coupled with sulfate reduction.

To test this hypothesis, thermodynamic calculations were performed to investigate the feasibility of the selected metabolic reactions using in situ temperature, pressure, and biogeochemical data presented by this study. Negative Gibbs free energy indicates energy-yielding (spontaneous) reactions and the environment is favorable for these reactions to take place. In contrast, positive Gibbs free energy indicates energy-consuming reactions such that an additional energy source would be required for these reactions to occur. The modeling results and their implications are discussed in Chapter 3.

(4) *To evaluate whether ridge-flank basement is a net source or sink for deep seawater dissolved organic carbon.*

Basement fluids originate from bottom seawater. Bottom seawater entrained into the basement initially carries ~40 µM DOC (Lang et al., 2006; Hansell et al., 2009). If there is no net removal or addition of DOC into the basement, basement fluids should maintain the same DOC concentrations as bottom seawater. Sediment porewater at the sediment-basement interface contains at least an order-of-magnitude higher DOC (Shipboard Scientific Party, 2004) than found in bottom seawater, so the porewater is a potential source of DOC for the basement. Chemosynthetic production of DOC within the basement environment has also been suggested by McCarthy et al. (2010). It is not known, however, whether the net biological production within basement and the

diffusional transport of DOC to basement together may exceed the net removal of DOC within basement due to biological consumption and abiotic reactions such as surface adsorption (Lang et al., 2006). An earlier study suggests that basement is a net sink for deep ocean DOC, based on the DOC concentrations in Baby Bare spring fluid and basement fluids collected from CORK 1026B (Lang et al., 2006). However, results of that study are potentially biased by sampling from an outcrop (Huber et al., 2006; Lang et al., 2006) and from old style CORKs (Cowen et al., 2003). This study aims to determine the DOC concentrations in ridge-flank basement fluids collected using advanced sampling methods from CORKs with FDLs at sites 1301A, 1362A and 1362B. Time-series sampling at CORK 1301A from 2008 to 2011 provides additional data to investigate the temporal variations in DOC concentrations.

Hypothesis 4: The ridge-flank basement is a net sink for refractory deep seawater DOC.

To test this hypothesis, DOC concentrations were analyzed in basement fluid samples and compared with that in bottom seawater. The ridge-flank basement fluid DOC concentrations were compared with global seawater DOC and are discussed in Chapter 2; non-ridge flank hydrothermal vent DOC concentrations are also presented in Chapter 5 for comparison. If DOC concentrations in the basaltic fluids are lower than that in bottom seawater, the basement environment must be a net sink for deep ocean DOC.

(5) *To assess whether ridge-flank basement is a net source or sink for labile organic carbon.*

Based on stable and radiocarbon isotopes of ridge-flank basement fluid DOC, McCarthy et al. (2010) suggest that DOC is synthesized from inorganic carbon within ridge-flank basement environments by chemosynthetic microbial communities. The production of fresh DOC should increase the amount of labile DOC and may result in exportation of labile DOC to the overlying ocean. Amino acids are the major labile components of DOC (Lee and Bada, 1975; McCarthy et al., 1997; Kaiser and Benner, 2009) and amino acid compositions would provide information on the fresher fraction of the DOC present in ridge-flank basement fluids.

Hypothesis 5: The basement is a net source of labile organic carbon such as amino acids.

To test this hypothesis, basement fluid samples from CORK 1301A, 1362A and 1362B were analyzed for dissolved amino acid concentrations and compared with those in North Pacific deep seawater. Higher concentrations of dissolved amino acids in the basement fluids would indicate that in situ production and/or transport of amino acids have occurred and export of dissolved amino acids into the overlying ocean is plausible. Concentrations of amino acids in ridge-flank basement fluids were also compared with those in deep ridge-flank sediment porewater from near the sediment-basement interface, and with non-ridge-flank hydrothermal fluids from various hydrothermal systems. Compositions of amino acids in ridge-flank basement fluids were also determined and compared with those in sediment porewater, deep seawater, and bacterial biomass to help identify potential sources. Degradation status was also inferred from the amino acid

compositions. The amino acid data and their implications are presented and discussed in Chapter 4.

1.2 References

Alt, J. C., Honnorez, J., Laverne, C., and Emmermann, R., 1986. Hydrothermal Alteration of a 1-Km Section through the Upper Oceanic-Crust, Deep-Sea Drilling Project Hole 504b - Mineralogy, Chemistry, and Evolution of Seawater-Basalt Interactions. *Journal of Geophysical Research-Solid Earth and Planets* **91**, 309-335.

Alt, J. C., Laverne, C., Vanko, D. A., Tartarotti, P., Teagle, D. A. H., Bach, W., Zuleger, E., Erzinger, J., Honnorez, I., and Pezard, P. A., 1996. Hydrothermal alteration of a section of upper oceanic crust in the eastern equatorial Pacific: A synthesis of results from Site 504 (DSDP Legs 69, 70, and 83, and ODP Legs 111, 137, 140, and 148). *Proc. Ocean Drill Program* **148**, 417-434.

Amend, J. P., McCollom, T. M., Hentscher, M., and Bach, W., 2011. Metabolic (catabolic and anabolic) energy for chemolithoautotrophs in deep-sea hydrothermal systems hosted in different rock types. *Geochim. Cosmochim. Acta* **75**, 5736-5748.

Amend, J. P. and Shock, E. L., 2001. Energetics of overall metabolic reactions of thermophilic and hyperthermophilic Archaea and Bacteria. *FEMS Microbiol. Rev.* **25**, 175-243.

Anderson, R. N., Langseth, M. G., and Sclater, J. G., 1977. The mechanisms of heat transfer through the floor of the Indian Ocean. *J. Geophys. Res.* **82**, 3391-3409.

Anderson, R. N., Zoback, M. D., Hickman, S. H., and Newmark, R. L., 1985. Permeability versus depth in the upper oceanic crust: In situ measurements in DSDP hole 504B, eastern equatorial Pacific. *Journal of Geophysical Research: Solid Earth (1978–2012)* **90**, 3659-3669.

Azam, F., Fenchel, T., Field, J., Gray, J., Meyer-Reil, L., and Thingstad, F., 1983. The ecological role of water-column microbes in the sea. *Marine ecology progress series. Oldendorf* **10**, 257-263.

Becker, K. and Fisher, A. T., 2000. Permeability of upper oceanic basement on the eastern flank of the Juan de Fuca Ridge determined with drill-string packer experiments. *J. Geophys. Res.* **105**, 897-912.

Becker, K., Sakai, H., Adamson, A., Alexandrovich, J., Alt, J., Anderson, R., Bideau, D., Gable, R., Herzig, P., and Houghton, S., 1989. Drilling deep into young oceanic crust, Hole 504B, Costa Rica Rift. *Reviews of Geophysics* **27**, 79-102.

Boetius, A., Ravenschlag, K., Schubert, C. J., Rickert, D., Widdel, F., Gieseke, A., Amann, R., Jorgensen, B. B., Witte, U., and Pfannkuche, O., 2000. A marine microbial consortium apparently mediating anaerobic oxidation of methane. *Nature* **407**, 623-626.

Carlson, C. A., 2002. Production and removal processes. In: *Biogeochemistry of marine dissolved organic matter* (eds. D. A. Hansell and C. A. Carlson). Elsevier.

Chapelle, F. H., O'Neill, K., Bradley, P. M., Methe, B. A., Ciufo, S. A., Knobel, L. L., and Lovley, D. R., 2002. A hydrogen-based subsurface microbial community dominated by methanogens. *Nature* **415**, 312-315.

Cowen, J. P., 2004. The microbial biosphere of sediment-buried oceanic basement. *Research in Microbiology* **155**, 497-506.

Cowen, J. P., Giovannoni, S. J., Kenig, F., Johnson, H. P., Butterfield, D., Rappe, M. S., Hutnak, M., and Lam, P., 2003. Fluids from aging ocean crust that support microbial life. *Science* **299**, 120-123.

Davis, E. and Lister, C., 1977. Heat flow measured over the Juan de Fuca Ridge: Evidence for widespread hydrothermal circulation in a highly heat transportive crust. *J. Geophys. Res.* **82**, 4845-4860.

Davis, E. E., Chapman, D. S., Wang, K., Villinger, H., Fisher, A. T., Robinson, S. W., Grigel, J., Pribnow, D., Stein, J., and Becker, K., 1999. Regional heat flow variations across the sedimented Juan de Fuca Ridge eastern flank: Constraints on lithospheric cooling and lateral hydrothermal heat transport. *Journal of Geophysical Research-Solid Earth* **104**, 17675-17688.

Ducklow, H. and Carlson, C., 1992. Oceanic bacterial production. *Advances in microbial ecology* **12**, 113-181.

Elderfield, H., Wheat, C. G., Mottl, M. J., Monnin, C., and Spiro, B., 1999. Fluid and geochemical transport through oceanic crust: a transect across the eastern flank of the Juan de Fuca Ridge. *Earth Planet. Sci. Lett.* **172**, 151-165.

Fisher, A. T., 2005. Marine hydrogeology: recent accomplishments and future opportunities. *Hydrogeol. J.* **13**, 69-97.

Fisher, A. T. and Becker, K., 2000. Channelized fluid flow in oceanic crust reconciles heat-flow and permeability data. *Nature* **403**, 71-74.

Fisher, A. T., Davis, E. E., Hutnak, M., Spiess, V., Zuhlsdorff, L., Cherkaoui, A., Christiansen, L., Edwards, K., Macdonald, R., Villinger, H., Mottl, M. J., Wheat, C. G., and Becker, K., 2003. Hydrothermal recharge and discharge across 50 km guided by seamounts on a young ridge flank. *Nature* **421**, 618-621.

Hansell, D. A., Carlson, C. A., Repeta, D. J., and Schlitzer, R., 2009. Dissolved organic matter in the ocean: a controversy stimulates new insights. *Oceanography* **22**, 202-211.

Hinrichs, K. U., Hayes, J. M., Sylva, S. P., Brewer, P. G., and DeLong, E. F., 1999. Methane-consuming archaebacteria in marine sediments. *Nature* **398**, 802-805.

Hoehler, T. M., Alperin, M. J., Albert, D. B., and Martens, C. S., 1998. Thermodynamic control on hydrogen concentrations in anoxic sediments. *Geochim. Cosmochim. Acta* **62**, 1745-1756.

Huber, J. A., Johnson, H. P., Butterfield, D. A., and Baross, J. A., 2006. Microbial life in ridge flank crustal fluids. *Environ. Microbiol.* **8**, 88-99.

Johnson, H. P. and Pruis, M. J., 2003. Fluxes of fluid and heat from the oceanic crustal reservoir. *Earth Planet. Sci. Lett.* **216**, 565-574.

Kaiser, K. and Benner, R., 2009. Biochemical composition and size distribution of organic matter at the Pacific and Atlantic time-series stations. *Mar. Chem.* **113**, 63-77.

Lang, S. Q., Butterfield, D. A., Lilley, M. D., Johnson, H. P., and Hedges, J. I., 2006. Dissolved organic carbon in ridge-axis and ridge-flank hydrothermal systems. *Geochim. Cosmochim. Acta* **70**, 3830-3842.

Lee, C. and Bada, J. L., 1975. Amino acids in equatorial Pacific Ocean water. *Earth and Planetary Science Letters* **26**, 61-68.

Lever, M., Heuer, V., Morono, Y., Masui, N., Schmidt, F., Alperin, M., Inagaki, F., Hinrichs, K. U., and Teske, A., 2010. Acetogenesis in deep subseafloor sediments

of the Juan de Fuca Ridge Flank: a synthesis of geochemical, thermodynamic, and gene-based evidence. *Geomicrobiol. J.*, 183-198.

Lister, C., 1972. On the thermal balance of a mid- ocean ridge. *Geophysical Journal of the Royal Astronomical Society* **26**, 515-535.

Lovley, D. R., Chapelle, F. H., and Woodward, J. C., 1994. Use of dissolved H2 concentrations to determine distribution of microbially catalyzed redox reactions in anoxic groundwater. *Environmental Science & Technology* **28**, 1205-1210.

Lovley, D. R. and Goodwin, S., 1988. Hydrogen concentrations as an indicator of the predominant terminal electron-accepting reactions in aquatic sediments. *Geochim. Cosmochim. Acta* **52**, 2993-3003.

Marescotti, P., Vanko, D. A., and Cabella, R., 2000. From oxidizing to reducing alteration: Mineralogical variations in pillow basalts from the east flank, Juan de Fuca Ridge. In: *Proceedings of the Ocean Drilling Program, Scientific Results* (eds. A. T. Fisher, E. E. Davis, and C. Escutia). Ocean Drilling Program.

McCarthy, M., Pratum, T., Hedges, J., and Benner, R., 1997. Chemical composition of dissolved organic nitrogen in the ocean. Nature Publishing Group.

McCarthy, M. D., Beaupre, S. R., Walker, B. D., Voparil, I., Guilderson, T. P., and Druffel, E. R. M., 2010. Chemosynthetic origin of C-14-depleted dissolved organic matter in a ridge-flank hydrothermal system. *Nat. Geosci.* **4**, 32-36.

Mottl, M. J., 2003. Partitioning of energy and mass fluxes between mid-ocean ridge axes and flanks at high and low temperature. In: *Energy and Mass Transfer in Marine Hydrothermal Systems* (eds. P. E. Halbach, V. Tunnicliffe, and J. R. Hein). Dahlem University Press, Berlin.

Mottl, M. J., Wheat, G., Baker, E., Becker, N., Davis, E., Feely, R., Grehan, A., Kadko, D., Lilley, M., Massoth, G., Moyer, C., and Sansone, F., 1998. Warm springs discovered on 3.5 Ma oceanic crust, eastern flank of the Juan de Fuca Ridge. *Geology* **26**, 51-54.

Nakagawa, S., Inagaki, F., Suzuki, Y., Steinsbu, B. O., Lever, M. A., Takai, K., Engelen, B., Sako, Y., Wheat, C. G., and Horikoshi, K., 2006. Microbial community in black rust exposed to hot ridge flank crustal fluids. *Appl. Environ. Microbiol.* **72**, 6789-6799.

Nealson, K. H., 1997. Sediment bacteria: who's there, what are they doing, and what's new? *Annu. Rev. Earth Pl. Sc.* **25**, 403-434.

Orphan, V. J., House, C. H., Hinrichs, K. U., McKeegan, K. D., and DeLong, E. F., 2001. Methane-consuming archaea revealed by directly coupled isotopic and phylogenetic analysis. *Science* **293**, 484-487.

Reynolds, C. and Davies, P., 2001. Sources and bioavailability of phosphorus fractions in freshwaters: a British perspective. *Biological Reviews of the Cambridge Philosophical Society* **76**, 27-64.

Ruttenberg, K. C. and Sulak, D. J., 2011. Sorption and desorption of dissolved organic phosphorus onto iron (oxyhydr)oxides in seawater. *Geochim. Cosmochim. Acta* **75**, 4095-4112.

Sherwood Lollar, B., Frape, S., Weise, S., Fritz, P., Macko, S., and Welhan, J., 1993. Abiogenic methanogenesis in crystalline rocks. *Geochim. Cosmochim. Acta* **57**, 5087-5097.

Sherwood Lollar, B., Lacrampe-Couloume, G., Slater, G. F., Ward, J., Moser, D. P., Gihring, T. M., Lin, L. H., and Onstott, T. C., 2006. Unravelling abiogenic and biogenic sources of methane in the Earth's deep subsurface. *Chem. Geol.* **226**, 328-339.

Sherwood Lollar, B., Lacrampe-Couloume, G., Voglesonger, K., Onstott, T. C., Pratt, L. M., and Slater, G. F., 2008. Isotopic signatures of CH_4 and higher hydrocarbon gases from Precambrian Shield sites: A model for abiogenic polymerization of hydrocarbons. *Geochim. Cosmochim. Acta* **72**, 4778-4795.

Sherwood Lollar, B., Westgate, T., Ward, J., Slater, G., and Lacrampe-Couloume, G., 2002. Abiogenic formation of alkanes in the Earth's crust as a minor source for global hydrocarbon reservoirs. *Nature* **416**, 522-524.

Shipboard Scientific Party, 1997. Introduction and summary: hydrothermal circulation in the oceanic crust and its consequences on the eastern flank of the Juan de Fuca Ridge *Proc. Ocean Drill. Program Initial Reports* **168**, 7–21.

Shipboard Scientific Party, 2004. Juan de Fuca hydrogeology: The hydrogeologic architecture of basaltic oceanic crust: compartmentalization, anisotropy, microbiology, and crustal-scale properties on the eastern flank of Juan de Fuca Ridge, eastern Pacific Ocean. *IODP Prel. Rept.* **301**.

Stein, C. A., Stein, S., and Pelayo, A. M., 1995. Heat flow and hydrothermal circulation. *Geophysical Monograph Series* **91**, 425-445.

Stevens, T. O. and McKinley, J. P., 1995. Lithoautotrophic microbial ecosystems in deep basalt aquifers. *Science* **270**, 450-454.

Stevens, T. O. and McKinley, J. P., 2000. Abiotic controls on H2 production from basalt-water reactions and implications for aquifer biogeochemistry. *Environmental Science & Technology* **34**, 826-831.

Teske, A., Dhillon, A., and Sogin, M. L., 2003. Genomic markers of ancient anaerobic microbial pathways: sulfate reduction, methanogenesis, and methane oxidation. *The Biological Bulletin* **204**, 186-191.

Weiss, R. F., Lonsdale, P., Lupton, J., Bainbridge, A., and Craig, H., 1977. Hydrothermal plumes in the Galapagos Rift.

Wheat, C. G., Elderfield, H., Mottl, M. J., and Monnins, C., 2000. Chemical composition of basement fluids within an oceanic ridge flank: Implications for along-strike and across-strike hydrothermal circulation. *J. Geophys. Res.* **105**, 13437-13447.

Wheat, C. G., Feely, R. A., and Mottl, M. J., 1996. Phosphate removal by oceanic hydrothermal processes: An update of the phosphorus budget in the oceans. *Geochim. Cosmochim. Acta* **60**, 3593-3608.

Wheat, C. G., Jannasch, H. W., Fisher, A. T., Becker, K., Sharkey, J., and Hulme, S., 2010. Subseafloor seawater-basalt-microbe reactions: Continuous sampling of borehole fluids in a ridge flank environment. *Geochem. Geophy. Geosy.* **11**, 1-18.

Wheat, C. G., Jannasch, H. W., Kastner, M., Plant, J. N., DeCarlo, E. H., and Lebon, G., 2004. Venting formation fluids from deep-sea boreholes in a ridge flank setting: ODP Sites 1025 and 1026. *Geochem. Geophy. Geosy.* **5**, 1-12.

Wheat, C. G., McManus, J., Mottl, M. J., and Giambalvo, E., 2003. Oceanic phosphorus imbalance: Magnitude of the mid-ocean ridge flank hydrothermal sink. *Geophys. Res. Lett* **30**, 1895.

Wheat, C. G. and Mottl, M. J., 2000. Composition of pore and spring waters from Baby Bare: Global implications of geochemical fluxes from a ridge flank hydrothermal system. *Geochim. Cosmochim. Acta* **64**, 629-642.

Williams, P., 1970. Heterotrophic utilization of dissolved organic compounds in the sea. *J. Mar, Biol. Assoc. UK* **50**, 859-870.

CHAPTER 2

Inorganic chemistry, gas compositions and dissolved organic carbon in fluids from sedimented young basaltic crust on the Juan de Fuca Ridge flanks

By

Huei-Ting Lin

James P. Cowen, Eric J. Olson, Jan P. Amend, Marvin D. Lilley (Coauthors)

Published in *Geochimica et Cosmochimica Acta*, 85, 213-227, March 2012

2.0. ABSTRACT

The permeable upper oceanic basement serves as a plausible habitat for a variety of microbial communities. There is growing evidence suggesting a substantial subseafloor biosphere. Here new time series data are presented on key inorganic species, methane, hydrogen and dissolved organic carbon (DOC) in ridge flank fluids obtained from subseafloor observatory CORKs (Circulation Obviation Retrofit Kits) at Integrated Ocean Drilling Program (IODP) boreholes 1301A and 1026B. These data show that the new sampling methods (Cowen et al., 2012) employed at 1301A result in lower contamination than earlier studies. Furthermore, sample collection methods permitted most chemical analyses to be performed from aliquots of single large volume samples, thereby allowing more direct comparison of the data. The low phosphate concentrations (0.06-0.2 μM) suggest that relative to carbon and nitrogen, phosphorus could be a limiting nutrient in the basement biosphere. Coexisting sulfate (17-18 mM), hydrogen sulfide (~0.1 μM), hydrogen (0.3-0.7 μM) and methane (1.5-2 μM) indicates that the basement aquifer at 1301A either draws fluids from multiple flow paths with different redox histories or is a complex environment that is not thermodynamically controlled and may allow co-occurring metabolic pathways including sulfate reduction and methanogenesis. The low DOC concentrations (11-18 μM) confirm that ridge flank basement is a net DOC sink and ultimately a net carbon sink. Based on the net amounts of DOC, oxygen, nitrate and sulfate removed (~30 μM, ~80 μM, ~40 μM and ~10 mM, respectively) from entrained bottom seawater, organic carbon may be aerobically or anaerobically oxidized in biotic and/or abiotic processes.

2.1. INTRODUCTION

Ocean crust consists of basaltic basement and the overlying sediments. Ocean basement, formed at the ridge axes, subsequently ages and is covered by increasingly thick sediments with increasing distance from the ridge. Hydrogeologic evidence indicates that hydrothermal fluid circulation persists within the upper basement to global average ages of at least 65 My (e.g. Becker and Fisher, 2000). These fluids originate from bottom seawater that penetrates highly permeable basement at mid-ocean ridges, unsedimented recharge seamounts and thinly sedimented young ridge flanks. The total fluid reservoir volume of the uppermost (40-500 m) basement aquifer is estimated to be about 2% of the ocean volume (Johnson and Pruis, 2003). Johnson and Pruis (2003) estimate that the total hydrothermal fluid flux from the oceanic crust into the ocean to be 20% of global riverine input although the hydrothermal flux from ridge flanks (crustal age older than 1 My) alone has been estimated to be 5-60% of riverine input (Mottl, 2003; Wheat et al., 2003).

There is growing evidence of a substantial subseafloor biosphere within this large water reservoir (Whitman et al., 1998; Parkes et al., 2000; Amend and Teske, 2005). Texture and chemical composition studies indicate that microbial processes are involved in the alteration of basaltic glass and rocks (Giovannoni et al., 1996; Fisk et al., 1998; Torsvik et al., 1998; Furnes et al., 2001a; Furnes et al., 2001b; Furnes et al., 2002; Bach and Edwards, 2003; Furnes et al., 2006). Concentration, speciation, and isotopic fractionation of sulfur also provide evidence of a subsurface biosphere in ridge flank basement (Rouxel et al., 2008; Alford et al., 2011; Alt and Shanks, 2011). However, while rock cores provide direct samples of surface-associated microbial communities,

core recovery is generally poor. Furthermore, the zones most likely to host the highest biomass are the highly fractured permeable zones with the poorest core recovery. On the other hand, indirect sampling through recovery of basement fluids provides a much larger biomass sample size and more frequent access to samples. Also, the fluid biogeochemistry provides an integrated composite view of past processes and potential contemporary reactivity (e.g., the energies and nutrients required for microbial activities) (Cowen et al., 2003; Wheat et al., 2004b).

In earlier studies, basement fluids were sampled from three study sites that are within 6 km of each other on the eastern flank of the Juan de Fuca Ridge (Fig. 2.1). Biogeochemical data of spring fluids from the unsedimented outcrop Baby Bare are reported by Mottl et al. (1998), Sansone et al. (1998), Lang et al. (2006) and Walker et al. (2008); microbial diversity data from the same site are published by Huber et al. (2006). However, earlier fluids collected at Baby Bare are likely contaminated with sediment despite a novel sampling device with plenty of flushing time designed to reduce contamination (Huber et al., 2006). The other two sites are Integrated Ocean Drilling Program (IODP) boreholes 1026B and 1301A (Fig. 2.1), which are equipped with Circulation Obviation Retrofit Kit (CORK) observatories (Becker and Davis, 2005) that allow routine sampling of basement fluids. Biogeochemical data of fluids ascending from CORK 1026B have been reported (e.g., Cowen et al., 2003; Wheat et al., 2004a; Lang et al., 2006; McCarthy et al., 2011). Although geochemical and microbial data indicate the conditions suitable for some level of microbial activity as well as the presence of diverse bacterial and archaeal communities (Cowen et al., 2003), fluids collected from CORK 1026B ascend through a low alloy steel casing potentially biasing results (Cowen et al.,

2003; Wheat et al., 2004a; Huber et al., 2006). Time series data from the continuous collection of small volumes of basement fluids at CORK 1301A using downhole continuous osmotic-pump fluid samplers, or OSMOs, have provided new insights into basement fluid chemistry and its recovery from drilling-related perturbations (Wheat et al., 2004a; Wheat et al., 2010). However, the OSMO samplers are currently limited by small sample volumes collected over long time periods.

The present study focuses on collecting large volumes (Cowen et al., 2012) of basement fluids to provide sufficient fluids for the simultaneous characterization of fluid chemistry, genetics, and metabolic activities. Extensive geochemical data derived from these samples are used as a check on sample quality with respect to potential contamination by bottom seawater, CORK or sampling materials, and to investigate the dynamics of the basement environment over space and time, including thermodynamic modeling for potential metabolic pathways. The concentrations of the three major bioelements, carbon, nitrogen and phosphorous, in basement fluids are presented and discussed. Dissolved gas constituents, including hydrogen and methane, are important fuels for and products of biological activities and their concentrations are also presented and discussed.

Dissolved organic carbon (DOC) concentrations are an important measure of the organic fuels available for subseafloor heterotrophic activities, and also represent a link between the basement environment and the global carbon cycle. Bottom seawater entrained into the basement carries ~40 μM DOC. Because global oceans circulate through ocean crust aquifers on the order of once every 100-500 Kyr (Fisher, 2005b), the fate of this DOC reflects on the impact of the basement circulation on global ocean

chemistry generally, and global carbon cycles specifically. Moreover, ultrafiltration DOC (UDOC) carbon isotope data suggest that ridge-flank circulation may be extensive enough to export substantial fixed carbon to the overlying ocean (McCarthy et al., 2011). The DOC concentrations of samples collected are presented and their biogeochemical implications will be discussed.

2.2 MATERIALS AND METHODS

2.2.1 Study Sites

Boreholes 1301A and 1026B are only 1 km apart (Fig. 2.1), and the holes were drilled through similar sediment cover (262 and 265 m, respectively) (Shipboard Scientific Party, 2004) into upper basement of similar age (~3.5 Myr), alteration history and temperature (~65 °C) (Elderfield et al., 1999; Wheat et al., 2010). The CORKs installed in borehole 1301A and 1026B are equipped with 1/8" inner diameter stainless steel fluid delivery lines (FDLs), which allow collection of fluids with minimal exposure to the borehole's iron casing (Cowen et al., 2012). Corroded iron casings have been suggested to cause artifacts in sampling for molecular biological studies and for obtaining accurate hydrogen concentrations (Bjerg et al., 1997; Nakagawa et al., 2006). It is also easier to flush the much smaller inner diameter of the FDLs than the central iron casing (10 ¾") prior to sample collection. Although 1026B is equipped with FDLs, gas samples collected from 1026B for this study were from fluids free-flowing upward through the central casing and out the temporarily uncapped top of the CORK.

One sample collected from the CORK at borehole 1025C, 68 km to the west of 1301A (Fig. 2.1), is also reported on here for its dissolved organic carbon content. Borehole 1025C penetrates through ~100 m of sediment into 1.24 Myr old basaltic crust (Shipboard Scientific Party, 1997a). Upper basement temperatures at this site are ~38 °C. It is equipped with the original style CORK in which fluids rise through the center of the casing and are accessed at the seafloor via 2 m titanium pipe.

2.2.2 Sampling Method

The manned submersible Alvin (2008 and 2009) or the remotely operated vehicle Jason (2010 and 2011) were used to visit the CORK observatories and to connect fluid sampling gear to the CORK FDLs. The technique for sampling basement fluids via the CORK FDLs was improved significantly over the course of this study. In 2008, a deep sea pump (5010 series, Pelagic Electronics) was used to draw basement fluids up the FDL. Upstream of this pump, a submersible titanium pump (SBE-5T, Sea-Bird Electronics) was used to draw fluids from the primary fluid flow to a Large Volume Bag Sampler (LVBS), consisting of a custom-made 60 L Tedlar bag (MiDan Co.) housed in a Nalgene high density polyethylene (HDPE) box (Fig. 2b; Cowen et al., 2012). The temperature probe on the submersible *Alvin* was used to monitor the fluid temperature at the Pelagic pump's exhaust port. Sample bags were filled after the FDLs were thoroughly flushed (3x volume of the FDL) and elevated fluid temperatures were observed.

In 2009, 2010 and 2011 the Pelagic pump was replaced with the Mobil Pumping System's (MPS) more powerful pump motor and non-contaminating (inert) titanium and

Teflon pump head to pump the fluids up the FDLs and then push them past temperature and flow sensors directly into samplers (Cowen et al., 2012). An in-line SeaBird temperature probe monitored fluid temperature during flushing and sampling. Fluids from CORK 1301A were collected into sample bags once fluid temperature rose to a stable temperature (~20 ºC for an hour), indicating that the FDL had been sufficiently flushed. In 2009 and 2010, LVBS were used (Fig. 2.2c). Additional refinements in sampling methods were instituted in 2011 (Cowen et al., 2012); fluids were directed from the pump to one of six acid-cleaned, sterilized (gamma irradiation) custom-made Medium Volume Bag Samplers (MVBS; 15 L foil-lined, polyethylene inner liner, Jensen Inert Products). The LVBS was typically mounted on an independent elevator that was quickly returned to the ship within an hour after fluid collection, whereas the MVBS system was borne by the remotely operated vehicle. The fluid sampling rate when using the MPS was 200-600 mL/min for the 1301A CORK's 1/8" inside diameter FDL; sampling rates to >5 L/min were achieved when connected to ½'' inside diameter FDLs available on more recently installed CORKs (Cowen et al., 2012).

In 2008, four gas samples were collected at 1301A using titanium Gas-Tight Samplers (Edmond et al., 1992) through a funnel connected to the exhaust port of the SeaBird pump. In 2010, three gas samples were collected through a similar funnel connected to the MPS exhaust port (Fig. 2.2d). In 2008, two Gas-Tight samples were also collected at CORK 1026B when this CORK head was opened for redeployment of downhole instrument strings (Fig. 2.2e).

2.2.3 Sample Storage

On deck, samples were quickly distributed into sample vials through acid-washed Teflon tubing fitted with a short middle section of acid-washed Master-flex (silicon) pump tubing coupled to a peristaltic pump. Samples for the analysis of total organic carbon (TOC) and major ions (including Mg, Ca, K, and sulfate) were pumped directly into acid washed Nalgene HDPE bottles. Alkalinity, pH, Mg and Ca were analyzed at sea. Samples for DOC, total dissolved nitrogen (TDN), ammonium, nitrate, phosphate and total dissolved iron analysis were filtered through a combusted GF/Filter (550 ºC, 5 hours) in a Whatman filter holder connected to the end of the Teflon tubing. Subsamples for DOC, TDN, ammonium and nitrate analysis were stored frozen until thawed just before analysis at the shore-based laboratory.

Gas samples were stored in Gas-Tight samplers at room temperature until extracted under vacuum. The 2008 CORK 1301A and 1026B samples were stored for 5-12 days and the 2010 CORK 1301A samples were stored for 5-8 days before extraction. Each sample was acidified with sulfamic acid to obtain complete extraction of total CO_2. After gas extraction, the remaining fluids were transferred into HDPE bottles and kept at room temperature for major ion analysis.

2.2.4 Analytical Methods

Analytical methods followed established techniques (Table 2.1). Standardization for major ions analysis (Gieskes et al., 1991) employed International Association for the Physical Sciences of the Oceans (IAPSO) standard seawater (OSIL, Environmental Instruments and Systems). For DOC and TDN analysis, Analytical Reference Materials (ARM) supplied by Drs. Wen-Hao Chen and Dennis Hansel (RSMAS, U. of Miami)

were used as calibration standards before, during and after analysis of samples collected after 2009 (Sharp et al., 2002; Dickson et al., 2007). At least one ARM was measured every 5 samples. The average measured DOC concentration in the ARM is 42±2 µM (n=44), within the standards' reported value of 41-43 µM. Our detection limit for DOC was about 2 µM. The average measured TDN value of the ARMs is 32.5±0.6 µM (n=42), within the standard's reported value of 32.2-33.8 µM. The detection limit of TDN is about 0.5 µM.

Methane and hydrogen concentrations in samples were analyzed by gas chromatography. Gas components were separated using either Hayesep A or Hayesep Q porous polymer columns (18-24 ft ×1/8 inch) started at -50 °C and ramped to 120 °C. Quantitative injections of various commercially prepared mixed gas standards were used to calibrate the detector responses. The accuracy for both gases is about 5%. The precision of measured values in replicate samples for both gases is better than 5%.

2.2.5 Endmember Correction

During sampling, bottom seawater can be entrained into Gas-Tight samplers depending on the flow rate out of the access ports, the sampling rate of the Gas-Tight samplers and how deeply the sampler snorkel is inserted into the port (Fig. 2.2 d & e; Cowen et al., 2012). The entrained seawater component is subtracted from the measurement of each sample to obtain the endmember (true) basement fluid composition (Mottl et al., 1998; Wheat and Mottl, 2000) using a two end-member mixing model (Libes, 2009) and the endmember represented by the lowest Mg concentration measured under optimal sampling conditions for a particular basement environment. The lowest Mg

concentrations measured are 1.9 mM at 1301A (Wheat et al., 2010) and 2.3 mM at 1026B (Wheat et al., 2004a).

2.3 RESULTS

2.3.1 Inorganic Composition of Basement Fluids

The Mg concentrations measured by inductively coupled plasma optical emission spectroscopy, ion chromatography and titration agree well over a wide concentration range. The inorganic chemical compositions of these upper basement samples collected via FDL from the seafloor (this study) are very similar to those of downhole OSMO samples reported by Wheat et al. (2010). Upper basement fluids are depleted in alkalinity, sulfate, potassium, nitrate and phosphate, but enriched in ammonium, silicate, and total dissolved iron, relative to nearby bottom seawater (Table 2.1, Figs. 2.3 and 2.4). The average endmember sulfate concentration for our 2010 and 2011 samples are 18.0±0.2 mM and 18.2±0.1 mM, respectively, much lower than the bottom seawater value of 28.4±0.3 mM (Table 2.1). The average endmember phosphate concentrations are 0.06±0.06 µM and 0.10±0.04 µM for 2010 and 2011 samples, respectively (Table 2.1).

2.3.2 Dissolved Organic Carbon Concentrations

Values of basement fluid DOC at CORK 1301A are given in Table 2.1 and plotted against Mg in Fig. 2.4d. The measured DOC concentrations for the 2010 1301A fluids are 12±3 µM (n=5), compared to 39±0.8 µM for bottom seawater. The DOC concentrations in 1301A fluids collected in 2009 and 2008 are 13 µM and 21 µM, respectively. Due to the low Mg levels in these samples, the differences between the measured and calculated endmember DOC values are less than 2 µM, similar to the

analytical error. The endmember DOC values for 1301A fluids are highest in the 2008 sample (19 µM) and lowest in 2010 samples (11±3 µM). The DOC concentration of a single basement fluid sample collected from CORK 1025C is 22±1 µM, although CORK 1025C fluid value needs to be used cautiously because the fluids were collected through the CORK's central iron casing. The overall sampling blanks for DOC are below the detection limits (2 µM).

2.3.3 Gas Composition

1301A Gas-Tight Samples

The Mg endmember calculations show that basement fluid contributes from 5-11% and 30-40%, respectively, of the total Gas-Tight samples collected at 1301A in 2008 and 2010, with bottom seawater making up the rest (Fig 2.5, Table 2.2). The low basement fluid endmember components in Gas-Tight samples are expected because the rate of basement fluid delivered to the funnel port was low (from <100 mL to 600 mL/min depending on whether pelagic pump or MPS was used) compared to the rapid Gas-Tight fluid collection rate (~125 mL per few seconds), insuring that bottom seawater would be drawn into the funnel during sampling (Fig. 2.2d). The significant increase in the endmember component of 2010 samples resulted from the higher fluid pumping rate (200-600mL/min) of the more powerful MPS pump. It should be noted that the slow pump rates are a function of the tremendous drag presented by the over 250 m of narrow bore (1/8" ID) FDL available at 1301A (Cowen et al., 2012).

A methane versus Mg plot (Fig. 2.5b) for 2008 and 2010 samples shows a conservative mixing relationship, suggesting that very little or no methane oxidation

occurred within the Gas-Tight samplers before gases were extracted from the samples. As a consequence, the endmember-corrected methane concentrations of the 2010 and 2008 samples were extremely close despite the much lower endmember component of the 2008 samples. The Mg endmember-corrected methane concentrations are 1.6±0.2 µM (n=3) and 1.5±0.3 µM (n=4) for the 2010 and 2008 samples, respectively.

A hydrogen versus magnesium plot for CORK 1301A samples in 2008 shows a cluster of data while that for 2010 samples clearly shows a linear trend (Fig. 2.5c). The calculated endmember hydrogen concentrations for the 2008 and 2010 samples are 2±1 µM (n=4) and 0.3±0.2 µM (n=3), respectively (Table 2.2).

1026B Gas-Tight Samples

The two 1026B Gas-Tight samples have Mg concentrations (2.8 and 2.9 mM) very similar to the lowest Mg concentration ever reported for upper basement at this site (2.3 µM; Wheat et al., 2004a) (Fig. 2.2e & Fig. 2.5, Table 2.2), indicating minimal bottom seawater entrainment in these samples. This is not surprising as the open CORK at this overpressured hole allowed basement fluids to flow unrestricted up and out of the large diameter (10 ¾") central casing.

The endmember methane concentrations of the two 1026B basement fluids are very similar (1.9 µM and 2.0 µM), indicating good reproducibility of the overall sampling and analytical processes (Table 2.2). In contrast, the hydrogen concentrations of the two 1026B basement fluid samples differ substantially at 1.1 µM and 0.4 µM. Overall, we were successful in collecting fluid samples for analysis of gas constituents both from the fluid delivery line (CORK 1301A) and from the open hole (CORK 1026B).

2.4 DISCUSSION

2.4.1. Comparison with Previous Studies

The compositions of upper basement fluids at the CORK 1301A site were previously reported for the period from Aug 2004 to August 2008 for samples collected by downhole OSMO samplers (Wheat et al., 2010). The data from 1301A reported here, derived from basement fluid samples collected using the FDL-pumping systems during annual cruises 2008 - 2011, extend the time series from 4 to 7 years. The intake screen for the FDL is located exterior to the CORK casing at 280 mbsf (meters below seafloor), in close proximity to the perforated fluid intake for OSMO samplers deployed inside the steel casing at 280 to 285 mbsf (Wheat et al., 2010) (Fig. 2.2a). Consequently, since the last data point recorded by the OSMO sampler was at about the same time as the 2008 FDL-LVBS samples (i.e. August 2008), a direct comparison of geochemical data obtained by different sampling methods is possible. The most significant differences between the FDL-collected fluids and the OSMO samples are in ammonium and dissolved iron concentrations (Table 2.1, Fig. 2.3c), discussed in detail below. Methane and hydrogen compositions briefly mentioned in previous studies (Mottl et al., 1998; Lang et al., 2006) are compared here with our new data and discussed in detail.

2.4.1.1. Ammonium

The ammonium concentrations for all of the FDL samples range from 99 to 111 µM (2008~2011), significantly lower than the average concentration of 840 µM in the OSMO

samples (Wheat et al., 2010). The lower ammonium concentrations observed during the present study are more consistent with the ammonium concentrations (~246 µM) observed in sediment interstitial water near the sediment-basement interface collected from borehole 1301C and 1301D (Shipboard Scientific Party, 2004; Fisher et al., 2005). The concentration of ~100 µM in basement fluids also falls on the trend line of the sediment diffusion profile (Fig. 2.6), indicating that the source of the basement fluid ammonia is downward diffusion from the sediment interstitial water into the basement. Moreover, the ammonium concentrations measured in this study are similar to those for 1026B CORK fluids and Baby Bare spring fluids (Fig. 6, Johnson et al., 2003; Wheat et al., 2004a).

In contrast, the high ammonium concentrations of the OSMO samples indicate an additional (i.e., contamination) source of ammonium. It has been argued that these elevated levels result from disturbance of the drilling operations or diffusion of ammonium from overlying sediment interstitial water (Wheat et al., 2010). However, the ammonium concentration in the overlying interstitial water (246 µM) is lower than that of the OSMO samples (840 µM), eliminating downward diffusional flow as a realistic explanation. Since the OSMO sampler's intake was in the perforated steel casing, the flushing of fluids collected by the OSMO samplers is relatively restricted. The source of the additional ammonium (contamination) to the OSMO samplers is not clear, but our data show that FDL-MPS, with either the LVBS or MVBS, is an effective method for collecting basement fluid samples for ammonium analysis and for subsequent biological and molecular studies.

2.4.1.2. Iron Concentrations

The much lower total dissolved iron (predominantly Fe^{2+}) concentrations in the FDL-MPS samples, relative to the OSMO samples (Fig. 2.3d), demonstrates the benefits of employing the stainless steel FDL and titanium-Polyvinylidene fluoride (PVDF) MPS system, with extensive flushing of the FDL prior to actual sample collection. Oxygen diffusion into the LVBS sample bags prior to subsampling may have allowed some oxidation and precipitation of dissolved iron. However, the iron concentrations measured in fluids fixed in situ during seafloor sampling (sample bag pre-charged with Ferrozine) show no significant difference from shipboard analysis of unfixed samples, indicating that quick sample turnover and shipboard analysis have minimized the influence of iron precipitation within the bag samples.

2.4.1.3. Methane Concentrations

The methane concentrations measured in this study for basement fluids at 1301A (~1.6 μM) and 1026B (2.0 μM) are higher than those measured previously for Baby Bare spring fluids. Mottl et al. (1998) reported methane at high nM concentrations in Baby Bare spring fluids consistent with the 0.1-0.74 μM reported by Lang et al. (2006). The lower methane concentrations in Baby Bare spring fluids are likely caused by consumption of methane as the fluids ascend to the seafloor. Baby Bare is a lightly sedimented outcrop and the ascending fluid is more susceptible to influence from oxygenated bottom seawater than the deeply buried CORK 1301A and 1026B fluids.

2.4.1.4. Hydrogen Concentrations

The relatively high hydrogen values in 2008 1301A basement fluids may indicate overestimation due to the low endmember component of these samples. The regression line for the three 2010 samples did not pass through the hydrogen value for bottom seawater, suggesting loss of hydrogen relative to the change of Mg, possibly through hydrogen oxidation inside the Gas-Tight sampler prior to sample extraction.

The hydrogen concentrations measured in basement fluids from 1301A and 1026B (0.3-0.7 μM) are similar to the high nM concentrations reported for Baby Bare spring fluids by Mottl et al. (1998). The hydrogen concentrations in Baby Bare fluids were mistakenly reported as 0.03-0.67 mM (Lang et al., 2006), when, in fact, the value is <0.18 μM. The hydrogen concentrations in ridge flank fluids are consistently much lower than what have been observed at ridge axes (summarized in Amend et al., 2011), which are typically at mM levels. Nevertheless, the hydrogen concentrations in basement fluids are three orders of magnitude above detection limits (0.2 nM) and could provide fuel for basement microbes.

2.4.2. Essential Bioelements in the Basement Fluids

The low phosphate concentration (0.11±0.06 μM, average 2008-2011 endmember value) in 1301A basement fluids is consistent with, but even lower than, the phosphate concentrations in CORK 1026B fluids (0.9 μM; Wheat et al., 2000) and nearby Baby Bare spring fluids (0.3 μM; Wheat et al., 2004a). The low dissolved inorganic phosphate concentrations in the basement fluids possibly result from biological uptake, adsorption onto basaltic basement, and removal by iron oxyhydroxide particles (Wheat et al., 1996). Iron oxyhydroxide is one of the most abundant secondary minerals present in the 3.5 Myr

rock cores from this study site (Marescotti et al., 2000). Sorption of phosphate onto iron oxyhydroxide surfaces renders phosphate unavailable for biological uptake (Reynolds and Davies, 2001; Ruttenberg and Sulak, 2011). In contrast to the depleted phosphate concentrations, the high endmember ammonium concentrations of 104±5 μM (average 2008-2011 endmember value) in basement fluids at 1301A indicate that nitrogen is likely not a limiting bio-element for the basement biosphere at this site.

The alkalinity of 1301A basement fluid (0.46±0.06 meq/L, endmember value) is significantly lower than that of bottom seawater (2.48±0.1 meq/L). Calculated basement dissolved inorganic carbon (DIC, 0.45±0.06 mM), based on the measured alkalinity and pH (Zeebe and Wolf-Gladrow, 2001), is also substantially lower than that of bottom seawater (2.41±0.1 meq/L). The drastic decrease in alkalinity in basement fluids cannot be explained by the slight decrease in pH from bottom seawater (7.7±0.1) to 1301A basement fluid (7.4±0.1). Carbonate precipitation is a more likely explanation for the low alkalinity in basement fluids (Sansone et al., 1998) although biological uptake might also contribute. The stoichiometric ratio of dissolved inorganic carbon, nitrogen, and phosphorus (DIC:DIN:DIP) is 4064:945:1 and suggests that neither carbon nor nitrogen is a limiting factor for life in this basement environment; phosphate appears to be limited.

While the DIP concentrations suggest that the basement environment could be phosphate limited, microorganisms in the basement environment might be able to exploit dissolved organic phosphate (DOP). Some microorganisms are capable of using organic phosphorus (eg. Bjorkman and Karl, 1994) as their source of P. DOP concentrations in the basement fluid at our study site are unknown, but in deep North Pacific seawater (2515m Station M), DOP value is 0.073 μM (Loh and Bauer, 2000). If the loss of DOP

from the deep water is proportional to the loss of DOC along the basement circulation flow path, the DOP at site 1301A would be around 0.018 μM. The sum of DIP and DOP at site 1301A would still be no more than 0.13 μM. Future phosphate addition experiments are needed to verify whether phosphate is truly a limiting element.

2.4.3. Hypothesized Scenarios for a Non-Standard State Redox System

The 1301A basement fluids collected in this study contain significant amounts of sulfate (~18 mM). A trace amount of hydrogen sulfide (0.1-0.4 μM) is observed in the 2009 FDL-MPS-LVBS sample. Fluids from 1301A and 1026B also contain 1.6-2 μM CH_4 and 0.3-1.7 μM H_2. Following the thermodynamically controlled redox reaction sequence, as observed in shallow anoxic sediment columns, methane production should occur only after sulfate is exhausted. However, unlike sediments, the permeable and fractured basement allows for rapid channelized fluid flow (Fisher and Becker, 2000). The basement fluids collected from CORK 1301A likely derive from a mixture of less reduced sources (with sulfate and H_2S, no CH_4) and more reduced sources (depleted sulfate, with CH_4). Co-occurrence of these redox species could indicate a basement aquifer that draws from multiple flow paths (i.e., channels) and micro-habitats with different redox histories (Fig. 2.7a), a scenario consistent with an extensively fractured formation. Relatively rapid basement fluid flow rates, slow metabolic rates and rapid sampling/processing could explain the simultaneous presence of sulfate and methane in the basement fluids. Concurrence of sulfate reduction and methanogenesis (methane production) has been inferred and quantified based on simultaneous presence of methane and abundant sulfate in open-ocean deep sediment interstitial water (D'Hondt et al., 2002; Wang et al., 2008). Simultaneous presence of methane and abundant sulfate is also

observed in the basement fluids from CORK 1301A. We thus infer that in the basement environment, sulfate reduction and methanogenesis might co-occur as well (Fig. 2.7 b). Coexistence due to the absence of competitive exclusion, is consistent with the recent view concluded from both calculations of the usable energies for methanogens, sulfate reducers and iron reducers, and long-term bioreactor experiments simulating the deep continental groundwater environment (Bethke et al., 2011).

The low hydrogen sulfide together with low total dissolved iron suggests that sulfide produced through microbial sulfate reduction precipitates with dissolved iron, which is supported by the presence of secondary pyrite in the rock cores recovered from boreholes 1301A (Shipboard Scientific Party, 2004) and 1026B (Marescotti et al., 2000). Secondary sulfide precipitates in oceanic basaltic rocks recovered from the western Pacific (Rouxel et al., 2008) and eastern Pacific (Alt and Shanks, 2011) are enriched in the light ^{32}S isotope (negative $\delta^{34}S$), indicating microbial sulfate reduction as the source of the secondary sulfide.

In addition to abiotic production of hydrogen via water-rock reaction (Stevens and McKinley, 1995), fermentation is another potentially important source of hydrogen (e.g. Boone et al., 1989) to the basement environment. In the two scenarios proposed to explain coexisting sulfate and methane (Fig. 2.7), fermenters are present throughout the entire flow path once oxygen in the environment is exhausted, coexisting with other functional groups including sulfate reducers and methanogens.

Interestingly, the hydrogen concentrations measured in the basement fluids from CORKs 1301A and 1026B are well above 2 nM, the predicted value for the overlying

1301A sediment interstitial water (Lever et al., 2010) based on thermodynamic modeling. If the environment is thermodynamically controlled, the minimum hydrogen concentration in the environment is determined by the apparent minimum biological energy quantum (ΔG_r = -10 kJ/mol) of the dominant microbial metabolic processes, including hydrogenotrophic sulfate reduction, methanogenesis or acetogenesis (Lever et al., 2010). The highest H_2 concentration (30-1000 nM) is maintained for acetogenesis, followed by methanogenesis (1-10 nM) and sulfate reduction (0.02-2 nM), which is predicted to dominate the deeper sediment column (Lovley and Goodwin, 1988; Hoehler et al., 1998; Lever et al., 2010). The thermodynamically predicted H_2 concentrations for the basement fluids should be similar to that for deep sediment interstitial water since most of the inorganic concentrations (e.g., CO_2, SO_4^{2-}) are similar. Therefore, the relatively high hydrogen concentrations measured in the basement fluids (0.3-1.75 μM) suggest that the hydrogen concentration is not exclusively controlled by hydrogenotrophic sulfate reduction. It further suggests that the hydrogen may diffuse across the sediment-basement interface, providing support for hydrogenotrophic acetogenesis reactions in the sediment column to help explain the "light" acetate isotopes observed in the sediment interstitial waters (Lever et al., 2010).

The hydrogen concentrations measured in fluids escaping from the opened top of CORK 1026B should be used with caution because the fluids could have been influenced by the iron casing (Bjerg et al., 1997). In contrast, the influence of the extensively flushed stainless steel FDL and plastic MPS-LVBS (or MVBS) system on H_2 concentrations from 1301A should have been minimal; it has been shown that compared with low alloy iron,

stainless steel installed in continental ground water boreholes generated 2-3 orders of magnitude less H_2 (Bjerg et al., 1997).

Overall, the inorganic chemistry of fluids collected during this study between 2008 and 2011 suggests a non-equilibrium redox system, where sulfate, hydrogen sulfide, methane and hydrogen coexist. These redox species provide electron donors and acceptors for diverse potential chemolithoautotrophic and heterotrophic metabolisms (eg. McCollom, 2000; Amend and Shock, 2001), not unlike what is commonly observed in continental hot springs and marine hydrothermal systems (Amend et al., 2003; Shock et al., 2010; Amend et al., 2011).

2.4.4. Implications of the DOC Data

2.4.4.1. Ridge Flank Basement as a Net DOC Sink

The consistently low DOC concentration of the basement fluid samples, relative to bottom seawater, demonstrates the successful evolution of our CORK seafloor sampling and analytical process, seen especially in the 2009-2011 samples from CORK 1301A. More importantly, the low detection limit (2 µM) and the small analytical uncertainty (±1 µM) allow examination of DOC temporal variations. The endmember DOC concentration for the 2009 sample (12.8 µM) was within the range of 2010 samples (7-14 µM, average 11±3 µM). The 2008 sample had a slightly higher concentration (18.6 µM). The variation of up to 7 µM observed among the five samples collected in 2010 (Fig. 2.4d) is similar to that observed in samples collected from nearby borehole 1026B (8-17 µM, average 13±4 µM; Lang et al., 2006) and Baby Bare warm spring (7-27 µM, average 11±3 µM; Lang et

al., 2006). It is possible that DOC concentrations of the basement fluids are moderately variable. Alternatively, the variation of the DOC may be caused by the drilling or sampling processes. As contamination tends to increase the DOC concentration, the lowest measured value should best represent the environmental value.

Although no significant spatial trend in DOC concentrations is observed along the flow direction from the younger Baby Bare to the slightly older 1301A and 1026B (Fig. 2.8), this study confirms earlier results that the ridge-flank basement environment is a net sink for ocean water DOC (Lang et al., 2006; McCarthy et al., 2011). When the DOC concentrations of the basement fluids (1301A, 1026B and Baby Bare) are plotted against their corresponding dissolved inorganic carbon $\Delta^{14}C$ values (Elderfield et al., 1999; Walker et al., 2008), basement fluid DOC data fall below a linear extension of the deep water DOC trend line (Fig. 2.8), suggesting a dynamic removal of even deep ocean refractory DOC within the low energy basement environment. The rapid decrease in DOC concentration with time (decreasing radiocarbon content) resulted from surface ocean DOC being rapidly removed during its cycling through the deep ocean (Hansell et al., 2009). Deep water DOC is lost more slowly with time. The DOC of basement fluids decreases at similar or more rapid rates than the deep water DOC.

2.4.4.2. DOC Net Removal Rate

The net DOC removal rates from entrained bottom seawater, calculated using DOC data from available basement fluid samples, provide insight into the reactivity of the DOC and its possible removal mechanisms. Dissolved inorganic radiocarbon ages

(Elderfield et al., 1999; Walker et al., 2008) and the average DOC concentrations for basement fluids at CORK 1301A, CORK 1025C (this study), CORK 1026B (Lang et al., 2006) and Baby Bare Spring (Lang et al., 2006) are used for the rate estimates. All DOC and C-14 ages are summarized in Table 2.3. The calculated net removal rates are 2.4±0.7, 2.4±0.7 and 2.9±0.7 nmol C/L/year based on 1301A, 1026B and Baby Bare DOC data, respectively. The removal rates are remarkably similar to the 3 nmol C/L/year net DOC removal rate calculated for circulating bottom seawater (Hansell et al., 2009; Table 3). Comparing the DOC removal rates in the lower water column to rates of biological and abiotic activities, Hansell et al. (2009) suggested that both biotic and abiotic processes are involved. Although rates of abiotic or biotic activities are not available yet for the basement environment, comparison of the net amount of DOC removed with the amount of redox couples removed or generated may shed light on possible mechanisms for the removal of entrained DOC during circulation of the basement fluids.

The net amounts of DOC (~30 µM) and nitrate (39-40 µM) removed from the entrained bottom seawater are comparable (Table 2.1), but less than the amount of oxygen removed (~80 µM; based on the O_2 concentration in the bottom seawater, 80±1 µM). At 1301A, nitrate in basement fluids is depleted to exhaustion (endmember 0-0.8µM), and following the redox hierarchy, oxygen concentration should equal zero in basement fluids. The net amount of DOC removed is negligible compared with the amount of sulfate removed (~10 mM) from the entrained bottom seawater. These comparisons suggest that the DOC removed from the entrained bottom seawater can be potentially coupled to either or both aerobic (oxygen consumption) or anaerobic (nitrate and sulfate reduction) heterotrophic activities to produce the observed increase in

ammonium, hydrogen sulfide and methane in the 1301A basement fluids. However, oxidation of basaltic rocks (Mottl et al., 1998), mineral precipitation and diffusion into overlying sediments (Elderfield et al., 1999) must also account for the loss of much of the oxygen, nitrate and sulfate from the entrained seawater.

The potential addition to basement DIC (~30 μM) from the total oxidation of entrained bottom water DOC is small relative to the observed large decrease in DIC concentration from entrained seawater (2.4 mM) to 1301A basement fluid (0.44 mM). Nevertheless, the depleted carbon isotopic value of DIC in the basement fluids collected at CORK 1026B and Baby Bare (Walker et al., 2008), relative to bottom seawater, may indicate secondary DIC sources including biological respiration of organic matter.

The above discussion of net DOC removal only considers the DOC entrained in bottom seawater at basement recharge zones. Other potential sources of DOC to the basement include diffusion of DOC across the sediment-basement interface and in situ production by chemolithoautotrophic organisms. The DOC concentration in the overlying deep sediment pore waters (Shipboard Scientific Party, 2004) is two orders of magnitude higher than the DOC concentration in the basement fluids. Inevitably, sediment interstitial DOC must diffuse into the basement. Moreover, the inorganic chemical compositions of the basement fluids and formation minerals suggest that the environment is conducive to chemolithoautotrophic production, which could contribute DOC. Calculations of Gibbs energies of reaction, ΔG_r, using extensive chemical and physical data from 1301A, indicate that basement conditions are thermodynamically conducive to a wide spectrum of metabolic reactions (Boettger, 2011). For example, the coupling of sulfate reduction with oxidation of hydrogen or various organic acids is energy yielding.

Chemolithoautotrophic organisms capable of such metabolisms may thrive within certain channels of the basement and contribute to the DOC pool. Moreover, the similar $\Delta^{14}C$ of UDOC and DIC of fluids collected from CORK 1026B suggests a chemolithoautotrophic origin of the UDOC and possibly of the total DOC (McCarthy et al., 2011). It has also been suggested that in situ abiotic production of DOC can be thermodynamically favorable under hydrothermal conditions (Amend and Shock, 1998; LaRowe and Regnier, 2008; Konn et al., 2009; Shock and Canovas, 2010). Consequently, the estimates for net DOC removal rates based solely on loss of seawater DOC likely underestimates the "actual" DOC removal rate in the basement environment.

2.5. CONCLUSIONS

Large volumes of high quality basement fluids were collected through the CORK 1301A stainless steel fluid delivery line using a clean mobile pumping system for the first time. The fluid delivery line supplies basement fluid with little or no ammonium and iron contamination, relative to fluid collected through the CORK's central casing. Interestingly, the fluids contain a significant amount of sulfate coexisting with hydrogen sulfide, methane and hydrogen. Hypothesized scenarios to explain these observations include an aquifer supplied by multiple fluids channels with different redox histories and a subsurface biosphere not controlled exclusively by equilibrium thermodynamics, where sulfate reduction and methanogenesis (and redox reactions) are both exergonic in the same fluid. The low measured DOC concentrations in basement fluids demonstrate good control over sampling and analytical procedures. Overall, the differences in DOC

between bottom seawater (~40 μM) and the basement fluids from 1301A (~12 μM) indicate a conservative net DOC removal rate of ~2.4 nmol/L/yr, similar to the net deep ocean DOC removal rate, as well as estimated DOC removal rates based on basement fluid data from 1026B and Baby Bare. Comparison of the net DOC removal with the removal of terminal electron acceptors such as oxygen, nitrate and sulfate suggest that heterotrophic activities could account for the removal of DOC. The actual DOC removal rate must be higher to account for the DOC diffused from sediment interstitial water across the sediment-basement interface and any additional DOC from in situ chemolithoautotrophic production.

Acknowledgments. We thank Chih-Chaing Hsieh, Ryan Matsumoto, Sean Jungbluth, Michael Matzinger, Natalie Hamada, Kathryn Hu, Joshua Bninski, and Brian Glazer for their fantastic technical field and lab support and the Alvin, Jason and R/V Atlantis crews for their support in field sampling. We also like to thank Dr. Chittaranjan Ray and Joseph Lichwa for providing access to the analytical instruments at the Water Resource Research Center at the University of Hawaii. This study benefitted from stimulating discussion with Alberto Robador, Dennis Hansell, Andy Fisher, Mark Lever, Fabien Kenig, Mike Mottl and Yuan-Hui (Telu) Li. We are very grateful to Geoff Wheat, two other anonymous reviewers and the associate editor Jeff Alt for their positive and helpful suggestions to help us improve the quality of this manuscript significantly. This project is supported by NSF-MCB06-04014, OCE0946381, and the UH NASA Astrobiology Institute. This is SOEST contribution no. 8542 and C-DEBI contribution no. 125.

2.6. REFERENCES

Alford, S. E., Alt, J. C., and Shanks Iii, W. C., 2011. Sulfur geochemistry and microbial sulfate reduction during low-temperature alteration of uplifted lower oceanic crust: Insights from ODP Hole 735B. *Chem. Geol.* **286**, 185-195.

Alt, J. C. and Shanks, W. C., 2011. Microbial sulfate reduction and the sulfur budget for a complete section of altered oceanic basalts, IODP Hole 1256D (eastern Pacific). *Earth and Planetary Science Letters* **310**, 73-83.

Amend, J. P., McCollom, T. M., Hentscher, M., and Bach, W., 2011. Metabolic (catabolic and anabolic) energy for chemolithoautotrophs in deep-sea hydrothermal systems hosted in different rock types. *Geochim. Cosmochim. Acta* **in review**.

Amend, J. P., Rogers, K. L., Shock, E. L., Gurrieri, S., and Inguaggiato, S., 2003. Energetics of chemolithoautotrophy in the hydrothermal system of Vulcano Island, southern Italy. *Geobiology* **1**, 37-58.

Amend, J. P. and Shock, E. L., 1998. Energetics of amino acid synthesis in hydrothermal ecosystems. *Science* **281**, 1659-1662.

Amend, J. P. and Shock, E. L., 2001. Energetics of overall metabolic reactions of thermophilic and hyperthermophilic Archaea and Bacteria. *FEMS Microbiol. Rev.* **25**, 175-243.

Amend, J. P. and Teske, A., 2005. Expanding frontiers in deep subsurface microbiology. *Palaeogeogr. Palaeocl.* **219**, 131-155.

Bach, W. and Edwards, K. J., 2003. Iron and sulfide oxidation within the basaltic ocean crust: Implications for chemolithoautotrophic microbial biomass production. *Geochim. Cosmochim. Acta* **67**, 3871-3887.

Becker, K. and Davis, E., 2005. A review of CORK designs and operations during the Ocean Drilling Program. *Proceedings of the Integrated Ocean Drilling Program* **301**.

Becker, K. and Fisher, A. T., 2000. Permeability of upper oceanic basement on the eastern flank of the Juan de Fuca Ridge determined with drill-string packer experiments. *J. Geophys. Res.* **105**, 897-912.

Becker, K. and Fisher, A. T., 2008. Borehole packer tests at multiple depths resolve distinct hydrologic intervals in 3.5-Ma upper oceanic crust on the eastern flank of Juan de Fuca Ridge. *J. Geophys. Res.* **113**, 1-12.

Bethke, C. M., Sanford, R. A., Kirk, M. F., Jin, Q., and Flynn, T. M., 2011. The thermodynamic ladder in geomicrobiology. *American Journal of Science* **311**, 183.

Bjerg, P. L., Jakobsen, R., Bay, H., Rasmussen, M., Albrechtsen, H.-J., and Christensen, T. H., 1997. Effects of Sampling Well Construction on H_2 Measurements Made for Characterization of Redox Conditions in a Contaminated Aquifer. *Environ. Sci. Technol.* **31**, 3029-3031.

Bjorkman, K. and Karl, D. M., 1994. Bioavailabiliy of inorganic and organic phosphorus-compounds to natural assemblages of microorganisms in Hawaiian costal water. *Marine Ecology-Progress Series* **111**, 265-273.

Boettger, J., 2011. Geochemical constraints on microbial metabolisms in the basement fluid of the Juan de Fuca Ridge flank, B.S. thesis, Washington Univ.

Boone, D. R., Johnson, R. L., and Liu, Y., 1989. Diffusion of the interspecies electron carriers H2 and formate in methanogenic ecosystems and its implications in the measurement of Km for H2 or formate uptake. *Appl. Environ. Microbiol.* **55**, 1735.

Cowen, J. P., Copson, D. A., Jolly, J., Hsieh, C.-C., Lin, H.-T., Glazer, B. T., and Wheat, C. G., 2012. Advanced instrument system for real-time and time-series microbial geochemical sampling of the deep (basaltic) crustal biosphere. *Deep-Sea Res. Pt. I* **61**, 43-56.

Cowen, J. P., Giovannoni, S. J., Kenig, F., Johnson, H. P., Butterfield, D., Rappe, M. S., Hutnak, M., and Lam, P., 2003. Fluids from aging ocean crust that support microbial life. *Science* **299**, 120-123.

D'Hondt, S., Rutherford, S., and Spivack, A. J., 2002. Metabolic activity of subsurface life in deep-sea sediments. *Science* **295**, 2067-2070.

Dickson, A., Sabine, C., and Christian, J., 2007. *Guide to best practices for ocean CO_2 measurements*. PICES Science Report.

Edmond, J., Massoth, G., and Lilley, M., 1992. Submersible-deployed samplers for axial vent waters. *Ridge Events* **3**, 23-24.

Elderfield, H., Wheat, C. G., Mottl, M. J., Monnin, C., and Spiro, B., 1999. Fluid and geochemical transport through oceanic crust: a transect across the eastern flank of the Juan de Fuca Ridge. *Earth Planet. Sci. Lett.* **172**, 151-165.

Fisher, A. T., 2004. Rates of flow and patterns of fluid circulation. In: *Hydrogeology of the oceanic lithosphere* (eds. E. E. Davis and H. Elderfield). Cambridge University Press, Cambridge.

Fisher, A. T., 2005. Marine hydrogeology: recent accomplishments and future opportunities. *Hydrogeol. J.* **13**, 69-97.

Fisher, A. T. and Becker, K., 2000. Channelized fluid flow in oceanic crust reconciles heat-flow and permeability data. *Nature* **403**, 71-74.

Fisher, A. T., Urabe, T., Klaus, A., and Scientists, E., 2005. Site U1301. *Proc. IODP* **301**.

Fisk, M. R., Giovannoni, S. J., and Thorseth, I. H., 1998. Alteration of oceanic volcanic glass: Textural evidence of microbial activity. *Science* **281**, 978-980.

Furnes, H., Dilek, Y., Muehlenbachs, K., and Banerjee, N. R., 2006. Tectonic control of bioalteration in modern and ancient oceanic crust as evidenced by carbon isotopes. *Isl. Arc* **15**, 143-155.

Furnes, H., Muehlenbachs, K., Torsvik, T., Thorseth, I. H., and Tumyr, O., 2001a. Microbial fractionation of carbon isotopes in altered basaltic glass from the Atlantic Ocean, Lau Basin and Costa Rica Rift. *Chem. Geol.* **173**, 313-330.

Furnes, H., Muehlenbachs, K., Torsvik, T., Tumyr, O., and Shi, L., 2002. Bio-signatures in metabasaltic glass of a Caledonian ophiolite, West Norway. *Geol. Mag.* **139**, 601-608.

Furnes, H., Staudigel, H., Thorseth, I. H., Torsvik, T., Muehlenbachs, K., and Tumyr, O., 2001b. Bioalteration of basaltic glass in the oceanic crust. *Geochem. Geophys. Geosyst.* **2**.

Gieskes, J. M., Gamo, T., and Brumsack, H., 1991. Chemical methods for interstitial water analysis aboard JOIDES Resolution. *ODP Tech. Note* **15**, 119-136.

Giovannoni, S. J., Fisk, M. R., Mullins, T. D., and Furnes, H., 1996. Genetic evidence for endolithic microbial life colonizing basaltic glass/seawater interfaces. *Proc. Ocean Drill. Program Sci. Results* **148**, 207-214.

Hansell, D. A., Carlson, C. A., Repeta, D. J., and Schlitzer, R., 2009. Dissolved organic matter in the ocean: a controversy stimulates new insights. *Oceanography* **22**, 202-211.

Hoehler, T. M., Alperin, M. J., Albert, D. B., and Martens, C. S., 1998. Thermodynamic control on hydrogen concentrations in anoxic sediments. *Geochim. Cosmochim. Acta* **62**, 1745-1756.

Huber, J. A., Johnson, H. P., Butterfield, D. A., and Baross, J. A., 2006. Microbial life in ridge flank crustal fluids. *Environ. Microbiol.* **8**, 88-99.

Johnson, H., Party, L. S., Sheffer, N., Enzel, Y., Waldmann, N., Grodek, T., Benito, G., Gill, T., Zobeck, T., and Tulaczyk, S., 2003. Probing for life in the ocean crust with the LEXEN program. *EOS, Tran. AGU* **84**, 12.

Johnson, H. P. and Pruis, M. J., 2003. Fluxes of fluid and heat from the oceanic crustal reservoir. *Earth Planet. Sci. Lett.* **216**, 565-574.

Jones, R. D., 1991. An improved fluorescence method for the determination of nanomolar concentrations of ammonium in natural-waters. *Limnology and Oceanography* **36**, 814-819.

Kelley, D. S., Lilley, M. D., Lupton, J. E., and Olson, E. J., 1998. Enriched H_2, CH_4, and ^3He concentrations in hydrothermal plumes associated with the 1996 Gorda Ridge eruptive event. *Deep Sea Research Part II: Topical Studies in Oceanography* **45**, 2665-2682.

Konn, C., Charlou, J. L., Donval, J. P., Holm, N. G., Dehairs, F., and Bouillon, S., 2009. Hydrocarbons and oxidized organic compounds in hydrothermal fluids from Rainbow and Lost City ultramafic-hosted vents. *Chem. Geol.* **258**, 299-314.

Lang, S. Q., Butterfield, D. A., Lilley, M. D., Johnson, H. P., and Hedges, J. I., 2006. Dissolved organic carbon in ridge-axis and ridge-flank hydrothermal systems. *Geochim. Cosmochim. Acta* **70**, 3830-3842.

LaRowe, D. E. and Regnier, P., 2008. Thermodynamic Potential for the Abiotic Synthesis of Adenine, Cytosine, Guanine, Thymine, Uracil, Ribose, and Deoxyribose in Hydrothermal Systems. *Origins of Life and Evolution of Biospheres* **38**, 383-397.

Lever, M., Heuer, V., Morono, Y., Masui, N., Schmidt, F., Alperin, M., Inagaki, F., Hinrichs, K. U., and Teske, A., 2010. Acetogenesis in deep subseafloor sediments of the Juan de Fuca Ridge Flank: a synthesis of geochemical, thermodynamic, and gene-based evidence. *Geomicrobiol. J.*, 183-198.

Libes, S. M., 2009. Salinity as a conservative tracer. In: *Introduction to marine biogeochemistry* (eds. S. M. Libes). Academic Press, Burlington.

Loh, A. N. and Bauer, J. E., 2000. Distribution, partitioning and fluxes of dissolved and particulate organic C, N and P in the eastern North Pacific and Southern Oceans. *Deep-Sea Res. Pt. I* **47**, 2287-2316.

Lovley, D. R. and Goodwin, S., 1988. Hydrogen concentrations as an indicator of the predominant terminal electron-accepting reactions in aquatic sediments. *Geochim. Cosmochim. Acta* **52**, 2993-3003.

Marescotti, P., Vanko, D. A., and Cabella, R., 2000. From oxidizing to reducing alteration: Mineralogical variations in pillow basalts from the east flank, Juan de Fuca Ridge. In: *Proceedings of the Ocean Drilling Program, Scientific Results* (eds. A. T. Fisher, E. E. Davis, and C. Escutia). Ocean Drilling Program.

McCarthy, M. D., Beaupre, S. R., Walker, B. D., Voparil, I., Guilderson, T. P., and Druffel, E. R. M., 2011. Chemosynthetic origin of C-14-depleted dissolved organic matter in a ridge-flank hydrothermal system. *Nat. Geosci.* **4**, 32-36.

McCollom, T. M., 2000. Geochemical constraints on primary productivity in submarine hydrothermal vent plumes. *Deep-Sea Res. Pt. I* **47**, 85-101.

Mottl, M. J., 2003. Partitioning of energy and mass fluxes between mid-ocean ridge axes and flanks at high and low temperature. In: *Energy and Mass Transfer in Marine Hydrothermal Systems* (eds. P. E. Halbach, V. Tunnicliffe, and J. R. Hein). Dahlem University Press, Berlin.

Mottl, M. J., Wheat, G., Baker, E., Becker, N., Davis, E., Feely, R., Grehan, A., Kadko, D., Lilley, M., Massoth, G., Moyer, C., and Sansone, F., 1998. Warm springs discovered on 3.5 Ma oceanic crust, eastern flank of the Juan de Fuca Ridge. *Geology* **26**, 51-54.

Nakagawa, S., Inagaki, F., Suzuki, Y., Steinsbu, B. O., Lever, M. A., Takai, K., Engelen, B., Sako, Y., Wheat, C. G., and Horikoshi, K., 2006. Microbial community in black rust exposed to hot ridge flank crustal fluids. *Appl. Environ. Microbiol.* **72**, 6789-6799.

Parkes, R. J., Cragg, B. A., and Wellsbury, P., 2000. Recent studies on bacterial populations and processes in subseafloor sediments: A review. *Hydrogeol. J.* **8**, 11-28.

Reynolds, C. and Davies, P., 2001. Sources and bioavailability of phosphorus fractions in freshwaters: a British perspective. *Biological Reviews of the Cambridge Philosophical Society* **76**, 27-64.

Rouxel, O., Ono, S., Alt, J., Rumble, D., and Ludden, J., 2008. Sulfur isotope evidence for microbial sulfate reduction in altered oceanic basalts at ODP Site 801. *Earth and Planetary Science Letters* **268**, 110-123.

Ruttenberg, K. C. and Sulak, D. J., 2011. Sorption and desorption of dissolved organic phosphorus onto iron (oxyhydr)oxides in seawater. *Geochim. Cosmochim. Acta* **75**, 4095-4112.

Sansone, F. J., Mottl, M. J., Olson, E. J., Wheat, C. G., and Lilley, M. D., 1998. CO2-depleted fluids from mid-ocean ridge-flank hydrothermal springs. *Geochim. Cosmochim. Acta* **62**, 2247-2252.

Sharp, J. H., Carlson, C. A., Peltzer, E. T., Castle-Ward, D. M., Savidge, K. B., and Rinker, K. R., 2002. Final dissolved organic carbon broad community intercalibration and preliminary use of DOC reference materials. *Mar. Chem.* **77**, 239-253.

Shipboard Scientific Party, 1997. Introduction and summary: hydrothermal circulation in the oceanic crust and its consequences on the eastern flank of the Juan de Fuca Ridge *Proc. Ocean Drill. Program Initial Reports* **168**, 7–21.

Shipboard Scientific Party, 2004. Juan de Fuca hydrogeology: The hydrogeologic architecture of basaltic oceanic crust: compartmentalization, anisotropy, microbiology, and crustal-scale properties on the eastern flank of Juan de Fuca Ridge, eastern Pacific Ocean. *IODP Prel. Rept.* **301**.

Shock, E. and Canovas, P., 2010. The potential for abiotic organic synthesis and biosynthesis at seafloor hydrothermal systems. *Geofluids* **10**, 161-192.

Shock, E. L., Holland, M., Meyer-Dombard, D. A., Amend, J. P., Osburn, G. R., and Fischer, T. P., 2010. Quantifying inorganic sources of geochemical energy in hydrothermal ecosystems, Yellowstone National Park, USA. *Geochim. Cosmochim. Acta* **74**, 4005-4043.

Stevens, T. O. and McKinley, J. P., 1995. Lithoautotrophic microbial ecosystems in deep basalt aquifers. *Science* **270**, 450-454.

Torsvik, T., Furnes, H., Muehlenbachs, K., Thorseth, I. H., and Tumyr, O., 1998. Evidence for microbial activity at the glass-alteration interface in oceanic basalts. *Earth Planet. Sci. Lett.* **162**, 165-176.

Walker, B. D., McCarthy, M. D., Fisher, A. T., and Guilderson, T. P., 2008. Dissolved inorganic carbon isotopic composition of low-temperature axial and ridge-flank hydrothermal fluids of the Juan de Fuca Ridge. *Mar. Chem.* **108**, 123-136.

Wang, G. Z., Spivack, A. J., Rutherford, S., Manor, U., and D'Hondt, S., 2008. Quantification of co-occurring reaction rates in deep subseafloor sediments. *Geochim. Cosmochim. Acta* **72**, 3479-3488.

Wheat, C. G., Elderfield, H., Mottl, M. J., and Monnins, C., 2000. Chemical composition of basement fluids within an oceanic ridge flank: Implications for along-strike and across-strike hydrothermal circulation. *J. Geophys. Res.* **105**, 13437-13447.

Wheat, C. G., Feely, R. A., and Mottl, M. J., 1996. Phosphate removal by oceanic hydrothermal processes: An update of the phosphorus budget in the oceans. *Geochim. Cosmochim. Acta* **60**, 3593-3608.

Wheat, C. G., Jannasch, H. W., Fisher, A. T., Becker, K., Sharkey, J., and Hulme, S., 2010. Subseafloor seawater-basalt-microbe reactions: Continuous sampling of borehole fluids in a ridge flank environment. *Geochem. Geophy. Geosy.* **11**, 1-18.

Wheat, C. G., Jannasch, H. W., Kastner, M., Plant, J. N., DeCarlo, E. H., and Lebon, G., 2004a. Venting formation fluids from deep-sea boreholes in a ridge flank setting: ODP Sites 1025 and 1026. *Geochem. Geophy. Geosy.* **5**, 1-12.

Wheat, C. G., McManus, J., Mottl, M. J., and Giambalvo, E., 2003. Oceanic phosphorus imbalance: Magnitude of the mid-ocean ridge flank hydrothermal sink. *Geophys. Res. Lett* **30**, 1895.

Wheat, C. G. and Mottl, M. J., 2000. Composition of pore and spring waters from Baby Bare: Global implications of geochemical fluxes from a ridge flank hydrothermal system. *Geochim. Cosmochim. Acta* **64**, 629-642.

Wheat, C. G., Mottl, M. J., Fisher, A. T., Kadko, D., Davis, E. E., and Baker, E., 2004b. Heat flow through a basaltic outcrop on a sedimented young ridge flank. *Geochem. Geophy. Geosy.* **15**, 1-18.

Whitman, W. B., Coleman, D. C., and Wiebe, W. J., 1998. Prokaryotes: The unseen majority. *P. Natl. Acad. Sci. U.S.A.* **95**, 6578-6583.

Zeebe, R. E. and Wolf-Gladrow, D. A., 2001. *CO_2 in seawater: equilibrium, kinetics, isotopes*. Elsevier Science.

Table 2.1. Inorganic chemical compositions of basement fluids collected from CORK 1301A.

Sample site		**CORK 1301A**									**Bottom seawater**	
Sampling time		**2011 July**		**2010 July**		**2009 Aug**		**2008 August**		**2007 Sep~ 2008 Aug**	**2008-2010**	
Variables	unit	**Uncorr. n=5**	Mg $_{corr.}$	**Uncorr. n=5**	Mg $_{corr.}$	**Uncorr.**	Mg $_{corr.}$	**Uncorr.**	Mg $_{corr.}$	OSMO[a]	-	**n=5**
pH		**-**	-	**7.4** (0.1)	-	**7.4**	-	**7.5**	-	-	**7.7**	(0.1)
Magnesium[b,c,d]	mM	**2.2** (0.2)	***1.9***	**3.4** (0.6)	***1.9***	**2.0**	***1.9***	**6.9**	***1.9***	1.9	**53.7**	(0.3)
Calcium[b,c,d]	mM	**55** (0.2)	55 (1)	**53** 1	54 (1)	**55**	55	**52**	56	57.2	**10.4**	(0.03)
Alkalinity[c]	meq/L	**0.42** (0.04)	0.41 (0.04)	**0.52** (0.04)	0.46 (0.05)	**0.42**	0.41	**0.73**	0.54	-	**2.48**	(0.05)
DOC[e]	µM	**12** (1)	12 (1)	**12** (3)	11 (3)	**13**	13	**21**	19	-	**39**	(1)
TOC[e]	µM	**11** (1)	11 (1)	**12** (2)	11 (2)	**13**	13	**21**	19	-	**39**	(1)
TDN[e]	µM	**102** (2)	103 (2)	**101** (2)	103 (2)	**102**	102	**101**	107	-	**44**	(1)
TN[e]	µM	**101** (2)	102 (2)	**101** (1)	103 (1)	**102**	102	**100**	106	-	**44**	(1)
Nitrate[f]	µM	**0.2** (0.1)	0.0 (0.2)	**1.5** (0.6)	0.3 (0.1)	**0.6**	0.5	**4.7**	0.8	0.0	**40.8**	(0.4)
Ammonium[g]	µM	**98** (2)	99 (2)	**100** (1)	103 (1)	**102**	103	**98**	111	861	**<0.05**	-
Sulfate[d]	mM	**18.2** (0.1)	18.2 (0.1)	**18.3** (0.3)	18.0 (0.6)	**17.2**	17.2	**18.7**	17.6	18.0	**28.4**	(0.3)
Chloride[d]	mM	**550** (2)	550 (11)	**557** (5)	557 (11)	**547**	547	**548**	548	567	**541**	(14)
Sodium[d]	mM	-	-	**471** (2)	471 (10)	**462**	462	**458**	457	475	**467**	(13)
Potassium[d]	mM	-	-	**6.4** (0.4)	6.3 (0.4)	**6.0**	6.0	**6.4**	6.0	7.1	**10.2**	(0.3)
Silicate[f]	µM	**1146** (5)	1152 (24)	**1137** (15)	1166 (15)	**1150**	1152	**1048**	1142	1189	**173**	(9)
Phosphate[f]	µM	**0.13** (0.04)	0.10 (0.04)	**0.14** (0.04)	0.06 (0.06)	**0.10**	0.10	**0.45**	0.2	-	**2.89**	(0.08)
Dissolved iron[b,f]	µM	**0.9** (0.3)	0.9 (0.3)	**0.6** (0.2)	0.6 (0.2)	**1.1**	1.1	**0.8**	0.8	4.1	**<0.1**	-

[a] Wheat et al. (2010); [b] inductively coupled plasma optical emission spectrometry; [c] titration; [d] ion chromatography; [e] high temperature combustion (Dickson et al., 2007); [f] colorimetry; [g] fluorescence (Jones, 1991).

Table 2.2. Methane and hydrogen concentrations of basement fluids.

		Mg (mM)	$Mg_{corr.}$ (mM)	$Mg_{corr.}$ CH_4 (μM)	$Mg_{corr.}$ H_2 (μM)
1301A	***2010***	34.8	1.9	1.8	0.5
		37.1		1.5	0.3
		39.0		1.4	0.2
			Average	***1.6***	***0.3***
			±	*0.2*	*0.2*
1301A	***2008***	50.1	1.9	1.4	1.9
		50.3		1.5	0.8
		48.6		2.0	0.6
		51.7		1.3	3.7
			Average	***1.5***	***2***
			±	*0.3*	*1*
1026B	***2008***	2.8	2.3	1.9	1.1
		2.9		2.0	0.4
			Average	***2.0***	***0.7***
			±	*0.1*	*0.5*
Seawater[a]		52.4		**0.0002**	**0.0004**

[a] Kelley et al. (1998)

Table 2.3. Estimated net DOC removal rates.

	Bottom seawater	1301A	1026B	Baby Bare	1025C
Fluid ^{14}C age (yr)	2285[a] ± 42	13008[a] ± 180	13008[a] ± 180	11893[a] ± 286	9926[b] ± 65
$Mg_{corr.}$ [DOC](μM)	39 ± 1	13 ± 4	14[c] ± 4	11[c] ± 3	22 ± 1
[DOC] net removal (nM/yr)	~ 3[d]	2.4 ± 0.7	2.4 ± 0.7	2.9 ± 0.7	2.2 ± 0.1

a. Fluid ^{14}C ages from Walker et al., 2008; the 1301A age is assume to be the same as 1026B.
b. Data from Elderfield et al., 1999.
c. Data from Lang et al., 2006.
d. Bottom seawater DOC removal rate from Hansell et al. 2009.

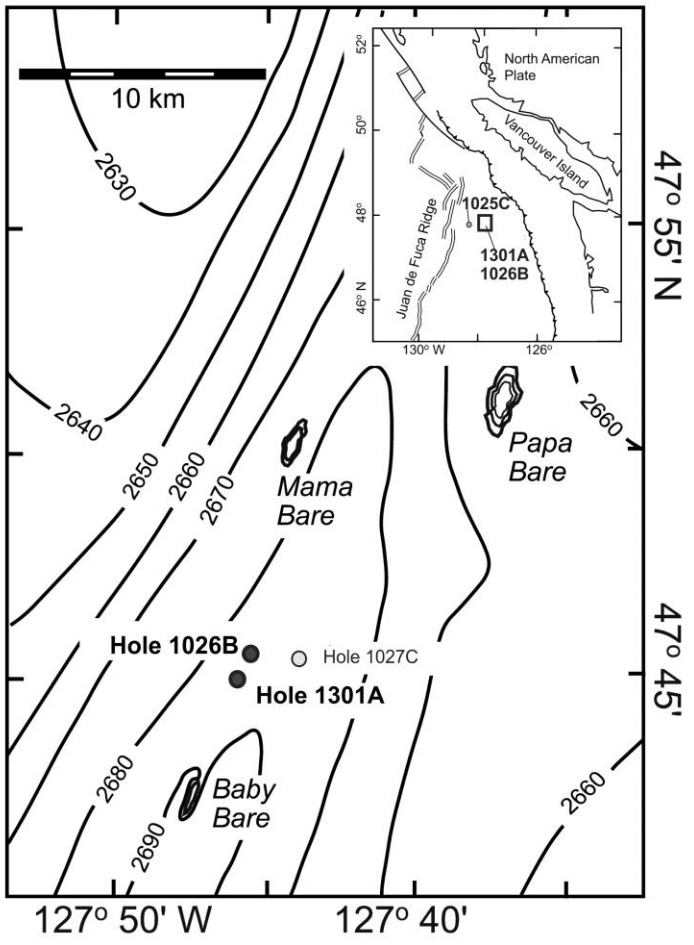

Fig. 2.1. Site Maps. Regional bathymetric map showing locations of borehole CORKs and outcrop seamounts. CORK 1026B is 1 km northeast and Baby Bare is 5 km southwest from CORK 1301A. The insert shows the location relative to the continents and CORK 1025C, which is 68 km to the west of CORK 1301A. Modified from (Becker and Fisher, 2008).

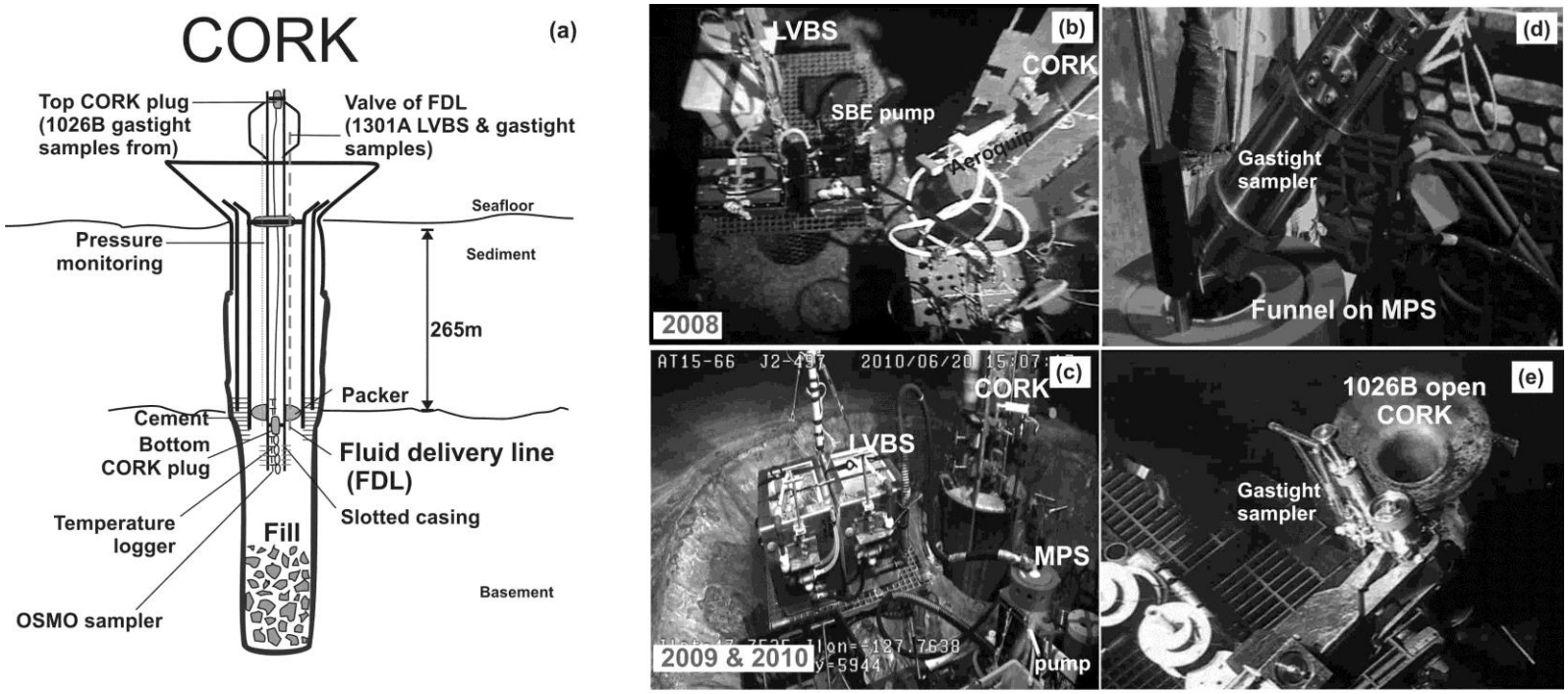

Fig. 2.2. Sampling methods. (a) Diagram showing the design of a new style CORK (1301A and 1026B). Note that the location of stainless steel fluid delivery line (FDL) is outside of the iron casing. The diagram is not drawn to scale. (b) Sampler used in 2008. A SeaBird pump was used to redirect the main flow drawn up by a Pelagic pump (not shown). (c) Sampler used in 2009 and 2010. The powerful & clean mobile pump sampler (MPS) and the large volume bag sampler (LVBS) are shown. CORK is also shown in the background. (d) Gas-Tight sampler was inserted into a funnel on the MPS. (e) Free flowing of warm basement fluid through 1026B open CORK; a Gas-Tight sampler ready to be inserted into the CORK for sampling is visible at bottom of panel.

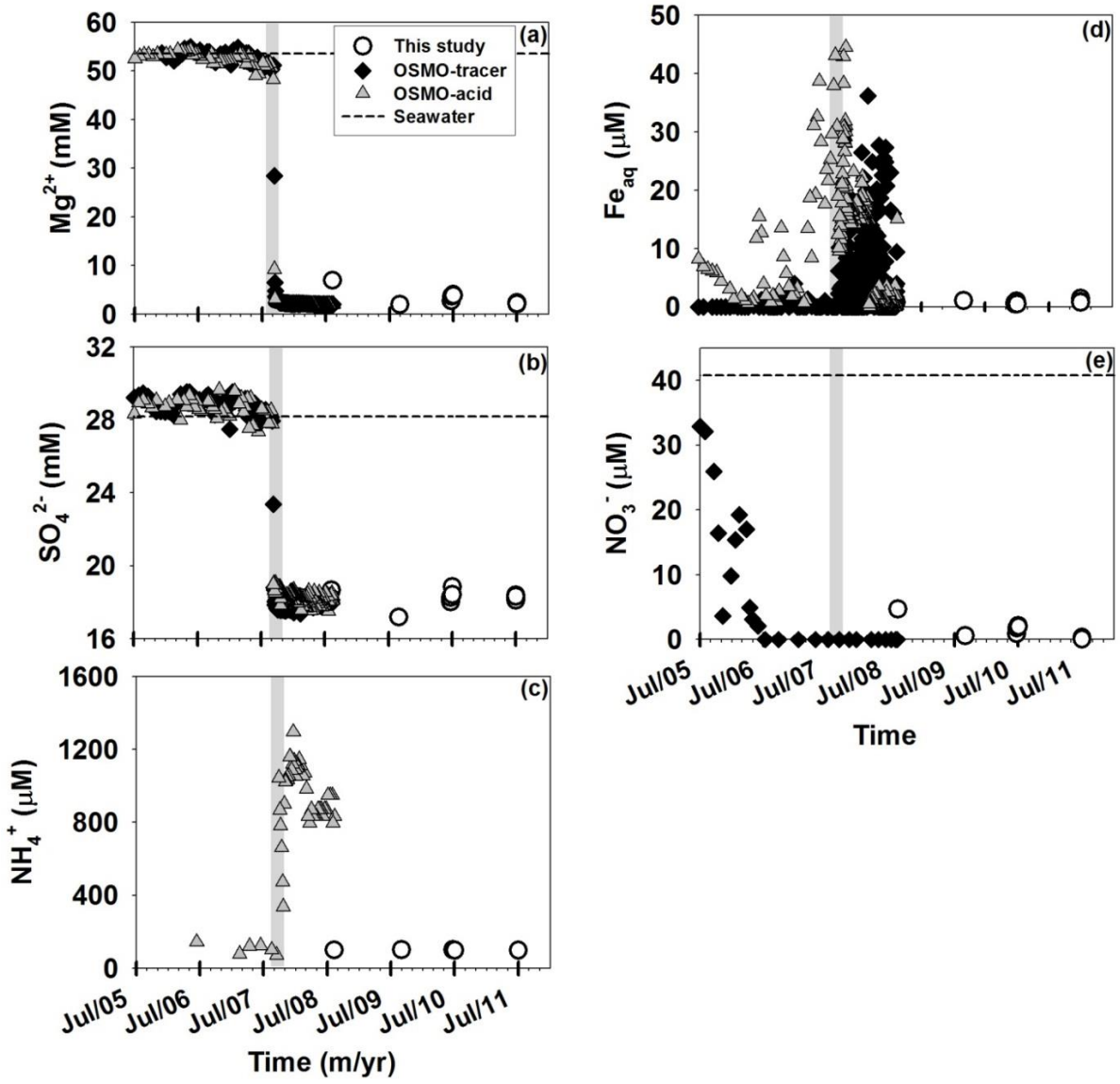

Fig. 2.3. Concentrations of (a) magnesium (b) sulfate (c) ammonium (d) total dissolved iron and (e) nitrate in CORK 1301A fluids collected over time. The gray bar indicates the time (~Sep, 2007) when borehole pressure conditions stabilized and started to return to overpressure condition (Wheat et al., 2010). Data from the current study, collected on 08/09/2008, 08/30/2009, 06/19~30/2010, 07/04/2011, are indicated by open circles. 'OSMO-tracer' samples, tagged in-situ with an unreactive chemical tracer (Wheat et al., 2010), are indicated by solid diamond, while 'OSMO-acid' (acidified in situ; Wheat et al., 2010) sample data are indicated by a triangle. OSMO sampler collected fluids between 9/2/2004 and 08/11/2008 (Wheat et al., 2010); data before 07/01/2005 were not plotted. Ammonium data were not reported for OSMO-tracer sampler while nitrate data were not reported for OSMO-acid sampler.

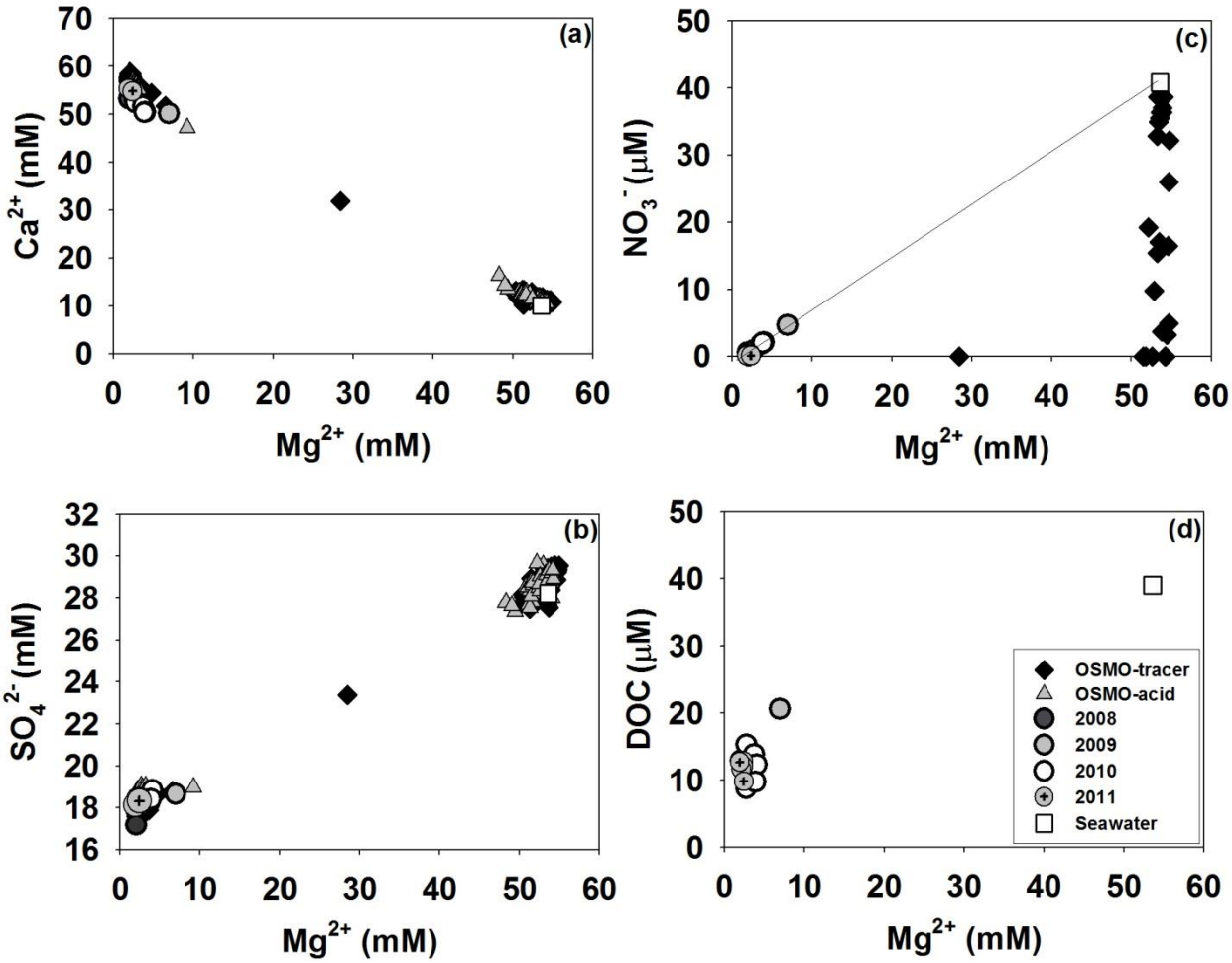

Fig. 2.4. Plots of concentrations of (a) calcium (b) sulfate (c) nitrate and (d) dissolved organic carbon (DOC) versus magnesium for 1301A basement fluid samples. Data from this study are indicated by the year of their collection: 2008, black-filled circle; 2009, grey-filled circle; 2010, open circle; 2011, circle with dot. Data from OSMO samples (Wheat et al., 2010) are plotted where data are available: OSMO-tracer, solid diamond; OSMO-acid, grey-filled triangle. The open square indicates average bottom seawater values.

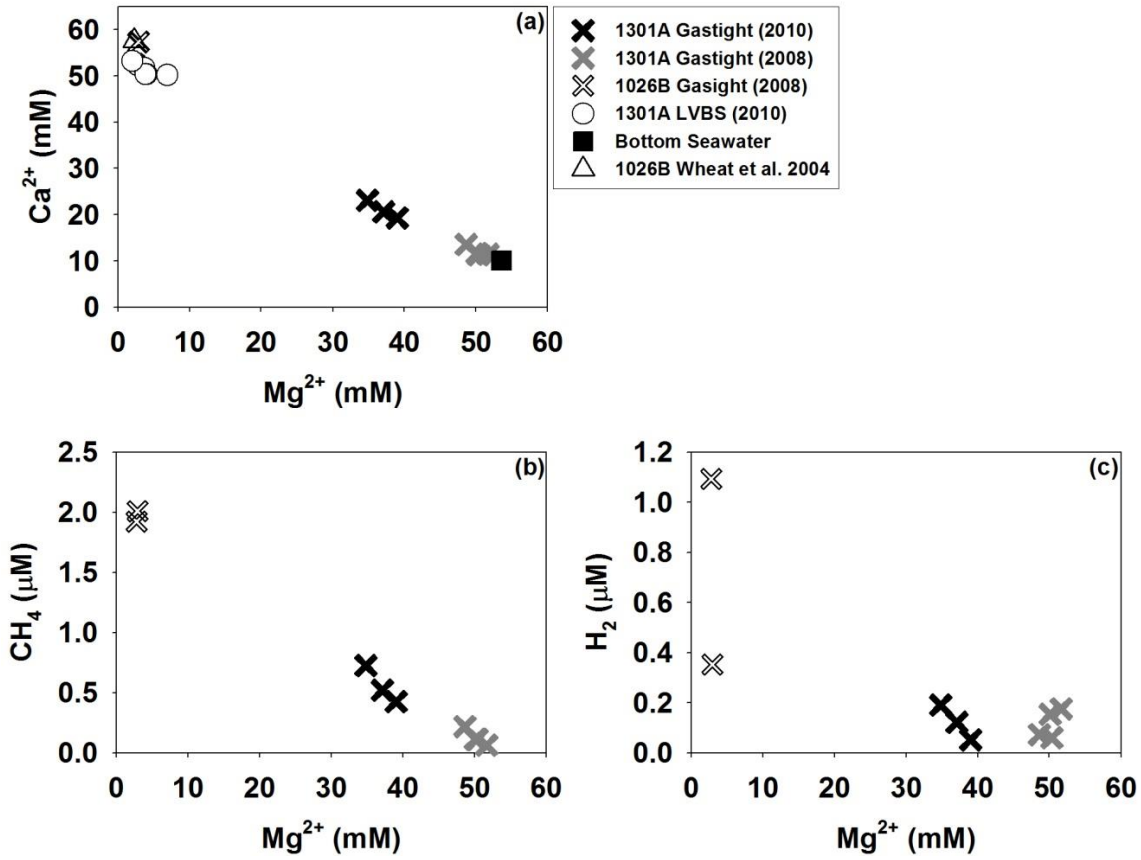

Fig. 2.5. Plots of uncorrected concentrations of (a) calcium (b) methane and (c) hydrogen versus magnesium in Gas-Tight samples of basement fluid from 1301A. The concentrations of Ca versus Mg for large volume bag samples (this study) are also plotted for comparison. Symbols represent data collected by GasTight samplers at 1301A in 2010 (black-filled X) and 2008 (grey-filled X), by GasTight sampler at 1026B in 2008 (unfilled X), and by LVBS at 1301A in 2010 (open circle). Calcium vs magnesium data are also shown for bottom seawater (filled square) and from OSMO data from 1026B (open triangle; Wheat et al., 2004a).

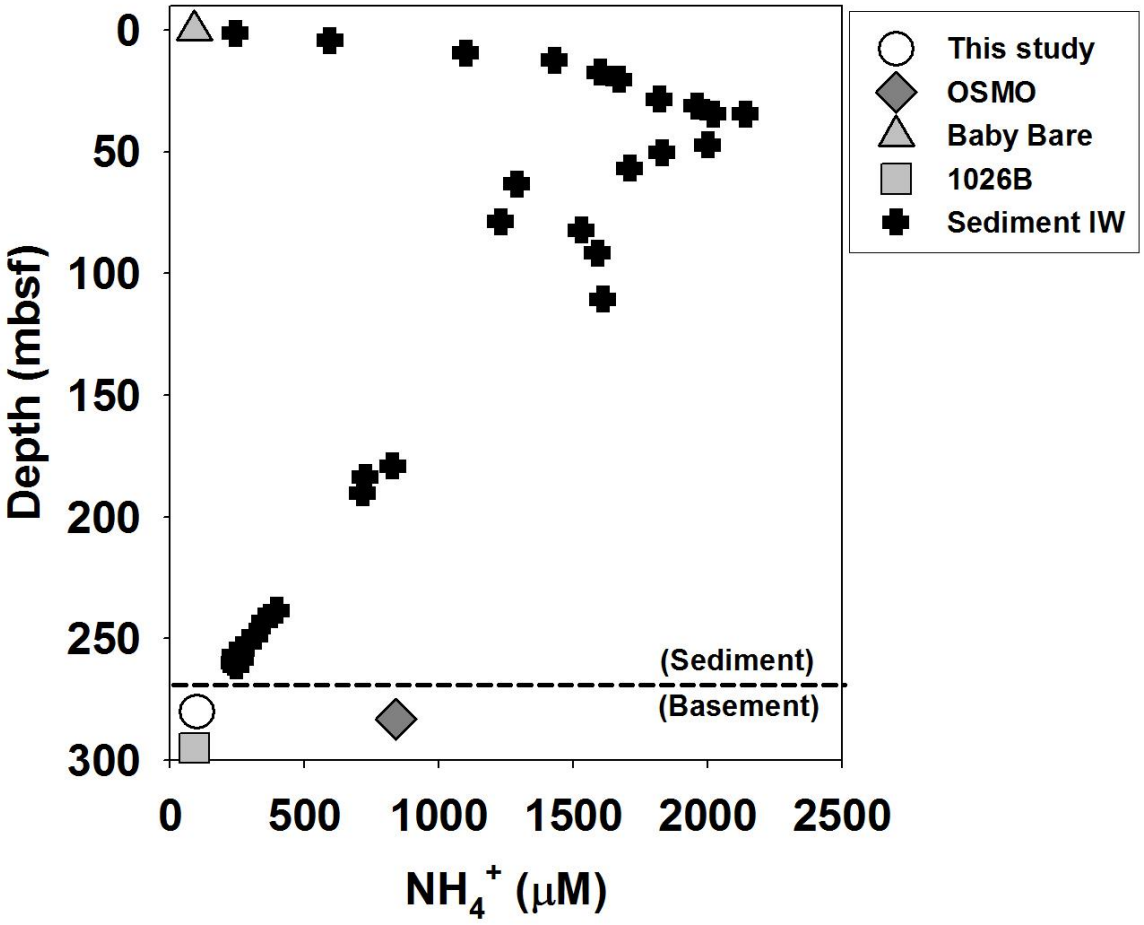

Fig. 2.6. Average ammonium concentrations for basement fluids from 1301A collected during this study (open circle) in comparison to 1026B data (Johnson et al., 2003) and OSMO sampler 1301A data (Wheat et al., 2010). Sediment interstitial waters (IW) for IODP site 1301A (Shipboard Scientific Party, 2004) and Baby Bare spring fluids (closed triangle; Johnson et al., 2003).

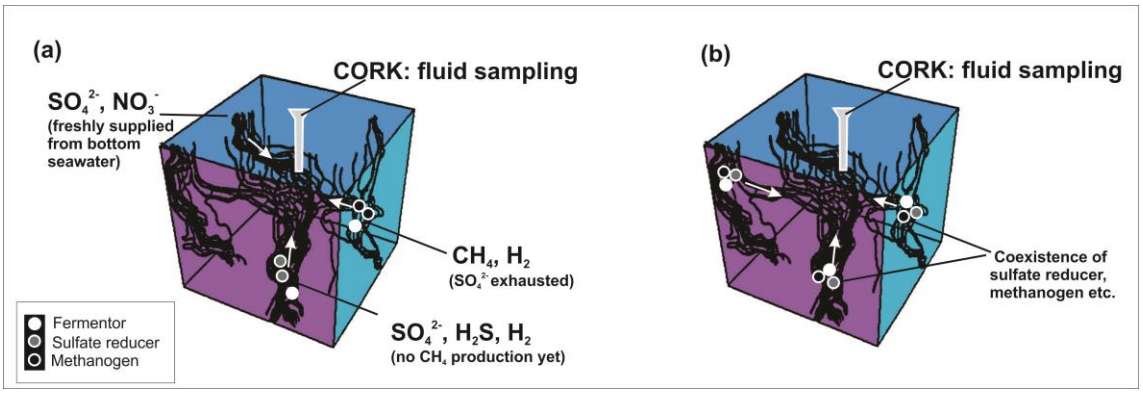

Fig. 2.7. Hypothesized scenarios to explain coexisting nitrate, sulfate, hydrogen sulfide, methane and hydrogen in fluid samples collected from 1301A. (a) Basement aquifer draws fluids from multiple flow paths with different redox histories. (b) Co-occurring metabolic processes such as sulfate reduction, methanogenesis, fermentation etc. within the aquifer. Figures modified from (Fisher, 2004).

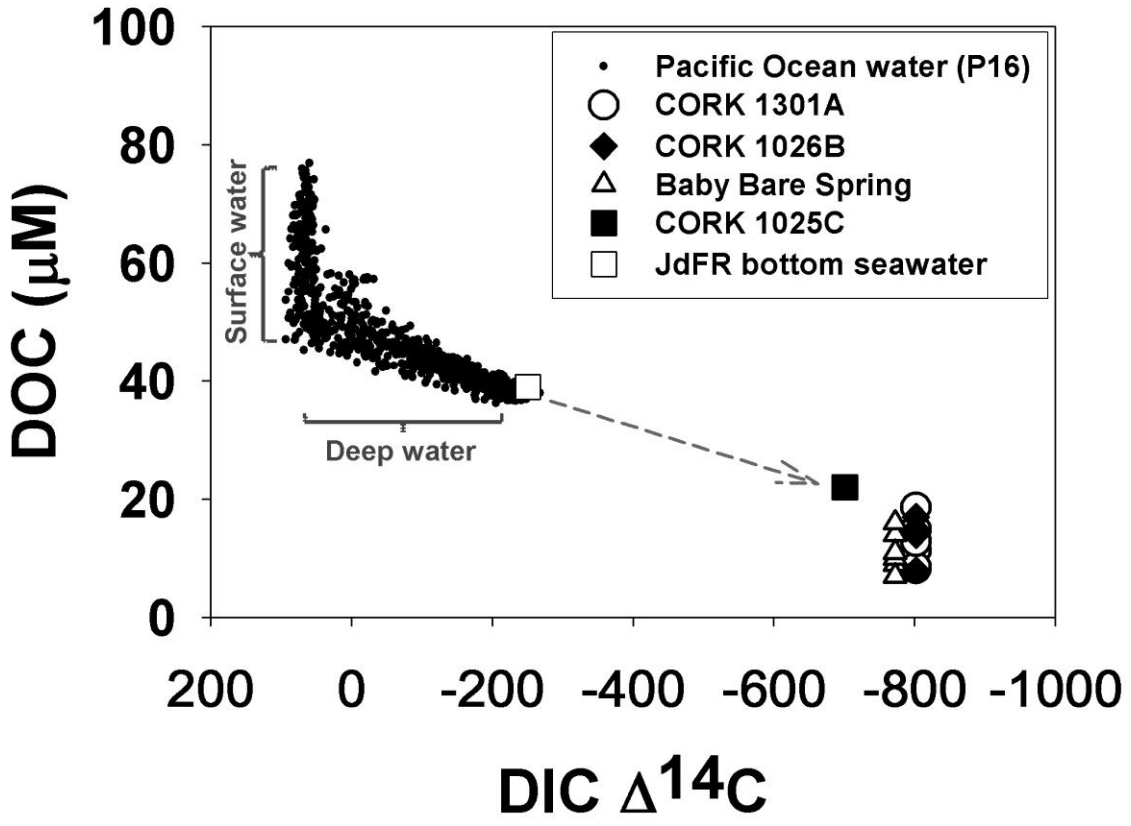

Fig. 2.8. Plot of concentrations of DOC versus Δ^{14}C-DIC, modified from Hansell et al., (2009). The Pacific Ocean water column data is along CLIVAR line P16 (Hansell et al., 2009). DOC concentrations for basement fluids collected from CORKs 1301A (open circles) and 1025C (closed squares), and for bottom seawater near 1301A (open square), are from this study. DOC concentrations for 1026B (closed diamonds) and Baby Bare (open triangle) fluids are from Lang et al., (2006). Δ^{14}C data for 1026B and Baby Bare are from Walker et al., (2008) and 1025C from (Elderfield et al., 1999). We assume 1301A has same Δ^{14}C as 1026B.

CHAPTER 3

Biogeochemistry of dissolved methane and hydrogen within basement fluids of the sediment-buried Juan de Fuca Ridge flank at CORK-fitted borehole 1362A, 1362B and 1301A

By

Huei-Ting Lin

James P. Cowen, Eric J. Olson, Marvin D. Lilley, Sean Jungbluth, Mike Rappe, Sam Wilson (coauthors)

Manuscript prepared for submission to Geochimica et Cosmochimica Acta

3.0. ABSTRACT

The ocean crust is the largest aquifer system on Earth. Within the sediment-buried 3.5 Myr basaltic crust of the eastern Juan de Fuca Ridge (JFR) flank, the circulating basement fluids have moderate temperature (~65°C) and potentially harbor a substantial subseafloor biosphere. With dissolved oxygen and nitrate exhausted, sulfate may serve as the major electron acceptor in this environment. This study aims to evaluate the availability and the biogeochemistry of two important electron donors, methane and hydrogen, for the subseafloor biosphere.

Basement fluids were collected via stainless steel and ethylene-tetrafluoroethylene fluoropolymer (ETFE or Tefzel^{TM}) fluid delivery lines associated with Integrated Ocean Drilling Program (IODP) Circulation Obviation Retrofit Kits (CORKs) that extend from basement depths to outlet ports at the seafloor. Three CORKs were visited; 1301A, 1362A and 1362B lie within 200 to 500 m of each other, and their fluid intakes lie at ~30, ~60, and ~50 m below the sediment-basement interface (mbs), respectively. In addition, CORK 1362A contains a second intake at a deep (~200 mbs) horizon.

The basement fluids from the three CORKs contained significantly higher concentrations of methane (1.5-13 μM) and hydrogen (0.05-1.1 μM) than in bottom seawater (0.002 and 0.0004 μM, respectively), indicating that prevalence and availability of both methane and hydrogen as electron donors for the subseafloor biosphere. Thermodynamic calculations show that sulfate reduction coupled with either methane or hydrogen oxidation is energy yielding in the oceanic basement. The $\delta^{13}C$ values of methane ranged from -43±1‰ to -58±0.3‰; this isotopic composition suggests that it is of biogenic origin in the basement

fluid. Interestingly, the δ^2H values of methane in CORKs 1301A, 1362A and 1362B fluids were 57±5‰, -262±2‰, -209±2‰, respectively. The δ^2H value of methane in the CORK 1301A fluids is much more positive than found in all other marine environments investigated to date. This is best explained by partial microbial oxidation of biogenic methane, which has an initial isotopic composition similar to that of methane from CORK 1362A and 1362B borehole fluid. High-throughput sequencing of the small subunit ribosomal RNA gene indicates the presence of methanogenic *Euryarchaeota* (e.g. *Methanobacteria*) in each of the borehole fluid samples described here. On average, fluid samples from boreholes 1362A and 1362B possessed a relatively higher abundance of known methanogens compared to borehole 1301A. Methane-oxidizing bacterial lineages from the phyla *Proteobacteria* and *Verrucomicrobia* were also detected; however, these groups were less abundant relative to the putative methane-producing groups. In conclusion, our study shows that methane and hydrogen are available electron donors and that methane is produced and potentially consumed by microorganisms in the oceanic basement. The data presented will guide incubation experiments using basement fluid in order to better understand the methane production and utilization processes within the oceanic basement.

3.1 Introduction

The upper (40-500 m) ocean crustal aquifer holds an amount of seawater-derived fluid equal to about 2% of the ocean volume, and thus represents the largest aquifer on earth (Johnson and Pruis, 2003). Heat flow data indicate that thermally driven circulation of seawater persists within the upper basement to a global average age of at least 65 My (Parsons and Sclater, 1977).

Basement fluids are recharged primarily by bottom seawater that penetrates the highly permeable basement at mid-ocean ridges and through thinly sedimented young ridge flanks and unsedimented rocky seamounts. Most of the flow occurs through ridge flanks at relatively low temperature (Shipboard Scientific Party, 2010). Johnson and Pruis (2003) estimated that the total hydrothermal fluid flux from the oceanic crust into the ocean is about 20% of global riverine input; Mottl (2003) and Wheat et al. (2003) estimated the hydrothermal flux from ridge flanks (crustal age older than 1 My) alone to be 5-60% of riverine input. Direct observations of hydrothermal discharge have been made at seamounts on the eastern flanks of the Juan de Fuca Ridge (Mottl et al., 1998; Wheat et al., 2000).

The circulating fluids within the ocean crust provide a suitable environment for microbial life. Evidence from the alteration of basaltic glass and rocks, including their texture and chemical and isotopic compositions, suggest a subseafloor biosphere within the ridge flank basement (Giovannoni et al., 1996; Fisk et al., 1998; Torsvik et al., 1998; Furnes et al., 2001a; Furnes et al., 2001b; Furnes et al., 2002; Bach and Edwards, 2003; Furnes et al., 2006; Rouxel et al., 2008; Alford et al., 2011; Alt and Shanks, 2011). Geochemical

and microbial data derived from the analyses of ridge flank crustal fluids also indicate that conditions there are suitable for some level of microbial activity (Cowen et al., 2003; Huber et al., 2006; Orcutt et al., 2011; Lin et al., 2012; Boettger et al., 2013; Jungbluth et al., 2013). The deep subseafloor ocean crust also plays an important role in regulating global biogeochemical cycles, such as the removal of magnesium (Mottl, 2003), phosphate (Wheat et al., 1996) and dissolved organic carbon (Lang et al., 2006; Lin et al., 2012).

Despite the immense volume of the ocean crustal aquifer, access to ocean basement fluids for study and sampling is limited. Unprecedented opportunities to collect basement fluids from sediment-covered ridge flanks are provided by Circulation Obviation Retrofit Kit (CORK) observatories (Becker and Davis, 2005). A cluster of CORKs have been installed in selected Ocean Drilling Program (ODP) and Integrated Ocean Drilling Program (IODP) boreholes on the eastern flanks of the Juan de Fuca Ridge, which penetrate through the sediment and into basement (Fig. 3.1) and thus allow the monitoring/testing of hydrogeological parameters and basement fluid sampling for geochemical and biological studies.

Hydrogen is an important energy source for a diverse group of microorganisms, including methanogens, sulfate reducers and iron reducers (e.g. Amend and Shock, 2001; Kashefi et al., 2002; Takai et al., 2002; Joye et al., 2009). Similarly, methane is an important energy and carbon source for a wide variety of methanotrophs (e.g. Balch et al., 1979; Knittel and Boetius, 2009; Merkel et al., 2013). Whether the ridge flank basement environment contains available hydrogen and/or methane for subseafloor microorganisms, and whether the basement environment is a source or a sink for hydrogen and/or methane,

has not been widely investigated. Significant methane production via anaerobic organic matter degradation is thought to occur after sulfate is exhausted (<1 mM, versus seawater concentration of ~28mM) and is widely observed in organic-rich coastal and continental margin marine sediments (e.g. Barnes and Goldberg, 1976; Claypool and Kvenvolden, 1983; Crill and Martens, 1986; Hoehler et al., 1994; Hoehler et al., 1998; D'Hondt et al., 2002). In contrast to organic-rich marine sediments, the 3.5 Ma old basaltic basement of our study sites on the Juan de Fuca Ridge flanks is a relatively organic-poor but sulfate-rich environment, with a total dissolved organic carbon concentration of about 14 μM and a sulfate concentration of about 18mM (Lin et al., 2012). Despite low organic carbon and abundant sulfate, small amounts of methane and hydrogen (1.5 μM and 1.1 μM, respectively) have been observed in this environment (Lin et al., 2012). In this study, we present new methane and hydrogen concentrations in basement fluids collected from two new sites, and the carbon and hydrogen isotopic compositions of methane to help understand the methane and hydrogen biogeochemistry in the ridge flank basement environment, and we discuss their implications for fluid circulation.

Background

Geological and hydrological settings

Most of the eastern flank of the Juan de Fuca Ridge is covered by hemipelagic mud and turbidite sediment transported from the nearby continental margin during the Pleistocene, resulting in rapid burial of basement rocks at a relatively young age (Davis et al., 1992; Underwood et al., 2005). Sediment is ~250m thick overlying the ~3.5 Ma basement at our study sites on the eastern flank of the Juan de Fuca Ridge (Fig. 3.1). The thick

sediment layer acts as a hydraulic seal, preventing direct exchange between bottom seawater and the basement (Davis et al., 1992; Wheat and Mottl, 1994; Shipboard Scientific Party, 1997b, a; Becker and Fisher, 2008). Direct exchange with bottom seawater is only available through seamounts and smaller basement outcrops protruding through the sediments to the north (Mama Bare) and south (Baby Bare and Grizzly Bare) of our study site (Fig.3.1). Heat flow (Fisher and Becker, 2000; Fisher et al., 2003; Hutnak et al., 2006) and geochemical and isotopic data (Wheat et al., 2000; Walker et al., 2008; Orcutt et al., 2010) around these seamounts and outcrops suggest a significant component of south-to-north fluid flow within the ~3.5 Ma basement.

This study utilizes three CORK observatories installed in boreholes drilled through overlying sediments into ~3.5 Ma basement on the eastern Juan de Fuca Ridge flank. Borehole 1301A was drilled and equipped with a CORK during IODP Expedition 301 in 2004 (Shipboard Scientific Party, 2004). Two new boreholes (1362A and 1362B, Fig. 3.1a & b) were drilled and had advanced CORKs installed during the IODP Expedition 327 in 2010 (Shipboard Scientific Party, 2010). The boreholes were positioned along the hypothesized basement fluid flow path, from the recharge seamount Grizzly Bare in the southwest toward the discharge outcrop Baby Bare in the northeast. CORK 1362B is located ~550 m north-northwest of CORK 1301A; CORK 1362A is ~331 m further NNW of 1362B (Fig. 3.1c). The three CORKs penetrate to different depth within the basaltic basement, permitting fluid circulation to be monitored at different crustal depths. The fluid intake is ~30 m below sediment-basement interface (mbs) at CORK 1301A, 200 mbs at CORK 1362A and ~50 mbs at CORK 1362B (Fig. 3.1c).

3.2 Methods

3.2.1. Sampling methods

Basement fluids were collected via fluid delivery lines (FDL, Fig. 3.2) that run exterior to the CORK's iron casing from basement depths to the seafloor outlet port. The FDL of CORK 1301Aconsists of stainless steel whereas the FDLs of CORKs 1362A and 1362B consist of ethylene-tetrafluoroethylene fluoropolymer (ETFE or Tefzel^{TM}) tubing. The seafloor outlet port of CORK 1301A is equipped with a male-part of an Aeroquip connector (Fig. 3.2f) whereas the seafloor outlet port of CORK 1361A and 1362B is equipped with a male-part of a 'Jannasch'-connector (Fig. 3.2; Wheat et al., 2011).

For this study, a mobile pump system (MPS, Fig.3.2c) equipped with a female-part of an Aeroquip connector or of a Jannasch connector was used to pump the fluid up the lengthy FDLs. The MPS directed fluids into a hydrothermal-fluid-trap (Fig. 3.2c) attached to the MPS. The hydrothermal-fluid-trap was used as an intermediate fluid reservoir for a gastight sampler (Fig. 3.2d, Edmond et al., 1992) or a Ti-major (Fig. 3.2e) to sample from. Snorkels of a gastight sampler or a Ti-major sampler punctured through a self-seal septum on the hydrothermal-fluid-trap to prevent bottom seawater entrainment during sampling. The MPS also directed fluids into each of six 15L foil-lined, gamma irradiated medium volume bag samplers (MVBS) for biogeochemical analysis (Cowen et al., 2012; Lin et al., 2012) and for analysis of methane isotopic compositions.

As soon as samples were sent back shipboard, sample fluids collected by a Ti-major were quickly transferred into pre-evacuated and poisoned (with mercuric chloride) glass flasks for storage until the extraction of dissolved gases in the fluids. Aliquots of sample fluids

in foil-lined bags were gravity-fed into 160 mL serum bottles, over flown for at least 80 mL, preserved with saturated mercuric chloride (1 mL per 100 mL sample), and kept in dark until the analysis for isotopic compositions of dissolved methane.

3.2.2. H_2 production experiment

To investigate whether the differences in FDL materials (316-stainless steel and Tefzel^{TM}) may be a source of hydrogen, an incubation experiment was conducted. 1.5m-long 316-stainless steel wires were coiled to make a wire bundle (Fig. 3.3). Twenty 1.5m-long (30 m total) wire bundles, yielding 364.6 cm^2 surface area, were placed in each of several 300-mL Wheaton bottles providing a surface-to-volume ratio similar to what the basement fluid is subjected to during its ascent through a 6.35 mm outer diameter stainless steel fluid delivery line. Polyvinylidene fluoride (PVDF) strips (each 6.3mm×610mm long, Fig. 3.3) with a total surface area of 670 cm^2 served as a negative control. PVDF is chemically very similar to ETFE used for selected CORK 1362A and 1362B FDLs. All of these materials and 0.2 μm filtered surface seawater from station ALOHA, 22°45'N, 158°W (Karl et al., 1996) were autoclaved at 121°C and 2 bar for 30 minutes. The autoclaved seawater was then purged with helium for 30 minutes to remove oxygen (Wilson et al., 2012). This deoxygenated seawater was transferred under positive pressure into the 300-mL Wheaton bottlesbottle filled with either stainless steel wire or PVDF strips. The samples were incubated in a shaking water bath for 2 hours at 45°C, an intermediate temperature between the basement fluid at our study sites (65°C) and our sampling temperature at the seafloor (~10°C).

To measure the dissolved hydrogen concentrations, a headspace analysis method was used to extract the hydrogen from the incubated deoxygenated seawater (Wilson et al., 2012).The incubated fluids were drawn into a 50-mL glass gas-tight syringe that had been rinsed at least twice with sample fluids. Thirty mL of sample were drawn and 10mL of air added to create a headspace. Hydrogen was then extracted from the water sample into the headspace by shaking the syringe vigorously for 3 minutes. The headspace was subsequently injected into a hydrogen analyzer described below.

3.2.3. Analytical methods

a. Gas concentrations

i. Gastight & Ti-major samples

Methane and hydrogen concentrations in basement fluid samples collected using gastight and Ti-major samplers were analyzed by gas chromatography. Gases were separated with either Hayesep A or Hayesep Q porous polymer columns (5.5-7.3m ×3.175mm). The temperature gradient started at -50 °C and ramped up to 120 °C. Quantitative injections of various commercially prepared mixed gas standards were used to calibrate. Analytical accuracy was ~5% for both gases. Reproducibility was better than 5% of the measured values in replicate samples for both gases.

ii. 316 stainless steel H_2 production experiment

H_2 was quantified with a reduced gas analyzer that couples a mercuric oxide (HgO) bed to a reducing compound photometer (Peak Laboratories, USA). The stoichiometric reduction of HgO by H_2 gas releases mercury vapor which is quantified using an ultraviolet absorption photometer located immediately downstream of the HgO

bed. Prior to the detector, the carrier gas (Ultra High Purity air) passes through two analytical columns maintained at 104 °C. The first column is packed with Unibeads 1S (60/80 mesh, 0.32 cm diameter and 41.9 cm length), and the second column with Molecular Sieve 13X (60/80 mesh, 0.32 cm diameter and 206 cm length). Analytical precision was ±2% estimated by analyzing air (H_2=~0.3 nmol l^{-1}) four times. The analyzer was calibrated using a 1 ppmv H_2 standard (Scott Marrin) that was diluted up to 100-fold using zero-H_2 air. The concentration of dissolved H_2 in equilibrium with seawater at the temperature during the analysiswas calculated using the Bunsen solubility coefficients of Wiesenburg and Guinasso (1979). The temperature of the equilibrated seawater sample was measured following injection of the headspace using a digital thermometer (Fluke) and inserting a thermocouple through the injection syringe tip.

b. Isotopic compositions of CH_4

The isotope data are reported as δ values (e.g. $\delta^{13}C$, $\delta^{2}H$) expressed in permil (‰):

$$\delta = \left(\frac{R_{sample}}{R_{standard}} - 1\right) \times 1000‰$$

where R is the $^{13}C/^{12}C$ or $^{2}H/^{1}H$ ratios. The standards for carbon and hydrogen isotopic composition are PDB (Craig, 1957) and SMOW (Craig, 1961), respectively.

i. Carbon isotopic composition of CH_4 in samples collected in 2010

The carbon isotopic compositions of CH_4 in samples collected in 2010 were analyzed at the Biogeochemical Stable Isotope Facility at the University of Hawaii at Manoa. Gas components within the fluid samples were separated with a Varian CP-PorabondQ column (25m ×0.32mm). Temperature was held at 10°C and then forced through a

furnace at 1050°C in the presence of nickel oxide to convert methane into carbon dioxide. The resulting CO_2 was then introduced into an isotope gas ratio mass spectrometer for isotopic analysis (Finnigan MAT252). A CO_2 tank with known carbon isotopic composition, characterized using international reference materials, was used to normalize the isotopic measurements to the PDB standard. The reproducibility of four replicates (including subsampling uncertainties) is about ± 2 ‰.

ii. *Carbon and hydrogen isotopic compositions of methane in samples collected in 2011*

The carbon and hydrogen isotopic compositions of CH_4 in samples collected in 2011 were analyzed at the Stable Isotope Facility at the University of California Davis. Methane dissolved in the basement fluid samples were first extracted from the 160mL serum bottles with high purity helium and transferred to pre-evacuated exetainers. The CH_4 was separated by Rt-Q-BOND GC column (30 m × 0.32 mm) at 30 °C. After CH_4 elutes from the separation column, CH_4 was oxidized to CO_2 by reaction with nickel oxide at 1000°C or was pyrolyzed in an empty alumina tube heated to 1350 °C to H_2. The resulting CO_2 or H_2 is transferred to a Thermo Scientific GasBench-PreCon trace gas system interfaced to a Delta V Plus isotope ratio mass spectrometer for isotopic analysis. A pure CO_2 or H_2 reference gas was used to calculate provisional δ value of the sample peak. Laboratory standards, commercially prepared CH_4 gas diluted in helium or air calibrated against standards provided by National Institute of Standards and Technology (NIST 8559, 8560 and 8561), are used to correct for changes in linearity of calibration curves and instrumental drift. The long-term standard analytical precision is 0.2‰ for $\delta^{13}C\text{-}CH_4$ and 2‰ for $\delta^{2}H\text{-}CH_4$.

3.2.4. Basement fluid end-member correction

All of the measured values were corrected for bottom seawater entrainment into gastights and Ti-majors during seafloor sampling. The degree of seawater entrainment depends on the flow rate out of the access ports, the sampling rate of the Gas-Tight and Ti-major samplers and how deeply the sampler snorkel is inserted into the port (Cowen et al., 2012). The entrained seawater component is subtracted from the measurement of each sample to obtain the endmember (true) basement fluid composition (Mottl et al., 1998; Wheat and Mottl, 2000) using a two end-member mixing model (Libes, 2009) and the endmember represented by the lowest Mg concentration measured under optimal sampling conditions for a particular basement environment (Lin et al., 2012).

3.2.1. Thermodynamic calculation

The amount of energy released or required from a chemical reaction can be expressed as Gibbs free energy of reaction (ΔG_r), calculated as:

$$\Delta G_r = \Delta G_r^\circ + RT \ln Q_r, \qquad (1)$$

where ΔG_r° is the standard state Gibbs energy of reaction at the temperature and pressure of interest, R is the gas constant, and T is the temperature in ºKelvin. Q_r is the reaction quotient and can be calculated as:

$$Q = \Pi\left(a_i^{v_{i,r}}\right), \qquad (2)$$

where a_i denotes the activity of chemical species i, and $v_{i,r}$ is its stoichiometric coefficient in reaction r, which is negative for reactants and positive for products. The activity is

computed using the concentrations of the species (Table 3.1) and their individual ion activity coefficients at in situ temperatures. Values of $\Delta G_r°$ at in situ temperature (65°C) and pressure (270 bar) were computed using the SUPCRT 92 software package (Johnson et al., 1992). Metabolic reactions are evaluated, including formate and acetate; hydrogenotrophic methanogenesis; hydrogenotrophic sulfate reduction; hydrogenotrophic iron reduction; and anaerobic methane oxidation coupled with sulfate reduction. The reactions are listed in Table 3.2. Since formate and acetate concentrations in CORK 1301A fluids are below the limits of detection (0.1 μM), a wide range of estimated concentrations (0.0005 to 0.1 μM) are used for the thermodynamic calculation.

3.2.2. Microbial Phylogenetic Classification

Details of the sample collection, DNA extraction, polymerase chain reaction, gene cloning and sequencing, and phylogenetic methods used have been described elsewhere (Jungbluth et al., 2013). Environmental DNA was extracted from samples using either commercial nucleic acid extraction kits (MO BIO Laboratories, Carlsbad, CA) or using an implementation of the phenol:chloroform extraction protocol (Chomczynski and Sacchi, 2006). Small subunit ribosomal RNA (SSU rRNA) gene fragments were amplified via the polymerase chain reaction (PCR, Saiki et al., 1988) using the universal oligonucleotide forward and reverse primers 519F (5'-CAGCMGCCGCGGTAATWC-3') and 1406R (5'-ACGGGCGGTGTGTRC-3'), respectively. Amplification products of the anticipated length were cloned using commonly-employed commercial cloning kits and clones were sequenced unidirectionally using classical sequencing techniques (Sanger et al., 1977). For purposes of phylogenetic classification, DNA sequences were aligned with

SILVA database version SSURef_106 (Prusse et al., 2011) using the ARB software package (Ludwig et al., 2004).

3.3 Results

3.3.1 Magnesium concentration

Magnesium concentrations of sample fluids collected by Ti-major samplers from CORK 1362A range from 2.5 to 3.2 mM (Fig. 3.4). The lowest Mg concentration measured from the samples for gas analysis is identical to the lowest Mg concentration measured from foil-bag samples collected at about the same time (Table 3.1). The lowest Mg value (2.5 mM) is used as the CORK 1362A basement fluid end-member for endmember corrections to account for any bottom seawater entrained during seafloor sampling (Lin et al. 2012).

Magnesium concentrations in fluid samples collected with gastight and Ti-major samplers from CORK 1362B are 2.3-3.3 mM (Fig. 3.4), slightly higher than the lowest Mg (1.6 mM) measured in fluids collected from this site with MVBS (Table 3.1). The 1.6 mM value is used as the CORK 1362B's Mg-end-member. The high Mg in 1301A gastight samples collected in previous years (2008 and 2010, Fig. 3.4) indicates that more than 60% seawater was entrained into the sampler during seafloor sampling (Lin et al. 2012). The low percentage of seawater entrained into 1362A and 1362B fluid samples for dissolved gas analysis demonstrates the significant improvements in the hydrothermal-fluid-trap (Fig. 3.2c), MPS (Cowen et al., 2012) and the 'Jannasch'-connector (Wheat et al., 2011) used to collect samples.

3.3.2 Hydrogen and methane concentrations in basement fluids

The Mg-corrected hydrogen concentrations in fluids from CORK 1362A (0.05±0.02 μM, n=6, Table 3.1) are similar to those in CORK 1362B (0.08±0.03 μM, n=3), but the small difference is still statistically significant (t-test, p=0.05). Hydrogen concentrations in both 1362A and 1362B are significantly lower than those in CORK 1301A (0.3-2 μM, n=7; t-test, p=0.05 and p=0.05, respectively). Significantly higher methane concentrations (13±1 μM, n=4) are observed in CORK 1362B fluids than in CORK 1362A fluids (6.2±0.4 μM, n=6, t-test, p=0.001); methane concentrations in fluids from both 1362B and 1362A are significantly higher than in CORK 1301A fluids (1.5±0.2 μM, n=7; t-test, p=0.001 and p=0.001, respectively). The methane and hydrogen concentrations in basement fluids from the three CORK sites are at least two orders of magnitude higher than what are observed in bottom seawater (Kelley et al., 1998).

3.3.3 Carbon and hydrogen isotopic compositions of methane

The methane carbon isotopic compositions of methane in basement fluids are -56.5‰, -58.3 ‰ and -42.8‰ at site 1362B, 1362A and 1301A, respectively (Table 3.1). The hydrogen isotopic compositions of methane are -209‰, -262‰ and 57‰ at 1362B, 1362A and 1301A, respectively.

3.3.4 Stainless steel H_2 production experiment

Over two hours of incubation time, hydrogen concentrations in the low nanomolar-range were produced in both stainless-steel amended and PVDF amended deoxygenated seawater (0.0025±0.0002 μM and 0.0047 ±0.0022 μM, n=3, respectively). The concentrations of hydrogen produced in the bottle experiment were, however, small

compared with those observed in the stainless steel FDL-CORK 1301A fluids (0.2-3.7 μM).

3.3.5 Thermodynamic calculations

Fermentation using formate and acetate to form hydrogen (Table 3.2) yields negative or positive Gibbs free energy within CORK 1301A fluids depending on the formate and acetate concentrations (Fig. 3.5); higher concentrations favor the fermentation reaction.

The value of Gibbs free energy for hydrogenotrophic methanogenesis is positive at site 1362A and 1362B (2.7 and 2.3 KJ/mol e^-, respectively, Table 3.2), but negative at site 1301A (-2.3 KJ/mol e^-). The calculated values of Gibbs free energy for hydrogenotrophic sulfate reduction, hydrogenotrophic iron reduction and anaerobic methane oxidation for 1362A, 1362B and 1301A are all negative and range from -2.7 to -11.3 KJ/mol e^-.

3.4 Discussion

3.4.1. Sample quality

The Mg concentrations of basement fluids collected using MVBS from site 1301A, 1362A and 1362B are very low, indicating good sample quality in respect to low/minimum bottom seawater entrianment (Lin et al., 2012). The low Mg concentrations of the fluid samples collected with Ti-majors at 1362A indicate that fluids contain 99-100% basement fluid (less than 1% seawater). The slightly higher Mg concentrations of fluid samples collected with gastights and Ti-mjors at 1362B indicate that 97-99% fluids are basement fluids (less than 3% seawater).

3.4.2. Potential sources of hydrogen and methane

Potential hydrogen sources

A few to tens of micromolar hydrogen are present in the basaltic fluids collected from all study sites. Although substantially lower than H_2 values found in fluids discharged from high temperature hydrothermal vents (0.04-1.7mM; summarized in Amend et al., 2011), these basement fluid concentrations are significantly greater than typical background seawater concentrations (0.0004 μM). Abiotic production of H_2 at neutral pH and warm temperature (60°C) from basalt reactions in aqueous solutions has been observed in lab experiments (Stevens and McKinley, 2000). Generalized behavior of Fe during serpentinization, expressed as (McCollom and Bach, 2009):

$$2(FeO)_{rock} + H_2O \rightarrow (Fe_2O_3)_{rock} + H_2 \qquad (3)$$

is the primary mechanism that produces high concentrations of hydrogen in mafic and ultramafic rock-hosted aquifers (12-16mM, Charlou et al., 2002; Kelley et al., 2005). High contents of ferrous iron minerals, such as olivine and pyroxene, and low silica activity (McCollom and Bach, 2009) are responsible for generating high concentrations of hydrogen in mafic rocks. Although basalts contain much lower contents of olivine and pyroxene than do peridotites, micromolar levels of hydrogen were observed in the Columbia River Basalt group (Stevens and McKinley, 1995, 2000), which are similar to or higher than the concentrations observed in the subseafloor basement fluids. Laboratory experiments demonstrate that common ferrous silicate minerals, such as olivine found in basalt, although are low in abundance, promote H_2 production through anaerobic water-rock reaction (Stevens and McKinley, 2000). Basalt-water reaction is likely a key mechanism of hydrogen production in the basement fluids collected in this study.

Fermentation, an organic carbon disproportionating reaction, is another important mechanism of hydrogen production in terrestrial groundwater settings and in marine sediments (e.g. Lovley and Goodwin, 1988; Boone et al., 1989; Lovley et al., 1994). The concentration of dissolved organic carbon in the subseafloor basement fluids (~12μM, Lin et al., 2012) is much lower than in sediment porewater. Formate and acetate are organic substrates with the potential to produce hydrogen in the basement environment. Results from thermodynamic calculations of formate and acetate fermentation reactions show that the concentrations of formate and acetate in the basement fluids from CORK 1301A need to be greater than 26 nM and 0.5 nM, respectively, for the reactions to proceed in the direction written (Fig. 3.5). Even for formate and acetate concentrations near the detection limit (0.1 μM), formation of hydrogen via formate and acetate fermentation would be favorable within the basement at 1301A. Without more sensitive analyses for formate and acetate, it remains inconclusive whether organic fermentation is a likely source of hydrogen in the organic-carbon-scarce fluids circulating within this 3.5 Ma old crust. In addition, if fermentation does take place in the basement environment, the concentrations of hydrogen that could be produced via microbial fermentation would likely be in the range of 0.05 to ~10nM (Stevens and McKinley, 1995), one to two orders of magnitude lower than what were observed at the subseafloor basement fluids at the three CORKs.

The hydrogen concentrations in CORK 1301A basement fluids are twenty-two and fourteen times higher than those in CORK 1362B and 1362A fluids, respectively. The much higher hydrogen concentrations in CORK 1301A fluids raise the concern that hydrogen may be produced from the CORK 1301A's stainless steel fluid delivery line

due to anaerobic corrosion of the steel via the following reaction (e.g. Smart et al., 2002a, b):

$$Fe_{(s)} + 2H_2O_{(l)} \rightarrow H_{2(g)} + Fe(OH)_{2(aq)} \quad (4)$$

However, only ~0.0025 μM H_2 was produced during a 2-hour-incubation of stainless steel in anaerobic seawater, indicating that the 0.3-2 μM hydrogen observed in CORK 1301A fluids was probably not produced via anaerobic corrosion of iron during the short (<1 hr) transit of basement fluids through the stainless steel fluid delivery line. Since the production of hydrogen by anaerobic corrosion of steel depends on the reaction time, a rapid fluid pumping rate and sampling from a well-flushed FDL greatly reduces the chance of contamination.

Potential methane sources

Anaerobic degradation of organic matter in buried marine sediment leads to the production of methane (Martens and Val Klump, 1980; Claypool and Kvenvolden, 1983). Methane production within deep sea sediments is also apparent at IODP U1301 (Fig. 3.6, Shipboard Scientific Party, 2004). However, the concentration of CH_4 in sediment porewater decreased drastically from 1.03-5.37 mM at 73 to 111 meters below seafloor (mbsf) to <3 μM below 142 mbsf (Shipboard Scientific Party, 2004). The methane concentrations in sediment porewater near the sediment-basement interface (2-3 μM, Fig. 3.6) indicate that net diffusion of methane from the overlying sediment into basement may be occurring near CORK 1301A (1.5-1.6 μM CH_4), but not for the much higher CH_4 concentrations found in basement fluids from CORKs 1362A (6.2 μM) and 1362B (13

μM). Methane at CORKs 1362A and 1362B must have been produced within the basaltic basement environment, which could then diffuse upward into the overlying sediments.

Thermodynamic calculations were performed to test the feasibility of methane production from hydrogen in the subseafloor basement. The reaction for methane production using hydrogen is (Amend and Shock, 2001):

$$HCO_3^- + 4H_2 + H^+ \rightarrow CH_4 + 3H_2O \qquad (5)$$

The results show that for the hydrogen concentration in the CORK 1301A fluids, methane production from hydrogen is thermodynamically favorable (exergonic, negative Gibbs free energy, Table 3.2). In contrast, at the much lower hydrogen concentrations found in CORKs 1362A and 1362B fluids, the reaction would be endergonic; the environment is not favorable for abiotic methane production from hydrogen, and microorganisms would need to couple methanogenesis with other energy-yielding reactions.

Based on field and laboratory studies, microbial methane can be conventionally distinguished by its much greater depletion in ^{13}C relative to thermogenic methane (Fig. 3.7). The depletion of ^{13}C of biogenic methane is due to a large ^{13}C fractionation during microbial methanogenesis via CO_2 reduction or acetate (methyl group) fermentation (Whiticar et al., 1986; Sherwood Lollar et al., 2002). In contrast, thermogenic methane inherits its higher $\delta^{13}C$ values from its source organic matter produced via photosynthesis (Schoell, 1988; Sherwood Lollar et al., 2002; Sherwood Lollar et al., 2006). Based on environmental data, abiogenic methane tends to be more depleted in ^{2}H than biogenic

methane, and much more depleted in ^{2}H than thermogenic methane (Fig. 3.7, Sherwood Lollar et al., 1993a; Sherwood Lollar et al., 2006). The depletion of ^{2}H in abiogenic methane is likely due to kinetically controlled polymerization, metamorphism of graphite-carbonate bearing rocks, and serpentinization (Sherwood Lollar et al., 2006; Sherwood Lollar et al., 2008), whereas while the less depleted ^{2}H biogenic methane is likely due to relatively small fractionation during biogenic methanogenesis (Valentine et al., 2004).

The carbon and hydrogen isotopic compositions of methane in CORK 1362A and 1362B fluids fall within the range of those in conventionanly defined biogenic and thermogenic methane (Fig. 3.7, Whiticar, 1999; Sherwood Lollar et al., 2006). Moreover, the $\delta^{13}C$ value of CH_4 for CORK 1362A and 1362B is within the range of ^{13}C-depleted methane (-54 to -65 ‰) produced within subsamples from the interior of rock samples collected from IODP U1301A during a two-year long incubation at 65°C in anoxic, sulfate-rich media containing H_2, acetate, methanol, and dimetheyl sulfide as energy substrates, and during another 5-year long incubation with basalt as substrate (Lever et al., 2013). The ^{13}C-depleted methane has been suggested to be produced by microbes residing inside the rock samples (Lever et al., 2013); and thus it is likely that the methane in the 1362A and 1362B fluids are biogenic. In contrast, the $\delta^{13}C$ and $\delta^{2}H$ values of methane in CORK 1301A fluids are higher compared with that in CORK 1362A and 1362B fluids, and fall outside the ranges of the values of conventionally defined biogenic, thermogenic and abiogenic methane. The carbon and hydrogen isotopic compositions of the methane in 1301A fluids are not indicative of the origin of the methane but rather, it is likely resulted

from isotope fractionation via processes such as microbial methane oxidation, and is discussed in a greater detail in the following section.

Although thermogenic methane can be produced at earth surface temperatures (10-25°C), the production rate is extremely slow (Claypool and Kvenvolden, 1983). Significant thermogenic methane forms only when organic-rich materials such as marine sediments are heated to greater than 80°C (Claypool and Kvenvolden, 1983). Since the basement fluids at our study sites have a low organic carbon content at relatively low temperatures (<65^{o}C) (Lin et al., 2012), thermogenic methane production in the basement is likely not significant.

It is interesting that 16S rRNA gene-based community structures reconstructed from analysis of particles filtered from CORK 1301A basement fluids do not indicate the presence of known methanogens. Methanogens have, thus far, only been detected from the Euryarchaeota branch of the Archaeal domain, from lineages such as Methanosarcina, Methanococcus, Methanothermobacter, etc. (Whitman et al., 2006; Valentine, 2011), and none of these groups have been observed in CORK 1301A borehole fluids analyzed thus far. 'Universal' primers used for PCR amplification of SSU rRNA gene fragments were checked to verify that methanogenic groups would be targeted, so the absence of these groups from our data appears legitimate. However, there are some sequences from Euryarchaeota lineages (and other lineages) in CORK 1301A fluid samples that have no cultivated members (e.g. MBG-E, Misc. Euryarcheotic Group; Jungbluth et al., 2013; Jungbluth et al., unpublished results). Further investigations are needed to determine unequivocally whether methanogens are present in the upper basement of site 1301A.

3.4.3. Methane oxidation in the basement- Rayleigh fractionation model

The methane in 1301A basement fluids is lower in concentration and more enriched in both ^{13}C and ^{2}H relative to that in 1362A and 1362B fluids, and fall outside of the conventionally defined ranges of source methane isotopic compositions (Fig. 3.7). The $\delta^{2}H$ value (57‰) of methane in 1301A fluids is much higher than that in anoxic sediment porewater (-268 to -64 ‰, Martens et al., 1999), in Black Sea water column (-230 to -75‰, Kessler et al., 2006; Reeburgh et al., 2006), in Skan Bay water column (-160 to -110 ‰, Kessler et al., 2008), in Santa Barbara Basin water column (-140 to -90‰, Kessler et al., 2008), in Santa Monica Basin water column (-380 to -100‰, Kessler et al., 2008) and in Cariaco Basin water column (-180 to -80‰, Kessler et al., 2008), and is closer to the $\delta^{2}H$ of methane (~35‰) remaining after an inoculation of methane oxidizers for several months at 26°C (Coleman et al., 1981). Since methane oxidation has been shown to cause a large fractionation in both carbon and hydrogen isotopes of methane (e.g. Alperin et al., 1988; Martens et al., 1999; Cowen et al., 2002; Kessler et al., 2006; Reeburgh et al., 2006; Kessler et al., 2008; Holler et al., 2009), we evaluate whether methane oxidation may explain the ^{13}C and ^{2}H-enriched methane in 1301A fluid by a Rayleigh fractionation model (e.g. Coleman et al., 1981; Cowen et al., 2002; Grant and Whiticar, 2002; Keir et al., 2009). The equation is as following:

$$\delta^{13}C_{reactant} = \delta^{13}C_{initial} - \varepsilon\{\ln(f)\}$$

where f is the fraction of reactant (i.e. methane) remaining, $\delta^{13}C_{initial}$ is the $\delta^{13}C$ value of the initial reactant methane pool, and ε is the kinetic isotope effect of the transformation. We assumed that the initial methane at site 1301A has concentration and isotopic

compositions same as those in 1362A (Fig. 3.8 a, b) or 1362B fluids (Fig. 3.8 c, d). Kinetic isotope effects by anaerobic methane oxidation were estimated to be between 7.5 and 10.2 for carbon and 180-134 for hydrogen (Alperin et al., 1988). The modeling results show that methane isotopic compositions in 1301A fluids fall within or near the range of those modeled by Rayleigh fractionation caused by anaerobic methane oxidation, suggesting that anaerobic methane oxidation have occurred to result in the observed methane isotopic compositions in 1301A fluids.

The $\delta^{13}C$ and $\delta^{2}H$ values of methane in 1301A, 1362A and 1362B fluids show a positive correlation, with r-squared value of 0.997 on a $\delta^{13}C$-CH_4 versus $\delta^{2}H$-CH_4 plot (Fig. 3.7), suggesting that methane oxidation may govern the variation in methane isotopic compositions in all three sites. However, one may argue that 1362B fluid has the highest methane concentration among the three sites but the isotopic compositions of methane in 1362B fluids fall between those in 1362A and 1301A fluids on a $\delta^{13}C$-CH_4 versus $\delta^{2}H$-CH_4 plot (Table 3.1 and Fig. 3.7). One plausible explanation is that the initial methane concentration at site 1362B is much higher than its current concentration (13 μM) whereas the initial methane concentration at site 1362A is not much higher than its current concentration (6 μM), the fraction of methane remaining in 1362A fluid is higher than that in 1362B fluid, resulting a less positive carbon and hydrogen isotopic composition of methane in 1362A fluids than that in 1362B fluids. Since the $\delta^{13}C$ value of methane produced by microbes in the incubated rock samples from U1301A was as low as -65‰ (Lever et al., 2013), the slightly more positive $\delta^{13}C$ values of methane in 1362A (-58.3‰) and 1362B fluids (-56.6‰) could result from partial methane oxidation of carbon isotopically lighter methane as observed in the incubated rock samples.

3.4.4. Energy yields for H_2 and CH_4 oxidation

Diverse chemolithoautotrophic microorganisms can use hydrogen as an electron donor, coupled with electron acceptors such as sulfate (e.g. Alt et al., 2007), carbon dioxide (e.g. Kurr et al., 1991) or iron (e.g. Kashefi et al., 2002), to produce organic matter. Hydrogen-based subsurface biospheres have been suggested for continental settings (Stevens and McKinley, 1995; Chapelle et al., 2002; Lin et al., 2006). Thermodynamic calculations were made to investigate the energy available to microorganisms via hydrogen oxidation coupled with sulfate, carbon dioxide (i.e. methanogenesis) and ferric iron within the Juan de Fuca Ridge flank upper basement aquifer (Table 3.2). More free energy is available at higher concentrations of hydrogen in the CORK 1301A fluids, than at the lower concentrations in CORK 1362A or 1362B fluids. Even so, hydrogen oxidation coupled with sulfate and iron reduction is still energy-yielding at all three sites. The fluid chemistry and the results of thermodynamic calculations are consistent with the observation of depleted ^{34}S in pyrite, likely produced biologically, from basaltic rock collected from site 1301 cores (Ono et al., 2012; Lever et al., 2013). In contrast, hydrogen oxidation coupled with carbon dioxide reduction (methanogenesis) provides energy only at CORK 1301A, and not at CORK 1362A and 1362B. Thermodynamic calculations also suggest that the microbial communities at the three boreholes may differ due to the available energy that can be derived from hydrogen.

Methane is another important electron donor for diverse aerobic and anaerobic microorganisms (e.g. Zehnder and Brock, 1979; Hinrichs et al., 1999; Boetius et al., 2000; Biddle et al., 2006; Inagaki et al., 2006; Leloup et al., 2007). The importance of methane

in the global carbon cycle has been widely recognized in various settings such as coastal ocean, marine sediment, deep ocean and hydrothermal systems (Claypool and Kvenvolden, 1983; Crill and Martens, 1986; Valentine et al., 2001; Cowen et al., 2002; Biddle et al., 2006). Basement fluids from sediment-buried 3.5 Ma Juan de Fuca Ridge flank crusts are anoxic but still contain a significant amount of sulfate (17-18 mM, Cowen et al., 2003; Wheat et al., 2004a; Wheat et al., 2010; Lin et al., 2012). Thermodynamic calculations show that anaerobic methane oxidation coupled with sulfate reduction is energy-yielding at all three study sites (Table 3.2). Although direct measurement of anaerobic methane oxidation has not been made for basement fluid from the Juan de Fuca Ridge flank, the carbon and hydrogen isotopic compositions of methane in the basement fluids suggest that methane oxidation had occurred. Potential anaerobic methane oxidation rates have also been measured throughout the entire sediment column at site 1301A (Engelen et al., 2008). In deep sediment at 1301A, peak methane occurred only within the zone where sulfate was exhausted; methane decreased significantly at depths where sulfate is supplied to the sediment porewater by diffusion from overlying seawater or from basement fluids across the basement-sediment interface (Fig. 3.6, Shipboard Scientific Party, 2004). Consumption of methane by sulfate reducers is an important mechanism for removing methane from deep sediment porewater (Reeburgh and Heggie, 1977; Claypool and Kvenvolden, 1983; Boetius et al., 2000; Shipboard Scientific Party, 2004), and the inverse relationship between sulfate and methane in the 1301A sediment porewater is best explained by anaerobic methane oxidation by sulfate reduction (Shipboard Scientific Party, 2004). The energy-yielding basement environment and the presence of anaerobic methane oxidizers in the deep sediment column (Engelen

et al., 2008) suggest that anaerobic methane oxidizers may also be present in the basement environment.

Detection of methanotrophs, which fall within the Verrucomicrobia (Dunfield et al., 2007) as well as the Alpha-, Beta-, and Gammaproteobacteria lineages (Valentine, 2011), are rare in CORK 1301A, 1362A and 1362B borehole fluids that have been sequenced thus far (Jungbluth et al., 2013). An uncultivated group called Hyd24-01 that seems to fit within the Methylcoccales lineage (Gammaproteobacteria) was found, as was a lineage closely related to Methylophaga (Gammaproteobacteria) in 1301A fluid from 2010, but both were detected only once. As for the methanogens, there were many uncultivated lineages from the Alpha-, Beta-, and Gammaproteobacteria lineages and a couple from the Verrucomicrobia. More studies, including new sequencing technologies, culturing and characterization and metabolic rate measurements, need to be carried out to determine whether methanotrophs are present in the basement environment.

3.4.5. Spatial differences in methane and hydrogen: implications for hydrogeological circulation

There is no discernible systematic horizontal, or vertical, variation in the methane concentrations of the basement fluids. The methane concentrations in basement fluids increase from 1.5 μM at the southernmost site (CORK 1301A) to 13 μM at the intermediate site (CORK 1362B) and then decrease to 6.1 μM at the northernmost site (CORK 1362A). The methane data from the three CORKs do not support a hypothesized north-south flow direction, although the penetration depths of the three CORKs into basement vary. Methane concentrations are 1.5 μM at the shallowest site (30 mbs, CORK

1301A), 13 μM at the slightly deeper site (50 mbs, CORK 1362B), but only 6.1 μM at the deepest site (200 mbs, CORK 1362A).

In contrast, hydrogen concentrations decrease systematically from 1.1 μM at the southernmost site (CORK 1301A) to 0.08 μM at the intermediate site (CORK 1362B) to 0.05 μM at the northernmost site (CORK 1362A). The hydrogen data from the three sites do suggest a north-south trend but not necessarily a flow direction. Hydrogen concentrations also decrease systematically from the shallowest site to the deepest site. However, unlike other geochemical parameters, which are controlled mainly by water-rock reactions (Wheat et al., 2000; Wheat et al., 2010) or by time (Walker et al., 2008), multiple potential sources and sinks for hydrogen and methane complicate the use of variations in their concentrations in the basement fluids to evaluate basement fluid flow pathways.

Nevertheless, the methane and hydrogen data presented in this study do not support a well-mixed and homogeneous aquifer on the scale of the 300 to 800 m horizontal separation among the three sites, despite the high upper basement permeability (Shipboard Scientific Party, 2010). Spatial heterogeneity in permeability has been inferred through packer experiments (Becker and Fisher, 2008; Fisher et al., 2008), and observations of recovered rock cores from the U1362 site show high vertical heterogeneity (Shipboard Scientific Party, 2010), suggesting diverse niches for both biological and abiological reactions, with highly variable flow and reaction histories which could contribute to the observed spatial differences in fluid methane and hydrogen concentrations.

3.5 Conclusion

This study provides new hydrogen and methane data for oceanic basement fluids. The data show that the sediment-buried basement on the eastern flank of the JFR is a source for both H_2 and CH_4. Thermodynamic calculations show that formation of CH_4 via H_2 oxidation is favorable at 1301A but the concentration of methane in CORK 1301A fluids is the lowest among the three sites. Stable carbon and hydrogen isotopic values for CH_4 in CORK 1301A fluids suggest that methane oxidation may have occurred. Although thermodynamic calculations indicate that the basement environment at 1362A and 1362B is not conducive to formation of CH_4, the stable carbon and hydrogen isotopic compositions of methane indicate that source of methane may still be biogenic. Nevertheless, the presence of H_2 and CH_4 in basement fluids provides a significant amount of energy for hydrogenotrophic sulfate reduction, hydrogenotrophic iron reduction and anaerobic methane oxidation at all sites investigated. Differences in H_2 and CH_4 concentrations in fluids from the three sites also suggest an incompletely mixed circulation system with diverse microhabitats.

Acknowledgement

This work is supported by NSF-Microbial Observatory Project (NSF XXXXX). We would like to thank crews of R/V Atlantis, HOV Alvin & ROV Jason for smooth cruises and submersible operations. We thank Chih-Chiang Hsieh for his help with the sample collection and his and Kathryn Hu's technical support and assistance on biogeochemicl analysis. We also thank David Karl's generosity in providing instruments for conducting and analysis of the H2 production experiment. We thank Brian Popp and Mike Mottl's comments and editorial assistance to greatly improve this manuscript. SOEST contribution number XXXX. C-DEBI contribution number XXXX.

3.6 References

Alford, S.E., Alt, J.C., Shanks Iii, W.C., 2011. Sulfur geochemistry and microbial sulfate reduction during low-temperature alteration of uplifted lower oceanic crust: Insights from ODP Hole 735B. Chemical Geology 286, 185-195.

Alperin, M.J., Reeburgh, W.S., Whiticar, M.J., 1988. Carbon and hydrogen isotope fractionation resulting from anaerobic methane oxidation. Global biogeochemical cycles 2, 279-288.

Alt, J.C., Honnorez, J., Laverne, C., Emmermann, R., 1986. Hydrothermal Alteration of a 1-Km Section through the Upper Oceanic-Crust, Deep-Sea Drilling Project Hole 504b - Mineralogy, Chemistry, and Evolution of Seawater-Basalt Interactions. Journal of Geophysical Research-Solid Earth and Planets 91, 309-335.

Alt, J.C., Laverne, C., Vanko, D.A., Tartarotti, P., Teagle, D.A.H., Bach, W., Zuleger, E., Erzinger, J., Honnorez, I., Pezard, P.A., 1996. Hydrothermal alteration of a section of upper oceanic crust in the eastern equatorial Pacific: A synthesis of results from Site 504 (DSDP Legs 69, 70, and 83, and ODP Legs 111, 137, 140, and 148). Proceedings of the Ocean Drilling Program 148, 417-434.

Alt, J.C., Shanks III, W.C., Bach, W., Paulick, H., Garrido, C.J., Beaudoin, G., 2007. Hydrothermal alteration and microbial sulfate reduction in peridotite and gabbro exposed by detachment faulting at the Mid-Atlantic Ridge, 15 20′ N (ODP Leg 209): a sulfur and oxygen isotope study. Geochemistry Geophysics Geosystems 8, Q08002.

Alt, J.C., Shanks, W.C., 2011. Microbial sulfate reduction and the sulfur budget for a complete section of altered oceanic basalts, IODP Hole 1256D (eastern Pacific). Earth and Planetary Science Letters 310, 73-83.

Amend, J.P., McCollom, T.M., Hentscher, M., Bach, W., 2011. Metabolic (catabolic and anabolic) energy for chemolithoautotrophs in deep-sea hydrothermal systems hosted in different rock types. Geochimica et Cosmochimica Acta 75, 5736-5748.

Amend, J.P., Rogers, K.L., Shock, E.L., Gurrieri, S., Inguaggiato, S., 2003. Energetics of chemolithoautotrophy in the hydrothermal system of Vulcano Island, southern Italy. Geobiology 1, 37-58.

Amend, J.P., Shock, E.L., 1998. Energetics of amino acid synthesis in hydrothermal ecosystems. Science 281, 1659-1662.

Amend, J.P., Shock, E.L., 2001. Energetics of overall metabolic reactions of thermophilic and hyperthermophilic Archaea and Bacteria. Fems Microbiology Reviews 25, 175-243.

Amend, J.P., Teske, A., 2005. Expanding frontiers in deep subsurface microbiology. Palaeogeography, Palaeoclimatology, Palaeoecology 219, 131-155.

Anderson, R.N., Langseth, M.G., Sclater, J.G., 1977. The mechanisms of heat transfer through the floor of the Indian Ocean. Journal of Geophysical Research 82, 3391-3409.

Anderson, R.N., Zoback, M.D., Hickman, S.H., Newmark, R.L., 1985. Permeability versus depth in the upper oceanic crust: In situ measurements in DSDP hole 504B, eastern equatorial Pacific. Journal of Geophysical Research: Solid Earth (1978–2012) 90, 3659-3669.

Azam, F., Fenchel, T., Field, J., Gray, J., Meyer-Reil, L., Thingstad, F., 1983. The ecological role of water-column microbes in the sea. Marine ecology progress series. Oldendorf 10, 257-263.

Bach, W., Edwards, K.J., 2003. Iron and sulfide oxidation within the basaltic ocean crust: Implications for chemolithoautotrophic microbial biomass production. Geochim. Cosmochim. Acta 67, 3871-3887.

Balch, W., Fox, G., Magrum, L., Woese, C., Wolfe, R., 1979. Methanogens: reevaluation of a unique biological group. Microbiological reviews 43, 260.

Barnes, R., Goldberg, E., 1976. Methane production and consumption in anoxic marine sediments. Geology 4, 297-300.

Becker, K., Davis, E., 2005. A review of CORK designs and operations during the Ocean Drilling Program. Proceedings of the Integrated Ocean Drilling Program 301.

Becker, K., Fisher, A.T., 2000. Permeability of upper oceanic basement on the eastern flank of the Juan de Fuca Ridge determined with drill-string packer experiments. Journal of Geophysical Research 105, 897-912.

Becker, K., Fisher, A.T., 2008. Borehole packer tests at multiple depths resolve distinct hydrologic intervals in 3.5-Ma upper oceanic crust on the eastern flank of Juan de Fuca Ridge. J. Geophys. Res. 113, 1-12.

Becker, K., Sakai, H., Adamson, A., Alexandrovich, J., Alt, J., Anderson, R., Bideau, D., Gable, R., Herzig, P., Houghton, S., 1989. Drilling deep into young oceanic crust, Hole 504B, Costa Rica Rift. Reviews of Geophysics 27, 79-102.

Bethke, C.M., Sanford, R.A., Kirk, M.F., Jin, Q., Flynn, T.M., 2011. The thermodynamic ladder in geomicrobiology. American Journal of Science 311, 183.

Biddle, J.F., Lipp, J.S., Lever, M.A., Lloyd, K.G., Sorensen, K.B., Anderson, R., Fredricks, H.F., Elvert, M., Kelly, T.J., Schrag, D.P., Sogin, M.L., Brenchley, J.E., Teske, A., House, C.H., Hinrichs, K.U., 2006. Heterotrophic Archaea dominate sedimentary subsurface ecosystems off Peru. Proceedings of the National Academy of Sciences of the United States of America 103, 3846-3851.

Bjerg, P.L., Jakobsen, R., Bay, H., Rasmussen, M., Albrechtsen, H.-J., Christensen, T.H., 1997. Effects of Sampling Well Construction on H_2 Measurements Made for Characterization of Redox Conditions in a Contaminated Aquifer. Environ. Sci. Technol. 31, 3029-3031.

Bjorkman, K., Karl, D.M., 1994. Bioavailabiliy of inorganic and organic phosphorus-compounds to natural assemblages of microorganisms in Hawaiian costal water. Marine Ecology-Progress Series 111, 265-273.

Boetius, A., Ravenschlag, K., Schubert, C.J., Rickert, D., Widdel, F., Gieseke, A., Amann, R., Jorgensen, B.B., Witte, U., Pfannkuche, O., 2000. A marine microbial consortium apparently mediating anaerobic oxidation of methane. Nature 407, 623-626.

Boettger, J., 2011. Geochemical constraints on microbial metabolisms in the basement fluid of the Juan de Fuca Ridge flank, B.S. thesis, Department of Earth and Planetary Sciences and Division of Biology and Biomedical Sciences. Washington Univ., St. Louis.

Boettger, J., Lin, H.-T., Cowen, J.P., Henstscher, M., Amend, J.P., 2013. Energy yields from chemolithotrophic metabolisms in igneous basement of the Juan de Fuca ridge flank system. Chemical Geology 337-338, 11-19.

Boone, D.R., Johnson, R.L., Liu, Y., 1989. Diffusion of the interspecies electron carriers H2 and formate in methanogenic ecosystems and its implications in the measurement of Km for H2 or formate uptake. Applied and Environmental Microbiology 55, 1735.

Carlson, C.A., 2002. Production and removal processes, in: Hansell, D.A., Carlson, C.A. (Eds.), Biogeochemistry of marine dissolved organic matter. Elsevier, pp. 91–151.

Chapelle, F.H., O'Neill, K., Bradley, P.M., Methe, B.A., Ciufo, S.A., Knobel, L.L., Lovley, D.R., 2002. A hydrogen-based subsurface microbial community dominated by methanogens. Nature 415, 312-315.

Charlou, J., Donval, J., Fouquet, Y., Jean-Baptiste, P., Holm, N., 2002. Geochemistry of high H_2 and CH_4 vent fluids issuing from ultramafic rocks at the Rainbow hydrothermal field (36°14′ N, MAR). Chemical Geology 191, 345-359.

Chomczynski, P., Sacchi, N., 2006. The single-step method of RNA isolation by acid guanidinium thiocyanate–phenol–chloroform extraction: twenty-something years on. Nature protocols 1, 581-585.

Claypool, G.E., Kvenvolden, K.A., 1983. Methane and other hydrocarbon gases in marine sediment. Annual Review of Earth and Planetary Sciences 11, 299.

Coleman, D.D., Risatti, J.B., Schoell, M., 1981. Fractionation of carbon and hydrogen isotopes by methane-oxidizing bacteria. Geochimica et Cosmochimica Acta 45, 1033-1037.

Cowen, J.P., 2004. The microbial biosphere of sediment-buried oceanic basement. Research in Microbiology 155, 497-506.

Cowen, J.P., Copson, D.A., Jolly, J., Hsieh, C.-C., Lin, H.-T., Glazer, B.T., Wheat, C.G., 2012. Advanced instrument system for real-time and time-series microbial geochemical sampling of the deep (basaltic) crustal biosphere. Deep Sea Research Part I: Oceanographic Research Papers 61, 43-56.

Cowen, J.P., Giovannoni, S.J., Kenig, F., Johnson, H.P., Butterfield, D., Rappe, M.S., Hutnak, M., Lam, P., 2003. Fluids from aging ocean crust that support microbial life. Science 299, 120-123.

Cowen, J.P., Wen, X., Popp, B.N., 2002. Methane in aging hydrothermal plumes. Geochimica et Cosmochimica Acta 66, 3563-3571.

Craig, H., 1957. Isotopic standards for carbon and oxygen and correction factors for mass-spectrometric analysis of carbon dioxide. Geochimica et cosmochimica acta 12, 133-149.

Craig, H., 1961. Standard for reporting concentrations of deuterium and oxygen 18 in natural waters. Science 133, 1833-1834.

Crill, P.M., Martens, C.S., 1986. Methane production from bicarbonate and acetate in an anoxic marine sediment. Geochimica et Cosmochimica Acta 50, 2089-2097.

D'Hondt, S., Rutherford, S., Spivack, A.J., 2002. Metabolic activity of subsurface life in deep-sea sediments. Science 295, 2067-2070.

Davis, E., Lister, C., 1977. Heat flow measured over the Juan de Fuca Ridge: Evidence for widespread hydrothermal circulation in a highly heat transportive crust. Journal of Geophysical Research 82, 4845-4860.

Davis, E.E., Chapman, D.S., Mottl, M.J., Bentkowski, W.J., Dadey, K., Forster, C., Harris, R., Nagihara, S., Rohr, K., Wheat, G., Whiticar, M., 1992. Flank flux - an

experiment to study the nature of hydrothermal circulation in young oceanic-crust. Can. J. Earth. Sci. 29, 925-952.

Davis, E.E., Chapman, D.S., Wang, K., Villinger, H., Fisher, A.T., Robinson, S.W., Grigel, J., Pribnow, D., Stein, J., Becker, K., 1999. Regional heat flow variations across the sedimented Juan de Fuca Ridge eastern flank: Constraints on lithospheric cooling and lateral hydrothermal heat transport. Journal of Geophysical Research-Solid Earth 104, 17675-17688.

Dickson, A., Sabine, C., Christian, J., 2007. Guide to best practices for ocean CO_2 measurements. PICES Science Report.

Ducklow, H., Carlson, C., 1992. Oceanic bacterial production. Advances in microbial ecology 12, 113-181.

Dunfield, P.F., Yuryev, A., Senin, P., Smirnova, A.V., Stott, M.B., Hou, S., Ly, B., Saw, J.H., Zhou, Z., Ren, Y., 2007. Methane oxidation by an extremely acidophilic bacterium of the phylum Verrucomicrobia. Nature 450, 879-882.

Edmond, J., Massoth, G., Lilley, M., 1992. Submersible-deployed samplers for axial vent waters. Ridge Events 3, 23-24.

Elderfield, H., Wheat, C.G., Mottl, M.J., Monnin, C., Spiro, B., 1999. Fluid and geochemical transport through oceanic crust: a transect across the eastern flank of the Juan de Fuca Ridge. Earth Planet. Sci. Lett. 172, 151-165.

Engelen, B., Ziegelmueller, K., Wolf, L., Kopke, B., Gittel, A., Cypionka, H., Treude, T., Nakagawa, S., Inagaki, F., Lever, M.A., Steinsbu, B.O., 2008. Fluids from the oceanic crust support microbial activities within the deep biosphere. Geomicrobiol. J. 25, 56-66.

Fisher, A.T., 2004. Rates of flow and patterns of fluid circulation, in: Davis, E.E., Elderfield, H. (Eds.), Hydrogeology of the oceanic lithosphere. Cambridge University Press, Cambridge, pp. 337-375.

Fisher, A.T., 2005. Marine hydrogeology: recent accomplishments and future opportunities. Hydrogeol. J. 13, 69-97.

Fisher, A.T., Becker, K., 2000. Channelized fluid flow in oceanic crust reconciles heat-flow and permeability data. Nature 403, 71-74.

Fisher, A.T., Davis, E.E., Becker, K., 2008. Borehole-to-borehole hydrologic response across 2.4 km in the upper oceanic crust: Implications for crustal-scale properties. Journal of Geophysical Research-Solid Earth 113.

Fisher, A.T., Davis, E.E., Hutnak, M., Spiess, V., Zuhlsdorff, L., Cherkaoui, A., Christiansen, L., Edwards, K., Macdonald, R., Villinger, H., Mottl, M.J., Wheat, C.G., Becker, K., 2003. Hydrothermal recharge and discharge across 50 km guided by seamounts on a young ridge flank. Nature 421, 618-621.

Fisher, A.T., Urabe, T., Klaus, A., Scientists, E., 2005. Site U1301. Proc. IODP 301.

Fisk, M.R., Giovannoni, S.J., Thorseth, I.H., 1998. Alteration of oceanic volcanic glass: Textural evidence of microbial activity. Science 281, 978-980.

Furnes, H., Dilek, Y., Muehlenbachs, K., Banerjee, N.R., 2006. Tectonic control of bioalteration in modern and ancient oceanic crust as evidenced by carbon isotopes. Isl. Arc 15, 143-155.

Furnes, H., Muehlenbachs, K., Torsvik, T., Thorseth, I.H., Tumyr, O., 2001a. Microbial fractionation of carbon isotopes in altered basaltic glass from the Atlantic Ocean, Lau Basin and Costa Rica Rift. Chemical Geology 173, 313-330.

Furnes, H., Muehlenbachs, K., Torsvik, T., Tumyr, O., Shi, L., 2002. Bio-signatures in metabasaltic glass of a Caledonian ophiolite, West Norway. Geological Magazine 139, 601-608.

Furnes, H., Staudigel, H., Thorseth, I.H., Torsvik, T., Muehlenbachs, K., Tumyr, O., 2001b. Bioalteration of basaltic glass in the oceanic crust. Geochemistry, Geophysics, Geosystems 2.

Gieskes, J.M., Gamo, T., Brumsack, H., 1991. Chemical methods for interstitial water analysis aboard JOIDES Resolution. ODP Tech. Note 15, 119-136.

Giovannoni, S.J., Fisk, M.R., Mullins, T.D., Furnes, H., 1996. Genetic evidence for endolithic microbial life colonizing basaltic glass/seawater interfaces. Proc. Ocean Drill. Program Sci. Results 148, 207-214.

Grant, N.J., Whiticar, M.J., 2002. Stable carbon isotopic evidence for methane oxidation in plumes above Hydrate Ridge, Cascadia Oregon Margin. Global Biogeochemical Cycles 16, 1124.

Hansell, D.A., Carlson, C.A., Repeta, D.J., Schlitzer, R., 2009. Dissolved organic matter in the ocean: a controversy stimulates new insights. Oceanography 22, 202-211.

Hinrichs, K.U., Hayes, J.M., Sylva, S.P., Brewer, P.G., DeLong, E.F., 1999. Methane-consuming archaebacteria in marine sediments. Nature 398, 802-805.

Hoehler, T.M., Alperin, M.J., Albert, D.B., Martens, C.S., 1994. Field and laboratory studies of methane oxidation in an anoxic marine sediment-evidence for a methanogen-sulfate reducer consortium. Global Biogeochemical Cycles 8, 451-463.

Hoehler, T.M., Alperin, M.J., Albert, D.B., Martens, C.S., 1998. Thermodynamic control on hydrogen concentrations in anoxic sediments. Geochimica et Cosmochimica Acta 62, 1745-1756.

Holler, T., Wegener, G., Knittel, K., Boetius, A., Brunner, B., Kuypers, M.M.M., Widdel, F., 2009. Substantial 13C/12C and D/H fractionation during anaerobic oxidation of methane by marine consortia enriched in vitro. Environmental microbiology reports 1, 370-376.

Huber, J.A., Johnson, H.P., Butterfield, D.A., Baross, J.A., 2006. Microbial life in ridge flank crustal fluids. Environmental Microbiology 8, 88-99.

Hutnak, M., Fisher, A.T., Zuhlsdorff, L., Spiess, V., Stauffer, P.H., Gable, C.W., 2006. Hydrothermal recharge and discharge guided by basement outcrops on 0.7-3.6 Ma seafloor east of the Juan de Fuca Ridge: Observations and numerical models. Geochemistry Geophysics Geosystems 7.

Inagaki, F., Nunoura, T., Nakagawa, S., Teske, A., Lever, M., Lauer, A., Suzuki, M., Takai, K., Delwiche, M., Colwell, F.S., Nealson, K.H., Horikoshi, K., D'Hondt, S., Jorgensen, B.B., 2006. Biogeographical distribution and diversity of microbes in methane hydrate-bearing deep marine sediments, on the Pacific Ocean Margin. Proceedings of the National Academy of Sciences of the United States of America 103, 2815-2820.

Johnson, H., Party, L.S., Sheffer, N., Enzel, Y., Waldmann, N., Grodek, T., Benito, G., Gill, T., Zobeck, T., Tulaczyk, S., 2003. Probing for life in the ocean crust with the LEXEN program. EOS, Tran. AGU 84, 12.

Johnson, H.P., Pruis, M.J., 2003. Fluxes of fluid and heat from the oceanic crustal reservoir. Earth Planet. Sci. Lett. 216, 565-574.

Johnson, J.W., Oelkers, E.H., Helgeson, H.C., 1992. SUPCRT92: A software package for calculating the standard molal thermodynamic properties of minerals, gases, aqueous species, and reactions from 1 to 5000 bar and 0 to 1000 C. Computers & Geosciences 18, 899-947.

Jones, R.D., 1991. An improved fluorescence method for the determination of nanomolar concentrations of ammonium in natural-waters. Limnology and Oceanography 36, 814-819.

Joye, S.B., Samarkin, V.A., Orcutt, B., Macdonald, R., Hinrichs, K.U., Elvert, M., Teske, A., Lloyd, K.G., Lever, M., Montoya, J.P., Meile, C.D., 2009. Metabolic variability in seafloor brines revealed by carbon and sulphur dynamics. Nature Geoscience 2, 349-354.

Jungbluth, S.P., Grote, J., Lin, H.T., Cowen, J.P., Rappé, M.S., 2013. Microbial diversity within basement fluids of the sediment-buried Juan de Fuca Ridge flank. ISME Journal 7, 161-172.

Kaiser, K., Benner, R., 2009. Biochemical composition and size distribution of organic matter at the Pacific and Atlantic time-series stations. Marine Chemistry 113, 63-77.

Karl, D., Christian, J., Dore, J., Hebel, D., Letelier, R., Tupas, L., Winn, C., 1996. Seasonal and interannual variability in primary production and particle flux at Station ALOHA. Deep Sea Research Part II: Topical Studies in Oceanography 43, 539-568.

Kashefi, K., Tor, J.M., Holmes, D.E., Van Praagh, C.V.G., Reysenbach, A.L., Lovley, D.R., 2002. Geoglobus ahangari gen. nov., sp. nov., a novel hyperthermophilic archaeon capable of oxidizing organic acids and growing autotrophically on hydrogen with Fe (III) serving as the sole electron acceptor. International Journal of Systematic and Evolutionary Microbiology 52, 719-728.

Keir, R.S., Schmale, O., Seifert, R., Sültenfuß, J., 2009. Isotope fractionation and mixing in methane plumes from the Logatchev hydrothermal field. Geochemistry, Geophysics, Geosystems 10.

Kelley, D.S., Karson, J.A., Fruh-Green, G.L., Yoerger, D.R., Shank, T.M., Butterfield, D.A., Hayes, J.M., Schrenk, M.O., Olson, E.J., Proskurowski, G., Jakuba, M., Bradley, A., Larson, B., Ludwig, K., Glickson, D., Buckman, K., Bradley, A.S., Brazelton, W.J., Roe, K., Elend, M.J., Delacour, A., Bernasconi, S.M., Lilley, M.D., Baross, J.A., Summons, R.T., Sylva, S.P., 2005. A serpentinite-hosted ecosystem: The lost city hydrothermal field. Science 307, 1428-1434.

Kelley, D.S., Lilley, M.D., Lupton, J.E., Olson, E.J., 1998. Enriched H_2, CH_4, and ^3He concentrations in hydrothermal plumes associated with the 1996 Gorda Ridge eruptive event. Deep Sea Research Part II: Topical Studies in Oceanography 45, 2665-2682.

Kessler, J.D., Reeburgh, W.S., Tyler, S.C., 2006. Controls on methane concentration and stable isotope (δ2H- CH4 and δ13C- CH4) distributions in the water columns of the Black Sea and Cariaco Basin. Global biogeochemical cycles 20.

Kessler, J.D., Reeburgh, W.S., Valentine, D.L., Kinnaman, F.S., Peltzer, E.T., Brewer, P.G., Southon, J., Tyler, S.C., 2008. A survey of methane isotope abundance (14C, 13C, 2H) from five nearshore marine basins that reveals unusual

radiocarbon levels in subsurface waters. Journal of Geophysical Research: Oceans (1978–2012) 113.

Knittel, K., Boetius, A., 2009. Anaerobic oxidation of methane: progress with an unknown process. Annual review of microbiology 63, 311-334.

Konn, C., Charlou, J.L., Donval, J.P., Holm, N.G., Dehairs, F., Bouillon, S., 2009. Hydrocarbons and oxidized organic compounds in hydrothermal fluids from Rainbow and Lost City ultramafic-hosted vents. Chemical Geology 258, 299-314.

Kurr, M., Huber, R., König, H., Jannasch, H.W., Fricke, H., Trincone, A., Kristjansson, J.K., Stetter, K.O., 1991. Methanopyrus kandleri, gen. and sp. nov. represents a novel group of hyperthermophilic methanogens, growing at 110 C. Archives of Microbiology 156, 239-247.

Lang, S.Q., Butterfield, D.A., Lilley, M.D., Johnson, H.P., Hedges, J.I., 2006. Dissolved organic carbon in ridge-axis and ridge-flank hydrothermal systems. Geochimica et Cosmochimica Acta 70, 3830-3842.

LaRowe, D.E., Regnier, P., 2008. Thermodynamic Potential for the Abiotic Synthesis of Adenine, Cytosine, Guanine, Thymine, Uracil, Ribose, and Deoxyribose in Hydrothermal Systems. Origins of Life and Evolution of Biospheres 38, 383-397.

Lee, C., Bada, J.L., 1975. Amino acids in equatorial Pacific Ocean water. Earth and Planetary Science Letters 26, 61-68.

Leloup, J., Loy, A., Knab, N.J., Borowski, C., Wagner, M., Jorgensen, B.B., 2007. Diversity and abundance of sulfate-reducing microorganisms in the sulfate and methane zones of a marine sediment, Black Sea. Environmental Microbiology 9, 131-142.

Lever, M., Heuer, V., Morono, Y., Masui, N., Schmidt, F., Alperin, M., Inagaki, F., Hinrichs, K.U., Teske, A., 2010. Acetogenesis in deep subseafloor sediments of the Juan de Fuca Ridge Flank: a synthesis of geochemical, thermodynamic, and gene-based evidence. Geomicrobiol. J., 183-198.

Lever, M., Rouxel, O., Alt, J.C., Shimizu, N., Ono, S., Coggon, R.M., Shanks III, W.C., Lapham, L., Elvert, M., Prieto-Mollar, X., Hinrichs, K.U., Inagaki, F., Teske, A., 2013. Evidence for microbial carbon and sulfur cycling in deeply buried ridge flank basalt. Science 339, 1305-1308.

Libes, S.M., 2009. Salinity as a conservative tracer, in: Libes, S.M. (Ed.), Introduction to marine biogeochemistry. Academic Press, Burlington, p. 92.

Lin, H.T., Cowen, J.P., Olson, E.J., Amend, J.P., Lilley, M.D., 2012. Inorganic chemistry, gas compositions and dissolved organic carbon in fluids from sedimented young basaltic crust on the Juan de Fuca Ridge flanks. Geochimica et Cosmochimica Acta 85, 213-227.

Lin, L.H., Wang, P.L., Rumble, D., Lippmann-Pipke, J., Boice, E., Pratt, L.M., Lollar, B.S., Brodie, E.L., Hazen, T.C., Andersen, G.L., 2006. Long-term sustainability of a high-energy, low-diversity crustal biome. Science 314, 479-482.

Lister, C., 1972. On the thermal balance of a mid- ocean ridge. Geophysical Journal of the Royal Astronomical Society 26, 515-535.

Loh, A.N., Bauer, J.E., 2000. Distribution, partitioning and fluxes of dissolved and particulate organic C, N and P in the eastern North Pacific and Southern Oceans. Deep Sea Research Part I: Oceanographic Research Papers 47, 2287-2316.

Lovley, D.R., Chapelle, F.H., Woodward, J.C., 1994. Use of dissolved H2 concentrations to determine distribution of microbially catalyzed redox reactions in anoxic groundwater. Environmental Science & Technology 28, 1205-1210.

Lovley, D.R., Goodwin, S., 1988. Hydrogen concentrations as an indicator of the predominant terminal electron-accepting reactions in aquatic sediments. Geochimica et Cosmochimica Acta 52, 2993-3003.

Ludwig, W., Strunk, O., Westram, R., Richter, L., Meier, H., Buchner, A., Lai, T., Steppi, S., Jobb, G., Förster, W., 2004. ARB: a software environment for sequence data. Nucleic acids research 32, 1363-1371.

Marescotti, P., Vanko, D.A., Cabella, R., 2000. From oxidizing to reducing alteration: Mineralogical variations in pillow basalts from the east flank, Juan de Fuca Ridge, in: Fisher, A.T., Davis, E.E., Escutia, C. (Eds.), Proceedings of the Ocean Drilling Program, Scientific Results. Ocean Drilling Program, pp. 119-136.

Martens, C.S., Albert, D.B., Alperin, M.J., 1999. Stable isotope tracing of anaerobic methane oxidation in the gassy sediments of Eckernforde Bay, German Baltic Sea. American Journal of Science 299, 589-610.

Martens, C.S., Val Klump, J., 1980. Biogeochemical cycling in an organic-rich coastal marine basin—I. Methane sediment-water exchange processes. Geochimica et Cosmochimica Acta 44, 471-490.

McCarthy, M., Pratum, T., Hedges, J., Benner, R., 1997. Chemical composition of dissolved organic nitrogen in the ocean. Nature Publishing Group, pp. 150-154.

McCarthy, M.D., Beaupre, S.R., Walker, B.D., Voparil, I., Guilderson, T.P., Druffel, E.R.M., 2010. Chemosynthetic origin of C-14-depleted dissolved organic matter in a ridge-flank hydrothermal system. Nat. Geosci. 4, 32-36.

McCarthy, M.D., Beaupre, S.R., Walker, B.D., Voparil, I., Guilderson, T.P., Druffel, E.R.M., 2011. Chemosynthetic origin of C-14-depleted dissolved organic matter in a ridge-flank hydrothermal system. Nat. Geosci. 4, 32-36.

McCollom, T.M., 2000. Geochemical constraints on primary productivity in submarine hydrothermal vent plumes. Deep Sea Research Part I: Oceanographic Research Papers 47, 85-101.

McCollom, T.M., Bach, W., 2009. Thermodynamic constraints on hydrogen generation during serpentinization of ultramafic rocks. Elsevier, pp. 856-875.

Merkel, A.Y., Huber, J.A., Chernyh, N.A., Bonch-Osmolovskaya, E.A., Lebedinsky, A.V., 2013. Detection of Putatively Thermophilic Anaerobic Methanotrophs in Diffuse Hydrothermal Vent Fluids. Applied and Environmental Microbiology 79, 915-923.

Mottl, M.J., 2003. Partitioning of energy and mass fluxes between mid-ocean ridge axes and flanks at high and low temperature, in: Halbach, P.E., Tunnicliffe, V., Hein, J.R. (Eds.), Energy and Mass Transfer in Marine Hydrothermal Systems. Dahlem University Press, Berlin, pp. 271–286.

Mottl, M.J., Wheat, G., Baker, E., Becker, N., Davis, E., Feely, R., Grehan, A., Kadko, D., Lilley, M., Massoth, G., Moyer, C., Sansone, F., 1998. Warm springs discovered on 3.5 Ma oceanic crust, eastern flank of the Juan de Fuca Ridge. Geology 26, 51-54.

Nakagawa, S., Inagaki, F., Suzuki, Y., Steinsbu, B.O., Lever, M.A., Takai, K., Engelen, B., Sako, Y., Wheat, C.G., Horikoshi, K., 2006. Microbial community in black

rust exposed to hot ridge flank crustal fluids. Applied and Environmental Microbiology 72, 6789-6799.
Nealson, K.H., 1997. Sediment bacteria: who's there, what are they doing, and what's new? Annu. Rev. Earth Pl. Sc. 25, 403-434.
Ono, S., Keller, N.S., Rouxel, O., Alt, J.C., 2012. Sulfur-33 constraints on the origin of secondary pyrite in altered oceanic basement. Geochimica et Cosmochimica Acta.
Orcutt, B., Wheat, C.G., Edwards, K.J., 2010. Subseafloor ocean crust microbial observatories: Development of FLOCS (FLow-through Osmo Colonization System) and evaluation of borehole construction materials. Geomicrobiology Journal.
Orcutt, B.N., Sylvan, J.B., Knab, N.J., Edwards, K.J., 2011. Microbial Ecology of the Dark Ocean above, at, and below the Seafloor. Microbiology and Molecular Biology Reviews 75, 361-422.
Orphan, V.J., House, C.H., Hinrichs, K.U., McKeegan, K.D., DeLong, E.F., 2001. Methane-consuming archaea revealed by directly coupled isotopic and phylogenetic analysis. Science 293, 484-487.
Parkes, R.J., Cragg, B.A., Wellsbury, P., 2000. Recent studies on bacterial populations and processes in subseafloor sediments: A review. Hydrogeology Journal 8, 11-28.
Parsons, B., Sclater, J.G., 1977. An analysis of the variation of ocean floor bathymetry and heat flow with age. J. Geophys. Res., Solid Earth 82, 803–827.
Prusse, E., Quast, C., Yilmaz, P., Ludwig, W., 2011. SILVA: Comprehensive Databases for Quality Checked and Aligned Ribosomal RNA Sequence Data Compatible with ARB. Handbook of Molecular Microbial Ecology I: Metagenomics and Complementary Approaches 1, 393.
Reeburgh, W.S., Heggie, D.T., 1977. Microbial methane consumption reactions and their effect on methane distributions in freshwater and marine environments. Limnology and Oceanography, 1-9.
Reeburgh, W.S., Tyler, S.C., Carroll, J., 2006. Stable carbon and hydrogen isotope measurements on Black Sea water-column methane. Deep Sea Research Part II: Topical Studies in Oceanography 53, 1893-1900.
Reynolds, C., Davies, P., 2001. Sources and bioavailability of phosphorus fractions in freshwaters: a British perspective. Biological Reviews of the Cambridge Philosophical Society 76, 27-64.
Rouxel, O., Ono, S., Alt, J., Rumble, D., Ludden, J., 2008. Sulfur isotope evidence for microbial sulfate reduction in altered oceanic basalts at ODP Site 801. Earth and Planetary Science Letters 268, 110-123.
Ruttenberg, K.C., Sulak, D.J., 2011. Sorption and desorption of dissolved organic phosphorus onto iron (oxyhydr)oxides in seawater. Geochimica et Cosmochimica Acta 75, 4095-4112.
Saiki, R., Gelfand, D., Stoffel, S., Scharf, S., Higuchi, R., Horn, G., Mullis, K., Ehrlich, H., 1988. Primer-directed enzymatic amplification of DNA. Science 239, 487-491.
Sanger, F., Nicklen, S., Coulson, A.R., 1977. DNA sequencing with chain-terminating inhibitors. Proceedings of the National Academy of Sciences 74, 5463-5467.

Sansone, F.J., Mottl, M.J., Olson, E.J., Wheat, C.G., Lilley, M.D., 1998. CO2-depleted fluids from mid-ocean ridge-flank hydrothermal springs. Geochim. Cosmochim. Acta 62, 2247-2252.

Schoell, M., 1988. Multiple origins of methane in the earth. Chemical Geology 71, 1-10.

Sharp, J.H., Carlson, C.A., Peltzer, E.T., Castle-Ward, D.M., Savidge, K.B., Rinker, K.R., 2002. Final dissolved organic carbon broad community intercalibration and preliminary use of DOC reference materials. Mar. Chem. 77, 239-253.

Sherwood Lollar, B., Frape, S., Fritz, P., Macko, S., Welhan, J., Blomqvist, R., Lahermo, P., 1993a. Evidence for bacterially generated hydrocarbon gas in Canadian Shield and Fennoscandian Shield rocks. Geochimica et Cosmochimica Acta 57, 5073-5085.

Sherwood Lollar, B., Frape, S., Weise, S., Fritz, P., Macko, S., Welhan, J., 1993b. Abiogenic methanogenesis in crystalline rocks. Geochimica et Cosmochimica Acta 57, 5087-5097.

Sherwood Lollar, B., Lacrampe-Couloume, G., Slater, G.F., Ward, J., Moser, D.P., Gihring, T.M., Lin, L.H., Onstott, T.C., 2006. Unravelling abiogenic and biogenic sources of methane in the Earth's deep subsurface. Chemical Geology 226, 328-339.

Sherwood Lollar, B., Lacrampe-Couloume, G., Voglesonger, K., Onstott, T.C., Pratt, L.M., Slater, G.F., 2008. Isotopic signatures of CH_4 and higher hydrocarbon gases from Precambrian Shield sites: A model for abiogenic polymerization of hydrocarbons. Geochimica et Cosmochimica Acta 72, 4778-4795.

Sherwood Lollar, B., Westgate, T., Ward, J., Slater, G., Lacrampe-Couloume, G., 2002. Abiogenic formation of alkanes in the Earth's crust as a minor source for global hydrocarbon reservoirs. Nature 416, 522-524.

Shipboard Scientific Party, 1997a. Introduction and summary: hydrothermal circulation in the oceanic crust and its consequences on the eastern flank of the Juan de Fuca Ridge Proceedings of the Ocean Drilling Program, Initial Reports 168, 7–21.

Shipboard Scientific Party, 1997b. Rough basement transect (Sites 1026 and 1027). Proceedings of the Ocean Drilling Program, Initial Reports 168, 101–160.

Shipboard Scientific Party, 2004. Juan de Fuca hydrogeology: The hydrogeologic architecture of basaltic oceanic crust: compartmentalization, anisotropy, microbiology, and crustal-scale properties on the eastern flank of Juan de Fuca Ridge, eastern Pacific Ocean. IODP Prel. Rept. 301.

Shipboard Scientific Party, 2010. Juan de Fuca Ridge-flank hydrogeology: the hydrogeologic architecture of basaltic oceanic crust: compartmentalization, anisotropy, microbiology, and crustal-scale properties on the eastern flank of Juan de Fuca Ridge, eastern Pacific Ocean. IODP Prel. Rept. 327.

Shock, E., Canovas, P., 2010. The potential for abiotic organic synthesis and biosynthesis at seafloor hydrothermal systems. Geofluids 10, 161-192.

Shock, E.L., Holland, M., Meyer-Dombard, D.A., Amend, J.P., Osburn, G.R., Fischer, T.P., 2010. Quantifying inorganic sources of geochemical energy in hydrothermal ecosystems, Yellowstone National Park, USA. Geochimica et Cosmochimica Acta 74, 4005-4043.

Smart, N., Blackwood, D., Werme, L., 2002a. Anaerobic corrosion of carbon steel and cast iron in artificial groundwaters: Part 1-Electrochemical aspects. Corrosion 58, 547-559.

Smart, N., Blackwood, D., Werme, L., 2002b. Anaerobic corrosion of carbon steel and cast iron in artificial groundwaters: Part 2-Gas generation. Corrosion 58, 627-637.

Stein, C.A., Stein, S., Pelayo, A.M., 1995. Heat flow and hydrothermal circulation. Geophysical Monograph Series 91, 425-445.

Stevens, T.O., McKinley, J.P., 1995. Lithoautotrophic microbial ecosystems in deep basalt aquifers. Science 270, 450-454.

Stevens, T.O., McKinley, J.P., 2000. Abiotic controls on H2 production from basalt-water reactions and implications for aquifer biogeochemistry. Environmental Science & Technology 34, 826-831.

Takai, K., Inoue, A., Horikoshi, K., 2002. Methanothermococcus okinawensis sp. nov., a thermophilic, methane-producing archaeon isolated from a Western Pacific deep-sea hydrothermal vent system. International Journal of Systematic and Evolutionary Microbiology 52, 1089-1095.

Teske, A., Dhillon, A., Sogin, M.L., 2003. Genomic markers of ancient anaerobic microbial pathways: sulfate reduction, methanogenesis, and methane oxidation. The Biological Bulletin 204, 186-191.

Torsvik, T., Furnes, H., Muehlenbachs, K., Thorseth, I.H., Tumyr, O., 1998. Evidence for microbial activity at the glass-alteration interface in oceanic basalts. Earth Planet. Sci. Lett. 162, 165-176.

Underwood, M.B., Hoke, K.D., Fisher, A.T., Davis, E.E., Giambalvo, E., Zühlsdorff, L., Spinelli, G.A., 2005. Provenance, stratigraphic architecture, and hydrogeologic influence of turbidites on the mid-ocean ridge flank of northwestern Cascadia Basin, Pacific Ocean. Journal of Sedimentary Research 75, 149-164.

Valentine, D.L., 2011. Emerging topics in marine methane biogeochemistry. Annual Review of Marine Science 3, 147-171.

Valentine, D.L., Blanton, D.C., Reeburgh, W.S., Kastner, M., 2001. Water column methane oxidation adjacent to an area of active hydrate dissociation, Eel river Basin. Geochimica et Cosmochimica Acta 65, 2633-2640.

Valentine, D.L., Chidthaisong, A., Rice, A., Reeburgh, W.S., Tyler, S.C., 2004. Carbon and hydrogen isotope fractionation by moderately thermophilic methanogens. Geochimica et Cosmochimica Acta 68, 1571-1590.

Walker, B.D., McCarthy, M.D., Fisher, A.T., Guilderson, T.P., 2008. Dissolved inorganic carbon isotopic composition of low-temperature axial and ridge-flank hydrothermal fluids of the Juan de Fuca Ridge. Mar. Chem. 108, 123-136.

Wang, G.Z., Spivack, A.J., Rutherford, S., Manor, U., D'Hondt, S., 2008. Quantification of co-occurring reaction rates in deep subseafloor sediments. Geochim. Cosmochim. Acta 72, 3479-3488.

Weiss, R.F., Lonsdale, P., Lupton, J., Bainbridge, A., Craig, H., 1977. Hydrothermal plumes in the Galapagos Rift.

Wheat, C.G., Elderfield, H., Mottl, M.J., Monnins, C., 2000. Chemical composition of basement fluids within an oceanic ridge flank: Implications for along-strike and across-strike hydrothermal circulation. J. Geophys. Res. 105, 13437-13447.

Wheat, C.G., Feely, R.A., Mottl, M.J., 1996. Phosphate removal by oceanic hydrothermal processes: An update of the phosphorus budget in the oceans. Geochim. Cosmochim. Acta 60, 3593-3608.

Wheat, C.G., Jannasch, H., Kastner, M., Hulme, S., Cowen, J., Edwards, K., Orcutt, B., Glazer, B., 2011. Fluid Sampling from Oceanic Borehole Observatories: Design and Methods for CORK Activities (1990-2010), AGU Fall Meeting Abstracts, p. 1458.

Wheat, C.G., Jannasch, H.W., Fisher, A.T., Becker, K., Sharkey, J., Hulme, S., 2010. Subseafloor seawater-basalt-microbe reactions: Continuous sampling of borehole fluids in a ridge flank environment. Geochem. Geophy. Geosy. 11, 1-18.

Wheat, C.G., Jannasch, H.W., Kastner, M., Plant, J.N., DeCarlo, E.H., Lebon, G., 2004a. Venting formation fluids from deep-sea boreholes in a ridge flank setting: ODP Sites 1025 and 1026. Geochem. Geophy. Geosy. 5, 1-12.

Wheat, C.G., McManus, J., Mottl, M.J., Giambalvo, E., 2003. Oceanic phosphorus imbalance: Magnitude of the mid-ocean ridge flank hydrothermal sink. Geophys. Res. Lett 30, 1895.

Wheat, C.G., Mottl, M.J., 1994. Hydrothermal circulation, Juan de Fuca Ridge eastern flank: factors controlling basement water composition. Journal of Geophysical Research 99, 3067-3080.

Wheat, C.G., Mottl, M.J., 2000. Composition of pore and spring waters from Baby Bare: Global implications of geochemical fluxes from a ridge flank hydrothermal system. Geochim. Cosmochim. Acta 64, 629-642.

Wheat, C.G., Mottl, M.J., Fisher, A.T., Kadko, D., Davis, E.E., Baker, E., 2004b. Heat flow through a basaltic outcrop on a sedimented young ridge flank. Geochem. Geophy. Geosy. 15, 1-18.

Whiticar, M.J., 1999. Carbon and hydrogen isotope systematics of bacterial formation and oxidation of methane. Chemical Geology 161, 291-314.

Whiticar, M.J., Faber, E., Schoell, M., 1986. Biogenic methane formation in marine and freshwater environments: CO_2 reduction *vs.* acetate fermentation—Isotope evidence. Geochimica et Cosmochimica Acta 50, 693-709.

Whitman, W.B., Bowen, T.L., Boone, D.R., 2006. The methanogenic bacteria. Prokaryotes 3, 165-207.

Whitman, W.B., Coleman, D.C., Wiebe, W.J., 1998. Prokaryotes: The unseen majority. Proceedings of the National Academy of Sciences of the United States of America 95, 6578-6583.

Wiesenburg, D.A., Guinasso Jr, N.L., 1979. Equilibrium solubilities of methane, carbon monoxide, and hydrogen in water and sea water. Journal of Chemical and Engineering Data 24, 356-360.

Williams, P., 1970. Heterotrophic utilization of dissolved organic compounds in the sea. J. Mar, Biol. Assoc. UK 50, 859-870.

Wilson, S.T., Böttjer, D., Church, M.J., Karl, D.M., 2012. Comparative Assessment of Nitrogen Fixation Methodologies, Conducted in the Oligotrophic North Pacific Ocean. Applied and Environmental Microbiology 78, 6516-6523.

Zeebe, R.E., Wolf-Gladrow, D.A., 2001. CO_2 in seawater: equilibrium, kinetics, isotopes. Elsevier Science.

Zehnder, A., Brock, T., 1979. Methane formation and methane oxidation by methanogenic bacteria. Journal of Bacteriology 137, 420.

Table 3.1. Magnesium corrected methane, hydrogen and dissolved iron concentrations

Sample site		CORK 1362B				CORK 1362A				CORK 1301A		Bottom seawater	
		2011				2011				2008-2011		2008-2010	
Variables	unit	Uncorr.	(n=9)	**Mg Corr.**	(n=9)	Uncorr.	n=6	**Mg Corr.**	(n=6)	**Mg Corr.**	(n=12)	-	(n=5)
Temperature	°C	65[a]	-	**65[a]**	-	65[a]	-	**65[a]**	-	**65**	-	1.7	-
Pressure	bar	271[b]	-	**271[b]**	-	271[b]	-	**271[b]**	-	**270**	-	270	-
pH	-	7.3	-	**7.3**	-	7.5	-	**7.5**	-	**7.4**	(0.1)	7.7	(0.1)
Magnesium	mM	2.4	(1.1)	**1.6**	-	2.8	(0.4)	**2.5**	-	**1.9**	-	53.7	(0.3)
Calcium	mM	55.2	(1.1)	**55.9**	(0.3)	54.1	(0.3)	**54.5**	(0.1)	**55.0**	(1)	10.4	(0.03)
Alkalinity	meq/L	0.50	(0.06)	**0.47**	(0.01)	0.60	(0.01)	**0.58**	(0.02)	**0.45**	(0.04)	2.48	(0.05)
Methane	µM	13	(1)	**13**	(1)	6.1	(0)	**6.1**	(0)	**1.5**	(0)	0.0002*	-
δ^{13}C-methane	‰ (PDB)	-57	(0.6)	-57	(0.6)	-58.3	(0.3)	-58.3	(0.3)	**-42.8**	(1)	-	-
δ^{2}H-methane	‰ (SMOW)	-206	(2)	-209	(2)	-262	(2)	-262	(2)	57	(5)	-	-
Hydrogen	µM	0.08	(0.03)	**0.08**	(0.03)	0.05	(0.02)	**0.05**	(0.02)	**1.1**	(1.2)	0.0004*	-
DOC	µM	12	(1)	**11**	(1)	16	(3)	**16**	(0.4)	**12**	(3)	39	(1)
TOC	µM	19.3	(10)	**15**	(3)	18.7	(3)	**18.7**	(0)	**12**	(3)	39	(1)
TDN	µM	103	(1)	**104**	(1)	103	(0)	**103**	(3)	**103**	(2)	44	(1)
TN	µM	104	(1)	**105**	(0)	105	(1)	**105**	(3)	**103**	(1)	44	(1)
Nitrate	µM	0.03	(0.03)	**0**	(0.09)	0.03	(0.03)	**0**	(0.22)	**0.21**	(0.32)	40.8	(0.39)
Ammonium	µM	100	(0.7)	**101**	(0.4)	98	(0.6)	**99**	(1.0)	**102**	(3.0)	<0.05	-
Sulfate	mM	18.9	(0.1)	**18.8**	(0.1)	18.9	(0.1)	**18.8**	(0.4)	**18.0**	(0.3)	28.4	(0.3)
Chloride	mM	552	(10)	**552**	(2)	548	(2)	**548**	(1)	**552**	(6)	541	(14)
Sodium	mM	-	-	**468[a]**	-	-	-	**468[a]**	-	**468**	(6)	467	(13)
Potassium	mM	-	-	**6.2[a]**	-	-	-	**6.2[a]**	-	**6.2**	(0.4)	10.2	(0.3)
Silicate	µM	1137	(8)	**1147**	(7)	1069	(3)	**1075**	(8)	**1156**	(9)	173	(9)
Phosphate	µM	0.06	(0.02)	**0.06**	(0.02)	0.11	(0.01)	**0.09**	(0.02)	**0.10**	(0.05)	2.89	(0.08)
Sulfide	µM	-	-	**0.17[a]**	-	-	-	**0.17[a]**	-	**0.17**	-		
Dissolved iron	µM	1.3	(0.21)	**1.4**	(0.20)	1.9	(0.34)	**1.9**	(0.37)	**0.8**	(0.27)	<0.1	-

a. Data not available, using values for CORK 1301A fluids.
b. Davis et al., unpublished

*Data from Kelley et al. (1998)

Table 3.2. Values of Gibbs free energy normalized to per electron transferred, $\Delta G_r/e^-$ (kJ/mol e^-), for potential metabolic reactions involving H_2 and CH_4 within basement fluids collected from CORK 1362A, 1362B and 1301A.

Metabolic Reaction	Examples of metabolic pathway	# of e^- transferred	$\Delta G_r/e^-$ (kJ/mol e-) 1362A	1362B	1301A
Methanogenesis	$4\mathbf{H_2}_{(aq)} + HCO_3^-{}_{(aq)} + H^+ \rightarrow \mathbf{CH_4}_{(aq)} + 3H_2O_{(l)}$	8	2.7	2.3	-2.3
Sulfate reduction	$4\mathbf{H_2}_{(aq)} + SO_4^{2-}{}_{(aq)} + 2H^+ \rightarrow HS^-_{(aq)} + 4H_2O_{(l)}$	8	-2.7	-3.4	-8.4
Iron reduction	$\mathbf{H_2}_{(aq)} + Fe_3O_{4(s)} + 6H^+ \rightarrow 3Fe^{2+}_{(aq)} + 4H_2O_{(l)}$	2	-6.7	-7.4	-11.3
Anaerobic methane oxidation	$\mathbf{CH_4}_{(aq)} + SO_4^{2-}{}_{(aq)} \rightarrow HS^-_{(aq)} + HCO_3^-{}_{(aq)} + H_2O_{(l)}$	8	-4.3	-4.5	-3.8

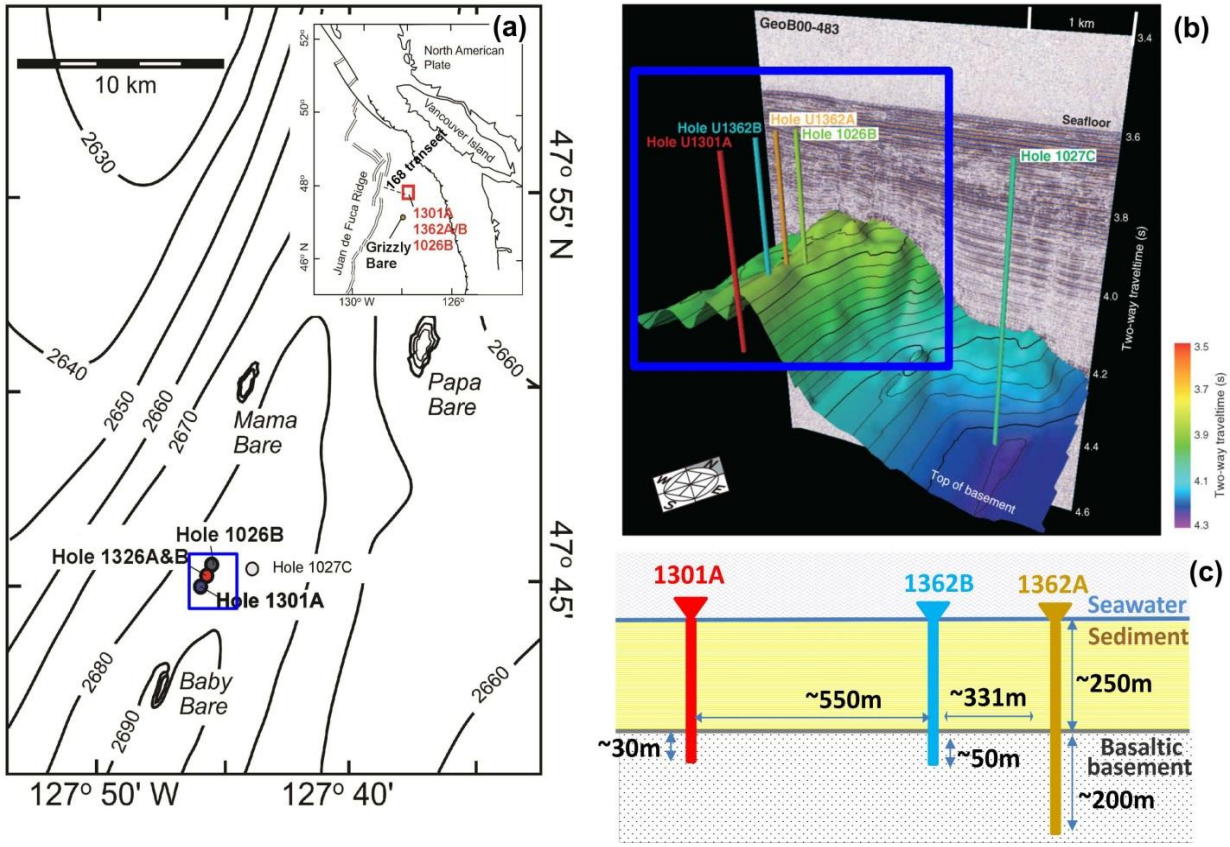

Figure 3.1. Site maps. (a) Regional bathymetric map showing locations of borehole Circulation Obviation Retrofit Kit (CORK) observatories and outcrop seamounts. Grizzly Bare Seamount (shown in insert) is 52km south-south west of Baby Bare shown at the bottom of figure 1a. Modified from Becker and Fisher (2008). (b) Three dimensional perspective view of basement around the CORK cluster. Holes 1362A, 1362B, 1301A and 1026B are all drilled through a topographic high on the seafloor. Figure modified from IODP 327 initial report (Shipboard Scientific Party, 2010). (c) A cartoon showing relative distances and penetration depths of CORKs 1362A, 1362B and 1301A.

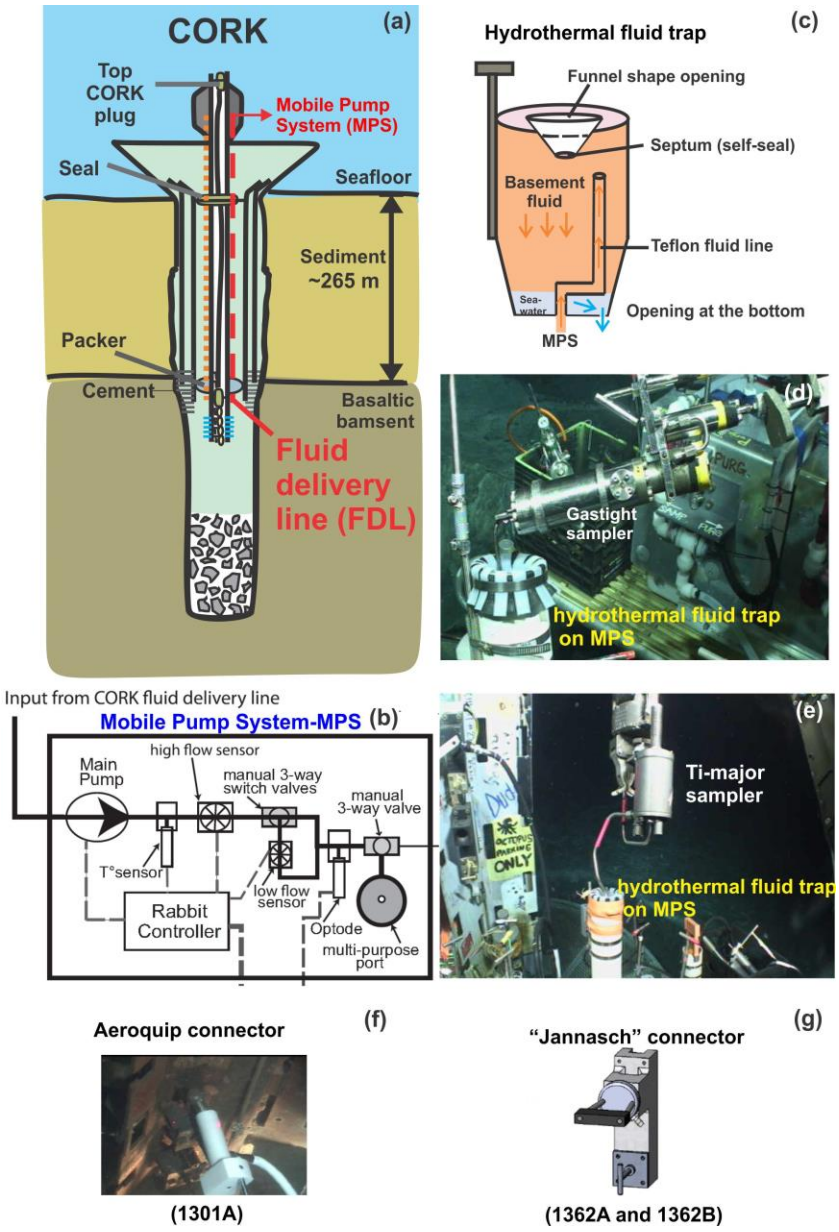

Figure 3.2. Sampling methods. (a) Schematic drawing of a Circulation Observatory Retrofit Kit (CORK). Note that fluid delivery lines, which transports basement fluids from the basement to the seafloor outlet port, runs exterior to the CORK's casing. (b) A diagram of a mobile pump system (MPS), consisting of a powerful pump with a titanium and Teflon pump head and flow rate, temperature and oxygen sensors (Cowen et al., 2012). (c) A hydrothermal-fluid-trap was designed to greatly reduce bottom seawater intrusion during sampling. Warm basement fluid rises up and replaces cold seawater, with several hydrothermal-fluid-trap reservoir volumes, to ensure high sample quality. (d) A gastight sampler is inserted through the septum on top of the hydrothermal-fluid-trap. (e) A Ti-major sampler is being inserted into the hydrothermal-fluid-trap. (f) Aeroquip connector on CORK 1301A. (g) Jannasch connector on CORK 1362A and 1362B.

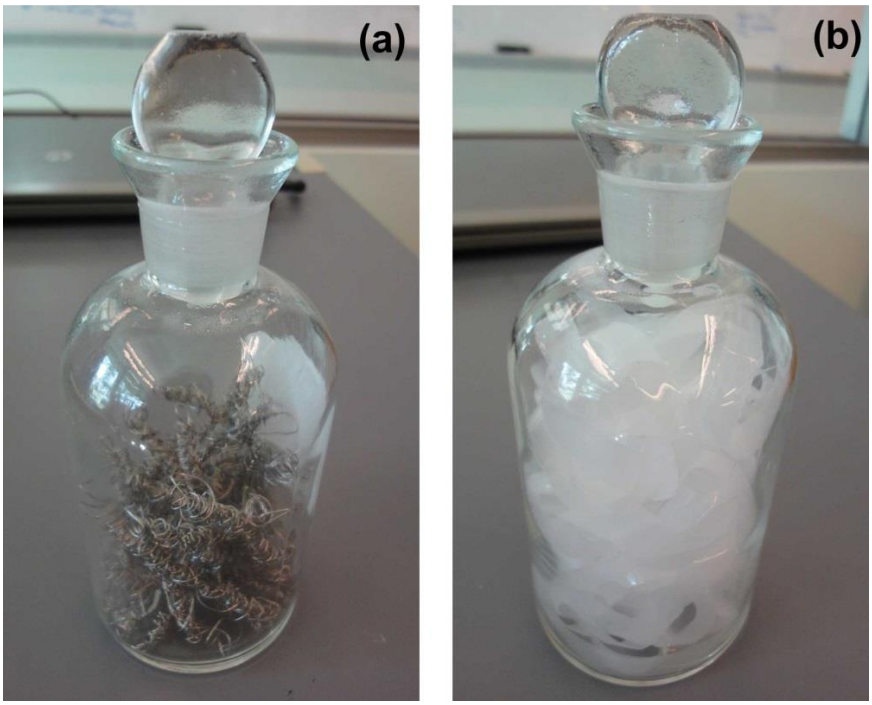

Figure 3.3. (a) Stainless steel bundle and (b) polyvinylidene fluoride (PVDF) strips for a bottle hydrogen production experiment.

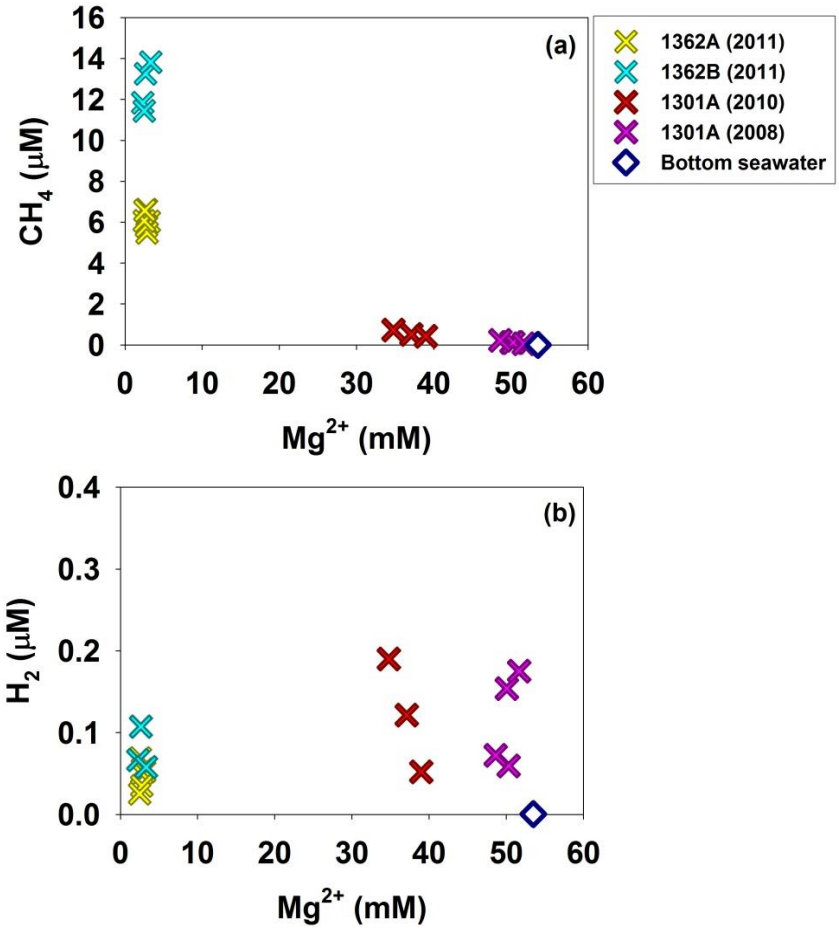

Figure 3.4. Concentration plots for (a) methane and (b) hydrogen versus magnesium for basement fluids collected at CORKs 1362A (light blue cross), 1362B (yellow cross) and 1301A (red cross for 2010 samples; pink cross for 2008 samples) gastight and Ti-major samples. Methane and hydrogen concentration values for seawater (blue open diamond) are also plotted for comparison (Kelley et al., 1998).

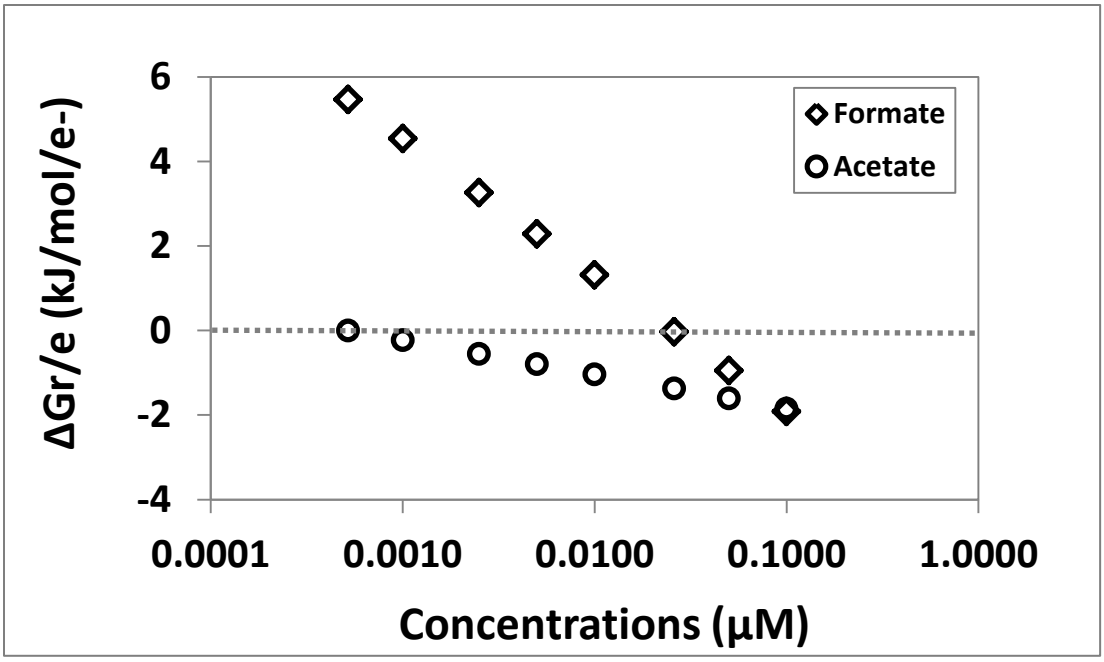

Figure 3.5. Values of Gibbs free energy normalized to per electron transferred, $\Delta Gr/e^-$ (kJ/mol e^-), for hydrogen-producing formate and acetate fermentation reaction at a wide range of formate and acetate concentrations. Formate fermentation: $HCOO^- + H_2O \rightarrow H_2 + HCO_3^-$; Acetate fermentation: $CH_3COO^- + 4H_2O \rightarrow 4H_2 + 2HCO_3^- + H^+$.

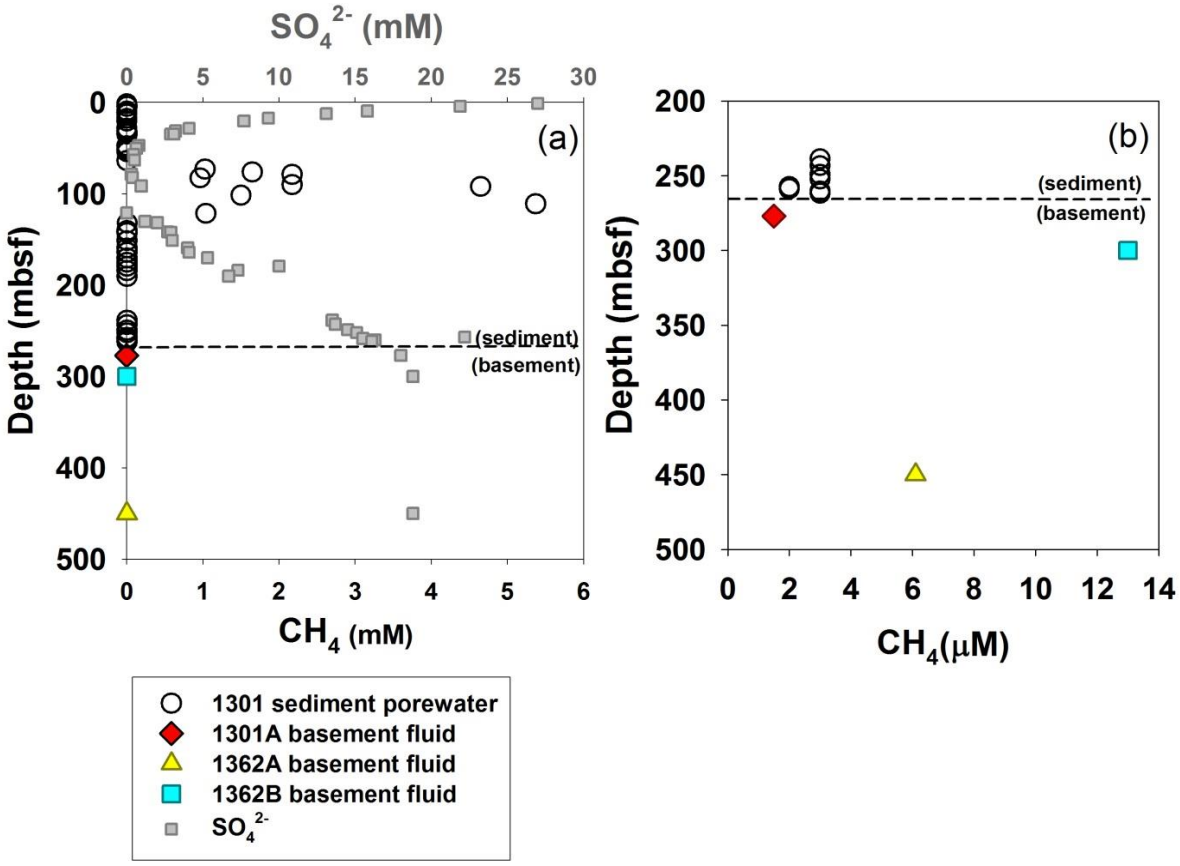

Figure 3.6. Methane concentrations for (a) basement fluids from 1362A, 1362B, 1301A and sediment porewater collected from IODP borehole 1301. (b) redraw of plot (a) with different scale; note the unit for x-axis is "μM" and the y-axis only extends from 200 to 500 meter below seafloor (mbsf). Sulfate concentrations for basement fluids (gray square symbol below the basement-sediment interface) and sediment porewater (gray square symbol above the basemen-sediment interface) are included for comparison. The depths of each basement fluid sample are based on the depth of the intake screen for the respective CORK's fluid delivery lines. IODP U1301 sediment porewater data derived from Shipboard Scientific Party (2004).

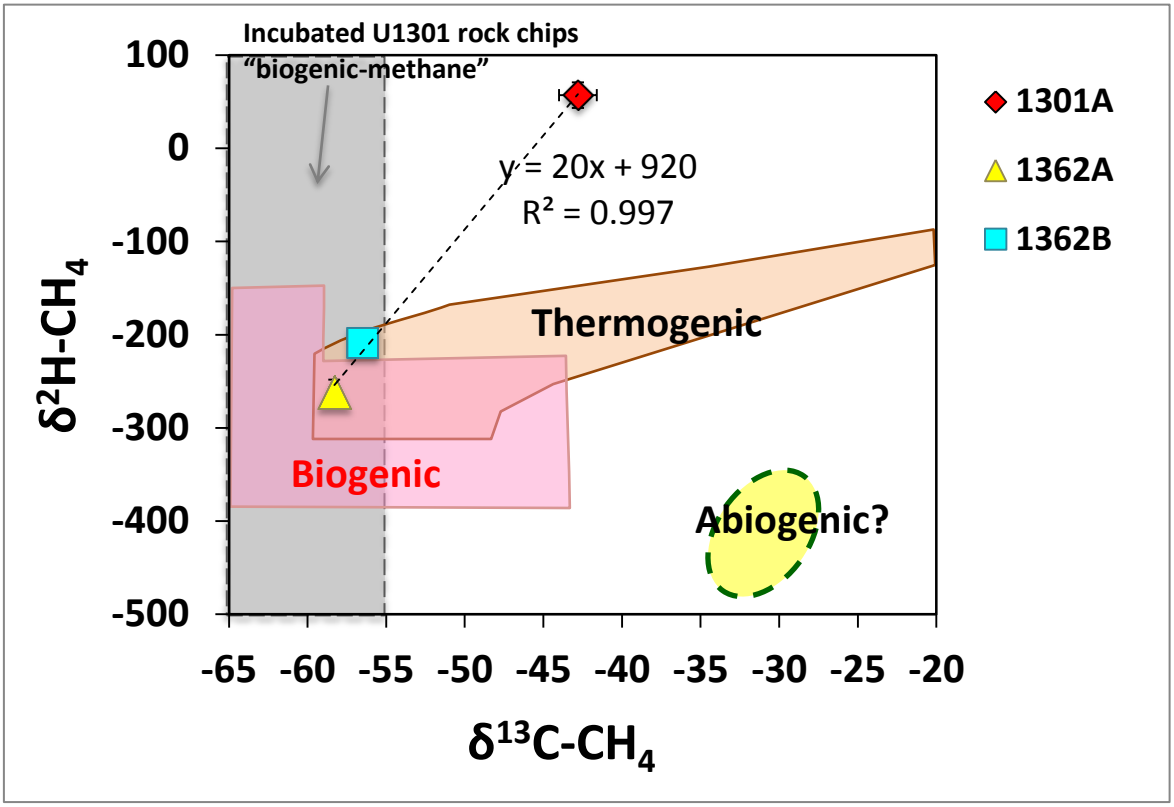

Figure 3.7. Plot of $\delta^{13}C$ versus $\delta^{2}H$ values for methane conventionally used to classify microbial, thermogenic and abiogenic methane. The $\delta^{13}C$-CH_4 and $\delta^{2}H$-CH_4 values for CORK 1301A, 1362A and 1362B basement fluids are plotted. A regression line of the three data points is shown and the equation and the r-squared values are shown next to the line. Plot modified from Sherwood Lollar et al. (2006); data for incubated U1301 rock chips from Lever et al. (2013).

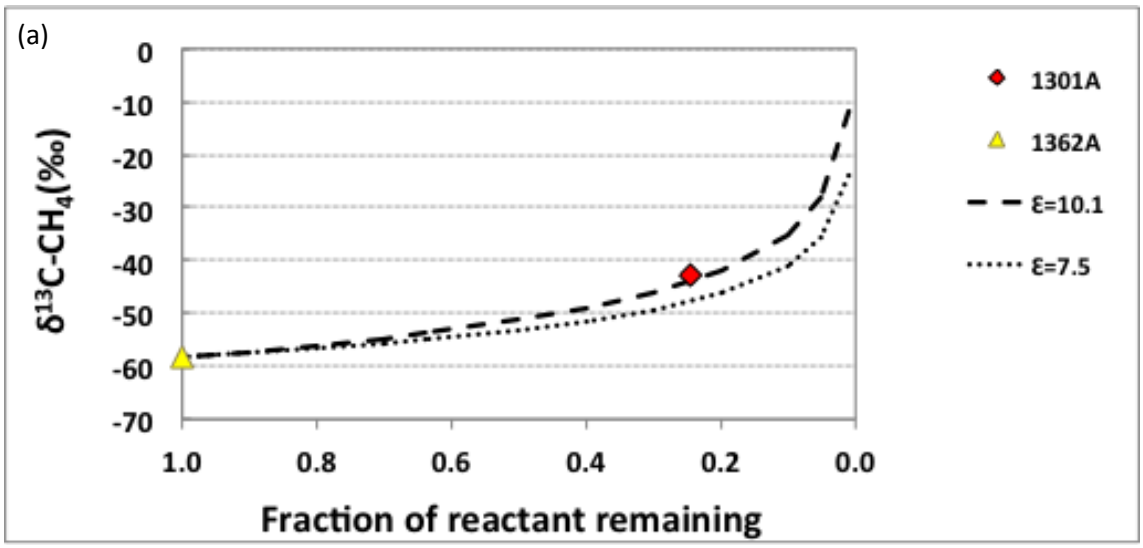
(a)
0
-10
-20
-30
-40
-50
-60
-70
δ13C-CH4(‰)
1.0
0.8
0.6
0.4
0.2
0.0
Fraction of reactant remaining
1301A
1362A
ε=10.1
ε=7.5

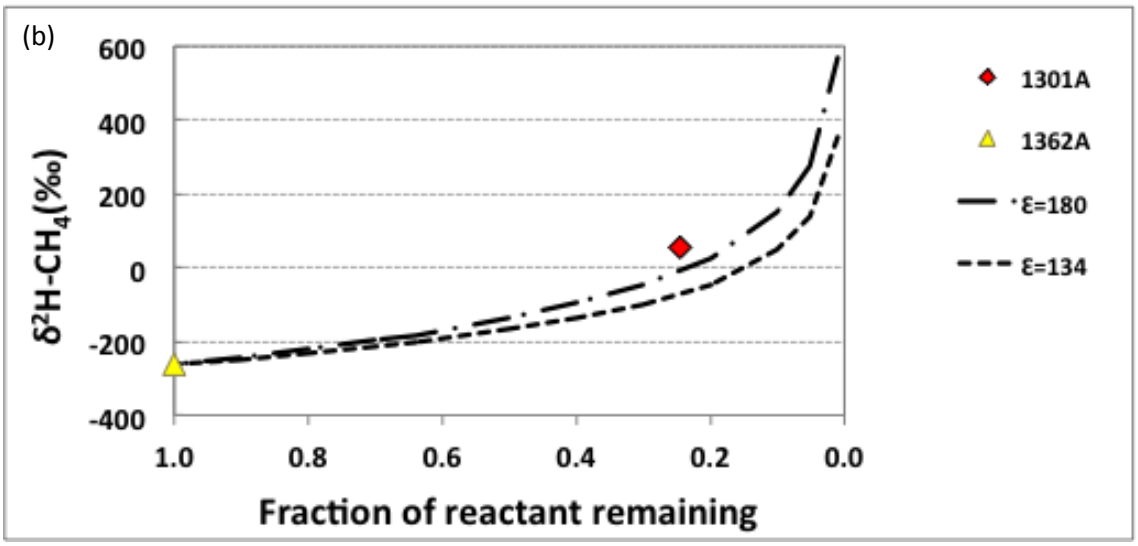
(b)
600
400
200
0
-200
-400
δ2H-CH4(‰)
1.0
0.8
0.6
0.4
0.2
0.0
Fraction of reactant remaining
1301A
1362A
ε=180
ε=134

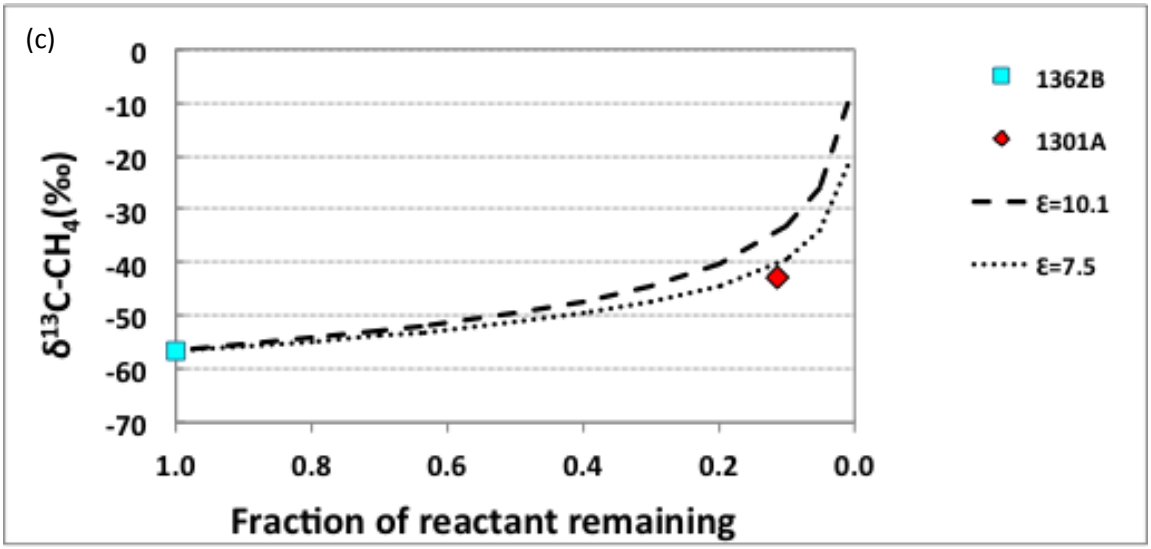

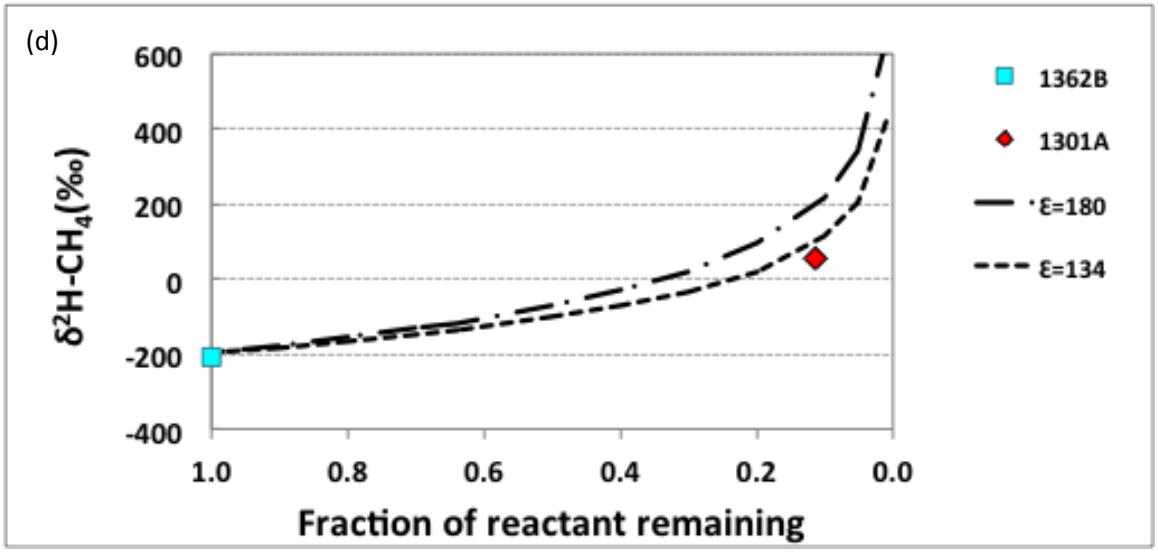

Figure 3.8. Rayleigh isotope fractionation models. (a) Carbon isotope fractionation. The concentration and carbon isotopic compositions of methane in CORK 1362A fluids are used as the initial values. (b) Hydrogen isotope fractionation; CORK 1362A fluid as initial condition. (c) Carbon isotope fractionation; CORK 1362B as initial condition. (d) Hydrogen isotope fractionation; CORK 1362B as initial condition. The fractionation effects, ε, for anaerobic methane oxidation were predicted to be 8.8±1.3 for carbon isotopes and 157± 23 for hydrogen isotopes (Alperin et al., 1988).

CHAPTER4

Dissolved amino acids in basement fluids from sediment-buried eastern Juan de Fuca Ridge flank

By

Huei-Ting Lin

James P. Cowen, Jan P. Amend, Jon-Paul Bingham (coauthors)

Manuscript prepared for submission to Geochimica et Cosmochimica Acta

4.0. Abstract

The ocean crust is the largest aquifer systems on Earth and likely hosts subseafloor biospheres with diverse microorganisms. Labile organic chemical components in the basement fluids, such as amino acids, comprise potential substrates for heterotrophic microorganisms but are largely unexplored. The extent to which the circulating basement fluids have influenced the quantity and quality of the deep ocean labile dissolved organic carbon pool remains unclear. This study provides data on concentrations and compositions of dissolved amino acids measured in fluids from sedimented ridge-flank basement aquifers.

Some dissolved free amino acid (DFAA) concentrations are slightly higher in basement fluids from site 1301A relative to that in bottom seawater. Concentrations of dissolved hydrolysable amino acids (DHAA) in basement fluids from sites 1301A, 1362A and 1362B are all elevated relative to North Pacific deep seawater. Export of fixed carbon in the form of amino acids from the ridge-flank basement fluids into the overlying ocean is plausible. Thermodynamic calculations indicate that the ridge-flank basement environment is not conducive to the abiotic synthesis of free amino acids. Thus, DFAA are likely produced biologically in situ, or imported from an external source such as diffusion from sediment porewaters across the sediment-basement interface. Similarity in mole percent distribution of the DHAA in basement fluids, bacteria biomass and deep sediment porewater supports this view. Differences in diagenetic status of the dissolved amino acids in basement fluid samples collected from different sites or years suggest a dynamic environment and that the basement fluids are not well-mixed at a scale of 200-700m.

4.1. Introduction

The upper (40-500 m) ocean crustal aquifer, representing the largest aquifer on earth, holds hydrothermal fluids equivalent to an estimated 2% of the ocean volume (Johnson and Pruis, 2003). The hydrothermal flux from ridge flanks (crustal age older than 1 My) is estimated to be 5-60% of the riverine input (Mottl, 2003; Wheat et al., 2003). Alteration evidence, including the texture and chemical and isotopic compositions of basaltic glass and rocks, suggests a subseafloor biosphere within the ridge-flank basement (Giovannoni et al., 1996; Fisk et al., 1998; Torsvik et al., 1998; Furnes et al., 2001a; Furnes et al., 2001b; Furnes et al., 2002; Bach and Edwards, 2003; Furnes et al., 2006; Rouxel et al., 2008; Alford et al., 2011; Alt and Shanks, 2011; Ono et al., 2012). Geochemical and microbial data derived from the analyses of ridge-flank crustal fluids also indicate that conditions there are suitable for some level of microbial activity (Cowen et al., 2003; Huber et al., 2006; Orcutt et al., 2011; Lin et al., 2012; Boettger et al., 2013; Jungbluth et al., 2013). The extent to which the deep subseafloor biosphere impacts the global ocean carbon cycle remains largely unexplored.

Organic carbon dynamics is an important and intensely studied component of ocean and global carbon cycling (e.g., Williams and Druffel, 1988, Engleton and Repeta, in press; Hansell and Carlson, 1998). The deep ocean is the largest reservoir of fixed carbon, with a global ocean abundance of dissolved organic carbon (DOC) approximately equal to atmospheric CO_2 (662 Pg C, Hansell et al., 2009). Global oceans circulate through the ocean crustal aquifer on the order of once every 100-500 Kyr (Fisher, 2005a) and the bottom seawater that recharges oceanic crustal fluids contains ~40 µM of DOC (Lang et al., 2006; Lin et al., 2012). When the DOC concentrations of basement fluids (3.5 Ma

upper basement, JFR; Lang et al. 2006, Lin et al. 2012) are plotted with water column DOC values against their corresponding Δ^{14}C-DIC values (Elderfield et al., 1999; Walker et al., 2008) basement fluid DOC data fall below a linear extension of the deep water DOC trend line (Lin et al., 2012), suggesting a dynamic removal of even refractory deep ocean DOC within the low energy basement environment. Yet the radiocarbon composition of the DOC in ridge-flank basement fluids suggests that the DOC is synthesized from inorganic carbon in ridge-flank basement fluids by chemosynthetic microbial communities and possibly resulting in exportation of substantial fixed carbon to the overlying ocean (McCarthy et al., 2010).

Dissolved amino acids are a subclass of bio-utilizable (or labile) dissolved organic carbon which can be readily taken up by microorganisms (e.g. Crawford et al., 1974; Wheeler and Kirchman, 1986), supporting both carbon and nitrogen demands (e.g. Keil and Kirchman, 1991b; Middelboe et al., 1995). Many microorganisms isolated from hydrothermal environments have been shown to utilize amino acids (e.g. Jannasch et al., 1988; Pledger and Baross, 1991; Hoaki et al., 1993; Hoaki et al., 1994; Dirmeier et al., 1998). While amino acids are important for supporting heterotrophic microorganisms, are ubiquitous in living organisms and are widely distributed on Earth's surface (Bada, 1991), their distribution and abundances within hydrothermal ecosystems have been only moderately explored in a few studies (Haberstroh and Karl, 1989; Takano et al., 2003a; Svensson et al., 2004; Klevenz et al., 2010; Lang et al., 2013).

Moreover, total dissolved amino acids (TDAA) only account for about 0.5% of the deep water DOC (Kaiser and Benner, 2009). As a consequence, hydrothermal fluids, including basement fluids, begin with only a small amount of total dissolved amino acids when

deep seawater recharges into a deep submarine hydrothermal system. Whether TDAA decreases as DOC decreases along the crustal fluid circulation pathways or TDAA abundance increases due to in situ production by chemolithoautotrophic production within the basement biospheres, as suggested by McCarthy et al. (2010), is unclear. In this study, we report the concentrations and compositions of dissolved amino acids in ridge-flank basement fluids to help understand the organic carbon pool within the basement and to investigate whether the ridge-flank basement is a source of fixed labile carbon. The new amino acid composition data also provide information on which amino acids are available to be assimilated and /or dissimilated by microorganisms in the basement environment.

In addition, abiotic production of dissolved free amino acids is favorable in some hydrothermal settings (Amend and Shock, 1998). A thermodynamic model is presented to evaluate the energy required for amino acid synthesis in the ridge-flank basaltic environment and to evaluate whether the amino acids observed in the basement fluids could originate from abiotic production.

4.2. Method and materials

4.2.1 Sampling sites

The Eastern flank of the Juan de Fuca Ridge, off the coast of Washington (USA) and British Columbia (Canada), is covered by hemipelagic mud and turbidites transported from the nearby continental margin during the Pleistocene (Davis et al., 1992; Underwood et al., 2005). Sediment thickness is ~250m-thick and overlies ~3.5 Ma basement at our study sites, about 100km east of the active spreading center of the Juan de Fuca Ridge (Figure 1). The thick sediment layer acts as a hydraulic seal preventing direct exchange between bottom seawater and the basement (Davis et al., 1992; Wheat and Mottl, 1994; Shipboard Scientific Party, 1997b, a; Becker and Fisher, 2008). Direct exchange with bottom seawater near these sites is only possible through seamounts and smaller basement outcrops protruding above the sediments to the north (Mama Bare) and south (Baby Bare and Grizzly Bare) of our main study site (Figure1 b). At our study sites, a cluster of boreholes was drilled through ~250m sediments into ~3.5 Ma basement and equipped with Circulation Obviation Retrofit Kit (CORK) observatories (Shipboard Scientific Party, 1997a; Shipboard Scientific Party, 2004; Shipboard Scientific Party, 2010) to provide access to the basement aquifer for hydrological and biogeochemical studies. This study focuses on boreholes1301A, 1362A and 1362B.

Borehole 1301A was drilled and equipped with a CORK during IODP Expedition 301 (Shipboard Scientific Party, 2004). Two new boreholes, 1362A and 1362B, were drilled and had advanced CORKs installed during the IODP Expedition 327 (Shipboard Scientific Party, 2010). CORK 1362B is located ~550 m north-northwest (NNW) of CORK 1301A; CORK 1362A is ~311 m further NNW of 1362B (Figure 1c). The three

CORKs penetrate to different depths within the basaltic basement, permitting monitoring of the circulating fluids at different crustal depths. The fluid intake is ~30 m below sediment-basement interface (mbs) at CORK 1301A, 200 mbs at CORK 1362A and ~50 mbs at CORK 1362B (Figure 1c).

This study also includes the analysis of deep sediment porewater samples from deep sediments on the flanks of Grizzly Bare outcrop. Grizzly Bare outcrop is a large basaltic feature 52 km to the south the CORK clusters (Figure 1d). Five boreholes were cored during IODP expedition 327 at site U1363 (Scientists, 2011b). Borehole 1363D has the thickest sediment cover, with a sediment-basement interface depth of 231 meter below seafloor (mbsf). Sediment was cored and sediment porewater samples collected from only the lower portion (200-222 mbsf) of the borehole (Scientists, 2011b). The geochemical compositions of the sediment porewater collected near the sediment-basement interface indicate that the deep portion of the sediment is influenced by basement hydrothermal fluids (Scientists, 2011b). The deep sediment porewater at site 1363D is more altered relative to seawater than it is in the other shallower boreholes at site 1363 but is less altered than the basement fluids at sites 1301A, 1362A and 1362B (chapter 2 and Table 3.1) or the spring fluids discharged from outcrop Baby Bare and Mama Bare spring fluids (Scientists, 2011b). Progressively altered basement fluid with increasing distance from Grizzly Bare outcrop is inferred by the sediment porewater geochemical data from the five boreholes (Scientists, 2011b).

4.2.2 Sampling methods

Sampling methods for this study have been described in Cowen et al. (2012) and chapter 2. Briefly, basement fluids were collected via fluid delivery lines (FDL) that run exterior to the CORK's iron casing from basement depths to the seafloor outlet port. The FDLs consist of either 316 stainless steel (1301A) or Tefzel (ethylene-tetrafluoroethylene fluoropolymer) tubing (1362A and 1362B). A mobile pump system (MPS), transported and powered by the remotely operated vehicle (ROV) *Jason* or human-occupied vehicle (HOV) *Alvin* was used to pump the fluid up through the lengthy FDLs and direct it into 60L large volume Tedlar (polyvinyl fluoride) bag samplers (LVBS) in 2009 and 2010 from CORK 1301A and 15L foil-lined, gamma irradiated medium volume polyethylene inner-liner bag samplers (MVBS) from CORKs 1301A, 1362A and 1362B in 2011.

Aliquots of basement fluids were subsampled into acid-cleaned, 20mL combusted (550°C, 5 hours) glass scintillation vials once the LVBS or MVBS was returned to ship. Subsampling was conducted inside a laminar flow hood with high-efficiency particulate air (HEPA) filter. The fluid samples were then stored frozen at -20°C until analysis. Sampling blanks, including LVBS and MVBS sampling and shipboard subsampling, made by processing deionized water do not show significant amino acids contamination.

Details of sediment porewater sampling procedures are described in the IODP 327 proceeding report (Scientists, 2011a). Briefly, a titanium squeezer with a hydraulic press piston was used to squeeze sediment porewater from a 10-40cm whole-round sediment sample. Before pressing, the outside layer of the sediment core was

carefully scrapped to remove potential contamination from drill fluids and surface water. Porewater was passed through a prewashed Whatman number 1 filter above a titanium screen, filtered through a 0.45 µm Gelman polysulfone disposable filter and subsequently into an acid-cleaned, 20mL-combusted (550°C, 5 hours) glass scintillation vial. Porewater samples were kept frozen at -20°C until analysis.

4.2.3 Amino acids analysis

4.2.3.1 Hydrolysis

Fluid samples were hydrolyzed to obtain total dissolved hydrolysable amino acid (DHAA), which consists of dissolved free amino acids (DFAA) and dissolved combined amino acids (DCAA) such as peptides and proteins. DHAA is considered equivalent to the total dissolved amino acids (TDAA). Vapor phase hydrolysis was performed using a modified procedure described by Keil and Kirchman (Keil and Kirchman, 1991b), using a vacuum-heating hydrolysis system (PicoTag^{TM}, WATERS). Briefly, a 100µl-fluid sample was pipette into a muffled 1mL glass insert using an acid and methanol washed pipette tip (Kaiser and Benner, 2005). Eight to twelve glass inserts were placed into a 40mL hydrolysis reaction vial. The samples within the reaction vials were flushed with nitrogen three times and dried under vacuum until vacuum reached <80m Torr. Then 2.1 mL (12×0.175mL) of 7N, 10% trifluoroacetic acid, 0.1 % phenol was added to the reaction vial. The reaction vial was heated under vacuum to allow acid boiling for 20 seconds and flushed with nitrogen for three complete cycles to allow the hydrolysis be taken place under a nitrogen atmosphere (anoxic). Samples were hydrolyzed in the vapor phase at 156°C for 23 minutes. After hydrolysis, samples were dried under vacuum to remove any

acid and the hydrolysate was dissolved in 100 µl DI for subsequent free amino acid analysis by HPLC.

4.2.3.2 Amino acid characterization and quantification

Characterization and quantification of amino acids was carried out in an automated HPLC system (Alliance Separation Module 2690, Waters). The stationary system was a 2.1mm* 150mm Hypersil Gold column packed with 3 µm C-18 spheres (Thermo Scientific). Sample pH was first adjusted by adding a one-to-ten volume ratio of borate buffer (0.4 M, pH 10.5) into the sample (Grasshoff et al., 1999; Svensson et al., 2004). Then 10 µL of o-phthalaldehyde (OPA) derivatization reagent (100mg of OPA in 0.5 mL methanol and 0.05 mL of 2-mercaptoethanol) was added into 1mL of pH adjusted sample (Grasshoff et al., 1999) by the auto-sampler of the HPLC system and was allowed to react with the sample for exactly 10 minutes. 30 µL of derivatized sample were then injected into the separation column.

The mobile phases of the separation were 20 mM sodium acetate trihydrate with 0.3% tetrahydrofuran (pH adjusted to 7.1 using 2% acetic acid) and 100% methanol. The gradient started with 15% methanol and increased to 18% in the first 6 minutes. Then methanol increased to 22 % at 10 minutes, 38 % at 25 minutes, 55 % at 59 minutes and 100% at 70 minutes. The gradient was followed by 10 minutes of 100% methanol for column cleanup. This gradient system allows separation of 18 protein-forming amino acids, including aspartic acid (ASP), glutamic acid (GLU), glutamine (GLN), serine (SER), asparagine (ASN), histidine (HIS), glycine (GLY), threonine

(THR), arginine (ARG), alanine (ALA), tyrosine (TYR), tryptophan (TRY), methionine (MET), valine (VAL), phenylalanine (PHE), isoleucine (ILE), leucine (LEU) and lysine (LYS); and 2 non-protein amino acids, ϒ-aminobutyric acid (GABA) and β-alanine (BALA). The OPA derivatized amino acids were detected by a fluorescence detector (RF-20Axs, Shimadzu); excitation wavelength set at 340nM and emission at 420nM.

4.2.3.3 Calibration and limits of detection

Calibrations of amino acids were made by using a premixed Amino Acid Standard H, GABA and BALA standards (PIERCE). Since tryptophan degraded (e.g. Coffin, 1989), asparagine turned into aspartic acid, and glutamine turned into glutamic acid (e.g. Keil and Kirchman, 1991b) during the hydrolysis step, these three amino acids were not calibrated and reported. Limits of detection (S/N=3) were 3-30 fmol, equivalent to 0.1-1 nM at the 30uL injection volume for individual amino acids. Reagent blanks were estimated by analyzing deionized water every day and were 0.1-2 nM of individual amino acids; reagent blanks were subtracted from the DFAA measured on the same day as the reagent blanks (fresh OPA reagents were made daily). Hydrolysis blanks monitored for each batch of hydrolysis ranged from 16-42 nM total amino acids and were subtracted from the samples hydrolyzed at the same time. Lysine (LYS) was much less sensitive than all other amino acids with the column and derivatizing agent used and had a limit of detection of ~3 nM.

4.2.3.4 Ammonium removal

High concentrations of ammonium (> 10mM) in Guaymas Basin sediment porewaters are suggested to contribute to multiple uncharacterized peaks observed in OPA-derivatized chromatograms (Haberstroh and Karl, 1989). We also observe that much higher ammonium concentrations (>100 μM) relative to amino acids concentrations in the basement fluid (~50-90 nM) and sediment porewater samples (~200-3000 nM) cause interferences in quantifying phenylalanine, isoleucine and leucine. Purging of pH adjusted samples was conducted in a 12-mL combusted glass tube to remove the abundant ammonium. Exactly 3 mL of sample was added to 0.3 mL of borate buffer (0.4 M, pH 10.5). The final pH of the seawater samples was ~9.5 and ammonium was effectively removed (down to <5 μM) after 90 minutes of purging with nitrogen. Since purging also accelerated evaporation, samples were weighted before and after purging to evaluate the degree of pre-concentration of the dissolved constituents in the samples. Samples were typically concentrated about 1.4 times (n=36). The purging device was made with clean Tygon and Teflon tubes. Only acid-cleaned Teflon tubing was inserted into sample. The flow of nitrogen gas was adjusted so that enough fluid turbulence was created inside the glass tube but the fluid did not over flow. No significant change in amino acids compositions or concentrations (i.e. no contamination) was observed during the purging process based on several DI and surface seawater analysis. No significant differences were observed between concentrations of amino acids not affected by ammonium measured for purged and non-purged samples. Average values of these amino acids for purged and non-purged samples are reported. Concentrations of phenylalanine, isoleucine and leucine for the purged samples are reported.

4.2.4 Thermodynamic modeling

The amount of energy released or required from amino acid synthesis reactions can be expressed as the Gibbs free energy of reaction (ΔG_r), calculated as:

$$\Delta G_r = \Delta G_r^\circ + RT\ln Q_r, \quad (1)$$

where ΔG_r° is the standard state Gibbs energy of reaction at the temperature and pressure of interest and R and T are the gas constant and temperature in degrees Kelvin, respectively. Q_r is the reaction quotient and can be calculated according to:

$$Q_r = \Pi(a_i^{vi,r}), \quad (2)$$

where a_i denotes the activity of chemical species i, and $v_{i,r}$ is its stoichiometric coefficient in reaction r, which is negative for reactants and positive for products. The activity is calculated using the concentrations of the species and their individual ion activity coefficients at in situ temperatures. Values of ΔG_r° at in situ temperature (65°C) and pressure (270 bar) were computed using the SUPCRT 92 software package (Johnson et al., 1992). Reactions used for thermodynamic calculation are listed in Table 4.1. The physical and geochemical data used for the calculation are from table 1 in Chapter 2, table 1 in Chapter 3.

4.2.5 Statistics

Pearson correlation coefficients were calculated for the concentrations of DHAA in ridge-flank basement fluids to help decipher whether significant correlations exit among the investigated amino acids across sites and sampling times. Confidence intervals ($\alpha \leq 0.05$ and $\alpha \leq 0.01$) were used to describe the statistical significance of each correlation.

4.3. Results

4.3.1. Basement fluids

Concentrations and distributions of dissolved amino acids for the basement fluid samples collected from our study sites on the eastern flanks of Juan de Fuca Ridge are summarized in Table 4.2. The concentrations are also converted into mole percentages for easy comparison and are summarized in Table 4.3 and plotted in Figure 4.3. The total concentrations of DFAA and DHAA for the basement fluid samples range from 1-13 nM and 52-89 nM, respectively. Much higher concentrations of DHAA than DFAA are present in all of the basement fluid samples collected, and DFAA fraction represents only between 2 and 15% of the DHAA.

Although DFAA are only present in trace amount (near reagent blanks 0.1-2nM), the DFAA detected (>3 times deviation) in basement fluid samples include aspartic acid (ASP), serine (SER), histidine (HIS), glycine (GLY), alanine (ALA), valine (Val). The frequency of occurrence is the highest for alanine, which is present in CORK 1301A samples collected in 2009 and 2010, and in both CORK 1362A and 1362B samples collected in 2011. No phenylalanine (PHE), leucine (LEU), lysine (LYS), ϒ-aminobutyric acid (GABA) or β-alanine (BALA) are present as DFAA.

All amino acids measured except lysine were present in the DHAA fraction of the basement fluid samples. The more abundant amino acids (>10 mole %) of DHAA in all basement fluid samples collected include aspartic acid, glutamic acid, serine and glycine (Table 4.3). These four amino acids together represent 51-71% of the DHAA. The non-

protein amino acid ϒ-aminobutyric acid (GABA) is also abundant in CORK 1301A (11%) and in CORK 1362A (30%) basement fluid samples collected in 2011 (Table 4.3). DHAA comprise on average 2.2±0.7 % of the DOC in the basement fluid samples collected from the eastern flanks of Juan de Fuca Ridge.

4.3.2. Deep sediment porewater

The concentrations and distributions of dissolved amino acids in the deep sediment porewater samples collected from IODP borehole 1363D are summarized in Table 4.4 and the amino acids mole percentages are summarized in Table 4.3. The total concentrations of DFAA and DHAA for the sediment porewater samples range from 227-1653 nM and 815-3079 nM, respectively. Although the lowest concentrations of DFAA (227nM) and DHAA (815nM) are found in the deepest sediment porewater samples (222m), no significant variation in DFAA or DHAA concentrations with depth is observed over the limited depth range of sediment porewater analyzed.

The DFAA represents about 34% of the DHAA in the deepest sediment porewater sample (222m). The DFAA fraction comprises about 50-54 % of the DHAA in the porewater samples from the other three shallower depths. Except for lysine, all of the amino acids measured are detected in the DFAA fraction of the deep sediment porewater samples (Table 4.3 and 4.4). Aspartic acid (ASP), glutamic acid (GLU), serine (SER), glycine (GLY) and alanine (ALA) are the more abundant amino acids in the DFAA fraction, all together representing 64-75% of the entire DFAA pool. The DFAA represent between 1% and 4% of DOC within the deep sediment porewater samples, compared to <0.3% for the basement fluids (Table 4.2 and 4.4).

All of the 17 amino acids measured are present in the DHAA of the deep sediment porewater samples collected. The five most abundant amino acids (ASP, GLU, SER, GLY and ALA) found in the DFAA fraction are also very abundant in the the DHAA fraction, all together representing 64-78% of all the DHAA pool (Table 4.3). The DHAA pool comprises 2.7-6.9% of DOC within the deep sediment porewater samples (Table 4.4), compared to 1.4-3.3% for the basement fluid samples (Table 4.2).

4.3.3. Results of thermodynamic calculation

The results of the thermodynamic calculations are shown based on a wide range of hydrogen concentrations (i.e. redox conditions; Figure 4.2). Gibbs free energy is positive for the synthesis of each of the 20 protein-forming amino acids at the concentrations of H_2 observed in ridge-flank basement fluids (H_2=0.05-1.1 μM, see chapter 3). Energy requirement decreases with increasing hydrogen concentrations. Among the three study sites, the amount of energy required for synthesizing protein amino acids is smallest at site 1301A.

4.4. Discussions

4.4.1. Concentrations of amino acids in basement fluids

4.4.1.1. *DFAA*

The DFAA concentrations in basement fluids from sites 1301A, 1362A and 1362B (1-13 nM) are slightly higher than the undetectable DFAA (<1nM) in high temperature (152-319°C) smoker vent fluids at Guaymas Basin (Haberstroh and Karl, 1989). The undetectable DFAA in these Guaymas Basin fluids have been explained as the result of

the instability of the amino acids at extremely high temperatures and pressure (Haberstroh and Karl, 1989). Such an interpretation is confirmed by laboratory experiments which show complete decomposition of amino acids at 250°C after 240 hours (Ito et al., 2006). Although the same amino acid decomposition experiment does not cover the temperature of our study sites (65°C), much less decomposition was observed in the same study at 100°C than at higher temperatures (Ito et al., 2006). We infer that the thermal decomposition of particulate or combined amino acids into free amino acid will be minor at the modest temperature (65°C) within the ridge-flank basement environment; thus, the presence of DFAA is not surprising.

The concentrations of DFAA in the ridge-flank basement fluids (1-13 nM) is significantly lower than that in hydrothermal fluid samples collected from mid-Atlantic Ridge diffuse vents (0.035-24.9 μM, Klevenz et al., 2010) and from mid-Atlantic Ridge high temperature vents (0.038-0.377 μM, Klevenz et al., 2010). Diffuse vent systems tend to promote production of DOC (chapter 5; Lang et al., 2006), likely due to prosperous surface and subsurface biospheres that intensify the biological production of labile organic compounds including amino acids. In contrast, the basement environment is a DOC sink although it is still conducive to biological production; lower concentrations of DFAA in the ridge-flank basement environment than in the diffuse vent are expected. However, higher concentrations of DFAA in the mid-Atlantic high temperature vent fluid samples than that in the basement fluids are unexpected as heat degradation at 300°C should have destroyed the DFAA as suggested by Ito et al (2006); no explanations of this issue have been provided by Klevenz et al. (2010).

DFAA concentrations in the ridge-flank basement fluids (1-13 nM) are much lower in comparison to the micro-molar level of DFAA in deep sediment porewater from the Juan de Fuca Ridge flank (0.23-1.46 µM, Table 4.4), shallow submarine hydrothermal vents (1.33-1.92 µM, Svensson et al., 2004), geothermal wells (0.33-78 µM, Svensson et al., 2004) and hydrothermal-influenced surface marine sediment porewater (5-446 µM, Haberstroh and Karl, 1989; Hoaki et al., 1995). The high concentrations of DFAA in the non-ridge flank hydrothermal environments are consistent with the high DOC in these hydrothermal environments (56 to ~5000 µM, Haberstroh and Karl, 1989; Hoaki et al., 1995; Svensson et al., 2004) while the low DFAA in the ridge-flank basement fluids are accompanied by low DOC (12-16 µM, Table 4.2). The elevated concentrations of DFAA in the hydrothermal-influenced surface sediment porewater have been explained by indirect low-temperature heating (5-100°C), decomposition of sedimentary particulate organic carbon and the elevated numbers of microorganisms residing in the sediments sustained by the reduced inorganic substrates in the hydrothermal fluids percolating through the sediments (Haberstroh and Karl, 1989). The same mechanisms may explain the elevated DFAA (0.23-1.46 µM) observed in the deep marine sediment porewater from the Juan de Fuca Ridge flanks. The elevated DFAA in the deep sediment porewater could diffuse downward to contribute to the much lower DFAA basement fluids.

4.4.1.2. DHAA

Total DHAA in basement fluids (53-89 nM) is much lower than that in ~90°C deep submarine Lost City vent fluids (736-2300 nM, Lang et al., 2013, Table 4.5) and is equivalent to or lower than that in ~300°C high temperature vent fluids from Suiyo Seamount (67-1082 nM, Horiuchi et al., 2004). The high DHAA in the Lost City vent

fluids are attributed to intensified chemolithoautotrophic production as evidenced by the stable carbon isotopic values of the amino acids (Lang et al., 2013). The presence of higher concentrations of DHAA in the high temperature fluids than in the basement fluids are more surprising as heat degradation at 300°C should have degraded the DHAA as suggested by Ito et al (2006), although Horiuchi et al. (2004) did not offer explanations on this issue.

The DHAA in basement fluids (53-89 nM) are also much lower than the micro-molar levels of DHAA in shallow submarine hydrothermal vents (Svensson et al., 2004), terrestrial geothermal wells (Svensson et al., 2004), subterranean hydrothermal vent (Takano et al., 2003b), and in hydrothermal-influenced marine sediment porewater (Hoaki et al., 1995). Svensson et al., 2004 suggest that the high DHAA concentrations in the terrestrial geothermal wells result from lower adsorption of amino acids onto particles under elevated temperatures (~80°C) and low pH (~2, Svensson et al., 2004). As described earlier, the DOC concentrations (56-5000µM) in these hydrothermal ecosystems are much more elevated than in the ridge-flank basement (12-16 µM). There is also less particulate organic carbon (<1µmol-C/L, this study) that can be heat degraded to produce DHAA within the ridge-flank basement environment, contributing to the much lower observed DHAA. Overall, DHAA concentrations within the ridge-flank basement fluids are at the very low end of the range of DHAA observed in various hydrothermal fluids.

4.4.1.3. DFAA/DHAA ratio

DFAA/DHAA ratios for ridge-flank basement fluids range from 0.08 to 0.15 at site 1301A and between 0.02 and 0.03 at sites 1362B and 1362A. The low DFAA/DHAA ratios indicate that dissolved combined amino acids (DCAA) are the predominant form of dissolved amino acids in ridge-flank basement fluids. Low DFAA/DHAA ratios are generally observed for seawater samples (Lee and Bada, 1975; Keil and Kirchman, 1999; Kaiser and Benner, 2009) and have been explained by the preferential uptake of DFAA over DCAA by marine microorganisms (Keil and Kirchman, 1991a; Middelboe et al., 1995) and/or by the adsorption of DFAA onto particles (Lee and Bada, 1975). Similar mechanisms may explain the low DFAA/DCAA ratios for the basement fluids.

In contrast, DFAA/DHAA ratios for Vulcano shallow submarine hydrothermal vents and geothermal wells are between 0.33 and 0.87 and have been attributed to in situ acid hydrolysis and heat decomposition (Svensson et al., 2004). Unlike the acidic condition (pH=2-6.3) in the Vulcano hydrothermal solutions, ridge-flank basement fluids are at neutral pH. The production of DFAA via acid hydrolysis within ridge-flank basement fluids is unlikely and the low DFFF/DHAA ratios observed are not surprising.

4.4.2. Compositions of amino acids in basement fluids

The detectable amino acids within the basement fluids' DFAA pool include aspartic acid, serine, histidine, glycine and valine, while aspartic acid, glutamic acid, serine and glycine comprise the more abundant amino acids within the DHAA pool, with glycine being the most abundant (Table 4.3 and Figure 4.3). Glycine is also very abundant in marine DOC (Yamashita and Tanoue, 2003), marine high-molecular-weight (HMW) DOC (McCarthy et al., 1996) and unfiltered seawater (Kaiser and Benner, 2009). The similar distribution

of their total hydrolysable amino acids (THAA) suggests that marine DOC, HMW-DOC and sediment trap particle samples reflect a source-like (phytoplankton and bacteria) amino acid distribution (Aluwihare and Meador, 2008). A source-like pattern in the amino acid distribution is also observed for ridge-flank basement fluid DOC, North Pacific deep water (Kaiser and Benner, 2009), bacteria (Cowie and Hedges, 1992), deep seawater HMW-DOC(McCarthy et al., 1996) and deep sediment porewater DOC (Figure 4.3).

Some differences in amino acids compositions for ridge-flank basement fluid DOC, North Pacific deep water (Kaiser and Benner, 2009), bacteria (Cowie and Hedges, 1992), deep seawater HMW-DOC(McCarthy et al., 1996) and deep sediment porewater DOC, however, do exist and have been linked to the extent of organic matter degradation (Aluwihare and Meador, 2008; Kaiser and Benner, 2009). For example, the basement fluids are more enriched in both serine and glycine than bacteria (Figure 4.3). The accumulation of serine and glycine in marine sinking particulate organic matter (Cowie and Hedges, 1992), marine DOC (Hubberten et al., 1995; Yamashita and Tanoue, 2003) and HWM-DOC (McCarthy et al., 1996) has been attributed to the preferential preservation of the two amino acids during degradation (Dauwe et al., 1999; Aluwihare and Meador, 2008) since the two amino acids are enriched in the relatively unreactive cell wall proteins (Hecky et al., 1973). The relatively higher abundance of serine and glycine in ridge-flank basement fluids than in bacteria may be due to such preferential preservation mechanisms.

Another apparent difference is the enrichment of the non-protein amino acids ϒ-aminobutyric acid and β-alanine in the ridge-flank basement fluids relative to bacterial

biomass (Cowie and Hedges, 1992) and deep seawater HMW-DOC (McCarthy et al., 1996), although the enrichment of the two amino acids is also observed in deep seawater (Kaiser and Benner, 2009) and ridge-flank deep sediment porewater (Figure 4.3). ϒ-aminobutyric acid and β-alanine have been suggested to be produced from partial decarboxylation of glutamic acid and aspartic acid, respectively (Schroeder, 1975; Whelan, 1977; Lee and Cronin, 1982), and has generally been used as an indicator of organic carbon aging or diagenesis (Cowie and Hedges, 1994; Dauwe et al., 1999; Kaiser and Benner, 2009). The presence of ϒ-aminobutyric acid and β-alanine in basement fluids and deep sediment porewater may indicate that the DOC within the study sites at the time of sampling is aged and degraded.

A Pearson correlation matrix was generated to investigate the relative compositional variations in amino acids within the basement fluids across study sites and sampling times (Table 4.6). Concentrations of individual amino acids within the DHAA pool are, in many cases, correlated with each other. The correlated amino acids may imply similar or related source and sink mechanisms. For example, the well-correlated tyrosine (TYR) and glutamic acids (GLU) within the basement fluids (Figure 4.4a) can be explained by their relatively high concentration in cell plasma (Hecky et al., 1973) and since both tend to be depleted during degradation (Cowie and Hedges, 1994). The inverse concentration trend observed between ϒ-aminobutyric acid (GABA) and glutamic acids (GLU, Figure 4.4b) has been suggested to be a result of partial decarboxylation of glutamic acids that forms ϒ-aminobutyric acid (Schroeder, 1975; Whelan, 1977; Lee and Cronin, 1982). The inverse parent (GLU)-daughter (GABA) trend has often been observed in surface

sediments (e.g. Cowie and Hedges, 1994) and ocean water column (e.g. Kaiser and Benner, 2009).

4.4.3. Potential sources of amino acids in the basement fluids

The similarities in the distribution of amino acids within basement fluids, deep seawater, deep sediment porewater, and bacterial biomass (Figure 4.3) suggest that the amino acids within the basement fluids may originate from any combination of these sources. Since the total DHAA concentrations for basement fluids (52-89 nM) is greater than that in North Pacific deep seawater (~50nM, Kaiser and Benner, 2009), deep seawater that recharges into basement cannot be the sole source of DHAA in the ridge-flank basement fluids. In contrast, diffusional input from overlying sediment porewater is a likely source of amino acids to basement fluids as the DFAA concentration in the deep sediment porewater (277 nM) collected near the sediment-basement interface (222m) is one to two orders of magnitude higher than that in the basement fluids (1-13 nM); the DHAA in the same deep sediment porewater (815 nM) is 9-15 times higher than that in the ridge-flank basement fluids (Table 4.2 and 4.4).

Biological production of fixed carbon, including amino acids, by chemoautotrophic microorganisms in the basement environment and leaching of amino acids from these microorganisms into the basement fluids is also plausible. The basement fluids, despite their presumed anemic energy yields (Boettger et al., 2013), are conducive to a wide variety of chemolithoautotrophic metabolisms including hydrogenotrophic sulfate reduction, hydrogenotrophic iron reduction, anaerobic methane oxidation by sulfate (chapter 3) and anaerobic methane oxidation by ferric iron (Boettger et al., 2013). The

presence of chemolithoautotrophic activities within the ridge-flank basement environment is also supported by the low $\delta^{34}S$ values of pyrite from basaltic rock collected from site 1301 cores (Ono et al., 2012; Lever et al., 2013) and by the radiocarbon and stable carbon isotopic compositions of the DOC in ridge-flank basement fluids (McCarthy et al., 2010).

Abiotic production has long been proposed as a source of amino acids in hydrothermal systems and its potential has been evaluated by thermodynamic modeling (e.g. Shock, 1990; Amend and Shock, 1998; Shock and Canovas, 2010). In this study, thermodynamic calculations show that syntheses of none of the 20 protein-forming amino acids within the basement fluids at our study sites are favorable (i.e. endergonic, Figure 4.2) under the geochemical and physical conditions present at our study sites. In contrast, syntheses of 11 out of the 20 protein-forming amino acids would be favorable (exergonic) under simulated hot (100 °C) and reducing deep submarine hydrothermal fluid conditions. The contrasting results are not surprising since the measured hydrogen concentrations in ridge-flank basement fluids (0.05-1.1 μM, chapter 3) reported here are two orders of magnitude lower than that (~0.34 mM) used in the thermodynamic calculations by Amen and Shock (1998). As shown in Figure 2, higher hydrogen concentrations in the system yield higher Gibbs free energy, making the environment more favorable for the syntheses of amino acids to take place. Since the ridge-flank basement fluids are not favorable for synthesis of amino acids, abiotic production is an unlikely source for the amino acids observed in the basement fluids.

4.4.4. Diagenetic status

As noted above, variations in amino acid concentrations and mole percentage distributions may be linked to organic matter degradation within the basement fluids. For example, the enrichment in serine, glycine, ϒ-aminobutyric acid and β-alanine within the basement fluid samples relative to microbial biomass (Table 4.2 and Figure 4.3) suggest that common processes, including organic carbon degradation, are affecting the amino acids compositions (Cowie and Hedges, 1994; Davis et al., 2009). Furthermore, the systematic trends observed in plots of glutamic acid versus tyrosine and glutamic acid versus ϒ-aminobutyric acid for basement fluid samples (Figure 4.4) suggest that amino acids in basement fluids from different sites and times have been subjected to different degrees of diagenetic alteration (Cowie and Hedges, 1994; Dauwe et al., 1999; Kaiser and Benner, 2009). Basement fluid samples collected from site 1362A in 2011 contain the lowest concentrations of tyrosine and glutamic acid, and the highest concentrations of ϒ-aminobutyric acid relative to all the other basement fluid samples collected, suggesting that this sample may be the most diagenetically altered among all basement sites sampled (Figure 4.4). The high mole percent of ϒ-aminobutyric acid in basement fluids collected from site 1301A in 2011 (11±3 %) also suggest that the fluids circulating by this site were more altered than fluids collected from the same site in previous years (undetectable ϒ-aminobutyric acid, Table 4.4).

Carbon-normalized DHAA yields, defined as the percentage of organic carbon comprised by DHAA, have been suggested as sensitive indicators of diagenetic status (Cowie and Hedges, 1994; Davis et al., 2009; Kaiser and Benner, 2009). Amino acids are preferentially utilized during microbial decomposition of marine organic matter (Lee et

al., 2000; Amon et al., 2001; Lee et al., 2004), causing a decrease in carbon-normalized yield. Microbial decomposition experiments also demonstrate that carbon-normalized DHAA yields are an effective indicator for early diagenesis, while the mol% composition of the non-protein amino acid ϒ-aminobutyric acid is an effective indicator of advanced DOC diagenesis (Davis et al., 2009).

Calculated carbon-normalized amino acid yields for our ridge-flank basement fluid samples are summarized in Table 4.2. Basement fluid samples collected from site 1362A in 2011 contain the lowest carbon-normalized DHAA yield (1.4±0.4 %OC) among all the basement fluid samples, indicating that this sample is likely the most diagenetically altered among the basement fluids collected. The basement fluid sample collected from site 1301A in 2011 has the lowest carbon-normalized DHAA yield (2.0±0.6 %OC) relative to samples collected from the same site in years 2009 and 2010 (2.7 and 3.3±1.2%OC, respectively), suggesting that the 2011 sample is more diagenetically altered than those from 2009 and 2010. The carbon-normalized DHAA yield and the non-protein amino acid ϒ-aminobutyric mol% data suggest similar relative diagenetic status for the ridge-flank basement fluids analyzed.

The carbon-normalized DHAA yields for the ridge-flank basement fluids (1.4-3.3 %OC) are near the low end or generally lower than the range of values reported for ~90°C deep submarine Lost City vent fluids (2.5-15 %OC; Lang et al., 2013), Vulcano shallow submarine hydrothermal vents (10-15 %OC, Svensson et al., 2004), Vulcano geothermal wells (2-25%; Svensson et al., 2004), hydrothermal-influenced marine surface sediment porewater (15-23 %OC; Hoaki et al., 1995) and hydrothermal-influenced deep sediment porewater (2.5-6.9%, table 4.4). High carbon-normalized DHAA yields within the non-

ridge flank hydrothermal fluids indicate a high faction of labile organic matter (Hoaki et al., 1995; Svensson et al., 2004) and, in some cases, approach the carbon-normalized DHAA yield of marine plankton (~34 %OC; Kaiser and Benner, 2009).

In contrast, carbon-normalized DHAA yields for the ridge-flank basement fluids are higher than those for seawater and HMW-DOC (0.4-1.2 %OC; McCarthy et al., 1996; Kaiser and Benner, 2009). In addition, the carbon-normalized DHAA yields in marine DOC also decrease from ~1.2 %OC (surface ocean) to ~0.4 %OC (North Pacific deep ocean) along the thermohaline circulation pathway over a time span of about 1000 years (along the thermohaline circulation; Kaiser and Benner, 2009), consistent to the general observation that decreases in carbon-normalized DHAA yields correspond to a higher degree of diagenetic alteration (Cowie and Hedges, 1994; Davis et al., 2009). Higher carbon-normalized DHAA yields in basement fluids than in North Pacific deep seawater implies that the basement fluid DOC is relatively more labile than the North Pacific deep ocean water.

The differences in dissolved amino acids compositions and in their diagenetic status also suggest spatial and temporal variability in the ridge-flank basement fluids. This further implies that the basement environment is not a well-mixed and homogeneous aquifer on the scale of the 311 to 850 m horizontal separation among the three study sites. Such a conclusion is also supported by the variable hydrogen and methane concentrations in basement fluids collected from the same study sites (chapter 3).

4.4.5. Export of fixed carbon from ridge-flank basement

Based on the DFAA and DCAA concentrations, the basement fluid at our sedimented Juan de Fuca Ridge flank sites could be a net source of DFAA and DCAA to deep North Pacific seawater. DFAA concentrations (7-13 nM) measured in basement fluids collected from site 1301A during three consecutive years are higher than measured in local background seawater (5±2 nM) and thus basement fluids at site 1301A can potentially export fixed labile carbon as free amino acids to the overlying ocean. DCAA concentrations (52-89 nM) in all of the basement fluids collected during this study are also higher than DCAA concentrations (50 nM) reported for North Pacific deep seawater (Kaiser and Benner, 2009).

Although the ridge-flank basement is buried by thick sediments, dissolved amino acids can be exported from the basement to the ocean through seamounts and smaller basement outcrops protruding above the sediments. For example, Baby Bare, ~5 km south to our study site 1301A, is an outcrop of 3.5 Ma crust and act as a high-permeability conduit for venting warm basement fluids (Mottl et al., 1998). Based on the heat loss at ridge-flanks (12% of 53±5 $\times 10^{18}$ Cal/yr; Mottl, 2003) and venting at temperatures between 20-65°C, the maximum water flux through the Baby-Bare type warm ridge flank vents is estimated to be ~7.4-43$\times 10^{13}$ kg-seawater/year (Lang et al., 2006). Assuming that all ridge-flank basement fluids have DHAA similar to those measured in this study (52-89 nM) and that deep ocean water DHAA concentrations are ~50 nM (Kaiser and Benner, 2009), for a net input of 2-39 nM into the deep ocean ridge-flank basement could potentially export ~0.0013-0.086 $\times 10^{10}$g C-dissolved amino acids per year into the deep ocean. This is significantly less than the DOC that is lost from bottom seawater to the ridge-flank basement environment (2-13$\times 10^{10}$g C/year) or the DOC that is added to deep ocean

seawater (3-28×10^{10}gC/year) from low temperature diffuse vents (Lang et al., 2006). Nevertheless, while dissolved amino acids comprise a small portion of DOC mass, they are particularly important because they represent a highly desirable labile component (e.g. Keil and Kirchman, 1993; Keil and Kirchman, 1999). The export from ridge-flank basement may help to support some heterotrophic activities in the amino-acids-scarce deep ocean.

4.5. Conclusion

Concentrations and compositions of dissolved free and hydrolysable amino acids (DFAA and DCAA, respectively) in ridge-flank basement fluids are at the lower end of the range reported previously for other hydrothermal ecosystems including diffuse vents, high temperature smokers, shallow submarine vents, geothermal wells and hydrothermal-influenced sediment porewater. Low DFAA/DHAA ratios suggest rapid removal of DFAA from the basement fluids. Relative mole percentage amino acid compositions in the basement fluids suggest a source-like distribution and potential sources include in situ biological production and diffusion from overlying sediment porewater. Abiotic synthesis of amino acids is not favorable within the ridge-flank basement fluids. Variations in the amino acid compositions suggest different diagenetic histories for the basement fluids in time and space across study sites, indicating that the basement aquifer is not well mixed at the scale of hundreds of meters. Finally, our data indicate that amino acids in the basement fluids on the Juan de Fuca Ridge flanks can potentially be exported to the overlying ocean.

Acknowledgement

This work is supported by NSF-Microbial Observatory Project (NSF XXXXX). We would like to thank crews of R/V Atlantis, HOV Alvin & ROV Jason for smooth cruises and submersible operations. We thank Joseph Lichwa for his tremendous support and assistance at our early stage of method development for amino acid analysis. We also thank Ray Chittaranjan's generosity in providing an instrument for initial testing of the method for amino acid analysis. We thank Chih-Chiang Hsieh for his help with the sample collection, Kathryn Hu and Natalie Hamada's assistance in preparing lab wares needed for this study, and Douglas LaRowe's instructions on thermodynamic calculations. SOEST contribution number XXXX. C-DEBI contribution number XXXX.

4.6. References

Alford, S. E., Alt, J. C., and Shanks Iii, W. C., 2011. Sulfur geochemistry and microbial sulfate reduction during low-temperature alteration of uplifted lower oceanic crust: Insights from ODP Hole 735B. *Chem. Geol.* **286**, 185-195.

Alt, J. C. and Shanks, W. C., 2011. Microbial sulfate reduction and the sulfur budget for a complete section of altered oceanic basalts, IODP Hole 1256D (eastern Pacific). *Earth and Planetary Science Letters* **310**, 73-83.

Aluwihare, L. I. and Meador, T., 2008. Chemical composition of marine dissolved organic nitrogen. In: *Nitrogen in the marine environment* (eds. D. G. Capone, D. A. Bronk, M. R. Mulholland, and E. J. Carpenter). San Diego, CA, USA: Academic Press.

Amend, J. P. and Shock, E. L., 1998. Energetics of amino acid synthesis in hydrothermal ecosystems. *Science* **281**, 1659-1662.

Amon, R. M., Fitznar, H.-P., and Benner, R., 2001. Linkages among the bioreactivity, chemical composition, and diagenetic state of marine dissolved organic matter. *Limnology and Oceanography* **46**, 287-297.

Bach, W. and Edwards, K. J., 2003. Iron and sulfide oxidation within the basaltic ocean crust: Implications for chemolithoautotrophic microbial biomass production. *Geochim. Cosmochim. Acta* **67**, 3871-3887.

Bada, J. L., 1991. Amino acid cosmogeochemistry. *Philosophical Transactions of the Royal Society of London. Series B: Biological Sciences* **333**, 349-358.

Becker, K. and Fisher, A. T., 2008. Borehole packer tests at multiple depths resolve distinct hydrologic intervals in 3.5-Ma upper oceanic crust on the eastern flank of Juan de Fuca Ridge. *J. Geophys. Res.* **113**, 1-12.

Boettger, J., Lin, H.-T., Cowen, J. P., Henstscher, M., and Amend, J. P., 2013. Energy yields from chemolithotrophic metabolisms in igneous basement of the Juan de Fuca ridge flank system. *Chem. Geol.* **337-338**, 11-19.

Coffin, R. B., 1989. Bacterial uptake of dissolved free and combined amino acids in estuarine waters. *Limnology and Oceanography*, 531-542.

Cowen, J. P., Copson, D. A., Jolly, J., Hsieh, C.-C., Lin, H.-T., Glazer, B. T., and Wheat, C. G., 2012. Advanced instrument system for real-time and time-series microbial geochemical sampling of the deep (basaltic) crustal biosphere. *Deep-Sea Res. Pt. I* **61**, 43-56.

Cowen, J. P., Giovannoni, S. J., Kenig, F., Johnson, H. P., Butterfield, D., Rappe, M. S., Hutnak, M., and Lam, P., 2003. Fluids from aging ocean crust that support microbial life. *Science* **299**, 120-123.

Cowie, G. L. and Hedges, J. I., 1992. Sources and Reactivities of Amino-Acids in a Coastal Marine-Environment. *Limnology and Oceanography* **37**, 703-724.

Cowie, G. L. and Hedges, J. I., 1994. Biochemical indicators of diagenetic alteration in natural organic matter mixtures.

Crawford, C. C., Hobbie, J., and Webb, K., 1974. The utilization of dissolved free amino acids by estuarine microorganisms. *Ecology*, 551-563.

Dauwe, B., Middelburg, J. J., Herman, P. M. J., and Heip, C. H. R., 1999. Linking diagenetic alteration of amino acids and bulk organic matter reactivity. *Limnology and Oceanography* **44**, 1809-1814.

Davis, E. E., Chapman, D. S., Mottl, M. J., Bentkowski, W. J., Dadey, K., Forster, C., Harris, R., Nagihara, S., Rohr, K., Wheat, G., and Whiticar, M., 1992. Flank flux - an experiment to study the nature of hydrothermal circulation in young oceanic-crust. *Can. J. Earth. Sci.* **29**, 925-952.

Davis, J., Kaiser, K., and Benner, R., 2009. Amino acid and amino sugar yields and compositions as indicators of dissolved organic matter diagenesis. *Organic Geochemistry* **40**, 343-352.

Dirmeier, R., Keller, M., Hafenbradl, D., Braun, F.-J., Rachel, R., Burggraf, S., and Stetter, K. O., 1998. Thermococcus acidaminovorans sp. nov., a new hyperthermophilic alkalophilic archaeon growing on amino acids. *Extremophiles* **2**, 109-114.

Elderfield, H., Wheat, C. G., Mottl, M. J., Monnin, C., and Spiro, B., 1999. Fluid and geochemical transport through oceanic crust: a transect across the eastern flank of the Juan de Fuca Ridge. *Earth Planet. Sci. Lett.* **172**, 151-165.

Fisher, A. T., 2005. Marine hydrogeology: recent accomplishments and future opportunities. *Hydrogeol. J.* **13**, 69-97.

Fisk, M. R., Giovannoni, S. J., and Thorseth, I. H., 1998. Alteration of oceanic volcanic glass: Textural evidence of microbial activity. *Science* **281**, 978-980.

Furnes, H., Dilek, Y., Muehlenbachs, K., and Banerjee, N. R., 2006. Tectonic control of bioalteration in modern and ancient oceanic crust as evidenced by carbon isotopes. *Isl. Arc* **15**, 143-155.

Furnes, H., Muehlenbachs, K., Torsvik, T., Thorseth, I. H., and Tumyr, O., 2001a. Microbial fractionation of carbon isotopes in altered basaltic glass from the Atlantic Ocean, Lau Basin and Costa Rica Rift. *Chem. Geol.* **173**, 313-330.

Furnes, H., Muehlenbachs, K., Torsvik, T., Tumyr, O., and Shi, L., 2002. Bio-signatures in metabasaltic glass of a Caledonian ophiolite, West Norway. *Geol. Mag.* **139**, 601-608.

Furnes, H., Staudigel, H., Thorseth, I. H., Torsvik, T., Muehlenbachs, K., and Tumyr, O., 2001b. Bioalteration of basaltic glass in the oceanic crust. *Geochem. Geophys. Geosyst.* **2**.

Giovannoni, S. J., Fisk, M. R., Mullins, T. D., and Furnes, H., 1996. Genetic evidence for endolithic microbial life colonizing basaltic glass/seawater interfaces. *Proc. Ocean Drill. Program Sci. Results* **148**, 207-214.

Grasshoff, K., Ehrhardt, M., Kremling, K., and Almgren, T., 1999. Methods of seawater analysis.

Haberstroh, P. and Karl, D., 1989. Dissolved free amino acids in hydrothermal vent habitats of the Guaymas Basin. *Geochim. Cosmochim. Acta* **53**, 2937-2945.

Hansell, D. A. and Carlson, C. A., 1998. Deep-ocean gradients in the concentration of dissolved organic carbon. *Nature* **395**, 263-266.

Hansell, D. A., Carlson, C. A., Repeta, D. J., and Schlitzer, R., 2009. Dissolved organic matter in the ocean: a controversy stimulates new insights. *Oceanography* **22**, 202-211.

Hecky, R. E., Mopper, K., Kilham, P., and Degens, E. T., 1973. The amino acid and sugar composition of diatom cell-walls. *Mar. Biol.* **19**, 323-331.

Hoaki, T., Nishijima, M., Kato, M., Adachi, K., Mizobuchi, S., Hanzawa, N., and Maruyama, T., 1994. Growth requirements of hyperthermophilic sulfur-dependent

heterotrophic archaea isolated from a shallow submarine geothermal system with reference to their essential amino acids. *Appl. Environ. Microbiol.* **60**, 2898-2904.
Hoaki, T., Nishijima, M., Miyashita, H., and Maruyama, T., 1995. Dense Community of Hyperthermophilic Sulfur-Dependent Heterotrophs in a Geothermally Heated Shallow Submarine Biotope near Kodakara-Jima Island, Kagoshima, Japan. *Appl. Environ. Microbiol.* **61**, 1931-1937.
Hoaki, T., Wirsen, C. O., Hanzawa, S., Maruyama, T., and Jannasch, H. W., 1993. Amino acid requirements of two hyperthermophilic archaeal isolates from deep-sea vents, Desulfurococcus strain SY and Pyrococcus strain GB-D. *Appl. Environ. Microbiol.* **59**, 610-613.
Horiuchi, T., Takano, Y., Ishibashi, J.-i., Marumo, K., Urabe, T., and Kobayashi, K., 2004. Amino acids in water samples from deep sea hydrothermal vents at Suiyo Seamount, Izu-Bonin Arc, Pacific Ocean. *Organic Geochemistry* **35**, 1121-1128.
Hubberten, U., Lara, R. J., and Kattner, G., 1995. Refractory organic compounds in polar waters: Relationship between humic substances and amino acids in the Arctic and Antarctic. *Journal of Marine Research* **53**, 137-149.
Huber, J. A., Johnson, H. P., Butterfield, D. A., and Baross, J. A., 2006. Microbial life in ridge flank crustal fluids. *Environ. Microbiol.* **8**, 88-99.
Ito, M., Gupta, L. P., Masuda, H., and Kawahata, H., 2006. Thermal stability of amino acids in seafloor sediment in aqueous solution at high temperature. *Organic Geochemistry* **37**, 177-188.
Jannasch, H. W., Wirsen, C. O., Molyneaux, S. J., and Langworthy, T. A., 1988. Extremely thermophilic fermentative archaebacteria of the genus Desulfurococcus from deep-sea hydrothermal vents. *Appl. Environ. Microbiol.* **54**, 1203-1209.
Johnson, H. P. and Pruis, M. J., 2003. Fluxes of fluid and heat from the oceanic crustal reservoir. *Earth Planet. Sci. Lett.* **216**, 565-574.
Johnson, J. W., Oelkers, E. H., and Helgeson, H. C., 1992. SUPCRT92: A software package for calculating the standard molal thermodynamic properties of minerals, gases, aqueous species, and reactions from 1 to 5000 bar and 0 to 1000 C. *Computers & Geosciences* **18**, 899-947.
Jungbluth, S. P., Grote, J., Lin, H. T., Cowen, J. P., and Rappé, M. S., 2013. Microbial diversity within basement fluids of the sediment-buried Juan de Fuca Ridge flank. *ISME Journal* **7**, 161-172.
Kaiser, K. and Benner, R., 2005. Hydrolysis-induced racemization of amino acids.
Kaiser, K. and Benner, R., 2009. Biochemical composition and size distribution of organic matter at the Pacific and Atlantic time-series stations. *Mar. Chem.* **113**, 63-77.
Keil, R. G. and Kirchman, D. L., 1991a. Contribution of dissolved free amino acids and ammonium to the nitrogen requirements of heterotrophic bacterioplankton. *Mar. Ecol. Prog. Ser* **73**, 1-10.
Keil, R. G. and Kirchman, D. L., 1991b. Dissolved combined amino acids in marine waters as determined by a vapor-phase hydrolysis method. *Mar. Chem.* **33**, 243-259.
Keil, R. G. and Kirchman, D. L., 1993. Dissolved combined amino acids: Chemical form and utilization by marine bacteria. *Limnology and Oceanography*, 1256-1270.

Keil, R. G. and Kirchman, D. L., 1999. Utilization of dissolved protein and amino acids in the northern Sargasso Sea. *Aquatic Microbial Ecology* **18**, 293-300.

Klevenz, V., Sumoondur, A., Ostertag-Henning, C., and Koschinsky, A., 2010. Concentrations and distributions of dissolved amino acids in fluids from Mid-Atlantic Ridge hydrothermal vents. *Geochem. J.* **44**, 387.

Lang, S., Früh-Green, G., Bernasconi, S., and Butterfield, D., 2013. Sources of organic nitrogen at the serpentinite- hosted Lost City hydrothermal field. *Geobiology*.

Lang, S. Q., Butterfield, D. A., Lilley, M. D., Johnson, H. P., and Hedges, J. I., 2006. Dissolved organic carbon in ridge-axis and ridge-flank hydrothermal systems. *Geochim. Cosmochim. Acta* **70**, 3830-3842.

Lee, C. and Bada, J. L., 1975. Amino acids in equatorial Pacific Ocean water. *Earth and Planetary Science Letters* **26**, 61-68.

Lee, C. and Cronin, C., 1982. The vertical flux of particulate organic nitrogen in the sea: decomposition of amino acids in the Peru upwelling area and the equatorial Atlantic. *Journal of Marine Research* **40**, 227-251.

Lee, C., Wakeham, S., and Arnosti, C., 2004. Particulate organic matter in the sea: The composition conundrum. *AMBIO: A Journal of the Human Environment* **33**, 565-575.

Lee, C., Wakeham, S. G., and I Hedges, J., 2000. Composition and flux of particulate amino acids and chloropigments in equatorial Pacific seawater and sediments. *Deep-Sea Res. Pt. I* **47**, 1535-1568.

Lever, M., Rouxel, O., Alt, J. C., Shimizu, N., Ono, S., Coggon, R. M., Shanks III, W. C., Lapham, L., Elvert, M., Prieto-Mollar, X., Hinrichs, K. U., Inagaki, F., and Teske, A., 2013. Evidence for microbial carbon and sulfur cycling in deeply buried ridge flank basalt. *Science* **339**, 1305-1308.

Lin, H. T., Cowen, J. P., Olson, E. J., Amend, J. P., and Lilley, M. D., 2012. Inorganic chemistry, gas compositions and dissolved organic carbon in fluids from sedimented young basaltic crust on the Juan de Fuca Ridge flanks. *Geochim. Cosmochim. Acta* **85**, 213-227.

McCarthy, M., Hedges, J., and Benner, R., 1996. Major biochemical composition of dissolved high molecular weight organic matter in seawater. *Mar. Chem.* **55**, 281-297.

McCarthy, M. D., Beaupre, S. R., Walker, B. D., Voparil, I., Guilderson, T. P., and Druffel, E. R. M., 2010. Chemosynthetic origin of C-14-depleted dissolved organic matter in a ridge-flank hydrothermal system. *Nat. Geosci.* **4**, 32-36.

Middelboe, M., Borch, N. H., and Kirchman, D. L., 1995. Bacterial utilization of dissolved free amino acids, dissolved combined amino acids and ammonium in the Delaware Bay estuary: Effects of carbon and nitrogen limitation. *Marine Ecology-Progress Series* **128**, 109-120.

Mottl, M. J., 2003. Partitioning of energy and mass fluxes between mid-ocean ridge axes and flanks at high and low temperature. In: *Energy and Mass Transfer in Marine Hydrothermal Systems* (eds. P. E. Halbach, V. Tunnicliffe, and J. R. Hein). Dahlem University Press, Berlin.

Mottl, M. J., Wheat, G., Baker, E., Becker, N., Davis, E., Feely, R., Grehan, A., Kadko, D., Lilley, M., Massoth, G., Moyer, C., and Sansone, F., 1998. Warm springs

discovered on 3.5 Ma oceanic crust, eastern flank of the Juan de Fuca Ridge. *Geology* **26**, 51-54.
Ono, S., Keller, N. S., Rouxel, O., and Alt, J. C., 2012. Sulfur-33 constraints on the origin of secondary pyrite in altered oceanic basement. *Geochim. Cosmochim. Acta*.
Orcutt, B. N., Sylvan, J. B., Knab, N. J., and Edwards, K. J., 2011. Microbial Ecology of the Dark Ocean above, at, and below the Seafloor. *Microbiology and Molecular Biology Reviews* **75**, 361-422.
Pledger, R. J. and Baross, J. A., 1991. Preliminary description and nutritional characterization of a chemoorganotrophic archaeobacterium growing at temperatures of up to 110° isolated from a submarine hydrothermal vent environment. *Journal of general microbiology* **137**, 203-211.
Rouxel, O., Ono, S., Alt, J., Rumble, D., and Ludden, J., 2008. Sulfur isotope evidence for microbial sulfate reduction in altered oceanic basalts at ODP Site 801. *Earth and Planetary Science Letters* **268**, 110-123.
Schroeder, R. A., 1975. Absence of β-alanine and γ-aminobutyric acid in cleaned foraminiferal shells: Implications for use as a chemical criterion to indicate removal of non-indigenous amino acid contaminants. *Earth and Planetary Science Letters* **25**, 274-278.
Scientists, E., 2011a. Methods. In: *Proc. IODP* (eds. A. T. Fisher, T. Tsuji, K. Petronotis, and E. Scientists).
Scientists, E., 2011b. Site U1363. In: *Proc. IODP, 327* (eds. A. T. Fisher, T. Tsuji, K. Petronotis, and E. Scientists).
Shipboard Scientific Party, 1997a. Introduction and summary: hydrothermal circulation in the oceanic crust and its consequences on the eastern flank of the Juan de Fuca Ridge *Proc. Ocean Drill. Program Initial Reports* **168**, 7–21.
Shipboard Scientific Party, 1997b. Rough basement transect (Sites 1026 and 1027). *Proc. Ocean Drill. Program Initial Reports* **168**, 101–160.
Shipboard Scientific Party, 2004. Juan de Fuca hydrogeology: The hydrogeologic architecture of basaltic oceanic crust: compartmentalization, anisotropy, microbiology, and crustal-scale properties on the eastern flank of Juan de Fuca Ridge, eastern Pacific Ocean. *IODP Prel. Rept.* **301**.
Shipboard Scientific Party, 2010. Juan de Fuca Ridge-flank hydrogeology: the hydrogeologic architecture of basaltic oceanic crust: compartmentalization, anisotropy, microbiology, and crustal-scale properties on the eastern flank of Juan de Fuca Ridge, eastern Pacific Ocean. *IODP Prel. Rept.* **327**.
Shock, E. and Canovas, P., 2010. The potential for abiotic organic synthesis and biosynthesis at seafloor hydrothermal systems. *Geofluids* **10**, 161-192.
Shock, E. L., 1990. Geochemical Constraints on the Origin of Organic-Compounds in Hydrothermal Systems. *Origins Life Evol. B.* **20**, 331-367.
Svensson, E., Skoog, A., and Amend, J. P., 2004. Concentration and distribution of dissolved amino acids in a shallow hydrothermal system, Vulcano Island (Italy). *Organic Geochemistry* **35**, 1001-1014.
Takano, Y., Horiuchi, T., Kobayashi, K., Marumo, K., and Urabe, T., 2003a. Large enantiomeric excesses of L-form amino acids in deep-sea hydrothermal sub-vent of 156°Cfluids at the Suiyo Seamount, Izu-Bonin Arc, Pacific ocean.

Takano, Y., Sato, R., Kaneko, T., Kobayashi, K., and Marumo, K., 2003b. Biological origin for amino acids in a deep subterranean hydrothermal vent, Toyoha mine, Hokkaido, Japan. *Organic Geochemistry* **34**, 1491-1496.

Torsvik, T., Furnes, H., Muehlenbachs, K., Thorseth, I. H., and Tumyr, O., 1998. Evidence for microbial activity at the glass-alteration interface in oceanic basalts. *Earth Planet. Sci. Lett.* **162**, 165-176.

Underwood, M. B., Hoke, K. D., Fisher, A. T., Davis, E. E., Giambalvo, E., Zühlsdorff, L., and Spinelli, G. A., 2005. Provenance, stratigraphic architecture, and hydrogeologic influence of turbidites on the mid-ocean ridge flank of northwestern Cascadia Basin, Pacific Ocean. *Journal of Sedimentary Research* **75**, 149-164.

Walker, B. D., McCarthy, M. D., Fisher, A. T., and Guilderson, T. P., 2008. Dissolved inorganic carbon isotopic composition of low-temperature axial and ridge-flank hydrothermal fluids of the Juan de Fuca Ridge. *Mar. Chem.* **108**, 123-136.

Wheat, C. G., McManus, J., Mottl, M. J., and Giambalvo, E., 2003. Oceanic phosphorus imbalance: Magnitude of the mid-ocean ridge flank hydrothermal sink. *Geophys. Res. Lett* **30**, 1895.

Wheat, C. G. and Mottl, M. J., 1994. Hydrothermal circulation, Juan de Fuca Ridge eastern flank: factors controlling basement water composition. *J. Geophys. Res.* **99**, 3067-3080.

Wheeler, P. A. and Kirchman, D. L., 1986. Utilization of inorganic and organic nitrogen by bacteria in marine systems. *Limnology and Oceanography*, 998-1009.

Whelan, J. K., 1977. Amino acids in a surface sediment core of the Atlantic abyssal plain. *Geochim. Cosmochim. Acta* **41**, 803-810.

Williams, P. and Druffel, E., 1988. Dissolved organic matter in the ocean: comments on a controversy. *Oceanography* **1**, 14-17.

Yamashita, Y. and Tanoue, E., 2003. Distribution and alteration of amino acids in bulk DOM along a transect from bay to oceanic waters. *Mar. Chem.* **82**, 145-160.

Table 4.1. Net protein-forming amino acid synthesis reaction.

Amino acids	Net reaction								
Alanine	$3HCO_3^-$	+ $2H^+$	+ NH_4^+	+ $6H_2$		↔	$C_3H_7NO_2$	+	$7\,H_2O$
Arginine	$6HCO_3^-$	+ $3H^+$	+ $4NH_4^+$	+ $11H_2$		↔	$C_6H_{15}N_4O_2^+$	+	$16\,H_2O$
Asparagine	$4HCO_3^-$	+ $2H^+$	+ $2NH_4^+$	+ $6H_2$		↔	$C_4H_8N_2O_3$	+	$9\,H_2O$
Aspartate	$4HCO_3^-$	+ $2H^+$	+ NH_4^+	+ $6H_2$		↔	$C_4H_7NO_4^-$	+	$9\,H_2O$
Cysteine	$3HCO_3^-$	+ $3H^+$	+ NH_4^+	+ $5H_2$	+ HS^-	↔	$C_3H_7NO_2S$	+	$7\,H_2O$
Glutamate	$5HCO_3^-$	+ $3H^+$	+ NH_4^+	+ $9H_2$		↔	$C_5H_8NO_4^-$	+	$11\,H_2O$
Glutamine	$5HCO_3^-$	+ $3H^+$	+ $2NH_4^+$	+ $9H_2$		↔	$C_5H_8NO_4$	+	$11\,H_2O$
Glycine	$2HCO_3^-$	+ $1H^+$	+ NH_4^+	+ $3H_2$		↔	$C_2H_5NO_2$	+	$4\,H_2O$
Histidine	$6HCO_3^-$	+ $3H^+$	+ $3NH_4^+$	+ $10H_2$		↔	$C_6H_9N_3O_2$	+	$16\,H_2O$
Isolucine	$6HCO_3^-$	+ $5H^+$	+ NH_4^+	+ $15H_2$		↔	$C_6H_{13}NO_2$	+	$16\,H_2O$
Lucine	$6HCO_3^-$	+ $5H^+$	+ NH_4^+	+ $15H_2$		↔	$C_6H_{13}NO_2$	+	$16\,H_2O$
Lysine	$6HCO_3^-$	+ $5H^+$	+ $2NH_4^+$	+ $14H_2$		↔	$C_6H_{15}N_2O_2^+$	+	$16\,H_2O$
Methionine	$5HCO_3^-$	+ $5H^+$	+ NH_4^+	+ $11H_2$	+ HS^-	↔	$C_5H_{11}NO_2S$	+	$13\,H_2O$
Phenylalanine	$9HCO_3^-$	+ $8H^+$	+ NH_4^+	+ $20H_2$		↔	$C_9H_{10}NO_2$	+	$25\,H_2O$
Proline	$5HCO_3^-$	+ $4H^+$	+ NH_4^+	+ $11H_2$		↔	$C_5H_9NO_2$	+	$13\,H_2O$
Serine	$3HCO_3^-$	+ $2H^+$	+ NH_4^+	+ $5H_2$		↔	$C_3H_7NO_3$	+	$6\,H_2O$
Threonine	$4HCO_3^-$	+ $3H^+$	+ NH_4^+	+ $8H_2$		↔	$C_4H_9NO_3$	+	$9\,H_2O$
Tryptophan	$11HCO_3^-$	+ $9H^+$	+ $2NH_4^+$	+ $23H_2$		↔	$C_{11}H_{12}N_2O_2$	+	$31\,H_2O$
Tyrosine	$9HCO_3^-$	+ $8H^+$	+ NH_4^+	+ $19H_2$		↔	$C_9H_{11}NO_3$	+	$24\,H_2O$
Valine	$5HCO_3^-$	+ $4H^+$	+ NH_4^+	+ $12H_2$		↔	$C_5H_{11}NO_2$	+	$13\,H_2O$

Table 4.2. Concentrations of dissolved free amino acids (DFAA), total dissolved hydrolysable amino acids (DHAA), dissolved organic carbon (DOC) and carbon-normalized amino acid yields (AA yield %OC) of DHAA for subseafloor basement fluids. DFAA for local background bottom seawater are also shown for comparison. Numbers in parenthesis are deviations (1SD). Amino acids with significant amounts (>3 times deviation) are shown in bold.

	CORK 1301A								CORK 1362 B				CORK 1362A				JdFR bottom seawater	
	2009				2010				2011				2011					
	DFAA (n=5)		DHAA (n=1)		DFAA (n=5)		DHAA (n=2)		DFAA (n=4)		DHAA (n=3)		DFAA (n=4)		DHAA (n=3)		DFAA (n=2)		DHAA (n=2)		DFAA (n=3)	
ASP	1.5	(0.2)	14	-	-	-	**15**	(0.0)	0.6	(0.1)	**10**	(2)	-	-	**9**	(3)	-	-	**2**	(1)	-	-
GLU	-	-	13	-	0.9	(1.5)	**15**	(2.2)	1.5	(1.4)	**8**	(3)	-	-	**12**	(2)	-	-	**5**	(1)	-	-
SER	**6.0**	(1.3)	16	-	1.7	(1.1)	**13**	(0.7)	0.5	(0.2)	-	-	-	-	**13**	(0.6)	-	-	**7**	(1.1)	**0.7**	(0.2)
HIS	0.8	(1.1)	1	-	-	-	**1**	(0.0)	2.1	(0.8)	**4**	(2)	-	-	1	(1)	-	-	**3**	(0)	2.6	(1.1)
GLY	2.4	(1.3)	19	-	0.5	(0.5)	**17**	(4.2)	1.9	(1.0)	**4**	(5)	0.96	(0.7)	**14**	(2)	-	-	**17**	(5)	**0.6**	(0.2)
THR	-	-	5	-	1.2	(0.8)	**7**	(0.6)	-	-	-	-	-	-	1.4	(1.2)	-	-	**1.7**	(0.6)	-	-
ARG	-	-	3	-	1.3	(1.5)	3	(1.3)	0.7	(0.8)	-	-	-	-	**2.5**	(0.8)	0.3	(0.1)	**0.2**	(0.4)	-	-
ALA	**2.4**	(0.7)	5	-	0.9	(1.3)	2	(0.9)	0.2	(0.2)	**2.1**	(2)	**0.31**	(0.1)	4	(3)	0.5	(0.0)	**3**	(0.5)	-	-
TYR	0.2	(0.2)	2	-	-	-	2	(0.9)	-	-	0.5	(0.5)	-	-	1.1	(0.4)	-	-	0.4	(0.4)	-	-
MET	-	-	-	-	1.9	(3.2)	-	-	0.3	(0.1)	**2.3**	(1)	-	-	0.3	(0)	-	-	**2**	(0.2)	-	-
VAL	0.7	(0.9)	4	-	-	-	4	(1.8)	-	-	**0.9**	(1)	-	-	1.7	(1)	-	-	0.8	(1)	-	-
PHE	-	-	2	-	-	-	2	(0.9)	-	-	-	-	-	-	0.2	(0.3)	-	-	0.1	(0.1)	-	-
ILE	0.5	(0.3)	-	-	0	0	-	-	-	-	-	-	-	-	1.1	(0.3)	-	-	0.1	(0.1)	-	-
LEU	-	-	8	-	0	0	8	(6.7)	-	-	**3.5**	(2)	-	-	1.0	(1)	-	-	-	-	0.8	(0.4)
LYS	-	-	-	-	-	-	-	-	-	-	-	-	-	-	-	-	-	-	-	-	-	-
GABA	-	-	-	-	-	-	-	-	-	-	**6**	(2)	-	-	0.6	(1.1)	-	-	18.0	(0.4)	-	-
BALA	-	-	-	-	-	-	-	-	-	-	**1.1**	(0)	-	-	0.6	(0.8)	0.3	(0.0)	-	-	-	-
Total AA (nM)	14	(6)	89	-	9	(10)	88	(20)	8	(5)	43	(22)	1	(1)	65	(18)	1	(0)	60	(12)	5	(2)
DOC (μM-C)	13		13	-	11		11	(3)	12		12	(1)	11		11	(1)		16	16	(3)	39	
AA yield (%OC)	0.3		2.8	-	0.2		3.3	(1.2)	0.3		2.0	(0.6)	0.04		2.2	(0.7)		0.04	1.4	(0.4)	0.06	

ASP: aspartic acid; GLU: glutamic acid; SER: serine; HIS: histidine; GLY: glycine, THR: threonine; ARG: arginine; ALA: alanine; TYR: tyrosine; TRY: tryptophan; MET: methionine; VAL: valine; PHE: phenylalanine; ILE: isoleucine; LEU: leucine and LYS: lysine; GABA: ϒ-aminobutyric acid; BALA: β-alanine.
-: below detection limit (most amino acids <0.1-1nM, LYS<10nM).

Table 4.3. Mole percentage (mole%) of total dissolved hydrolysable amino acids (DHAA) for subseafloor basement fluids and deep marine sediment porewater from eastern flanks of Juan de Fuca Ridge. Data for North Pacific 2000m seawater from Station ALOHA (22°45'N, 158°W; Kaier & Benner, 2009) are shown for comparison.

	CORK 1301A			CORK 1362B	CORK 1362A	IODP 1363D sediment porewater								North Pacific 2000m
	2009	2010	2011	2011	2011	222m		215m		213m		207m		2000m
	DHAA	DHAA	DHAA	DHAA	DHAA	DFAA	DHAA	DFAA	DHAA	DFAA	DHAA	DFAA	DHAA	DHAA
ASP	16	17	20	14	3	14	7	9	6	11	8	13	7	9
GLU	14	17	16	18	8	7	10	2	9	4	9	5	13	9
SER	18	15	9	20	12	22	11	32	22	19	14	27	19	3
HIS	1	1	9	2	5	2	3	7	4	5	6	12	12	3
GLY	21	20	12	22	28	19	29	22	35	23	30	9	21	28
THR	5	8	0	2	3	5	3	1	2	2	4	7	8	4
ARG	3	4	0	4	0	1	1	6	4	4	3	2	1	4
ALA	5	2	4	7	5	12	6	8	6	13	9	9	6	20
TYR	2	2	1	2	1	1	1	2	1	1	1	3	2	1
MET	0	0	4	0	3	0	1	1	1	1	1	0	0	0
VAL	5	5	2	3	1	6	2	2	2	5	3	5	3	1
PHE	2	2	3	0	0	1	1	2	1	2	2	1	0	0
ILE	0	0	0	2	0	3	2	2	1	3	2	3	2	3
LEU	9	9	7	1	0	5	2	5	3	4	3	3	2	0
LYS	0	0	1	0	0	0	0	0	1	0	1	0	3	1
GABA	0	0	11	1	30	0	7	0	2	0	3	0	1	8
BALA	0	0	2	1	1	0	14	0	0	0	1	0	1	6

ASP: aspartic acid; GLU: glutamic acid; SER: serine; HIS: histidine; GLY: glycine, THR: threonine; ARG: arginine; ALA: alanine; TYR: tyrosine; TRY: tryptophan; MET: methionine; VAL: valine; PHE: phenylalanine; ILE: isoleucine; LEU: leucine and LYS: lysine; GABA: ϒ-aminobutyric acid; BALA: β-alanine.
*: data from Kaiser & Benner (2009).

Table 4.4. Concentrations of dissolved free amino acids (DFAA), total dissolved hydrolysable amino acids (DHAA), dissolved organic carbon (DOC) and carbon-normalized yields (%OC) of DHAA for deep marine sediment porewater from IODP borehole 1363D. Numbers in parenthesis are deviations (1SD).

	1363D sediment porewater							
	222m		215m		213m		207m	
	DFAA (n=2)	DHAA (n=5)	DFAA (n=2)	DHAA (n=2)	DFAA (n=2)	DHAA (n=2)	DFAA (n=2)	DHAA (n=2)
ASP	40 (2)	61 (3)	145 (8)	196 (1)	67 (5)	90 (4)	195 (19)	205 (18)
GLU	20 (4)	85 (5)	30 (2)	276 (3)	26 (1)	109 (1)	71 (19)	385 (20)
SER	60 (6)	93 (6)	530 (8)	673 (3)	114 (5)	170 (17)	396 (39)	533 (31)
HIS	7 (3)	21 (1)	111 (3)	118 (3)	28 (1)	66 (13)	171 (17)	348 (6)
GLY	54 (21)	239 (31)	357 (40)	1084 (85)	137 (15)	358 (39)	138 (14)	591 (26)
THR	15 (0.2)	22 (2)	23 (1)	50 (1)	12 (1)	47 (3)	98 (10)	229 (6)
ARG	3 (0.0)	7 (1)	103 (2)	118 (1)	23 (5)	40 (5)	22 (7)	27 (13)
ALA	33 (1.1)	48 (5)	124 (28)	187 (2)	79 (10)	105 (7)	134 (7)	168 (10)
TYR	2 (1.3)	6 (1)	33 (3)	43 (1)	7 (2)	15 (2)	48 (1)	48 (1)
MET	- -	5 (5)	16 (5)	16 (1)	7 (3)	7 (2)	1.4 1.0	2 (3)
VAL	17 (1.1)	20 (3)	37 (3)	50 (8)	30 (3)	36 (1)	77 (10)	77 (11)
PHE	3 (0.2)	8 (4)	30 (3)	42 (2)	12 (2)	18 (0.4)	15 (15)	13 (8)
ILE	9 (0.2)	15 (7)	30 (3)	36 (4)	20 (3)	26 (0.1)	45 (4)	45 (2)
LEU	13 (0.3)	16 (2)	82 (7)	87 (2)	27 (3)	37 (2)	49 (2)	51 (3)
LYS	- -	- -	- -	40 (20)	- -	17 (11)	- -	76 (27)
GABA	0.4 (0.2)	60 (10)	1.4 (1)	54 (10)	2 (1)	33 (4)	- -	42 (15)
BALA	0.7 (0.7)	110 (6)	0.9 (1)	10 (2)	2 (1)	7 (2)	- -	17 (8)
Total AA (nM)	277	815	1653	3079	593	1182	1461	2856
DOC (μM-C)	103	103	156	156	176	176	229	229
DHAA yield (%OC)	1.0	2.7	4.0	6.9	1.3	2.5	2.7	5.0

ASP: aspartic acid; GLU: glutamic acid; SER: serine; HIS: histidine; GLY: glycine, THR: threonine; ARG: arginine; ALA: alanine; TYR: tyrosine; TRY: tryptophan; MET: methionine; VAL: valine; PHE: phenylalanine; ILE: isoleucine; LEU: leucine and LYS: lysine; GABA: ϒ-aminobutyric acid; BALA: β-alanine.
-: below detection limit (most amino acids <0.1-1nM, LYS<10nM).

Table 4.5. Dissolved free amino acids (DFAA), dissolve hydrolysable amino acids (DHAA) concentrations, carbon-normalized amino acid yields (AA yield %OC), dissolved organic carbon (DOC), temperature and pH for hydrothermal fluids and hydrothermal-influenced sediment porewater in various hydrothermal systems.

Hydrothermal type and location	Temperature (°C)	pH	DFAA (μM)	DHAA (μM)	DOC (μM)	DHAA yield (OC%)	Reference
Oceanic basaltic basement fluids							
Juan de Fuca eastern flank (3.5 Ma basement)	65	~7.4	0.001-0.013	0.053-0.089	12-16	1.3-3	This study
Deep submarine hydrothermal vents							
Mid-Atlantic Ridge 30°N (Lost City)	~90[a]	9-11[a]	N.A.	0.736-2.3	~100	2.5-15	Lang et al. (2003)
Mid-Atlantic Ridge 15°N (Logatchev) and 4-9°S	~18	N.A.	0.035-24.9	N.A.	N.A.	N.A.	Klevenz et al. (2010)
Mid-Atlantic Ridge 15°N (Logatchev) and 4-9°S	~350-400	~3.5[b]	0.038-0.377	N.A.	N.A.	N.A.	Klevenz et al. (2010)
Suiyo Seamount, Izu-Bonin Arc, NW Pacific (water depth ~1400m)	300	N.A.	N.A.	0.067-1.082[c]	N.A.	N.A.	Horiuchi et al. (2004)
Guaymas Basin (water depth ~2000m)	152-319	N.A.	<0.001	N.A.	N.A.	N.A.	Haberstroh and Karl (1989)
Shallow submarine hydrothermal vents (~1 m deep)							
Baia di Levante, Vulcano, Italy	88	5.6	1.33-1.92	0.88-1.86	56-72	10-15	Svensson et al. (2004)
Geothermal wells							
Vulcano, Italy	42-81	2-6.3	0.33-78	0.39-35	34-1780	2-25	Svensson et al. (2004)
Subterranean hydrothermal vent							
Toyoha mine, Hokkaido, Japan	48-71	5.8-6.6	N.A.	2.6-6.1	N.A.	N.A.	Takano et al. (2003)
Hydrothermal-influenced marine sediment porewater							
Juan de Fuca eastern flank (sample depth: 207-222m)	N.A.	7.1-7.5	0.23-1.46	0.8-3.1	103-229	2.5-6.9	This study
Guaymas Basin (sample depth: 0-12 cm)	5-100	N.A.	5-446	N.A.	N.A.	N.A.	Haberstroh and Karl (1989)
Shallow submarine near Japan (sample depth: 0-30 cm)	80-104	7.2-7.5	22-196	98-338	2,742-4,942	15-23	Hoaki et al. (1995)

N.A.: Not available.
a: Temperature and pH derived from Lang et al. (2010).
b: pH derived from Schmidt et al. (2007).
c: End-member fluid compositions calculated based on data from Horiuchi et al. (2004).

Table 4.6. Pearson correlations of individual amino acids within the dissolved hydrolysable amino acids (DHAA) pool in ridge-flank basement fluids. Correlations of individual amino acids with total DHAA (AA sum), dissolved organic carbon (DOC) and the carbon-normalized amino acid yields (AA yield) are also presented for comparison.

	ASP	GLU	SER	HIS	GLY	THR	ARG	ALA	TYR	MET	VAL	PHE	ILE	LEU	GABA	BALA	AA sum	DOC	AA yield
ASP	1	*							*		*	*		*	*				*
GLU		1					*		**	*	*				**				**
SER			1	**			*		*	**	*					*	*		
HIS				1	*		**		*	**						*	*		
GLY					1											*			
THR						1			*		*					*			*
ARG							1		**	**	*					*	*		*
ALA								1											
TYR									1	*	**			*	*	*	*		**
MET										1	*					*	*		*
VAL											1			*		**	**		**
PHE												1		*					
ILE													1						
LEU														1			*		*
GABA															1			*	*
BALA																1	**		*
AA sum																	1		*
DOC																		1	
AA yeild																			1

* Correlation is significant at the $\alpha \leq 0.05$ level (1-tailed).

** Correlation is significant at the $\alpha \leq 0.01$ level (1-tailed).

Figure 4.1. (a) Site map showing the location of the eastern flanks of Juan de Fuca Ridge study sites. (b) Bathymetry map showing Integrated Ocean Drilling Program (IODP) site U1301, U1362 and U1363. (c) A cartoon showing relative distances and penetration depths of CORKs 1362A, 1362B and 1301A. (d) Bathymetry map around near Grizzly Bare outcrop. borehole 1363D. The sediment-basement interface is at about 222m below seafloor, i.e. sediment thickness 222m.

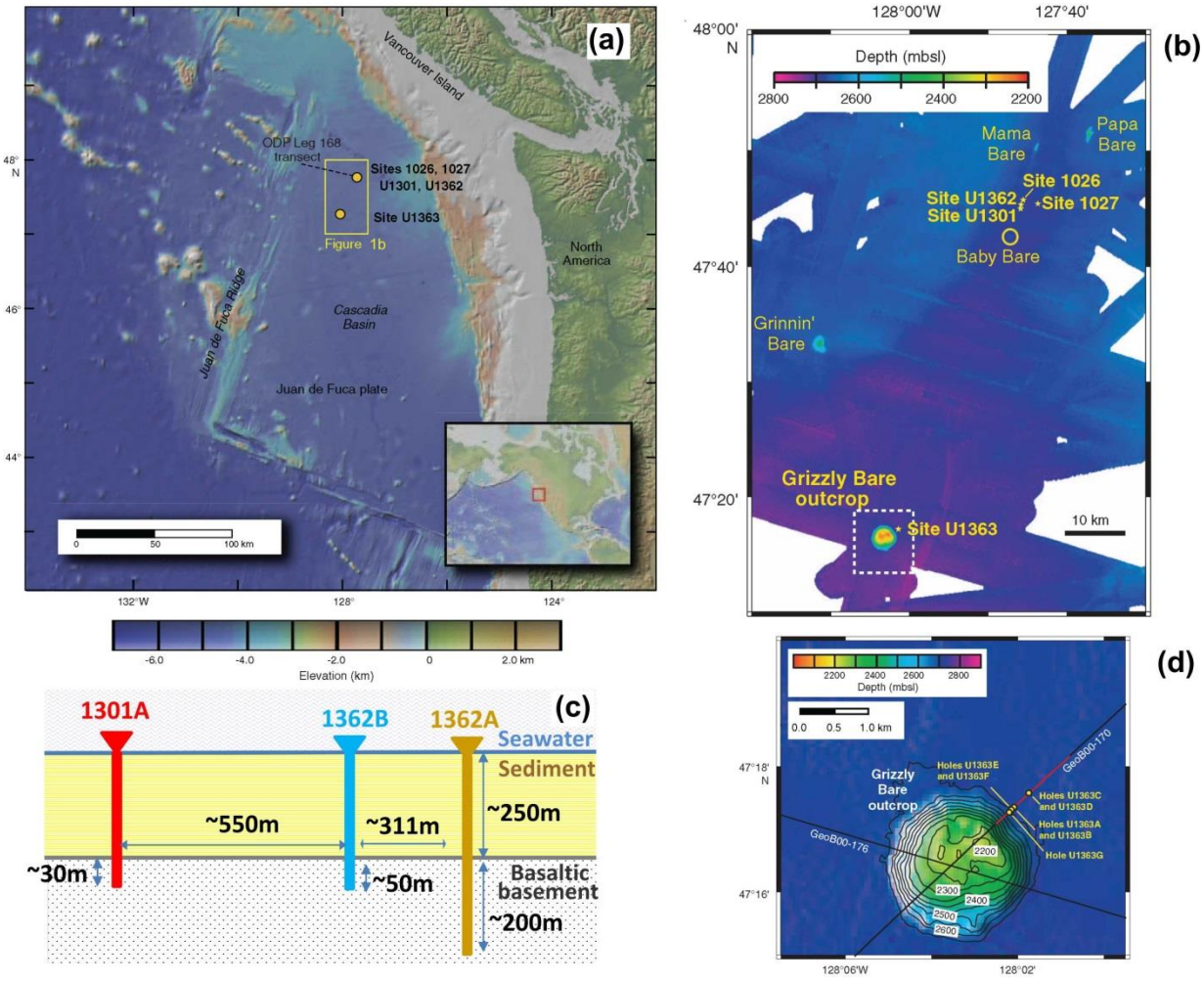

Figure 4.2. Energetics for amino acids synthesis based on equations listed in Table 1 by using average geochemical data (H_2, NH_4+, pH and bicarbonate) from CORK 1301A, 1362A and 1362B fluids (listed in table 3.1). Black dash lines indicate the hydrogen activities from the three sites.

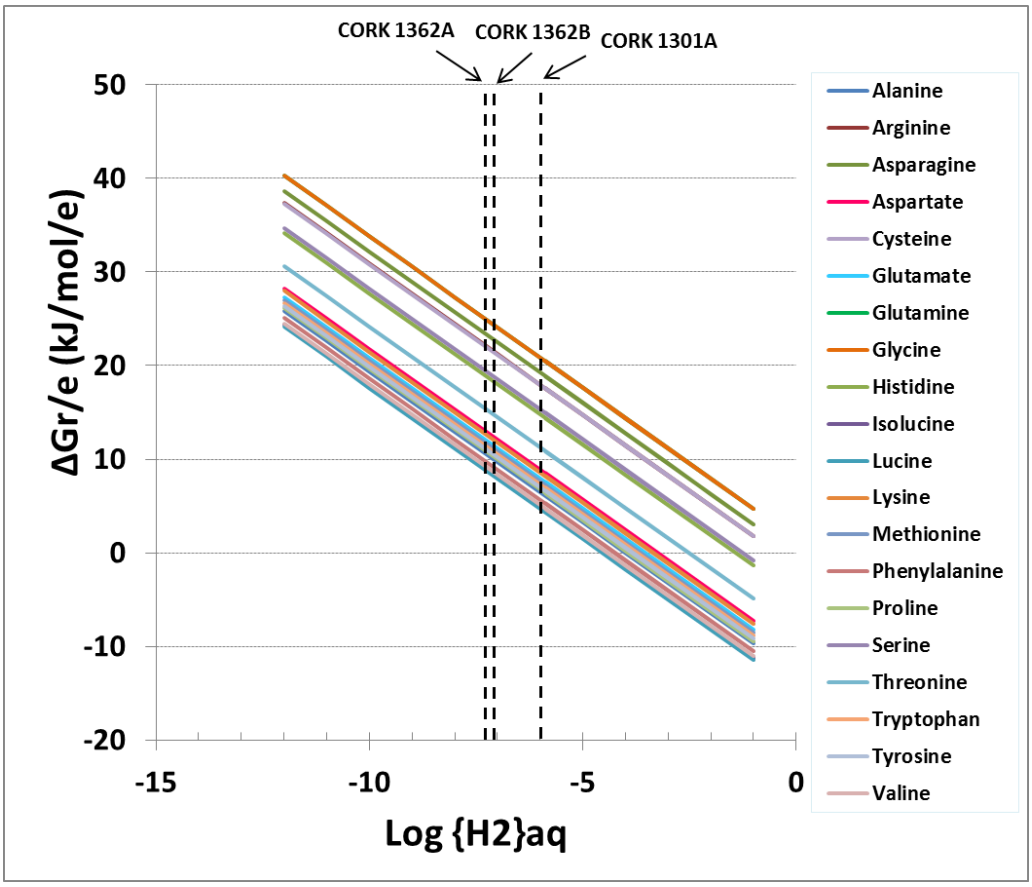

Figure 4.3. Mole percent distribution of dissolved hydrolysable amino acids, DHAA, in (a) ridge-flank basement fluids collected via CORK 1301A, 1362A and 1362B (b) North Pacific 2000m seawater (Kaiser and Benner, 2009) and bacteria (Cowie and Hedges, 1992) (c) deep hydrothermal-influenced marine sediment porewater collected from Juan de Fuca Ridge flank. (d) Mole percent distribution of dissolved free amino acids, DFAA, in deep hydrothermal-influenced marine sediment porewater collected from Juan de Fuca Ridge flank.

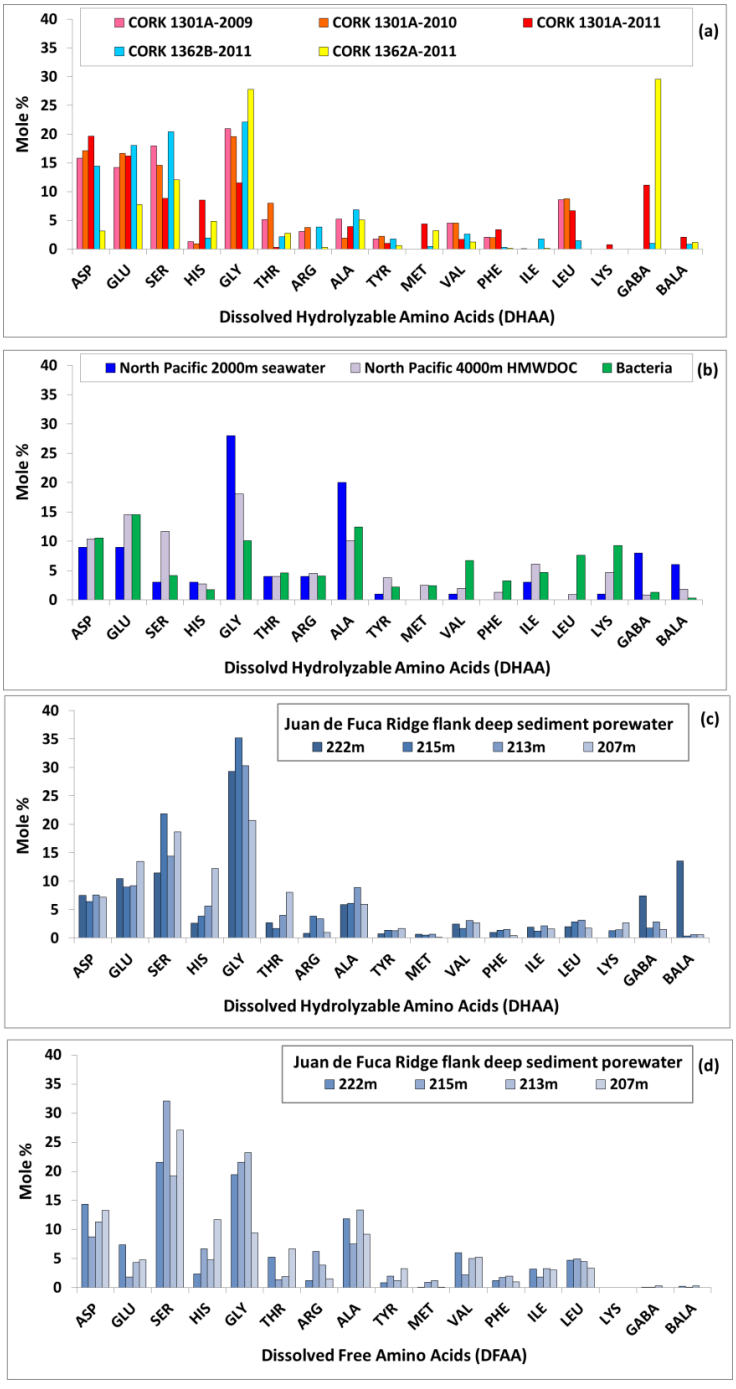

Figure 4.4. Scatter plots of selected well-correlated amino acids (Pearson correlation confidence level ≤0.01, Table 6). (a) Glutamic acids (GLU) versus tyrosine (TYR); (b) Glutamic acids versus ϒ-aminobutyric acid (GABA); (c) Carbon-normalized amino acid yields (AA yield %OC) versus GLU. Gray error bars are deviations (1SD); no replicate samples were run for CORK 1301A 2009 sample and the error bars for this sample are the average deviations of all other samples; dashed lines are used.

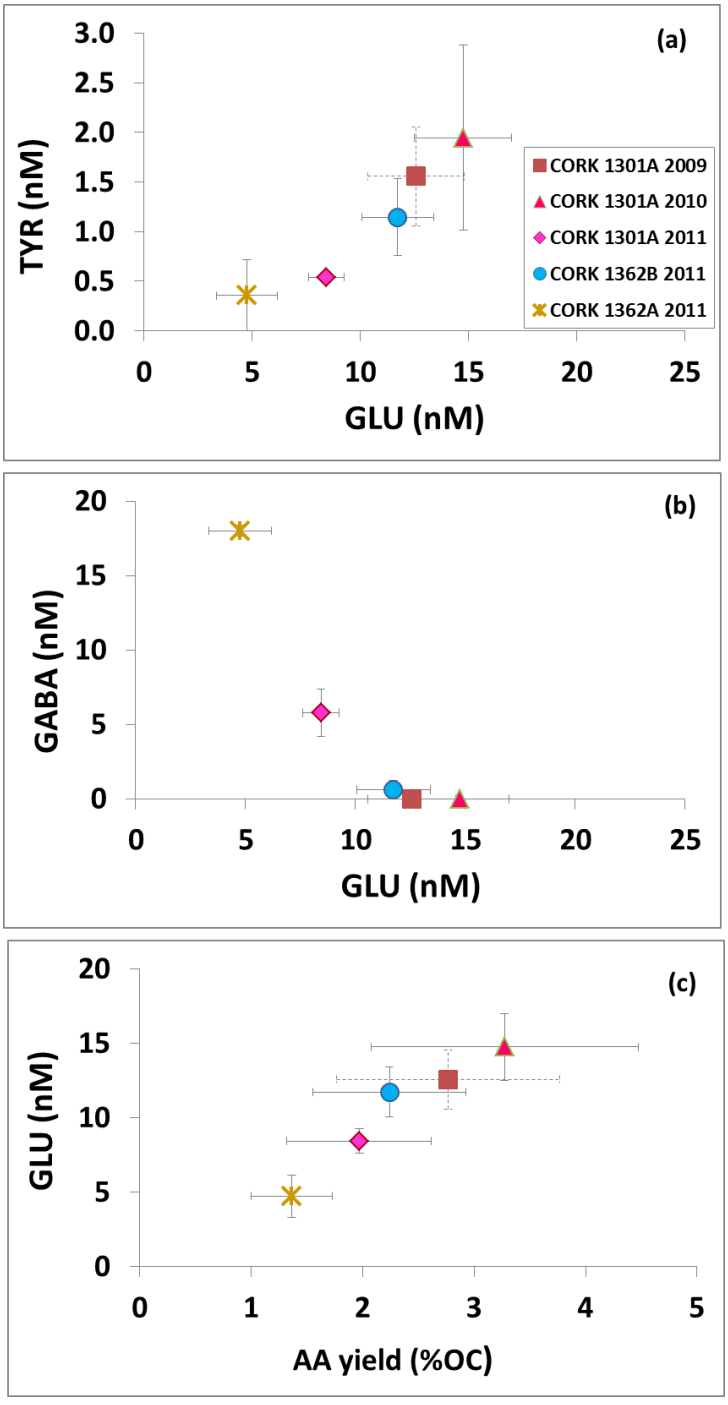

CHAPTER 5

Biogeochemistry of hydrothermal vents in NE Lau Basin: Dissolved and particulate organic carbon and total dissolved nitrogen

By

Huei-Ting Lin

James P. Cowen, David Butterfield, Edward T. Baker, Joseph A. Resing (co-author)

Manuscript prepared for submission to Geochimica et Cosmochimica Acta

5.0 Abstract

Dissolved organic carbon (DOC) is the largest carbon reservoir in the ocean. The impact of hydrothermal systems on seawater DOC could be profound, yet is poorly known. A rapid response cruise in May, 2009 to an on-going eruption at W. Mata, northeast Lau Basin, provided an unprecedented opportunity to measure DOC in fluids associated with a variety of seafloor hydrothermal environments. Hydrothermal fluid samples were collected from several diffuse vent sites, from two orifices of a focused black smoker vent and from fluids adjacent to molten lava. The impact of hydrothermal activity on the DOC in the overlying water column is also evaluated by measuring DOC concentrations in neutrally-buoyant hydrothermal plumes. Overall, results for our analyses show that hydrothermal activities induce biological activity, which produces DOC on the seafloor and in the sub-seafloor for export the from upper oceanic crust into the overlying water column.

The C/N ratio of particulate organic matter (POM) in fluids collected from diffuse vents is consistent with sources of POM from fresh marine and/or bacterial biomass. Concentrations of total dissolved nitrogen (TDN) in all diffuse and focused vent fluids sampled are lower than background seawater, in support of the presence of an active subsurface and/or surface vent biosphere. Elevated DOC and POM concentrations within neutrally-buoyant plumes over background seawater also indicate organic carbon production within the plume. DOC concentrations measured from the fluids collected adjacent to molten lava were found to be surprising high and cannot simply be explained by known sources of contamination. The high DOC may derive from circulating

hydrothermal fluids flushing DOC from potential sub-seafloor microbial habitats and/or sources of abiogenic DOC production.

5.1. Introduction

Organic carbon in the ocean can be operationally classified into dissolved and particulate forms. Combusted GF/F filter, which has nominal retention size of 0.7 μM, are commonly used to collect particulate organic carbon (POC) and the remaining organic carbon in the filtrate is defined as dissolved organic carbon (DOC). Dissolved organic carbon in the deep sea represents a significant carbon pool (662 Pg C, Hansell et al., 2009), equivalent to the total atmospheric carbon reservoir (MacKenzie, 1981; Siegenthaler and Sarmiento, 1993; Fasham et al., 2001). DOC plays important ecological roles as a byproduct of biological productivity and also as fuel for heterotrophic bacterial activity (e.g. Williams, 1970; Azam et al., 1983; Ducklow and Carlson, 1992; Carlson, 2002). Due to the utilization of DOC by microbial activity, the significance of a microbial carbon pump mechanism to convert atmospheric CO_2 into the deep ocean DOC has recently been proposed (Jiao et al., 2010) although the biological pumping mechanism via particulate organic matter (POM) has long been proposed (Volk and Hoffert, 1985) and widely-studied (reviewed by Honjo et al., 2008). Net production of DOC and POM in an environment results from the temporal and spatial decoupling of in situ biological production and consumption (Hansell and Carlson, 2001; Carlson, 2002; Honjo et al., 2008). Elevated concentrations of DOC are often observed in areas or at the time of vigorous biological activity, including increased primary production via extracellular release of DOC, intensified grazing-induced DOC produced by macro- and micro-zooplankton and elevated heterotrophic DOC production via release of extracellular

hydrolytic enzymes (e.g. Tanoue and Handa, 1979; Smith et al., 1992; Carlson et al., 2000; Hansell and Carlson, 2001; Carlson, 2002; Engel et al., 2012).

Deep seawater that recharges ocean crustal fluids contains ~40 µM of DOC (Hansell and Carlson, 1998; Hansell and Carlson, 2001; Hansell et al., 2009) and <1 µM-C of particulate organic carbon (Druffel et al., 1998; Loh and Bauer, 2000). Mixing of reduced hydrothermal fluids and oxic bottom seawater in the subsurface and at the seafloor provides a source of metabolic energy for chemolithotrophic microorganisms and supports an extensive seafloor and subseafloor hydrothermal ecosystems (McCollom and Shock, 1997; Amend et al., 2011). As a consequence, POM and DOC can be elevated in hydrothermal ecosystems where conditions are conducive to extensive chemolithoautotrophy, and can be exported to the deep ocean (Lang et al., 2006; Bennett et al., 2011b), contributing to the support of heterotrophic organisms in the deep ocean.

However, it is still uncertain whether the ocean crust is a net sink or a source for ocean water DOC (Eglinton and Repeta, in press). In addition, a significant proportion of marine DOC has been observed to be thermally altered (Dittmar and Paeng, 2009) and the input of such heat-altered DOC from deep-sea hydrothermal process is postulated (Eglinton and Repeta, in press). Some characterizations of DOC in hydrothermal fluids have been made, including hydrothermal hydrocarbons and hydrothermally-influenced sediment porewaters, to evaluate the impact of hydrothermal circulation on the deep ocean organic carbon reservoir (e.g. Simoneit et al., 1988; Simoneit, 1990; Simoneit and Sparrow, 2002; Lang et al., 2006; McCarthy et al., 2010; Bennett et al., 2011a; Bennett et al., 2011b; Lin et al., 2012). This paper presents new data on hydrothermal DOC and POC inputs to the deep ocean, including the first DOC measurements on fluids associated

with an on-going seafloor eruption. Moreover, whereas previously published hydrothermal fluid DOC and POC data are mainly derived from mid-ocean ridges (Lang et al., 2006; Bennett et al., 2011b), hot spot systems (Bennett et al., 2011a) or sediment-buried ridge flank oceanic crustal environments (Lang et al., 2006; McCarthy et al., 2010; Lin et al., 2012), the DOC data presented in this study are derived from a back-arc spreading system.

We hypothesize that high POC and DOC concentrations are expected in low temperature (<100°C) fluids, presumably associated with a well-developed subsurface microbial community (e.g. Lang et al., 2006). In contrast, lower POC and DOC is expected in high temperature (>>100°C) vent fluids due to low or absent microbial activity and thermal degradation (e.g. Lang et al., 2006); however, the DOC concentrations in high temperature fluids may be complicated by organic carbon entrained from other nearby subsurface biospheres. The lowest POC and DOC concentrations are expected in the vicinity of newly erupted basalt due to combustion of organic matter from the very high temperatures and the expected absence of subseafloor communities associated with new basalt flows.

This paper presents the DOC and POM measurements of hydrothermal fluids collected from six low temperature (<30°C) diffuse vents, one high temperature (315°C) focused vent and fluids adjacent to molten lava. The $\delta^{13}C$ values of POC from two low temperature sites are presented. Total dissolved nitrogen (TDN) and particulate nitrogen (PN) concentrations are also presented as another potential indicator of subseafloor biosphere activity. The DOC concentrations from the water column samples are used to assess the impact of the hydrothermal fluids on the water column above the eruptive sites.

5.2. Geological settings and methods

The Lau Basin is a triangular-shaped active back-arc basin (Fig. 5.1a). The basin is associated with the Tonga-Kermadec subduction zone in the western Pacific margin. Several hydrothermal fields were discovered and studied along the Lau Basin extensional zone in the early 1990s (e,g. Fouquet et al., 1990, 1991). There are multiple rifting and spreading centers in the Lau Back-arc Basin (Hawkins, 1995), the most northeastern of which is the Northeast Lau Spreading Center (NELSC). NELSC's maximum spreading rate is estimated to be about 94 mm/year (German et al. 2006). Between the NELSC and the frontal magmatic arc of the Tonga-Kermadec subduction zone lays several submarine volcanoes including West Mata. This entire area is hydrothermally very active (Falloon et al., 2007). During a cruise conducted by National Oceanic and Atmospheric Administration Pacific Marine Environmental Laboratory (NOAA-PMEL) in November 2008, two active eruption events were detected in this area. One was within the NELSC and the other at West Mata (Baker et al., 2011; Clague et al., 2011; Resing et al., 2011; Rubin et al., 2012).

5.2.1. Response *cruise and sampling sites*

In response to the two eruptions discovered in November, 2008 (Baker et al., 2011; Clague et al., 2011; Resing et al., 2011; Rubin et al., 2012), a research cruise was staged to Northeast Lau over May 5-13, 2009 on the R/V *T. G. Thomas* (Resing et al., 2011). During the cruise, seven dives by the remotely-operated-vehicle (ROV) JASON II (Woods Hole Oceanographic Institution) were conducted. Five dives were at the West

Mata area and two dives at the NELSC (Fig. 5.1a). Active eruptions were observed at West Mata during each dive there. Three eruption sites were identified: Hades, Akel's Afi and Prometheus (Fig. 5.1b). Near the eruptions sites, several low temperature diffuse vents were discovered: Creamsicle, Kohu, Shrimp City, Red Rock Ridge, Epsilon, Luo, and White Mat (Fig. 5.1b and 5.2; Table 5.1). In contrast, no eruptive activity was found at NELSC, although high temperature black-smoker type chimneys were relocated at Maka volcano in the southern NELSC (Fig. 5.1). Fluid samples were collected at this Maka vent from two fresh orifices formed when the ROV JASON broke the two chimneys sprouting from a single sulfide mound.

CTD operations were conducted from the R/V Thompson to assess the impact of the volcanic eruptions on water column chemistry and microbiology over and down current from the eruptive sites. One vertical cast (*V09C01*, Table 1) was made over the W. Mata eruptive site. A second vertical cast (*V09C02*, Table 1) was performed over the Maka high temperature black smoker vents with multiple chimneys and vent orifices. Two horizontal tows were made during which the CTD was continuously lowered then raised in a saw-toothed pattern (i.e., tow-yos; Baker 1998); samples from one of the tow-yos were collected for this study (Table 5.1). Sensors on the CTD measured conductivity, temperature, pressure, oxygen, optical backscatter, fluorescence, altimetry and oxidation-reduction potential (ORP). Anomalies in ORP indicate the presence of reduced chemical species such as H_2S and Fe^{2+}.

5.2.2. Sampling methods

Plume and background seawater samples were collected with Niskin bottles during CTD-rosette vertical and tow-yo casts (Table 1). Hydrothermal vent fluid samples were collected by JASON II using the PMEL Hydrothermal Fluid and Particulate Sampler (HFPS, Huber et al., 2002; Butterfield et al., 2004) and Ti-major samplers. The HFPS samples were collected into either 500mL Tedlar bags (HFPS-Bag) or 500mL Titanium piston type containers (HFPS-Piston). All diffuse vent samples used for this study were collected with the PMEL HFPS-Bag sampler.

The HFPS pistons and the lids for both the bags and the pistons were cleaned and sterilized with ethanol, followed by a vigorous deionized water rinse and finally by a filtered seawater rinse. Ethanol from a squirt bottle was sprayed on the filter holder components in the lid to sterilize and degrease the filter holder. The lid parts were then wiped off with a Kim-Wipe, rinsed under a stream of deionized water at the Millipore water purification dispenser, and assembled with the filter holder; Millipore water was circulated through the whole assembly. Finally, about 50ml of filtered seawater was passed through the lid.

DOC and TDN blanks for the samplers were collected in the shore-based laboratory by adding DI, 0.24 N HCl or 1N H_2SO_4 to HFPS-Bags and HFPS-Ti-Pistons to simulate the neutral to extremely low pH hydrothermal fluids that we could have sampled. The duration of the acid treatment provides an extreme condition to simulate how the samplers may contribute to DOC even when very acidic hydrothermal fluids are collected and temporarily stored. The samplers for the blank tests were treated the same as they were treated shipboard prior to actual sampling.

All fluid samples were filtered shipboard through combusted GF/F filters (550ºC for 5 hours) in acid-cleaned Whatman plastic filter holders. At least 50 mL of deionized water was passed through each filter just prior to use to ensure that a DOC blank below detection limit was achieved. The filtered samples were stored in acid-washed high-density polyethylene Nalgene bottles and kept frozen until thawed for analysis (Tupas et al., 1994).

Particulates were collected by in situ pumping 2-5 L of hydrothermal vent fluids through combusted GF/F filters (550ºC for 5 hours) using the HFPS. About 10 L of seawater collected with CTD-rosette Niskin bottles were filtered on board ship through combusted GF/F filters. Individual filters were wrapped in combusted foils and stored frozen until thawed for analysis.

5.2.3. Sample *analysis*

5.2.3.1.Dissolved organic carbon

Dissolved organic carbon (DOC) was measured by high-temperature combustion using a Shimadzu TOC-V_{CSH} analyzer. Combustion temperature was set at 720ºC. Samples were acidified to pH <2 within the autosampler syringe by adding 45 µL of 2N HCl to 3 mL samples. No acid contamination was observed throughout the analysis. Samples were purged with nitrogen to remove inorganic carbon. Five to six replicate analyses were performed using an injected sample volume of 150 µL. The reproducibility between replicate injections was <2 µM, i.e. <5% at 40 µM.

Two consensus reference materials (CRM, from University of Miami, Dickson et al. 2007), Florida Strait 700 m-deep seawater (DSW) and low carbon water (LCW), were

used extensively before, between and after sample analysis. At least one CRM was measured every 5 samples. The measured concentration of CRM-DSW was 42 ± 0.2 µM (n=23), which is consistent with the certified range of DOC concentration (41~43 µM). The average measured CRM-LCW value was 1.3 ± 0.4 µM (n=7), which also fell within the certified range of 1~2 µM. The detection limit was about 1 µM.

5.2.3.2.. Total dissolved nitrogen

Total dissolved nitrogen (TDN) was measured with a chemiluminescence detector in-line with the described Shimadzu TOC-V_{CSH} analyzer (Sharp, 2002). Consensus reference materials mentioned earlier were also used extensively to monitor the instrumental performance. Measured CRM-DSW is 33 ± 0.1 µM (n=23), the same as the certified value of 33 µM. The detection limit of TDN was about 0.5 µM.

5.2.3.3. Particulate organic carbon

A few drops of sulfurous acid (6-9% of H_2SO_3) were added to wet the filter and to remove inorganic carbon from the filter. The acidified filters were transferred to a 60°C oven for 24 hours. The dried filters were then transferred into a tin capsule before placing within a high-temperature combustion CN elemental analyzer (Costech, ECS 4010) connected in-line with a Mass Spectrometer (ThermoFinnigan Delta XP interfaced with a ConFloIV) for analysis of their organic carbon and nitrogen isotopic compositions.

5.2.3.4. pH measurement

Measurements of pH were made with an in-situ pH sensor (AMT, Rostock, Germany) connected to the home port of the HFPS. This pH sensor was repeatedly calibrated in the

lab and the post cruise calibration indicated that this sensor worked well throughout the cruise.

5.3. Results

5.3.1. Blank tests

The DOC and TDN blank values for DI in HFPS-Bag and HFPS-Ti-Piston samplers are below or only slightly elevated over the instrumental detection limit (~1μM and 0.5 μM, respectively) even after the DI sat in the bag or sampler for several hours (Table 5.2). Elevated DOC blank values (3-5μM) are observed after exposure of the HFPS-Bag and HFPS-Ti-pistons to 0.24N HCl over a course of 2 hours. Much higher DOC values (20-30 μM) are observed when the Ti pistons are exposed to 1N H_2SO_4 for 20 hours.

DOC blanks contributed by ethanol, which was used to sterilize the Ti pistons (section 5.2.2), were also evaluated. A 40mL combusted glass vial was first filled with ethanol, drained, filled with 40mL of DI, and then the DI was repeatedly drained out and filled with another 40mL of fresh DI. The resulting DOC value of the first DI-displacement in the glass vial is as high as 41.7 mM. The second 40mL DI displacement lowered the DOC blank ten-fold, the third to 63 μM, and the fourth to below 10 μM. The ethanol "rinse" blanks were prepared to provide the range of DOC that could be contributed from the sampler due to insufficient rinse after ethanol treatment.

In contrast, during our routine operation, the HFPS sampler is only exposed to a very small amount of ethanol (ethanol sprayed from a squirt bottle and dried with Kimwipes, section 2.2) and then is rinsed with copious amount of running deionized water. The rinse water should have displaced the ethanol with much more than four times the ethanol

volume. As a consequence, the overall sampler blanks summarized in Table 2 are the best representatives of our sampling blanks as the procedure for sampler blank collection followed the shipboard treatment.

5.3.2. DOC and TDN of vent fluids

The DOC concentrations for the diffuse vent fluids from the NE Lau Basin ranged from 39 µM to 521 µM (Table 5.3). Creamsicle and Red Rock vent fluid samples have DOC concentrations similar to those of bottom seawater in this area (39-45 µM, Table 5.3). The DOC concentrations of the diffuse vent fluid samples from the other sites are greater than that of bottom seawater. The highest DOC concentration observed in diffuse vent fluids (521 µM) derived from the Epsilon site. All the diffuse vent fluid samples have TDN concentrations within the 4.3-24.5 µM range, much lower than bottom seawater (39 µM, Table 5.3).

DOC concentrations in fluids collected from the two orifices of the focused high-temperature vent at Maka are 27 and 52 µM (Table 5.3), bracketing bottom seawater values (39 µM DOC). In contrast, the TDN concentrations for the focused vent fluid samples are 7 and 11 µM, considerably lower than that of deep seawater (39 µM TDN, Table 5.3).

The DOC concentration in fluids collected adjacent to the molten lava range from 63 to 1704 µM (Table 5.3), much higher than that of deep seawater. However, the TDN concentrations of these samples (34-40 µM) are about the same or slightly lower than that of bottom seawater (39 µM).

5.3.3. DOC, TDN, POC and PN of hydrothermal plume samples

A pronounced particle-rich layer was identified as a neutrally buoyant hydrothermal plume, ~80-100 m above the W. Mata eruption sites with greatly elevated light scattering anomalies (higher dNTU, anomaly in nephelometric turbidity units) and much lower oxidation-reduction potential (Fig. 5.3). The plume signal above Maka volcano was not as intense as the plume above W. Mata. The Maka plume had only slightly elevated light scattering anomalies and a minor dip in oxidation-reduction potential (Fig. 5.3). The DOC concentrations of the neutrally-buoyant plume samples above W. Mata is 45 ± 1 µM while those from above Maka volcano are 39±2 (Table 5.4). The DOC in background seawater samples is 39±1 µM (996m, 1598m & 1557m, Table 5.3). POC concentrations for W. Mata plume samples range from 0.28 to 0.56 µmolC/L, PN from 0.031 to 0.050 µmolN/L, and particulate-C/N ratios from 8.8 to 11.2 (Table 5.4), whereas the values for POC, PN and particulate-C/N ratios in the Maka plume samples are 0.29±0.08 µmolC/L, 0.036±0.01 µmolN/L and 8.2±0.5, respectively. Local background bottom seawater sample POC, PN and particulate-POC/PN values are 0.21±0.07 µmolC/L, 0.024±0.01 µmolN/L and 8.5±0.5, respectively (Table 5.4). TDN concentrations of plume samples above both W. Mata and Maka are uniformly 39 ± 1 µM, identical to that of background seawater.

5.3.4. POC and PN in vent fluids

The POC concentrations in Red Rock and Luo diffuse vent fluid samples are 2.45 and 3.08 µmol/L, respectively (Table 5.5), an order of magnitude higher than that for background seawater (no plume signal) above the vent (0.21±0.07 µmol/L, Table 5.4).

The POC concentration in the sample from Kohu vent is 0.48 µmol/L, also elevated relative to background seawater. The PN concentrations in Red Rock and Luo diffuse vent fluid samples are 0.398 and 0.605 µmol/L, respectively, much higher than that in background seawater (0.024 µmol/L). The PN concentration in Kohu vent fluid is 0.042 µmol/L, twice of that in background seawater.

5.4. Discussions

5.4.1. Sampler DOC blank

The low DOC blank of the HFPS-Bags is in good agreement with the replicate bag samples at Creamsicle, documenting the consistently low blanks for both sampling fluids with HFPS-Bags and our lab procedures. Although an elevated concentration of DOC was observed after samplers was subjected to 0.24N HCl for several hours, it is relatively small (e.g. about 10% of the background seawater value) and would not have a major impact on measurements of DOC at high concentrations. The 0.24N HCl should be a good representative of the acidic samples collected in hydrothermal vents; in fact, the pH (<0.6) of the 0.24N HCl blank tests is much lower than the lowest pH (1.6, eruptive sites, Table 5.3) of fluids collected for this study.

Although there is an increase of DOC after the Ti piston samplers were exposed to 1N H_2SO_4 for 20 hours, this acid treatment is much stronger than what the samplers would be exposed to the vent fluids; furthermore, the amount of DOC measured in the 1N H_2SO_4 treatment blanks is still relatively small compared to the very high DOC in fluids collected near eruptive sites with piston samplers (Table 5.3).

It is unlikely that the elevated DOC in the acid treatment experiment resulted from the DOC leached from fluorolube grease (Fluorolube GR 290, Fisher Scientific) used for lubricating the piston sampler. As much as 0.5g of fluorolube grease only contribute 1-5 µM total DOC and <0.4 µM TDN, even after sitting in DI, 0.1 N HCl or 1N H_2SO_4 for 24 hours (data not shown). Nevertheless, the acid treatment using 1N H_2SO_4 provide an upper limit for the DOC blank values that can be contributed from the HFPS-Piston sampler.

Ti-major samplers were used to collect high-temperature focused vent fluids in this study. No blank tests with Ti-major samplers were performed during this study. In a separate study, the DOC values are about 10-15 µM higher in oceanic deep crustal fluid samples collected using Ti-major samplers than using a newly developed clean sampler described in Cowen et al. (2011) and Lin et al. (2012). A similar level of DOC blank value (15.9 µM) for Ti-major sampler is reported by Bennett et al. (2011a). In contract, an undetectable DOC blank value is reported by Lang et al. (2006). Therefore, the DOC blank value for Ti-major is most likely somewhere between 0 and 15 µM. Here we used 15 µM as a conservative blank value to correct the DOC measured in fluids collected by Ti-majors.

5.4.2. Sample quality

Seawater entrainment is problematic during sampling of hydrothermal vent fluids at the seafloor. For high temperature vent fluids (>300^{0}C), the vent fluid end-member should contain very low Mg due to its removal during rapid water-rock reaction at high temperature (Mottl, 1983). In contrast, seawater contains much higher Mg (53mM). If a

conservative mixing relationship exists between Mg and the component of interest, e.g. DOC, Mg can be used to account for the signal contributed from seawater entrainment. However, since only two samples were collected from this particular vent type, it is not statistically possible to conclude whether a conservative mixing relationship between Mg and DOC existed at this study site. Nevertheless, the Mg concentrations of the two high temperature focused vent fluids are 4.2 and 4.7 mM (Table 5.3), much lower than that of bottom seawater, (53 mM), suggesting minimum (no more than 8%) seawater entrained in the two samples. The directly measured DOC values without applying Mg for seawater entrainment correction are reported. In addition, since non-zero Mg vent fluids have been observed (Ravizza et al., 2001), we also hesitate to assume that the end-member fluids from the Maka sulfide mound have zero-Mg for the correction.

It is more difficult to estimate the amount of seawater entrainment in low temperature diffuse vent fluids. Diffuse vent fluids are thought to derive from either subsurface mixing of high temperature fluids with seawater (Butterfield and Massoth, 1994; Butterfield et al., 1997) or from seawater that has been warmed by warm rocks (Cooper et al., 2000). The low temperature vents lack a focused conduit, making them more vulnerable to seawater entrainment during collection. The removal rate of Mg from fluids via water-rock reaction decreases significantly at lower reaction temperature (Mottl, 1983). As a result, the removal of Mg is much less significant at low temperature diffuse vents than at high temperature focused vents. The Mg concentrations of the diffuse vent fluid samples collected at W. Mata range from 49 to 57 mM (Table 5.3) bracketing the value for bottom seawater (53 mM). The high Mg concentrations in the diffuse vent fluids do not necessarily indicate high seawater entrainment during collection; rather, it

could indicate that diffuse vent fluids can result from the rapid warming of seawater with little removal of Mg. High integrity of the diffuse vent fluid samples is suggested by their much elevated silicate (>1000 µM) and dissolved iron (38-983 µM) concentrations relative to bottom seawater concentrations (silicate ~80 µM, dissolved iron <0.1 µM). Moreover, the higher temperatures (13-30°C) and much lower pH (2.8-5.8) of the diffuse fluids relative to surrounding bottom seawater (4°C, pH~8.0) also indicate that the diffuse vent fluids collected are distinct from bottom seawater. Due to the difficulty in obtaining a suitable factor for seawater entrainment correction, we report only the "uncorrected" values.

5.4.3. Elevated DOC in NE Lau diffuse vent fluids

The DOC concentration in the diffuse vent fluids from the NE Lau vent field varied from close to bottom seawater values (39 µM) at Creamsicle (40 µM) to a greatly elevated value at Luo (126 µM) and Epsilon (521 µM). Based on previous studies of vent fluids, the Epsilon DOC concentrations are much higher than expected. At Axial Volcano and Endeavour vent fields the DOC in diffuse vent fluids ranged from 34 to 71 µM (Lang et al., 2006). At 9°50'N East Pacific Rise vent field, the DOC in near-field plume fluids ranged from 37.9 to 47 µM (Bennett et al., 2011b). Although the DOC of vent fluids at Loihi seamount ranged from 54 to 92 µM (Bennett et al., 2011a), the range of values for porewater extracted from microbial mats recovered from the Loihi vent field (68-179 µM, Bennett et al., 2011a) bracket the elevated DOC of vent fluids from Luo at NE Lau (126 µM). The high Epsilon diffuse vent fluids DOC (521 µM) approaches the mM level of DOC measured in porewaters from microbial mats (e.g. Jonkers et al., 2003; Jonkers et al., 2005) and marine sediments (e.g. Simoneit and Sparrow, 2002). The young Epsilon

vent site had little sediment cover, but abundant filamentous microbial mats were observed at this study site (Fig.5.2f). Disturbance of the microbial mat during sampling could have caused DOC-rich porewater from microbial mats to mix with vent fluids. Interestingly, the elevated DOC at Epsilon is not accompanied by elevated TDN (Table 5.3).

5.4.4. DOC production and removal in hydrothermal systems

The elevated DOC concentrations of the low temperature diffuse vent fluids from the NE Lau Basin indicate that overall DOC input exceeds DOC removal processes within these vent systems. When bottom seawater recharges a hydrothermal system, it possesses ~40μM of DOC. Here, a model of DOC production and removal is proposed to describe the potential sources and sinks of DOC in a hydrothermal system (Fig. 5.4). Within the hydrothermal system, chemoorganotrophic organisms consume DOC and transfer carbon into the dissolved inorganic carbon (DIC) pool, decreasing the DOC pool, while on the other hand, chemolithoautotrophic organisms produce organic carbon from DIC (e.g. Karl, 1995). Some chemolithoautotrophic organisms such as acetogens and methanogens produce low molecular weight organic carbon (Lovley and Klug, 1983; Thauer, 1998). Macrofauna messy grazing can leak DOC (Carlson, 2002 and references therein) and POC can undergo cell lysis and other alterations to release carbon back to the DOC and the DIC pools (Fuhrman, 1992; Fuhrman, 1999; Carlson, 2002). Abiotic processes such as adsorption (Delacour et al., 2008; Ruttenberg and Sulak, 2011), heat degradation (Simoneit, 1984; Simoneit et al., 1992; Simoneit and Sparrow, 2002) and organic thermogenesis (Welhan and Lupton, 1987; Dittmar and Koch, 2006) also alter the bulk DOC concentration. The abiotic formation of low molecular weight organic carbon and

amino acids are thermodynamically favorable in some hydrothermal systems (Amend and Shock, 1998; Proskurowski et al., 2008), which can also contribute DOC to the system. Elevated dissolved organic carbon, formate and acetate relative to seawater have been observed in fluids from the Lost City vent field (Lang et al., 2010). A distinct inverse trend in the stable carbon and hydrogen isotopic composition of C1 to C4 hydrocarbon in Lost City vent fluids suggest abiotic origin (Proskurowski et al., 2008).

5.4.5. Biological production of organic carbon

All of the vent fluids collected during this study contained high concentrations of reducing species such as dissolved iron (dominantly Fe^{2+}), manganese and hydrogen sulfide (Table 5.3). The mixing of reducing vent fluids with oxic bottom seawater can yield significant energy via reactions such as iron, manganese and sulfide oxidation (McCollom and Shock, 1997). Abundant filamentous microbial mats were observed in several of the low temperature diffuse vent sites, such as Epsilon and Creamsicle (Fig. 5.2). Scattered microbial mats were also observed at low temperature diffuse vents Shrimp City and Luo, where high abundances of indigenous shrimps were also present (Fig. 5.2). Metabolism within these microbial mats could release dissolved organic carbon into the hydrothermal fluids. In this case, DOC was presumably produced by the mat community (macrofauna and microfauna activities) and entrained into the venting fluids. Subseafloor microbial communities residing at the interface between ascending anoxic warm fluids and descending recharge seawater could have contributed additional DOC to the venting fluids (Lang et al., 2006; Bennett et al., 2011a; Bennett et al., 2011b). The DOC measured in this study was the composite result of the DOC production and consumption activities both within the subseafloor and at the seafloor.

The elevated DOC within the vent fluids is consistent with the higher values for POC and PN measured in fluids from the Red Rock, Luo and Kohu diffuse vent sites relative to background seawater (Table 5.5). The elevated POC concentrations in the vent fluids from Red Rock (2.45 μmol/L) and Luo (3.08 μmol/L) are within the range of POC concentrations (0.87-3.81 μmol/L) observed in the near-field plume fluids from East Pacific Rise (Bennett et al., 2011b). Elevated POC concentrations (up to 18.3 μmol/L) have also been observed in warm diffuse vents at 21°N East Pacific Rise (Comita et al., 1984).

The POC in the Red Rock and Luo vent fluids have C/N ratios of 6.1 and 5.1, respectively, significantly lower than the C/N of POC collected from background seawater (8.9 ±1; Table 5.4 & 5.5). The low C/N ratios in Red Rock and Luo vent fluids are close to but even lower than the Redfield ratio (6.6, Redfield, 1958), suggesting that the POC was derived from a fresh marine source material and/or bacterial biomass (5.2-5.9, Meyers, 1994; Fukuda et al., 1998). Degradation of POC results in elevated C/N ratio (Meyers, 1994). Although the C/N of POC from Kohu vent is 11.4, much higher than from the Red Rock or Luo vents and is similar to nearby deep water POC values (Table 5.4 & 5.5), it still fell within the marine source range (Meyers, 1994; Fukuda et al., 1998).

Carbon isotope values of POC also reflect the potential carbon source and carbon assimilation pathways leading to the synthesis of POC (e.g. Sirevåg et al., 1977; Preuss et al., 1989; Popp et al., 1998; Hofmann et al., 2000; Hayes, 2001). The $\delta^{13}C$ values for the POC from Red Rock and Luo vents are -15.5 ‰ and -12.3 ‰, respectively (Table 5.5), which is higher than POC from nearby background seawater (-23±1 ‰, Table 5.5).

Provided that DIC in vent fluids has $\delta^{13}C$ values ranging from -2.5 to -9 ‰ (Zerkle et al., 2005; Walker et al., 2008), the ^{13}C enrichment in Red Rock and Luo vent fluid POC suggests that the resident microbes within the Red Rock and Luo vents may utilize carbon fixation pathways that lead to lower carbon isotope fractionation (Zerkle et al., 2005) than that associated with the most common photosynthetic pathway (C3 or Calvin-Benson cycle, Descolasgros and Fontugne, 1990; Zerkle et al., 2005). For example, carbon isotope fractionation is 2-5.5 ‰ via the reductive tricarboxylic acid (TCA) cycle and 0.2-3.6 ‰ via the 3-hydroxypropionate (3-HP) cycle (Zhang et al., 2002; House et al., 2003; Zerkle et al., 2005). The low $\delta^{13}C$ values of the POC from the background deep seawater (Table 5.5) most likely resulted from sinking particles produced in the surface ocean via the photosynthetic Calvin-Benson cycle (Meyers, 1994). In contrast, the high $\delta^{13}C$-POC values Red Rock and Luo vent fluids suggests that this POC was likely produced within the subsurface and/or at seafloor or vent surface biospheres through which the vent fluids circulate, as opposed to an accumulation from sinking photosynthesis-derived particles.

In addition to POC synthesized from DIC, methanotrophic activity can also leave an imprint on the carbon isotope value of biomass. Methane ($\delta^{13}C$=-16 to -55‰, Lilley et al., 1993) is another primary carbon source in hydrothermal systems. Since the carbon isotope fractionation between methane substrate and the biomass of methanotrophs range from -23.9 to -12.6 ‰ (Jahnke et al., 1999), methanotrophs would have $\delta^{13}C$ values in the range of -28.6 to -78.9‰. Since the POC in the Red Rock Ridge and Luo vent fluids is ^{13}C-enriched ($\delta^{13}C$=-15.5 ‰ and -12.3 ‰, respectively) relative to the biomass of potential methanotrophs ($\delta^{13}C$=-28.6 to -78.9‰), the POC isotope composition suggest

that methanotrophs are unlikely to be the dominant component of the POC. However, since POC provides a composite view, the δ^{13}C-POC values alone does not exclude the presence of methanotrophs in the two vent systems.

Lower concentrations of TDN in the diffuse and focused vents relative to bottom seawater (Table 5.3) also suggests a prosperous subseafloor and surface vent biosphere. Recharge local bottom seawater carries about 39 µM of TDN, as nitrate, into the subseafloor circulation system (Table 5.3). Biological activities such as nitrogen assimilation (e.g. chemosynthesis) and denitrification (ultimately to a gaseous end product) are known to decrease TDN in an aquatic environment (e.g. Jannasch, 1995; Cornwell et al., 1999; Devol, 2008). Similar to photosynthesis, chemosynthesis converts DIC and dissolved inorganic nitrogen (DIN) into particulate organic matter (e.g. Gruber, 2008). Moreover, in reducing environments, chemoautotrophic denitrifiers reduce nitrate, ultimately into nitrogen gas, decreasing the nitrate concentration in the fluids (Butterfield et al., 2004; Devol, 2008; Bourbonnais et al., 2012). The presence of ammonium in all of the diffuse vent fluids and the Maka high-temperature vent fluids also demonstrate the occurrence of nitrate reduction along the fluid flow paths. These subseafloor biological activities result in the production of organic carbon and, subsequently, increase DOC and lower the TDN in the circulating hydrothermal fluids.

5.4.6. Impact on the water column

Hydrothermal activities inject reducing species such as dissolved iron, hydrogen sulfide, hydrogen and ammonium into the overlying water column, inducing biological production and increasing POC and DOC concentrations (Cowen and Baker, 1998;

Bennett et al., 2011a; Bennett et al., 2011b). POC and PON concentrations observed within the W. Mata plume were twice those of the background seawater values (Table 5.4), consistent with previous observations from along the East Pacific Rise (Bennett et al., 2011b) and support the statement that hydrothermal activity can induce biological production in the deep ocean (Cowen and Baker, 1998; Cowen et al., 2001; Bennett et al., 2011a; Bennett et al., 2011b). The injection of hydrothermal fluids (e.g. Red Rock Ridge, Luo and Kohu, see section 4.5) that contain higher POC than background seawater, may contribute to the increased POC observed within the plume fluids. However, based on the dissolved Fe values of the W. Mata hydrothermal fluids (38-983 μM, Table 3) and plume fluids (<0.1 μM, Table 4), the hydrothermal diffuse vent fluid POC signal should also have been diluted by at least four-hundred times, although the oxidation of dissolved Fe to form particulate iron-oxyhyroxide can also accelerate the removal of dissolved Fe from the injected hydrothermal plume. Studies show that 3-5 orders of magnitude dilution factors are typical in forming neutrally buoyant plumes from seafloor hydrothermal vents (e.g. Lupton et al., 1985; Field and Sherrell, 2000; Cowen et al., 2003; Edmonds et al., 2003). Thus, enhanced POC found in some diffuse vent fluids are insufficient to account for the observed two-fold increase of POC in the plume fluids.

Consistent with the elevated POC, the concentrations of DOC in the W. Mata plume-samples (45±1 μM) are also significantly higher than that of background seawater (39±1 μM; two-tail t-test). The amount of increase in DOC in the W. Mata plume is comparable to the increase in DOC of plume samples collected from a site surveyed along the East Pacific Rise (plume DOC=43 μM; background seawater=38±1 μM, Bennett et al., 2011b). The increase in the W. Mata plume DOC is likely produced by more vigorous biological

activity (as suggested by higher POC) induced by the elevated supply of reducing species, as indicated by the anomaly in oxidation-reduction potential and more intensive particle layer (high turbidity NTU, Fig. 5.4).

In contrast, the DOC concentrations in Maka plume fluids are not significantly different from that in background seawaters. The unchanged DOC concentration is consistent with a second site surveyed over the East Pacific Rise (Bennett et al., 2011b). The Maka plume is much less intense than the W. Mata plume, although there is a slight elevation in POC concentrations to indicate production of POC within the plume, the biological activity may not be vigorous enough to reveal an increase in DOC.

5.4.7. Elevated DOC in high temperature fluids

Black smoker

The fluid collected from one orifice of a high temperature vent at Maka had a DOC concentration of 27 µM, less than background seawater but at the high end of the values reported for high temperature vent fluids at the Main Endeavour Field (12-26 µM) and Axial Volcano (8-24 µM, Lang et al., 2006). Plausible explanations for the lower DOC concentrations within the high temperature vent fluids, relative to seawater, include abiotic heat destruction (e.g. Simoneit et al., 1992; Mango and Elrod, 1999), heterotrophic consumption within lower temperature subsurface and seafloor environments (e.g. Cowen et al., 2003; Huber et al., 2006) and sorption of DOC onto mineral surfaces of basaltic rocks (Delacour et al., 2008; Ruttenberg and Sulak, 2011). The DOC concentration of fluids from another orifice of the same Maka high temperature vent is 52 µM, slightly higher than background seawater values (Table 5.2 and 5.3).

Since no known organisms can survive at temperatures as high as 315^{0}C, the production of DOC by microorganisms at an environment with such a high temperature is implausible. However, DOC produced at lower temperatures along the hydrothermal fluid flow path may still remain in the fluid. Cracking of crude oil (complex organic carbon) occurs at temperature higher than 150°C with the presence of transition metals as catalysts (Mango & Elrod, 1999). Complete oxidation of most marine and hydrothermal DOC into carbon dioxide using platinum as a catalyst occurs at a much higher temperature than 315°C. In fact, the combustion temperature for DOC analysis is typically set at 680°C or higher (we used 720°C) to insure complete oxidation of DOC for accurate measurements of marine and hydrothermal DOC (Suzuki et al., 1992; Carlson et al., 2010; Bennett et al., 2011a; Bennett et al., 2011b). Thus, the survival of DOC in 315^{0}C vent fluids is plausible.

As described earlier, elevated POC, PON and/or DOC, accompanied by lower TDN in vent fluids relative to background seawater, is good evidence for the occurrence of nitrogen assimilation (e.g. chemosynthesis) and/or denitrification along the fluid flow paths (e.g. Biddanda and Benner, 1997; Wohlers et al., 2009; Engel et al., 2011). Both Maka high temperature vent fluid samples are lower in TDN and both are higher in ammonium relative to background bottom seawater (Table 3). A DOC entrainment model is proposed (Fig. 5.5) to describe the high DOC and low TDN within the high temperature vent fluid sample. Chemosynthesis could occur within lower temperature subseafloor zones where microbes can thrive (<120^{0}C), most of the nitrogen is removed and DOC is added to the circulation fluids (Fig. 5.5). The fluids could be subsequently entrained into a high temperature zone, heated up to >300°C and discharged at the

seafloor. Although some of the DOC might be heat degraded, some DOC, possibly altered, could survive, yielding the elevated DOC observed within the high temperature vent fluid.

Eruption fluids

The DOC concentration in the eruption fluids is surprisingly high (Table 5.3). Sampler preparation procedure followed in this study was ultimately a compromise to best accommodate competing analytical demands. Insufficient rinsing of the sampler following ethanol sterilization treatment could have a large impact on the sampler DOC blank as described in section 3.1 although our overall sampler blank tests clearly show that the highest DOC blank from the samplers is not higher than 30 μM (Table 2 and section 3.1). In addition, positive trends are evident for these samples between DOC and Si and DOC and Fe (Fig.6). Both high Si and high Fe in hydrothermal fluids are good indicators of high temperature water-rock reactions (Butterfield et al., 1997), and higher DOC corresponds to elevated Si and Fe in all fluid samples collected adjacent to molten lava sites. Contamination cannot explain the trends between DOC and Si or DOC and Fe.

The DOC concentrations in fluids collected adjacent to eruption sites greatly exceed the diffusive vent fluids (39-521 μM) and approach the level of DOC observed in microbial mat porewaters (e.g. Jonkers et al., 2003; Jonkers et al., 2005). A DOC entrainment model plausibly explains the high DOC observed in these eruption-associated fluids (Figure 5). The model assumes that discharged fluids entrain high DOC fluids from nearby low temperature seafloor microbial mat and/or deeper subseafloor biospheres. However, there were no macrofauana or obvious microfauana (e.g., mats) on the seafloor

near the eruption sites (Fig.2h and 2i); thus, the entrainment of high DOC fluids from nearby seafloor biosphere was unlikely. In contrast, the combination of a deeper subseafloor biosphere community and eruption-influenced hydrothermal circulation may still be plausible. Thermophiles isolated from event plumes associated with the 1996 eruption at North Gorda Ridge implied that these thermophiles were members of a native subseafloor community that was present before the North Gorda Ridge eruption event (Summit and Baross, 1998). Similar to the discharge of microorganisms during an eruptive event, the observed high DOC could have been entrained from a productive deep subseafloor microbial community. The discharged fluids were not sufficiently heated to allow complete thermal degradation of the DOC, nor reacted with the molten lava, resulting in the high DOC values observed in the eruption fluids collected.

Another possible source for the high DOC in the eruption fluids is abiogenic organic carbon. Abiogenic hydrocarbons formed via catalytic Fischer-Tropsch type (FTT) synthesis at hydrothermal conditions have been synthesized in laboratory-controlled experiments (Foustoukos and Seyfried, 2004; McCollom and Seewald, 2006). Isotopic compositions of hydrocarbons and DOC, and the elevated acetate, formate and total DOC concentrations in fluids collected from the Lost City vent fields suggest that these organic compounds are abiogenic (Proskurowski et al., 2006; Lang et al., 2010). High concentrations of hydrogen (1-14 mmol/Kg) in the Lost City vent fluids could provide the reducing energy for the abiotic synthetic reaction (Proskurowski et al., 2006; Lang et al., 2010). High hydrogen concentrations (up to 18 nM; relative to background seawater of <0.2 nM) measured in the eruption-associated plume above W. Mata suggests that significant hydrogen is produced via lava-seawater interaction during eruptive events

(Baker et al., 2011; Resing et al., 2011). Excess hydrogen would support the abiogenic production of DOC. Future studies such as measurements of hydrogen concentrations and isotopic analysis of compound-specific organic carbon in the eruption-associated fluids will enhance our understanding of how each eruption event could impact the organic carbon cycle.

5.5. Conclusion

Relative to background seawater, higher DOC and POC, and lower TDN concentration were found in the diffuse and focused vent fluids of a back-arc spreading zone, indicating vigorous biological production within associated subseafloor and seafloor environments. The low C/N ratio of the POC in fluids discharged from W. Mata diffuse vents further suggests that the POC is freshly produced. The ^{13}C-enriched (elevated δ^{13}C) POC in vent fluids relative to that in background seawater suggests that resident organisms are capable of utilizing carbon-fixation pathways such as the reductive TCA cycle or 3-HP. The injection of reduced species into the water column via hydrothermal fluid discharge induced biological production within the plume waters, as suggested by their elevated POC concentration and slightly elevated δ^{13}C-POC values relative to that of the background seawater. Elevated DOC relative to bottom seawater in fluids collected adjacent to molten lava is surprising. The high DOC may derive from circulating hydrothermal fluids ejecting DOC produced within subseafloor biospheres and/or abiogenic DOC production.

Acknowledgments

We thank the *ROV Jason* and *R/V Thomas Thompson* crews for their skillful support during the field sampling and Chih-Chiang Hsieh, Natalie Hamada, Kathryn Hu for their fantastic lab support. This project was supported by NSF (OCE0929881, JPC), NOAA XXX and the UH NASA Astrobiology Institute. SOEST contribution no. XXXX, C-DEBI contribution no. XXXX.

5.6. References

Amend, J. P., McCollom, T. M., Hentscher, M., and Bach, W., 2011. Metabolic (catabolic and anabolic) energy for chemolithoautotrophs in deep-sea hydrothermal systems hosted in different rock types. *Geochim. Cosmochim. Acta* **75**, 5736-5748.

Amend, J. P. and Shock, E. L., 1998. Energetics of amino acid synthesis in hydrothermal ecosystems. *Science* **281**, 1659-1662.

Azam, F., Fenchel, T., Field, J., Gray, J., Meyer-Reil, L., and Thingstad, F., 1983. The ecological role of water-column microbes in the sea. *Marine ecology progress series. Oldendorf* **10**, 257-263.

Baker, E. T., Lupton, J. E., Resing, J. A., Baumberger, T., Lilley, M. D., Walker, S. L., and Rubin, K. H., 2011. Unique event plumes from a 2008 eruption on the Northeast Lau Spreading Center. *Geochem. Geophy. Geosy.* **12**, Q0AF02.

Bennett, S. A., Hansman, R. L., Sessions, A. L., Nakamura, K., and Edwards, K. J., 2011a. Tracing iron-fueled microbial carbon production within the hydrothermal plume at the Loihi seamount. *Geochim. Cosmochim. Acta* **75**, 5526-5539.

Bennett, S. A., Statham, P. J., Green, D. R. H., Le Bris, N., McDermott, J. M., Prado, F., Rouxel, O. J., Von Damm, K., and German, C. R., 2011b. Dissolved and particulate organic carbon in hydrothermal plumes from the East Pacific Rise, 9°50′N. *Deep-Sea Res. Pt. I* **58**, 922-931.

Biddanda, B. and Benner, R., 1997. Carbon, nitrogen, and carbohydrate fluxes during the production of particulate and dissolved organic matter by marine phytoplankton. *Limnology and Oceanography*, 506-518.

Bourbonnais, A., Lehmann, M. F., Butterfield, D. A., and Juniper, S. K., 2012. Subseafloor nitrogen transformations in diffuse hydrothermal vent fluids of the Juan de Fuca Ridge evidenced by the isotopic composition of nitrate and ammonium. *Geochem. Geophy. Geosy.* **13**, Q02T01, p1-23.

Butterfield, D. A., Jonasson, I. R., Massoth, G. J., Feely, R. A., Roe, K. K., Embley, R. E., Holden, J. F., McDuff, R. E., Lilley, M. D., and Delaney, J. R., 1997. Seafloor eruptions and evolution of hydrothermal fluid chemistry. *Philosophical Transactions of the Royal Society of London Series a-Mathematical Physical and Engineering Sciences* **355**, 369-386.

Butterfield, D. A. and Massoth, G. J., 1994. Geochemistry of north Cleft Segment vent fluids: temporal changes in chlorinity and their possible relation to recent volcanism. *Journal of Geophysical Research-Solid Earth* **99**, 4951-4968.

Butterfield, D. A., Roe, K. K., Lilley, M. D., Huber, J. A., Baross, J. A., Embley, R. W., and Massoth, G. J., 2004. Mixing, reaction and microbial activity in the sub-seafloor revealed by temporal and spatial variation in diffuse flow vents at Axial Volcano. *Geophysical monograph* **144**, 269-289.

Carlson, C. A., 2002. Production and removal processes. In: *Biogeochemistry of marine dissolved organic matter* (eds. D. A. Hansell and C. A. Carlson). Elsevier.

Carlson, C. A., Hansell, D. A., Nelson, N. B., Siegel, D. A., Smethie, W. M., Khatiwala, S., Meyers, M. M., and Halewood, E., 2010. Dissolved organic carbon export and subsequent remineralization in the mesopelagic and bathypelagic realms of the North Atlantic basin. *Deep Sea Research Part II: Topical Studies in Oceanography* **57**, 1433-1445.

Carlson, C. A., Hansell, D. A., Peltzer, E. T., and Smith Jr, W. O., 2000. Stocks and dynamics of dissolved and particulate organic matter in the southern Ross Sea, Antarctica. *Deep Sea Research Part II: Topical Studies in Oceanography* **47**, 3201-3225.

Clague, D. A., Paduan, J. B., Caress, D. W., Thomas, H., Chadwick, W. W., and Merle, S. G., 2011. Volcanic morphology of West Mata Volcano, NE Lau Basin, based on high-resolution bathymetry and depth changes. *Geochem. Geophy. Geosy.* **12**.

Comita, P. B., Gagosian, R. B., and Williams, P. M., 1984. Suspended particulate organic material from hydrothermal vent waters at 21^{o}N. *Nature* **307**, 450-453.

Cooper, M., Elderfield, H., and Schultz, A., 2000. Diffuse hydrothermal fluids from Lucky Strike hydrothermal vent field: Evidence for a shallow conductively heated system. *J. Geophys. Res.* **105**, 19369-19,375.

Cornwell, J. C., Kemp, W. M., and Kana, T. M., 1999. Denitrification in coastal ecosystems: methods, environmental controls, and ecosystem level controls, a review. *Aquatic Ecology* **33**, 41-54.

Cowen, J. P. and Baker, E. T., 1998. The 1996 Gorda Ridge event detection and response activities: historical perspective and future implications. *Deep Sea Research Part II: Topical Studies in Oceanography* **45**, 2503-2511.

Cowen, J. P., Bertram, M. A., Wakeham, S. G., Thomson, R. E., William Lavelle, J., Baker, E. T., and Feely, R. A., 2001. Ascending and descending particle flux from

hydrothermal plumes at Endeavour Segment, Juan de Fuca Ridge. *Deep-Sea Res. Pt. I* **48**, 1093-1120.

Cowen, J. P., Giovannoni, S. J., Kenig, F., Johnson, H. P., Butterfield, D., Rappe, M. S., Hutnak, M., and Lam, P., 2003. Fluids from aging ocean crust that support microbial life. *Science* **299**, 120-123.

Delacour, A., Früh-Green, G. L., Bernasconi, S. M., Schaeffer, P., and Kelley, D. S., 2008. Carbon geochemistry of serpentinites in the Lost City hydrothermal system (30 N, MAR). *Geochim. Cosmochim. Acta* **72**, 3681-3702.

Descolasgros, C. and Fontugne, M., 1990. Stable carbon isotope fractionation by marine-phytoplankton during photosynthesis. *Plant, Cell, and Environment* **13**, 207-218.

Devol, A., 2008. Denitrification including anammox. *Nitrogen in the Marine Environment, 2nd Edition, edited by: Capone, D., Bronk, D., Mulholland, M., and Carpenter, E., Elsevier, Amsterdam*, 263-301.

Dittmar, T. and Koch, B. P., 2006. Thermogenic organic matter dissolved in the abyssal ocean. *Mar. Chem.* **102**, 208-217.

Dittmar, T. and Paeng, J., 2009. A heat-induced molecular signature in marine dissolved organic matter. *Nature Geoscience* **2**, 175-179.

Druffel, E. R. M., Griffin, S., Bauer, J. E., Wolgast, D. M., and Wang, X. C., 1998. Distribution of particulate organic carbon and radiocarbon in the water column from the upper slope to the abyssal NE Pacific ocean. *Deep-Sea Research Part Ii-Topical Studies in Oceanography* **45**, 667-687.

Ducklow, H. and Carlson, C., 1992. Oceanic bacterial production. *Advances in microbial ecology* **12**, 113-181.

Edmonds, H., Michael, P., Baker, E., Connelly, D., Snow, J., Langmuir, C., Dick, H., Mühe, R., German, C., and Graham, D., 2003. Discovery of abundant hydrothermal venting on the ultraslow-spreading Gakkel ridge in the Arctic Ocean. *Nature* **421**, 252-256.

Eglinton, T. I. and Repeta, D. J., in press. Organic matter in the contemporary ocean. In: *Treatise on Geochemistry* (eds. M. J. Mottl).

Engel, A., Händel, N., Wohlers, J., Lunau, M., Grossart, H. P., Sommer, U., and Riebesell, U., 2011. Effects of sea surface warming on the production and composition of dissolved organic matter during phytoplankton blooms: results from a mesocosm study. *Journal of Plankton Research* **33**, 357-372.

Engel, A., Harlay, J., Piontek, J., and Chou, L., 2012. Contribution of combined carbohydrates to dissolved and particulate organic carbon after the spring bloom in the northern Bay of Biscay (North-Eastern Atlantic Ocean). *Continental Shelf Research* **45**, 42-53.

Fasham, M. J. R. B., B. M., Bowles, M. C., and et al., 2001. A new vision of ocean biogeochemistry after a decade of the Joint Global Ocean Flux Study (JGOFS). *Ambio* **10**, 4-31.

Field, M. P. and Sherrell, R. M., 2000. Dissolved and particulate Fe in a hydrothermal plume at 9° 45′ N, East Pacific Rise:: Slow Fe (II) oxidation kinetics in Pacific plumes. *Geochim. Cosmochim. Acta* **64**, 619-628.

Foustoukos, D. I. and Seyfried, W. E., 2004. Hydrocarbons in hydrothermal vent fluids: the role of chromium-bearing catalysts. *Science* **304**, 1002-1005.

Fuhrman, J., 1992. Bacterioplankton roles in cycling of organic matter: the microbial food web. *Primary productivity and biogeochemical cycles in the sea. Plenum Press, New York*, 361-383.

Fuhrman, J. A., 1999. Marine viruses and their biogeochemical and ecological effects. *Nature* **399**, 541-548.

Fukuda, R., Ogawa, H., Nagata, T., and Koike, I., 1998. Direct determination of carbon and nitrogen contents of natural bacterial assemblages in marine environments. *Appl. Environ. Microbiol.* **64**, 3352-3358.

Gruber, N., 2008. The marine nitrogen cycle: overview and challenges. In: *Nitrogen in the marine environment* (eds. D. G. Capone, D. A. Bronk, M. R. Mulholland, and E. J. Carpenter). Elsevier, Burlington.

Hansell, D. A. and Carlson, C. A., 1998. Deep-ocean gradients in the concentration of dissolved organic carbon. *Nature* **395**, 263-266.

Hansell, D. A. and Carlson, C. A., 2001. Marine dissolved organic matter and the carbon cycle. *Oceanography* **14**, 41-49.

Hansell, D. A., Carlson, C. A., Repeta, D. J., and Schlitzer, R., 2009. Dissolved organic matter in the ocean: a controversy stimulates new insights. *Oceanography* **22**, 202-211.

Hayes, J. M., 2001. Fractionation of carbon and hydrogen isotopes in biosynthetic processes. *Reviews in mineralogy and geochemistry* **43**, 225-277.

Hofmann, M., Wolf-Gladrow, D. A., Takahashi, T., Sutherland, S. C., Six, K. D., and Maier-Reimer, E., 2000. Stable carbon isotope distribution of particulate organic matter in the ocean: a model study. *Mar. Chem.* **72**, 131-150.

Honjo, S., Manganini, S. J., Krishfield, R. A., and Francois, R., 2008. Particulate organic carbon fluxes to the ocean interior and factors controlling the biological pump: a synthesis of global sediment trap programs since 1983. *Progress in Oceanography* **76**, 217-285.

House, C. H., Schopf, J. W., and Stetter, K. O., 2003. Carbon isotopic fractionation by Archaeans and other thermophilic prokaryotes. *Organic Geochemistry* **34**, 345-356.

Huber, J. A., Johnson, H. P., Butterfield, D. A., and Baross, J. A., 2006. Microbial life in ridge flank crustal fluids. *Environ. Microbiol.* **8**, 88-99.

Jahnke, L. L., Summons, R. E., Hope, J. M., and Des Marais, D. J., 1999. Carbon isotopic fractionation in lipids from methanotrophic bacteria II: the effects of physiology and environmental parameters on the biosynthesis and isotopic signatures of biomarkers. *Geochim. Cosmochim. Acta* **63**, 79-93.

Jannasch, H. W., 1995. Microbial interactions with hydrothermal fluids. *Geophysical Monograph Series* **91**, 273-296.

Jiao, N., Herndl, G. J., Hansell, D. A., Benner, R., Kattner, G., Wilhelm, S. W., Kirchman, D. L., Weinbauer, M. G., Luo, T. W., Chen, F., and Azam, F., 2010. Microbial production of recalcitrant dissolved organic matter: long-term carbon storage in the global ocean. *Nature Reviews Microbiology* **8**, 593-599.

Jonkers, H., Koh, I. O., Behrend, P., Muyzer, G., and De Beer, D., 2005. Aerobic organic carbon mineralization by sulfate-reducing bacteria in the oxygen-saturated photic zone of a hypersaline microbial mat. *Microbial ecology* **49**, 291-300.

Jonkers, H. M., Ludwig, R., Wit, R., Pringault, O., Muyzer, G., Niemann, H., Finke, N., and Beer, D., 2003. Structural and functional analysis of a microbial mat ecosystem from a unique permanent hypersaline inland lake:'La Salada de Chiprana'(NE Spain). *FEMS Microbiol. Ecol.* **44**, 175-189.

Karl, D., 1995. Ecology of free-living, hydrothermal vent microbial communities. In: *The Microbiology of Deep-Sea Hydrothermal Vents* (eds. D. Karl). CRC press New York.

Lang, S. Q., Butterfield, D. A., Lilley, M. D., Johnson, H. P., and Hedges, J. I., 2006. Dissolved organic carbon in ridge-axis and ridge-flank hydrothermal systems. *Geochim. Cosmochim. Acta* **70**, 3830-3842.

Lang, S. Q., Butterfield, D. A., Schulte, M., Kelley, D. S., and Lilley, M. D., 2010. Elevated concentrations of formate, acetate and dissolved organic carbon found at the Lost City hydrothermal field. *Geochim. Cosmochim. Acta* **74**, 941-952.

Lilley, M., Butterfield, D., Olson, E., Lupton, J., Macko, S., and McDuff, R., 1993. Anomalous CH4 and NH4+ concentrations at an unsedimented mid-ocean-ridge hydrothermal system. *Nature* **364**, 45-47.

Lin, H. T., Cowen, J. P., Olson, E. J., Amend, J. P., and Lilley, M. D., 2012. Inorganic chemistry, gas compositions and dissolved organic carbon in fluids from sedimented young basaltic crust on the Juan de Fuca Ridge flanks. *Geochim. Cosmochim. Acta* **85**, 213-227.

Loh, A. N. and Bauer, J. E., 2000. Distribution, partitioning and fluxes of dissolved and particulate organic C, N and P in the eastern North Pacific and Southern Oceans. *Deep-Sea Res. Pt. I* **47**, 2287-2316.

Lovley, D. R. and Klug, M. J., 1983. METHANOGENESIS FROM METHANOL AND METHYLAMINES AND ACETOGENESIS FROM HYDROGEN AND CARBON-DIOXIDE IN THE SEDIMENTS OF A EUTROPHIC LAKE. *Appl. Environ. Microbiol.* **45**, 1310-1315.

Lupton, J., Delaney, J., Johnson, H., and Tivey, M., 1985. Entrainment and vertical transport of deep-ocean water by buoyant hydrothermal plumes. *Nature* **316**, 621-623.

MacKenzie, F. T., 1981. Global carbon cycle: some minor sinks for CO_2. . In: *Flux of organic carbon by rivers to the ocean* (eds. G. E. Likens, F. T. MacKenzie, and J. E. S. Richey, J.R.

Turekain, K.K.). U.S. Dept. of Energy, Washington, DC. .

Mango, F. D. and Elrod, L., 1999. The carbon isotopic composition of catalytic gas: A comparative analysis with natural gas. *Geochim. Cosmochim. Acta* **63**, 1097-1106.

McCarthy, M. D., Beaupre, S. R., Walker, B. D., Voparil, I., Guilderson, T. P., and Druffel, E. R. M., 2010. Chemosynthetic origin of C-14-depleted dissolved organic matter in a ridge-flank hydrothermal system. *Nat. Geosci.* **4**, 32-36.

McCollom, T. M. and Seewald, J. S., 2006. Carbon isotope composition of organic compounds produced by abiotic synthesis under hydrothermal conditions. *Earth and Planetary Science Letters* **243**, 74-84.

McCollom, T. M. and Shock, E. L., 1997. Geochemical constraints on chemolithoautotrophic metabolism by microorganisms in seafloor hydrothermal systems. *Geochim. Cosmochim. Acta* **61**, 4375-4391.

Meyers, P. A., 1994. Preservation of elemental and isotopic source identification of sedimentary organic-matter. *Chem. Geol.* **114**, 289-302.

Mottl, M. J., 1983. Metabasalts, axial hot springs, and the structure of hydrothermal systems at mid-ocean ridges. *Geological Society of America Bulletin* **94**, 161.

Popp, B. N., Laws, E. A., Bidigare, R. R., Dore, J. E., Hanson, K. L., and Wakeham, S. G., 1998. Effect of phytoplankton cell geometry on carbon isotopic fractionation. *Geochim. Cosmochim. Acta* **62**, 69-77.

Preuss, A., Schauder, R., Fuchs, G., and Stichler, W., 1989. Carbon isotope fractionation by autotrophic bacteria with three different CO2 fixation pathways. *Zeitschrift für Naturforschung* **44**, 397-402.

Proskurowski, G., Lilley, M. D., Kelley, D. S., and Olson, E. J., 2006. Low temperature volatile production at the Lost City Hydrothermal Field, evidence from a hydrogen stable isotope geothermometer. *Chem. Geol.* **229**, 331-343.

Proskurowski, G., Lilley, M. D., Seewald, J. S., Fruh-Green, G. L., Olson, E. J., Lupton, J. E., Sylva, S. P., and Kelley, D. S., 2008. Abiogenic hydrocarbon production at Lost City hydrothermal field. *Science* **319**, 604-607.

Ravizza, G., Blusztajn, J., Von Damm, K. L., Bray, A. M., Bach, W., and Hart, S. R., 2001. Sr isotope variations in vent fluids from 9°46'-9°54'N East Pacific Rise: evidence of a non-zero-Mg fluid component. *Geochim. Cosmochim. Acta* **65**, 729-739.

Redfield, A. C., 1958. The biological control of chemical factors in the environment. *American Scientist* **46**.

Resing, J. A., Rubin, K. H., Embley, R. W., Lupton, J. E., Baker, E. T., Dziak, R. P., Baumberger, T., Lilley, M. D., Huber, J. A., Shank, T. M., Butterfield, D. A., Clague, D. A., Keller, N. S., Merle, S. G., Buck, N. J., Michael, P. J., Soule, A., Caress, D. W., Walker, S. L., Davis, R., Cowen, J. P., Reysenbach, A.-L., and Thomas, H., 2011. Active submarine eruption of boninite in the northeastern Lau Basin. *Nature Geoscience* **4**, 799-806.

Rubin, K. H., Soule, S. A., Chadwick, W. W., Fornari, D. J., Clague, D. A., Embley, R. W., Baker, E. T., Perfit, M. R., Caress, D. W., and Dziak, R. P., 2012. Volcanic Eruptions in the Deep Sea. *Oceanography* **25**, 142-157.

Ruttenberg, K. C. and Sulak, D. J., 2011. Sorption and desorption of dissolved organic phosphorus onto iron (oxyhydr)oxides in seawater. *Geochim. Cosmochim. Acta* **75**, 4095-4112.

Siegenthaler, U. and Sarmiento, J. L., 1993. Atmospheric carbon-dioxide and the ocean. *Nature* **365**, 119-125.

Simoneit, B., Goodfellow, W., and Franklin, J., 1992. Hydrothermal petroleum at the seafloor and organic matter alteration in sediments of Middle Valley, Northern Juan de Fuca Ridge. *Applied Geochemistry* **7**, 257-264.

Simoneit, B. R. T., 1984. Hydrothermal effects on organic matter—high vs low temperature components. *Organic Geochemistry* **6**, 857-864.

Simoneit, B. R. T., 1990. Organic matter in hydrothermal systems. *Appl. Geochem* **5**, 1-548.

Simoneit, B. R. T., Kawka, O., and Brault, M., 1988. Origin of gases and condensates in the Guaymas Basin hydrothermal system (Gulf of California). *Chem. Geol.* **71**, 169-182.

Simoneit, B. R. T. and Sparrow, M. A., 2002. Dissolved organic carbon in interstitial waters from sediments of Middle Valley and Escanaba Trough, Northeast Pacific, ODP Legs 139 and 169. *Applied Geochemistry* **17**, 1495-1502.

Sirevåg, R., Buchanan, B., Berry, J., and Troughton, J., 1977. Mechanisms of CO 2 fixation in bacterial photosynthesis studied by the carbon isotope fractionation technique. *Archives of Microbiology* **112**, 35-38.

Smith, D. C., Simon, M., Alldredge, A. L., and Azam, F., 1992. Intense hydrolytic enzyme activity on marine aggregates and implications for rapid particle dissolution. *Nature* **359**, 139-142.

Summit, M. and Baross, J. A., 1998. Thermophilic subseafloor microorganisms from the 1996 North Gorda Ridge eruption. *Deep Sea Research Part II: Topical Studies in Oceanography* **45**, 2751-2766.

Suzuki, Y., Tanoue, E., and Ito, H., 1992. A high-temperature catalytic-oxidation method for the determination of dissolved organic-carbon in seawater-analysis and improvement *Deep-Sea Research Part a-Oceanographic Research Papers* **39**, 185-198.

Tanoue, E. and Handa, N., 1979. Distribution of particulate organic carbon and nitrogen in the Bering Sea and northern North Pacific Ocean. *Journal of Oceanography* **35**, 47-62.

Thauer, R. K., 1998. Biochemistry of methanogenesis: a tribute to Marjory Stephenson. *Microbiology-Uk* **144**, 2377-2406.

Volk, T. and Hoffert, M. I., 1985. Ocean carbon pumps: Analysis of relative strengths and efficiencies in ocean-driven atmospheric CO2 changes. *The Carbon Cycle and Atmospheric CO2: Natural Variations Archean to Present, Geophys. Monogr. Ser* **32**, 99-110.

Walker, B. D., McCarthy, M. D., Fisher, A. T., and Guilderson, T. P., 2008. Dissolved inorganic carbon isotopic composition of low-temperature axial and ridge-flank hydrothermal fluids of the Juan de Fuca Ridge. *Mar. Chem.* **108**, 123-136.

Welhan, J. and Lupton, J., 1987. Light hydrocarbon gases in Guaymas Basin hydrothermal fluids: thermogenic versus abiogenic origin. *AAPG Bulletin* **71**, 215-223.

Williams, P., 1970. Heterotrophic utilization of dissolved organic compounds in the sea. *J. Mar, Biol. Assoc. UK* **50**, 859-870.

Wohlers, J., Engel, A., Zöllner, E., Breithaupt, P., Jürgens, K., Hoppe, H. G., Sommer, U., and Riebesell, U., 2009. Changes in biogenic carbon flow in response to sea surface warming. *Proceedings of the National Academy of Sciences* **106**, 7067-7072.

Zerkle, A. L., House, C. H., and Brantley, S. L., 2005. Biogeochemical signatures through time as inferred from whole microbial genomes. *American Journal of Science* **305**, 467-502.

Zhang, C. L. L., Ye, Q., Reysenbach, A. L., Gotz, D., Peacock, A., White, D. C., Horita, J., Cole, D. R., Fong, J., Pratt, L., Fang, J. S., and Huang, Y. S., 2002. Carbon isotopic fractionations associated with thermophilic bacteria Thermotoga maritima and Persephonella marina. *Environ. Microbiol.* **4**, 58-64.

Table 5.1. Sampling sites

Sampling site	JASON dive#	CTD cast #	Latitude (°S)	Longitude (°W)	Sampling depth (m)
W. Mata diffusive vents					
Creamsicle	J418	-	15.093645	173.747971	1206
Red Rock	J413	-	15.094602	173.748589	1183
Kohu	J414	-	15.093718	173.747666	1188
Shrimp City	J414	-	15.094023	173.748098	1187
Luo	J417	-	15.095635	173.750425	1277
Epsilon	J417	-	15.094530	173.748575	1179
Maka focused vent					
Maka black smoker	J416	-	15.422191	174.283780	~1531
Eruptive sties					
Akel's Afi	J418	-	15.094446	173.749047	1215
Hades	J413	-	15.094707	173.749115	1206
CTD operation					
Vertical cast					
above W. Mata	-	V09C01	15.094278	173.748523	949-1148
above Maka	-	V09C02	15.423150	174.284933	1195-1556
Tow-yo					
NE Lau Spreading Center	-	T09C01	15.381515	174.242577	1598
NE Lau Spreading Center	-	T09C01	15.390883	174.251013	996

Table 5.2. Dissolved organic carbon and total dissolved nitrogen blank values for sample storage materials (Tedlar bags and Ti piston sampler).

Material type	Fluid type	Sampler	Sample storing time (hours)	DOC (μM)	TDN (μM)
Tedlar	DI	500mL bag	0	0.6 ± 0.7	<0.5
Tedlar	DI	500mL bag	24	0.8 ± 0.1	<0.5
Tedlar	0.24 N HCl	500mL bag	2	5.2 ± 0.1	<0.5
Ti	DI	PMEL-HFPS	20	2.8 ± 0.5	<0.5
Ti	0.24 N HCl	PMEL-HFPS	20	3.2 ± 0.5	<0.5
Ti	1 N H_2SO_4	PMEL-HFPS	20	30.0 ± 7.5	<0.5

Table 5.3. Dissolved organic carbon (DOC) and total dissolved nitrogen (TDN) concentrations of hydrothermal fluids from diffuse vents, black smoker vents and adjacent to molten lava (eruptive site) during eruptive events at NE Lau Basin.

Vent type & name	Sampler type	Tmax (ºC)	pH	Mg (mM)	DOC (µM)	TDN (µM)	Si (µM)	Total Fe (µM)
Diffusive Vent								
Creamsicle	HFPS-Bag	29.3	3.0	53	39 ± 2	4.3 ± 0.1	2986	646
Creamsicle	HFPS-Bag	29.3	2.9	49	41 ± 5	5.8 ± 0.4	3104	660
Red Rock	HFPS-Bag	13.8	3.2	49	43 ± 1	24.5 ± 0.5	1173	802
Kohu	HFPS-Bag	30.8	3.0	57	86 ± 3	13.9 ± 0.3	3319	983
Shrimp City	HFPS-Bag	14.8	5.8	55	84 ± 2	10.8 ± 0.4	1084	51
Luo	HFPS-Bag	22.4	5.3	54	126 ± 7	12.7 ± 0.3	1570	38
Epsilon	HFPS-Bag	29.6	2.8	53	521 ± 5	21.5 ± 0.4	2235	928
Maka black smoker								
Orifice 1	Ti-Major	315	3.0	4.3	27 ± 2	7 ± 0.2	13496	15346
Orifice 2	Ti-Major	315	3.0	4.8	52 ± 5	11 ± 0.4	13640	10919
Eruptive site								
Akel's Afi	HFPS-Piston	27	1.8	43	1704 ± 3	39 ± 0.4	825	201
Hades	Ti-Major	N.A.	N.A.	51	63 ± 1	40 ± 1.0	142	0.13
Hades	HFPS-Piston	50	1.6	44	151 ± 3	38 ± 1.0	575	33
Hades	HFPS-Piston	49	1.6	48	1359 ± 4	34 ± 0.4	1773	598
Background seawater								
T09C-01, 996 m	Niskin-CTD	4	8?	53	40 ± 0.3	38 ± 1.0	69	<0.1
T09C-01, 1598 m	Niskin-CTD	4	8?	53	38 ± 0.7	39 ± 1.0	100	<0.1
V09C-02, 1557 m	Niskin-CTD	4	8?	53	38 ± 0.4	39 ± 0.7	103	<0.1

HFPS: PMEL Hydrothermal Fluid and Particulate Sampler. The samples either stored in a Tedlar bag (HFPS-Bag) or in Ti Piston (HFPS-Piston).
N.A.: Not available. Temperature & pH not measured during sampling or no aliquot was available for this analysis.
Table 5.4. Dissolved organic carbon (DOC), total dissolved nitrogen (TDN), particulate organic carbon (POC) and particulate nitrogen (PN) concentrations for seawater above W. Mata and Maka vent sites. Seawater samples were collected with Niskin bottles on a CTD.

Station (cast ID)	**Depth (m)**	**DOC (µM)**	**TDN (µM)**	**POC (µmol/L)**	**PN (µmol/L)**	**POC/PN**	**δ^{13}C-POC (‰)**	**Fe (µM)**	**Si (µM)**
Plume above W. Mata summit (15.09°S, 173. 75°W; above active eruption sites)									
V09C01	1092	45 ± 1.0	40 ± 0.8	0.28	0.031	8.8	-25	<0.1	N.A.
	1096	45 ± 0.9	39 ± 0.3	0.46	0.044	10.5	-22	<0.1	N.A.
	1099	44 ± 0.1	39 ± 0.6	0.50	0.045	11.0	-22	<0.1	78
	1134	45 ± 1.1	39 ± 0.8	0.56	0.050	11.2	-25	<0.1	78
Plume above Maka black smoker (15.42°S, 174. 28°W)									
V09C02	1297	41 ± 0.8	39 ± 0.7	N.A.	N.A.	N.A.	N.A.	<0.1	91
	1370	40 ± 2.0	39 ± 0.5	0.23	0.028	8.0	-24	<0.1	90
	1431	37 ± 1.2	39 ± 0.9	0.38	0.048	7.9	N.A.	<0.1	95
	1525	38 ± 0.4	39 ± 0.9	0.27	0.030	8.8	-24	<0.1	95
Background seawater (above and below W. Mata plume)									
	996-1598	39 ± 1	39 ± 1	0.21 ± 0.07	0.024 ± 0.01	8.9 ± 1	-23 ± 1	<0.1	69-103

N.A. Not available.

Table 5.5. Concentrations and isotopic compositions of particulate organic carbon (POC) and particulate nitrogen (PN) for suspended particles in hydrothermal fluids from three diffusive vents.

Sample name	POC (μmol/L)	PN (μmol/L)	POC/PN	δ^{13}C-POC (‰)	δ^{15}N-PN (‰)
Diffusive Vent					
Red Rock	2.45	0.398	6.1	-15.5	N.D.
Kohu	0.48	0.042	11.4	N.D.	N.D.
Luo	3.08	0.605	5.1	-12.3	4.3
Background Seawater					
	0.21	0.024	8.9	-23	N.D.

N.D.: Not detectable due to insufficient C and/or N materials collected for isotope analysis.

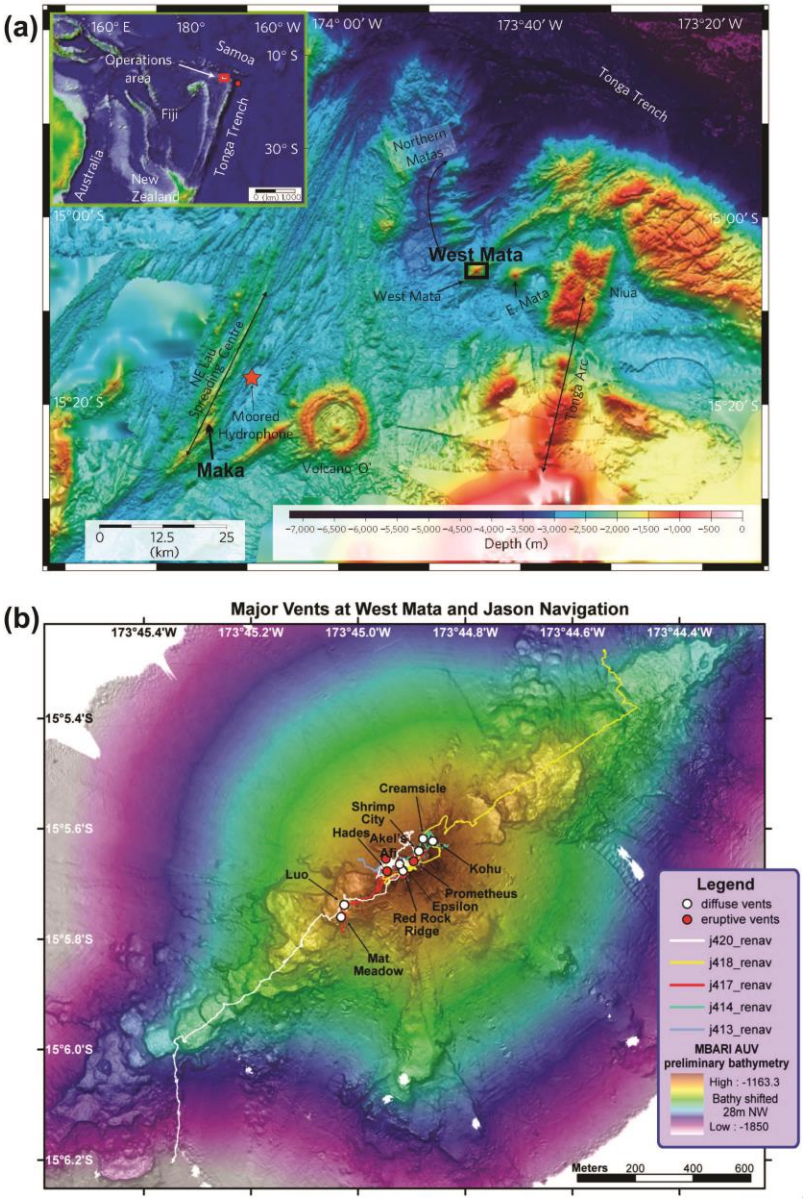

Fig 5.1. Map of the study site. (a) Regional map of NE Lau basin. The insert shows the location of the NE Lau basin relative to Fiji, Tonga and New Zealand. The red box indicates the operation area for this study and is enlarged in Fig 1(a). The two red circles indicate the locations of two background water column casts (15°S, 170°W; 14°S, 170°W), used for comparison to data obtained by this study. The area of West Mata is indicated by a black box and is enlarged in Fig 1(b). Maka sulfide mount is indicated with a black arrow. (b) Detailed bathymetric map of W. Mata. Diffuse venting sites are indicated by black filled triangles. Eruptive sites are shown by red filled triangles.

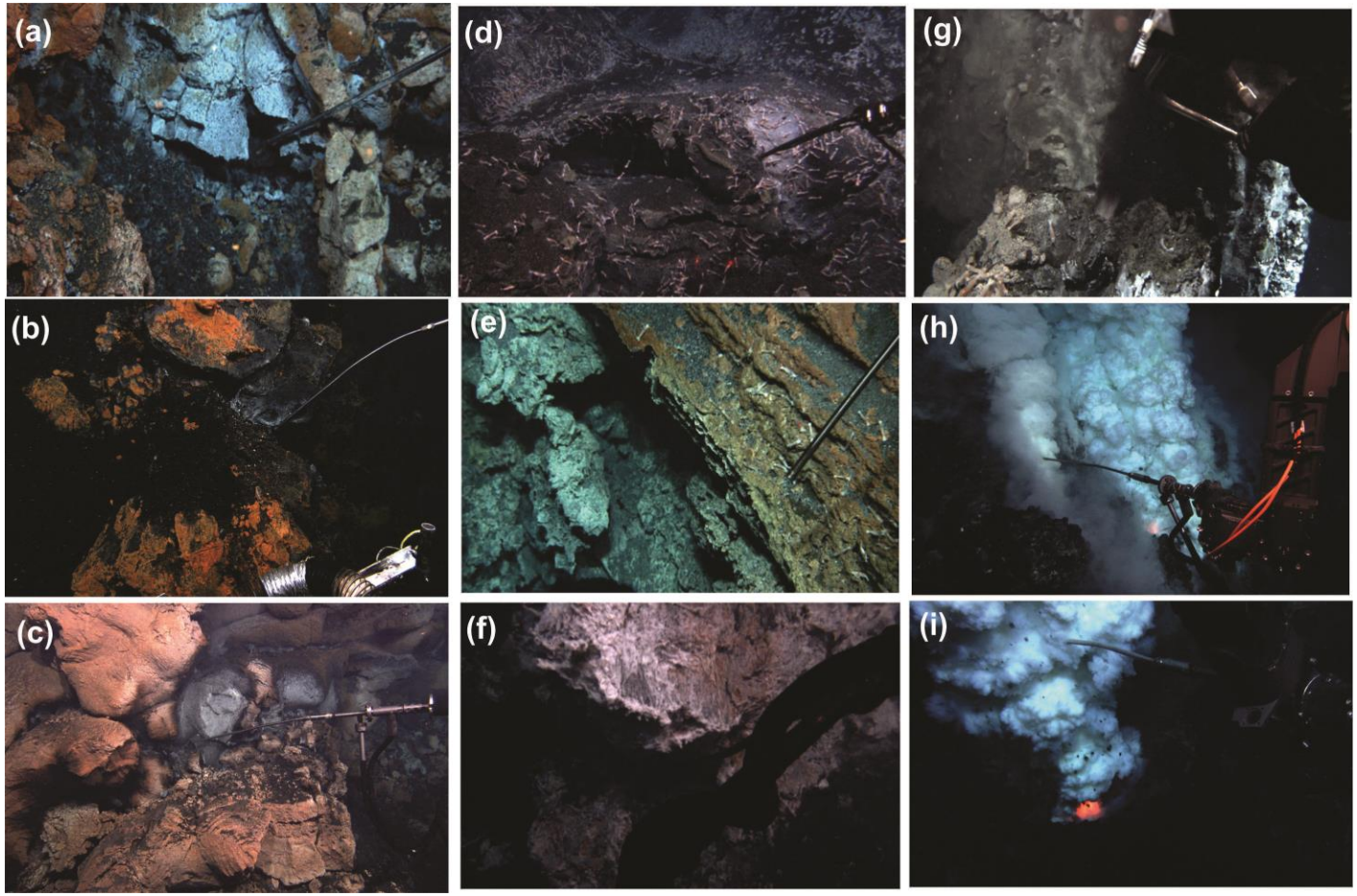

Fig 5.2. Sampling photos: diffuse vents (a) Creamsicle (b) Red Rock (c) Kohu (d) Shrimp (e) Luo (f) Epsilon; high-temperature vent (g) Maka; eruptive sites (h) Akel's Afi and (i) Hades.

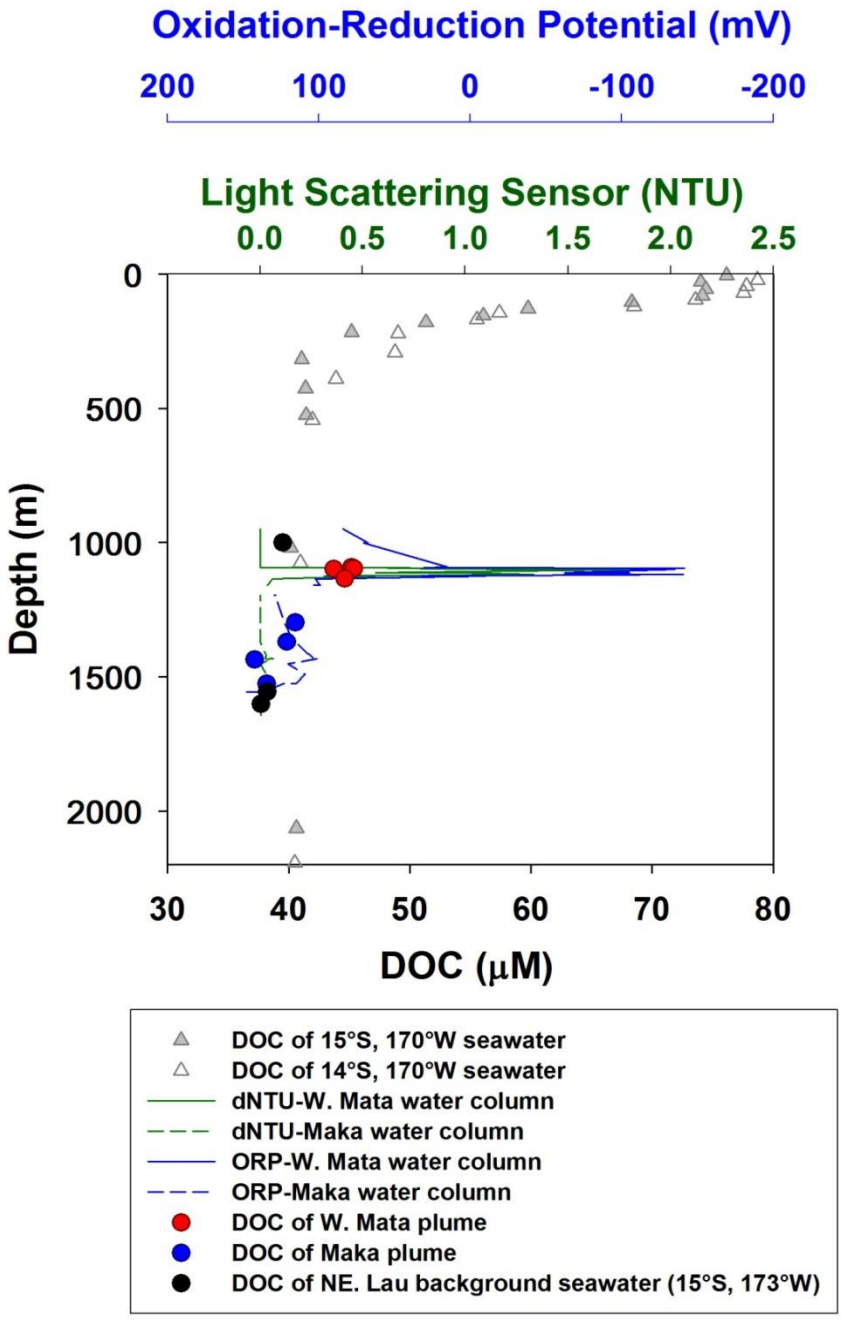

Fig 5.3. DOC concentrations in hydrothermal plume fluids and in background seawater. Filled circles are DOC data from this study. Open and filled triangles are DOC data generated by Dr. Hansell to provide additional local background seawater values(15°S, 170°W; 14°S, 170°W, transect P15S of WOCE/CLIVAR http://yyy.rsmas.miami.edu/groups/biogeochem/Data.html).

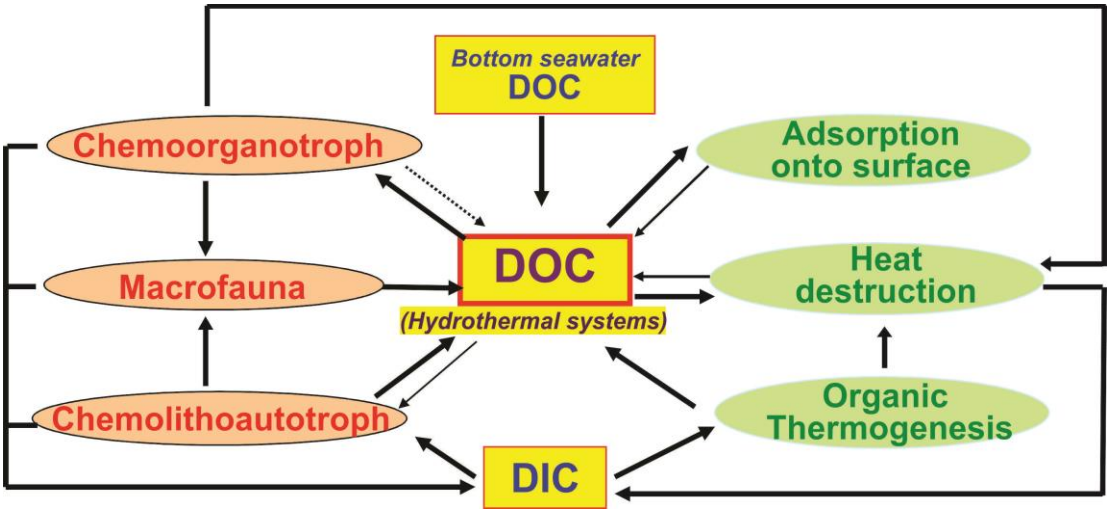

Fig 5.4. A model of DOC cycle in a general hydrothermal system. Rectangular boxes indicate different carbon reservoir. The ovals show various processes that remove or produce organic carbon. On the left are biologically mediated processes while on the right are abiological processes.

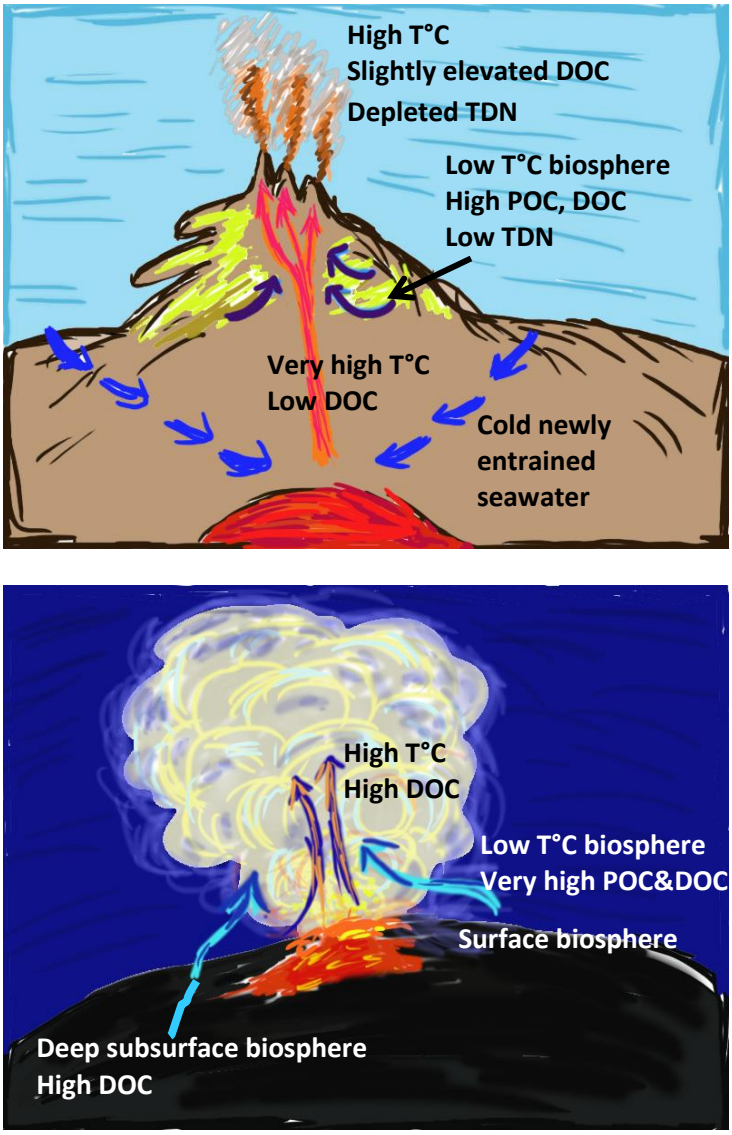

Fig 5.5. DOC entrainment models to describe high DOC in (a) high temperature black smoker type vents and (2) fluids adjacent to the molten basalt. In both models, high DOC is produced within the subsurface and/or at seafloor or vent surface biospheres. The circulating hydrothermal fluids entrain DOC before and/or after the fluids are heated up. Some DOC may be removed during the ascending of hydrothermal fluids but some DOC survives, resulting the high DOC observed in fluids collected.

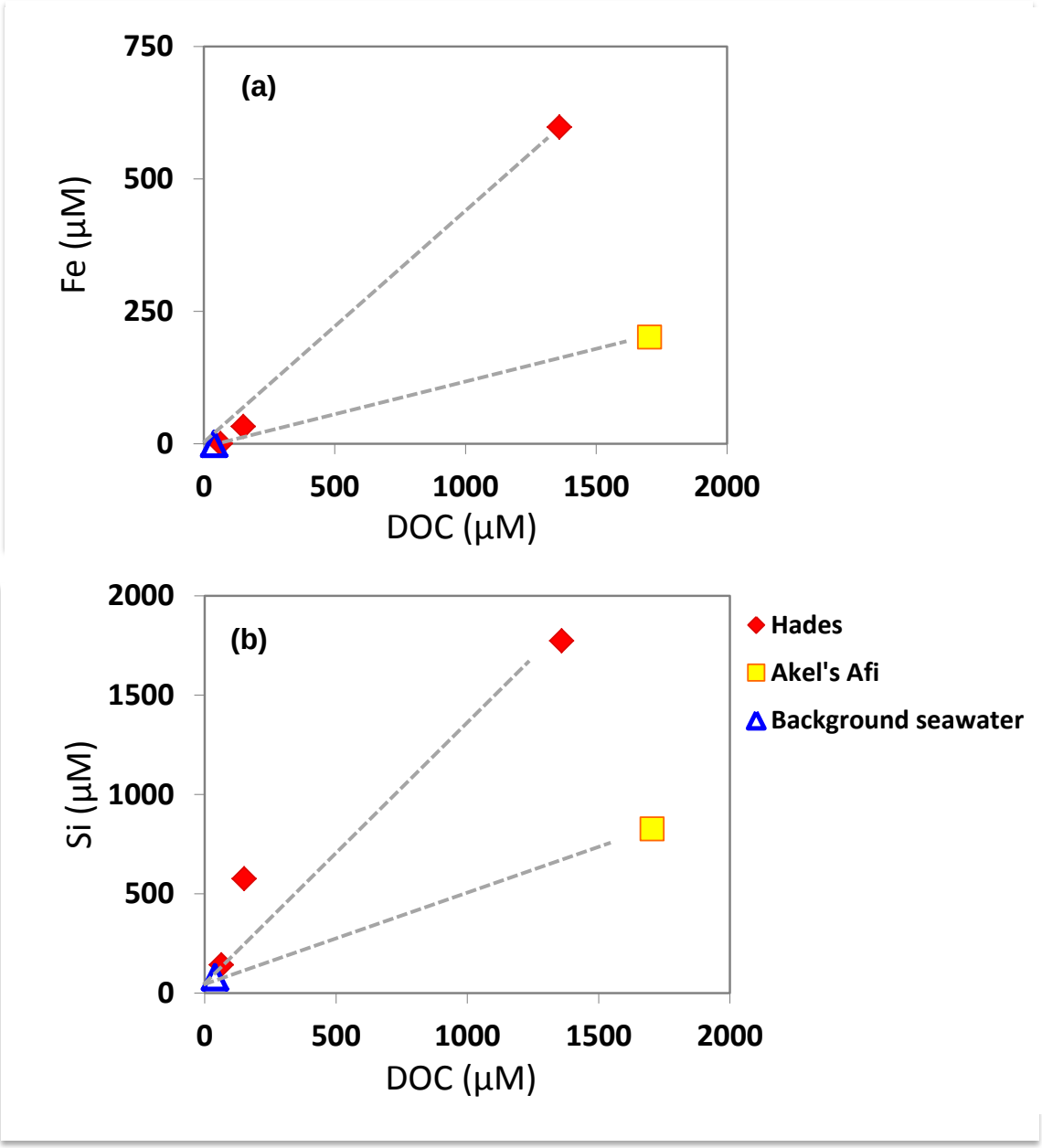

Fig 5.6. (a) Silicate and (b) dissolved iron versus DOC concentrations in fluids collected adjacent to molten lava. The gray dash lines are drawn to show the positive trends between the DOC and Fe and DOC and Si. Bottom seawater values are also shown for comparison.

CHAPTER 6

Summary and directions for future research

6.1 Summary

The overall goals of this study were to improve our understanding of the available nutrients, substrates and geochemical energy for the microbial biosphere in sediment-buried ridge-flank basement and to evaluate the impact that ridge-flank hydrothermal systems have on the global ocean organic carbon cycle. Major ions, bio-essential elements (nutrients), dissolved methane, dissolved hydrogen and dissolved amino acids were measured in high quality ridge-flank basement fluids. Basement fluids were collected from CORKs in IODP boreholes 1301A, 1362A and 1362B, all within ~800 m of each other and penetrating the overlying sediments and an additional 30m, 200m and 50m into the basement, respectively. Annual samplings from CORK 1301A between 2008 and 2011 provide a time-series data set. Thermodynamic calculations were applied extensively using the biogeochemical data from this study in order to investigate the energy yields (or requirements) of key metabolic and synthetic reactions. Important results and their implications are summarized below.

6.1.1. High quality ridge-flank basement fluid samples were obtained via advanced sampling techniques.

The employment of a powerful and clean pumping system to draw basement fluids through well-flushed fluid delivery lines has increased sample quality. Bottom seawater entrainment during seafloor sampling is low as evidenced by much depleted magnesium concentrations in all of the basement fluid samples collected (uncorrected 2.8±1.1 mM, n=23) relative to the seawater value (53.7±0.3 mM, n=5). As discussed in **Chapter 2**, the ammonium concentrations in basement fluid samples from CORK 1301A collected in

this study (102±3 μM) are consistent with those from Baby Bare (76-99 μM, Mottl et al., 1998; Johnson et al., 2003) and CORK 1026B (90-120 μM, Wheat et al., 2004), and also fall on the trend line of a downward diffusion profile from overlying sediment porewater (Shipboard Scientific Party, 2004). Our ammonium concentrations greatly contrast with those in fluid samples collected by osmotic samplers installed inside the casing of CORK 1301A (840 μM, Wheat et al., 2010). Consistently low dissolved iron concentrations (0.8±0.3 μM from 1301A; 1.4±0.2 μM from 1362B; 1.9±0.2 μM from 1362A) also indicate that the basement fluid samples collected in our study are not influenced by the CORK's rusty iron casing, as were fluids with highly variable iron concentrations collected by osmotic samplers from the same CORK (0-127 μM; Wheat et al., 2010).

6.1.2. Ridge-flank basement fluids from 3.5 Ma crust contain low but measurable phosphate; in contrast, nitrate is undetectable.

As discussed in **Chapter 2**, phosphate concentrations are 0.1±0.05 μM (average 2008-2011 endmember values), 0.06±0.02 μM and 0.09±0.02 μM in ridge-flank basement fluids collected from CORKs 1301A, 1362B and 1362A, respectively. These concentrations are consistent with, but even lower than those reported previously for samples collected from Baby Bare spring fluids (0.3 μM; Mottl et al., 1998) and CORK 1026B (0.9 μM; Wheat et al., 2004). The low phosphate concentrations in ridge-flank basement fluids are expected due to biological uptake and abiotic adsorption onto iron oxyhydroxide (Wheat et al., 1996), one of the most abundant secondary minerals present in the 3.5 Ma rock cores from site 1026B (Marescotti et al., 2000). The sorption of phosphate onto iron oxyhydroxide surfaces lowers the dissolved inorganic phosphate

concentration in the fluid and renders phosphate unavailable for biological uptake (Reynolds and Davies, 2001; Ruttenberg and Sulak, 2011).

Oxygen diffusion into our sampling bags prior to analysis may have allowed some dissolved iron to oxidize, forming iron oxyhydroxide that could remove phosphate from the sample fluids. However, the phosphate concentrations of fluids acidified in situ (sample bags pre-charged with acid to prevent formation of iron oxyhydroxide) show no significant differences from those in untreated fluid samples. The low phosphate concentrations (0.06-0.1 μM) found in this study should fairly represent the basement fluids circulating through the three sampling sites.

Verifying the concentration of nitrate in ridge-flank basement fluids was challenging. The detectable but highly variable nitrate in basement fluids collected from CORK 1301A (average 0.2±0.3 μM, n=12, 2008-2011 samples) may have resulted from an imperfect Aeroquip connector (Wheat et al., 2011) used for this CORK's seafloor sampling port, whichpermitted a small amount of nitrate-rich bottom seawater to leak into our sampling system. Improvements in the new style ('Jannasch') connectors installed on the seafloor sampling ports of CORKs 1362A and 1362B (Wheat et al., 2011) allow the collection of even higher quality basement fluids, with no bottom seawater entrainment. As expected, nitrate concentrations are below detection limits (<0.02μM) in basement fluid samples collected from CORK 1362A and 1362B. The absence of nitrate in the basement fluids indicates that the available geochemical energy for the basement biosphere is even lower than previously predicted based on samples from CORK 1301A, since nitrate reduction coupled with hydrogen, methane or hydrogen sulfide oxidation is much more exergonic (energy-yielding) than sulfate reduction or methanogenesis (Boettger et al., 2013).

6.1.3. The sedimented ridge-flank basement environment is a net source of hydrogen and methane, which provide energy for basement biospheres.

As discussed in **Chapter 2** and **Chapter 3**, ridge-flank basement fluids collected for this study all contain significantly higher methane and hydrogen concentrations (1.5-13μM and 0.05-2 μM, respectively) than bottom seawater (0.0002 and 0.0004 μM, respectively; Kelley et al., 1998) or deep sediment porewater (0.002 μM and 2-3 μM, respectively; Shipboard Scientific Party, 2004). The elevated methane and hydrogen concentrations within the basement fluids indicate that the sedimented ridge-flank basement is a net source of hydrogen and methane, supporting **hypothesis 2** presented in the introductory chapter of this dissertation.

Thermodynamic calculations demonstrate that hydrogenotrophic sulfate and iron reduction are energy-yielding at all sites investigated by this study, supporting part of **hypothesis 3**. The presence of methane in ridge-flank basement fluids also makes anaerobic methane oxidation energy yielding at all sites visited, supporting **hypothesis 3.** In contrast, hydrogenotrophic methanogenesis is only energy-yielding at site 1301A, where higher hydrogen concentrations are observed, a result consistent with geochemical data (Ono et al., 2012; Lever et al., 2013) and incubation experiments using rocks collected from the same site (Lever et al., 2013). Hydrogenotrophic methanogenesis is not favorable at sites 1362A and 1362B, refuting **hypothesis 3**.

6.1.4. The sedimented ridge-flank basement is a net sink for deep seawater dissolved organic carbon but a net source for deep seawater dissolved amino acids.

Low dissolved organic carbon (DOC) concentrations in basement fluids collected from all sites (11-16 μM, table 3.1) confirms that ridge-flank basement is a net DOC sink for deep seawater DOC (~40 μM), supporting **hypothesis 4** presented in chapter 1. When DOC concentrations in the basement fluids are plotted against their corresponding dissolved inorganic radiocarbon isotope values (Elderfield et al., 1999; Walker et al., 2008), basement fluid DOC data fall below a linear extension of the deep water DOC trend line (**Chapter 2: Figure 2.8**). The net rate of DOC removed from recharging bottom seawater during hydrothermal circulation within basement was estimated to be ~2.4 nmol C/year, a value very similar to the 3 nmol C/year removal rate calculated for circulating deep seawater (Hansell et al., 2009). The actual DOC removal rate should be higher, since DOC produced by chemolithoautotrophic activities along basement fluid circulation flow paths, and downward diffusion of DOC across the sediment-basement interface into the basement fluid, are not taken into account for the net rate estimation.

As discussed in **Chapter 4**, although the concentrations of total dissolved amino acids (53-89 nM) in ridge-flank basement fluids investigated for this study are at the lower end of the range reported previously for other hydrothermal systems (67 nM-338 μM; Hoaki et al., 1995; Takano et al., 2003; Horiuchi et al., 2004; Svensson et al., 2004; Klevenz et al., 2010; Lang et al., 2013), they all are elevated relative to North Pacific deep seawater (~50 nM; Kaiser and Benner, 2009). Deep seawater that recharges into basement therefore cannot be the sole source of dissolved amino acids in ridge-flank basement

fluids. Similarities in the distribution of amino acids in ridge-flank basement fluids, deep sediment porewater and bacterial biomass suggest that the additional sources may include diffusional transport from deep sediment porewater and in situ production by microorganisms in the basement environment (**Chapter 4: Fig 3**). High concentrations of total dissolved amino acids (815nM) in deep sediment porewater near the sediment-basement interface permit diffusional input of amino acids from sediment into basement. Thermodynamic calculations show that ridge-flank basement fluids are conducive to a wide variety of chemolithoautotrophic metabolisms (Chapter 3; Boettger et al., 2013), thus also supporting biological production of amino acids and their release to the basement fluids. In addition, although basement appears to be a net sink for total DOC, the elevated total dissolved amino acid concentrations suggest that basement is a net source of labile organic carbon, and that exportation of fixed carbon (in the form of amino acids) into overlying seawater is plausible, thus supporting **hypothesis 5**. The presence of dissolved amino acids also indicates that labile organic substrates are available for heterotrophic microorganisms in the basement environment.

6.1.5. Basement fluids are heterogeneous at a scale of 300-800 m.

As discussed in **Chapter 3**, the methane and hydrogen concentrations in basement fluids from the three sites investigated are all significantly different from each other. The dissolved gas data thus do not support a well-mixed and homogeneous aquifer at the scale of hundreds of meters. In **Chapter 4**, the differences in dissolved amino acid concentrations and in their diagenetic status in basement fluids from the three study sites also suggest spatial and temporal variability in ridge-flank basement fluids. These biogeochemical data are consistent with the spatial heterogeneity in permeability inferred

from packer experiments (Becker and Fisher, 2008; Fisher et al., 2008) and with the vertical heterogeneity of rock cores from borehole U1362 (Shipboard Scientific Party, 2010). The presence of variable micro niches for both biological and abiotic reactions, and the highly variable flow and reaction histories, could all contribute to the observed spatial and temporal differences in basement fluid biogeochemistry. As discussed in **Chapter 2**, coexisting sulfate, hydrogen sulfide, hydrogen and methane indicate that fluids collected from CORK 1301A derive either from multiple flow paths with different redox histories, or from a complex environment that allows co-occurring metabolic pathways including sulfate reduction and methanogenesis (**Chapter 2: Figure 7**). Despite the high upper basement permeability, the heterogeneous nature of the biogeochemical composition of basement fluids also suggests that variable microbial communities may be found at the three sites, as a result of the available energy (hydrogen and methane) and organic substrates (amino acids) that can be exploited by microorganisms residing in basement.

6.1.6. Contrasting ridge-flank and other hydrothermal systems.

As discussed in **Chapter 4**, DOC and amino acid concentrations in ridge-flank basement fluids are lower than those in previously reported hydrothermal systems, including deep submarine high temperature vent fluids (Horiuchi et al., 2004; Klevenz et al., 2010; Lang et al., 2013), shallow submarine hydrothermal vents (Svensson et al., 2004), terrestrial geothermal wells (Svensson et al., 2004), subterranean hydrothermal vents (Takano et al., 2003) and hydrothermal-influenced marine sediment porewater (Haberstroh and Karl, 1989; Hoaki et al., 1995). High concentrations of DOC have also been observed in the

low temperature diffusive vent fluids collected at W. Mata in northeast Lau Basin (39-521 μM, **Chapter 5**), equal to or much higher than the local background seawater value (39 μM) and much more elevated than that for ridge-flank basement fluids (11-16 μM, **Appendix A)**. Unlike ridge-flank basement fluids, W. Mata diffusive vent fluids are a source of deep seawater DOC. Elevated DOC in diffusive vent fluids from the N.E. Lau vent fields is probably produced biologically. The particulate organic carbon (POC) concentration in the vent fluids is more elevated than in background seawater and the C/N (5.1-11.4, Chapter 5) and stable carbon isotope values (-12.3 to -15.5 ‰) of this POC suggest that it is comprised of fresh marine and/or bacterial biomass. Total dissolved nitrogen (TDN) in the Lau diffuse vent fluids is depleted relative to background seawater, probably because of microbially-mediated nitrogen assimilation and denitrification (e.g. Jannasch, 1995; Cornwell et al., 1999; Devol, 2008), which likewise supports the presence of a prosperous subsurface and/or seafloor biosphere.

6.2 Future research directions

6.2.1. Identify additional sources of methane.

In **Chapter 3**, we discuss the potential sources for methane, including abiotic and biotic methane synthesis from hydrogen and heat degradation of organic matter. The $\delta^{13}C\text{-}CH_4$ values for CORK 1301A fluids (-42±2 ‰, n=4) fall near the middle of the ranges for both thermogenic (-20‰ to -62‰) and abiotic (-25‰ to -57‰) formation and near the heavy end of the biogenic values (-110‰ to -45‰; Whiticar, 1999; Sherwood Lollar et al., 2006). CORK 1301A fluids contain more ^{13}C-enriched methane than the biogenic methane observed in the enrichment incubation of interior of rock chips collected from

IODP U1301A (-54 to -65 ‰; Lever et al., 2013), suggesting that additional sources of methane contribute to the dissolved methane pool in the CORK 1301A fluid. Future hydrogen isotopic analysis of methane in subseafloor basement fluids should shed more light on the source of methane in this environment as abiogenic methane tends to be more depleted in ^{2}H than biogenic methane, and much more depleted in ^{2}H than thermogenic methane (Chapter 3: Fig. 7, Sherwood Lollar et al., 1993; Sherwood Lollar et al., 2006). Enrichment experiments with fluid samples (free living microorganisms) can also help to verify the presence of methanogens and to provide the isotope values of methane produced by free-living methanogens. These results from experiments with free-living microorganisms can be compared with those using the attached methanogens residing within the rock chips reported by Lever et al. (2013).

6.2.2. Look for bio-limiting factor(s) for ridge-flank basement biosphere.

The low phosphate concentrations in basement fluids collected during this study suggest that relative to carbon and nitrogen, phosphate could be a limiting nutrient in the basement biosphere. However, although phosphate concentrations (0.06-0.1 μM) are much lower in the ridge-flank basement fluids than in bottom seawater (2.89 μM), the concentrations are still higher those found in the oligotrophic open ocean such as the Sargasso sea (0.0002-0.001 μM, Wu et al., 2000). Despite the low phosphate availability, there remains little direct evidence for phosphorus limitation of primary production in the surface ocean (Van Mooy et al., 2009). Low phosphate concentrations or low phosphate to nitrogen ratios are insufficient to indicate whether an environment is phosphate limited.

Therefore, hypothesis 1 presented in the introductory chapter is not fully tested by this approach.

Substrate-addition bioassay experiments such as those described by Mills et al. (2008), with modifications, can be conducted to identify bio-limiting factors. Basement fluids can be amended with substrates that are suspected to be bio-limiting, including phosphate (Mills et al., 2008) and labile DOC (e.g. glucose, acetate, amino acids; Church et al., 2000; Longnecker et al., 2009), and then incubated in the dark at in situ temperature (65°C) and pressure (270 bars). If significantly more elevated microbial cell abundance and production are observed in the amended samples relative to the untreated ones, the amended substrate(s) can then be identified as a limiting factor(s) for free-living microbes residing in the basement fluids.

6.2.3. DOC characterization.

Ridge-flank basement has been shown to be a net sink for deep ocean DOC by this study. To fully understand the nature of DOC within basement fluids, we must characterize the fractions of DOC removed from recharged deep seawater and the fractions of DOC remaining in the basement fluids along the circulation paths. This study is the first to characterize the DOC in sedimented ridge-flank basement fluids by analyzing their amino acid content (**Chapter 4**). However, total dissolved amino acids only account for 1.4-3.3% of the DOC in ridge-flank basement fluids (**Chapter 4: table 2**), leaving 96-98% of the DOC uncharacterized. Partial characterization of DOC in seawater, groundwater or sediment porewater has been made for aldose by ion chromatography (McCarthy et al., 1997; Skoog and Benner, 1997), amino sugars by anion-exchange chromatography

(Kaiser and Benner, 2000; Kaiser and Benner, 2009), low-molecular-weight organic acids by liquid chromatography (Albert et al., 1995; Albert and Martens, 1997; Amend et al., 1998), functional groups by nuclear magnetic resonance spectroscopy (NMR; Benner et al., 1992; Aluwihare et al., 1997; Repeta et al., 2002; Aluwihare et al., 2005) and molecular compositions by electrospray ionization coupled with Fourier-transform ion cyclotron resonance mass spectrometry (ESI FT-ICR-MS; Koch et al., 2005; Dittmar and Koch, 2006; Kujawinski and Behn, 2006; Kujawinski et al., 2009; Schmidt et al., 2009; Longnecker and Kujawinski, 2011; Schmidt et al., 2011).

Aldose and amino sugars, together with amino acids, comprise large fractions of the organic carbon in fresh organisms (30-60 %; Cowie and Hedges, 1994; Kaiser and Benner, 2009) but account for less than 10% of organic carbon in deep seawater DOC (Kaiser and Benner, 2009). The labile nature of aldose and amino sugars, similar to amino acids, are good indicators of fresher DOC and can be used, in addition to amino acids, as diagenetic indexes (Cowie and Hedges, 1994; Davis et al., 2009; Kaiser and Benner, 2009) for DOC in ridge-flank basement fluids.

Low-molecular-weight organic acids (LMW-OAs, monocarboxylic acids with 1-5 carbon atoms per molecule) can be the key organic species in aqueous subsurface environments, including marine sediment porewater (e.g. Sansone and Martens, 1982; Heuer et al., 2009), hydrothermal-influenced marine sediment porewater (e.g. Martens, 1990; Wellsbury et al., 1997; Lever et al., 2010) and continental and submarine hydrothermal fluids (e.g. Amend et al., 1998; Cruse and Seewald, 2006). LMW-OAs, in particular acetate, are important metabolic intermediates in anaerobic bacterial metabolism, including sulfate reduction and methanogenesis (Sansone and Martens, 1981; Sørensen et

al., 1981; Jørgensen, 1982). While sulfate reduction and methanogenesis are likely to be key metabolic reactions in the sedimented ridge-flank basement environment (Chapter 3; Boettger et al., 2013), understanding the availability of LMW-OAs, especially acetate, is important.

Functional-group identification of marine DOC using NMR has shown that there are two chemically distinct pools of organic nitrogen present in the water column (Aluwihare et al., 2005). In the surface ocean, half of the high-molecular-weight dissolved organic nitrogen (HMW-DON) is present as N-acetyl amino polysaccharides (e.g. chitin and peptidoglycan, a more labile portion of DON) while in the deep ocean, most HMWDON is present as amides that resist both hydrolysis and biological degradation (McCarthy et al., 1997; Aluwihare et al., 2005). The pervasive distribution of these refractory amides throughout the water column and across stations suggest that either they are resistant to biological degradation in the marine environment and/or they are produced throughout the water column (Aluwihare and Meador, 2008). It is important to know whether such pervasive amides would persist long after deep seawater has recharged into the basement and circulated to ridge-flank basement fluid sampling sites (~eleven thousand years; Walker et al., 2008).

Up to 8% of marine DOC has been characterized using FT-ICR-MS (Hertkorn et al., 2006), greatly increasing our understanding from the previously 3% of marine DOC that was characterizable by biochemical analysis alone (Benner, 2002). Molecular structures inferred from FT-ICR-MS data can be linked to the organic molecule's physical and chemical properties (Hertkorn et al., 2006). For example, a major characterizable component of marine DOC, referred to as carboxyl-rich alicyclic molecules, is

considered to be refractory due to its abundant alicyclic rings and branching, which makes it more resistant to biodegradation, leading to its high abundance in marine DOC (Hertkorn et al., 2006). Another refractory organic component identified is thermally altered organic molecules, which are homogeneously distributed in the deep sea (Dittmar and Paeng, 2009) and comprise more than 2.4% of marine DOC (Dittmar and Koch, 2006). Venting of deep sea hydrothermal fluids has been suggested as the primary source of such thermally altered DOC (Dittmar and Koch, 2006). The upper ocean basement (~600m) is the largest reservoir for hydrothermal fluids and the hydrothermal fluid flux from ridge-flanks (crustal age >1Ma) alone is about 5-60% of the total hydrothermal fluid flux (Mottl, 2003; Wheat et al., 2003). Identification and quantification of thermally altered organic molecules in ridge-flank basement fluids can help us to understand whether hydrothermal fluids circulating within the upper basement are a source of these molecules to the overlying ocean.

6.3 References

Albert, D. B. and Martens, C. S., 1997. Determination of low-molecular-weight organic acid concentrations in seawater and pore-water samples via HPLC. *Mar. Chem.* **56**, 27-37.

Albert, D. B., Taylor, C., and Martens, C. S., 1995. Sulfate reduction rates and low-molecualr-weight fatty-acid concentrations in the water column and surficial sediments of the Black-Sea. *Deep-Sea Research Part I-Oceanographic Research Papers* **42**, 1239-1260.

Aluwihare, L. I. and Meador, T., 2008. Chemical composition of marine dissolved organic nitrogen. In: *Nitrogen in the marine environment* (eds. D. G. Capone, D. A. Bronk, M. R. Mulholland, and E. J. Carpenter). San Diego, CA, USA: Academic Press.

Aluwihare, L. I., Repeta, D. J., and Chen, R. F., 1997. A major biopolymeric component to dissolved organic carbon in surface sea water. *Nature* **387**, 166-169.

Aluwihare, L. I., Repeta, D. J., Pantoja, S., and Johnson, C. G., 2005. Two chemically distinct pools of organic nitrogen accumulate in the ocean. *Science* **308**, 1007-1010.

Amend, J. P., Amend, A. C., and Valenza, M., 1998. Determination of volatile fatty acids in the hot springs of Vulcano, Aeolian Islands, Italy. *Organic Geochemistry* **28**, 699-705.

Becker, K. and Fisher, A. T., 2008. Borehole packer tests at multiple depths resolve distinct hydrologic intervals in 3.5-Ma upper oceanic crust on the eastern flank of Juan de Fuca Ridge. *J. Geophys. Res.* **113**, 1-12.

Benner, R., 2002. Chemical composition and reactivity. In: *Biogeochemistry of marine dissolved organic matter* (eds. D. A. C. C. Hansell). Elsevier.

Benner, R., Pakulski, J. D., McCarthy, M., Hedges, J. I., and Hatcher, P. G., 1992. Bulk chemical characteristics of dissolved organic matter in the ocean. *Science* **255**, 1561-1564.

Boettger, J., Lin, H.-T., Cowen, J. P., Henstscher, M., and Amend, J. P., 2013. Energy yields from chemolithotrophic metabolisms in igneous basement of the Juan de Fuca ridge flank system. *Chem. Geol.* **337-338**, 11-19.

Church, M. J., Hutchins, D. A., and Ducklow, H. W., 2000. Limitation of bacterial growth by dissolved organic matter and iron in the Southern Ocean. *Appl. Environ. Microbiol.* **66**, 455-466.

Cornwell, J. C., Kemp, W. M., and Kana, T. M., 1999. Denitrification in coastal ecosystems: methods, environmental controls, and ecosystem level controls, a review. *Aquatic Ecology* **33**, 41-54.

Cowie, G. L. and Hedges, J. I., 1994. Biochemical indicators of diagenetic alteration in natural organic matter mixtures.

Cruse, A. M. and Seewald, J. S., 2006. Geochemistry of low-molecular weight hydrocarbons in hydrothermal fluids from Middle Valley, northern Juan de Fuca Ridge. *Geochim. Cosmochim. Acta* **70**, 2073-2092.

Davis, J., Kaiser, K., and Benner, R., 2009. Amino acid and amino sugar yields and compositions as indicators of dissolved organic matter diagenesis. *Organic Geochemistry* **40**, 343-352.

Devol, A., 2008. Denitrification including anammox. *Nitrogen in the Marine Environment, 2nd Edition, edited by: Capone, D., Bronk, D., Mulholland, M., and Carpenter, E., Elsevier, Amsterdam*, 263-301.

Dittmar, T. and Koch, B. P., 2006. Thermogenic organic matter dissolved in the abyssal ocean. *Mar. Chem.* **102**, 208-217.

Dittmar, T. and Paeng, J., 2009. A heat-induced molecular signature in marine dissolved organic matter. *Nature Geoscience* **2**, 175-179.

Elderfield, H., Wheat, C. G., Mottl, M. J., Monnin, C., and Spiro, B., 1999. Fluid and geochemical transport through oceanic crust: a transect across the eastern flank of the Juan de Fuca Ridge. *Earth Planet. Sci. Lett.* **172**, 151-165.

Fisher, A. T., Davis, E. E., and Becker, K., 2008. Borehole-to-borehole hydrologic response across 2.4 km in the upper oceanic crust: Implications for crustal-scale properties. *Journal of Geophysical Research-Solid Earth* **113**.

Haberstroh, P. and Karl, D., 1989. Dissolved free amino acids in hydrothermal vent habitats of the Guaymas Basin. *Geochim. Cosmochim. Acta* **53**, 2937-2945.

Hansell, D. A., Carlson, C. A., Repeta, D. J., and Schlitzer, R., 2009. Dissolved organic matter in the ocean: a controversy stimulates new insights. *Oceanography* **22**, 202-211.

Hertkorn, N., Benner, R., Frommberger, M., Schmitt-Kopplin, P., Witt, M., Kaiser, K., Kettrup, A., and Hedges, J. I., 2006. Characterization of a major refractory component of marine dissolved organic matter. *Geochim. Cosmochim. Acta* **70**, 2990-3010.

Heuer, V. B., Pohlman, J. W., Torres, M. E., Elvert, M., and Hinrichs, K. U., 2009. The stable carbon isotope biogeochemistry of acetate and other dissolved carbon species in deep subseafloor sediments at the northern Cascadia Margin. *Geochim. Cosmochim. Acta* **73**, 3323-3336.

Hoaki, T., Nishijima, M., Miyashita, H., and Maruyama, T., 1995. Dense Community of Hyperthermophilic Sulfur-Dependent Heterotrophs in a Geothermally Heated Shallow Submarine Biotope near Kodakara-Jima Island, Kagoshima, Japan. *Appl. Environ. Microbiol.* **61**, 1931-1937.

Horiuchi, T., Takano, Y., Ishibashi, J.-i., Marumo, K., Urabe, T., and Kobayashi, K., 2004. Amino acids in water samples from deep sea hydrothermal vents at Suiyo Seamount, Izu-Bonin Arc, Pacific Ocean. *Organic Geochemistry* **35**, 1121-1128.

Jannasch, H. W., 1995. Microbial interactions with hydrothermal fluids. *Geophysical Monograph Series* **91**, 273-296.

Johnson, H., Party, L. S., Sheffer, N., Enzel, Y., Waldmann, N., Grodek, T., Benito, G., Gill, T., Zobeck, T., and Tulaczyk, S., 2003. Probing for life in the ocean crust with the LEXEN program. *EOS, Tran. AGU* **84**, 12.

Jørgensen, B. B., 1982. Mineralization of organic matter in the sea bed—the role of sulphate reduction.

Kaiser, K. and Benner, R., 2000. Determination of amino sugars in environmental samples with high salt content by high-performance anion-exchange chromatography and pulsed amperometric detection. *Anal. Chem.* **72**, 2566-2572.

Kaiser, K. and Benner, R., 2009. Biochemical composition and size distribution of organic matter at the Pacific and Atlantic time-series stations. *Mar. Chem.* **113**, 63-77.

Kelley, D. S., Lilley, M. D., Lupton, J. E., and Olson, E. J., 1998. Enriched H_2, CH_4, and ^3He concentrations in hydrothermal plumes associated with the 1996 Gorda Ridge eruptive event. *Deep Sea Research Part II: Topical Studies in Oceanography* **45**, 2665-2682.

Klevenz, V., Sumoondur, A., Ostertag-Henning, C., and Koschinsky, A., 2010. Concentrations and distributions of dissolved amino acids in fluids from Mid-Atlantic Ridge hydrothermal vents. *Geochem. J.* **44**, 387.

Koch, B. P., Witt, M., Engbrodt, R., Dittmar, T., and Kattner, G., 2005. Molecular formulae of marine and terrigenous dissolved organic matter detected by electrospray ionization Fourier transform ion cyclotron resonance mass spectrometry. *Geochim. Cosmochim. Acta* **69**, 3299-3308.

Kujawinski, E. B. and Behn, M. D., 2006. Automated analysis of electrospray ionization Fourier transform ion cyclotron resonance mass spectra of natural organic matter. *Anal. Chem.* **78**, 4363-4373.

Kujawinski, E. B., Longnecker, K., Blough, N. V., Del Vecchio, R., Finlay, L., Kitner, J. B., and Giovannoni, S. J., 2009. Identification of possible source markers in marine dissolved organic matter using ultrahigh resolution mass spectrometry. *Geochim. Cosmochim. Acta* **73**, 4384-4399.

Lang, S., Früh-Green, G., Bernasconi, S., and Butterfield, D., 2013. Sources of organic nitrogen at the serpentinite-hosted Lost City hydrothermal field. *Geobiology*.

Lever, M., Heuer, V., Morono, Y., Masui, N., Schmidt, F., Alperin, M., Inagaki, F., Hinrichs, K. U., and Teske, A., 2010. Acetogenesis in deep subseafloor sediments of the Juan de Fuca Ridge Flank: a synthesis of geochemical, thermodynamic, and gene-based evidence. *Geomicrobiol. J.*, 183-198.

Lever, M., Rouxel, O., Alt, J. C., Shimizu, N., Ono, S., Coggon, R. M., Shanks III, W. C., Lapham, L., Elvert, M., Prieto-Mollar, X., Hinrichs, K. U., Inagaki, F., and Teske, A., 2013. Evidence for microbial carbon and sulfur cycling in deeply buried ridge flank basalt. *Science* **339**, 1305-1308.

Longnecker, K., Da Costa, A., Bhatia, M., and Kujawinski, E. B., 2009. Effect of carbon addition and predation on acetate-assimilating bacterial cells in groundwater. *FEMS Microbiol. Ecol.* **70**, 456-470.

Longnecker, K. and Kujawinski, E. B., 2011. Composition of dissolved organic matter in groundwater. *Geochim. Cosmochim. Acta*.

Marescotti, P., Vanko, D. A., and Cabella, R., 2000. From oxidizing to reducing alteration: Mineralogical variations in pillow basalts from the east flank, Juan de Fuca Ridge. In: *Proceedings of the Ocean Drilling Program, Scientific Results* (eds. A. T. Fisher, E. E. Davis, and C. Escutia). Ocean Drilling Program.

Martens, C. S., 1990. Generation of short chain acid anions in hydrothermally altered sediments of the Guaymas Basin, Gulf of California. *Applied Geochemistry* **5**, 71-76.

McCarthy, M., Pratum, T., Hedges, J., and Benner, R., 1997. Chemical composition of dissolved organic nitrogen in the ocean. Nature Publishing Group.

Mills, M. M., Moore, C., Langlois, R., Milne, A., Achterberg, E., Nachtigall, K., Lochte, K., Geider, R., and La Roche, J., 2008. Nitrogen and phosphorus co-limitation of bacterial productivity and growth in the oligotrophic subtropical North Atlantic. *Limnology and Oceanography* **53**, 824.

Mottl, M. J., 2003. Partitioning of energy and mass fluxes between mid-ocean ridge axes and flanks at high and low temperature. In: *Energy and Mass Transfer in Marine Hydrothermal Systems* (eds. P. E. Halbach, V. Tunnicliffe, and J. R. Hein). Dahlem University Press, Berlin.

Mottl, M. J., Wheat, G., Baker, E., Becker, N., Davis, E., Feely, R., Grehan, A., Kadko, D., Lilley, M., Massoth, G., Moyer, C., and Sansone, F., 1998. Warm springs discovered on 3.5 Ma oceanic crust, eastern flank of the Juan de Fuca Ridge. *Geology* **26**, 51-54.

Ono, S., Keller, N. S., Rouxel, O., and Alt, J. C., 2012. Sulfur-33 constraints on the origin of secondary pyrite in altered oceanic basement. *Geochim. Cosmochim. Acta*.

Repeta, D. J., Quan, T. M., Aluwihare, L. I., and Accardi, A. M., 2002. Chemical characterization of high molecular weight dissolved organic matter in fresh and marine waters. *Geochim. Cosmochim. Acta* **66**, 955-962.

Reynolds, C. and Davies, P., 2001. Sources and bioavailability of phosphorus fractions in freshwaters: a British perspective. *Biological Reviews of the Cambridge Philosophical Society* **76**, 27-64.

Ruttenberg, K. C. and Sulak, D. J., 2011. Sorption and desorption of dissolved organic phosphorus onto iron (oxyhydr)oxides in seawater. *Geochim. Cosmochim. Acta* **75**, 4095-4112.

Sansone, F. J. and Martens, C. S., 1981. Methane production from acetate and associated methane fluxes from anoxic coastal sediments. *Science* **211**, 707-709.

Sansone, F. J. and Martens, C. S., 1982. Volatile Fatty-Acid Cycling in Organic-Rich Marine-Sediments. *Geochim. Cosmochim. Acta* **46**, 1575-1589.

Schmidt, F., Elvert, M., Koch, B. P., Witt, M., and Hinrichs, K.-U., 2009. Molecular characterization of dissolved organic matter in pore water of continental shelf sediments. *Geochim. Cosmochim. Acta* **73**, 3337-3358.

Schmidt, F., Koch, B. P., Elvert, M., Schmidt, G., Witt, M., and Hinrichs, K.-U., 2011. Diagenetic Transformation of Dissolved Organic Nitrogen Compounds under Contrasting Sedimentary Redox Conditions in the Black Sea. *Environmental Science & Technology* **45**, 5223-5229.

Sherwood Lollar, B., Frape, S., Fritz, P., Macko, S., Welhan, J., Blomqvist, R., and Lahermo, P., 1993. Evidence for bacterially generated hydrocarbon gas in Canadian Shield and Fennoscandian Shield rocks. *Geochim. Cosmochim. Acta* **57**, 5073-5085.

Sherwood Lollar, B., Lacrampe-Couloume, G., Slater, G. F., Ward, J., Moser, D. P., Gihring, T. M., Lin, L. H., and Onstott, T. C., 2006. Unravelling abiogenic and biogenic sources of methane in the Earth's deep subsurface. *Chem. Geol.* **226**, 328-339.

Shipboard Scientific Party, 2004. Juan de Fuca hydrogeology: The hydrogeologic architecture of basaltic oceanic crust: compartmentalization, anisotropy, microbiology, and crustal-scale properties on the eastern flank of Juan de Fuca Ridge, eastern Pacific Ocean. *IODP Prel. Rept.* **301**.

Skoog, A. and Benner, R., 1997. Aldoses in various size fractions of marine organic matter: Implications for carbon cycling. *Limnology and Oceanography* **42**, 1803-1813.

Sørensen, J., Christensen, D., and Jørgensen, B. B., 1981. Volatile fatty acids and hydrogen as substrates for sulfate-reducing bacteria in anaerobic marine sediment. *Appl. Environ. Microbiol.* **42**, 5-11.

Svensson, E., Skoog, A., and Amend, J. P., 2004. Concentration and distribution of dissolved amino acids in a shallow hydrothermal system, Vulcano Island (Italy). *Organic Geochemistry* **35**, 1001-1014.

Takano, Y., Sato, R., Kaneko, T., Kobayashi, K., and Marumo, K., 2003. Biological origin for amino acids in a deep subterranean hydrothermal vent, Toyoha mine, Hokkaido, Japan. *Organic Geochemistry* **34**, 1491-1496.

Van Mooy, B. A., Fredricks, H. F., Pedler, B. E., Dyhrman, S. T., Karl, D. M., Koblí, and zcaron, M., 2009. Phytoplankton in the ocean use non-phosphorus lipids in response to phosphorus scarcity. *Nature* **458**, 69-72.

Walker, B. D., McCarthy, M. D., Fisher, A. T., and Guilderson, T. P., 2008. Dissolved inorganic carbon isotopic composition of low-temperature axial and ridge-flank hydrothermal fluids of the Juan de Fuca Ridge. *Mar. Chem.* **108**, 123-136.

Wellsbury, P., Goodman, K., Barth, T., Cragg, B. A., Barnes, S. P., and Parkes, R. J., 1997. Deep marine biosphere fuelled by increasing organic matter availability during burial and heating. *Nature* **388**, 573-576.

Wheat, C. G., Feely, R. A., and Mottl, M. J., 1996. Phosphate removal by oceanic hydrothermal processes: An update of the phosphorus budget in the oceans. *Geochim. Cosmochim. Acta* **60**, 3593-3608.

Wheat, C. G., Jannasch, H., Kastner, M., Hulme, S., Cowen, J., Edwards, K., Orcutt, B., and Glazer, B., 2011. Fluid Sampling from Oceanic Borehole Observatories: Design and Methods for CORK Activities (1990-2010)*AGU Fall Meeting Abstracts*.

Wheat, C. G., Jannasch, H. W., Fisher, A. T., Becker, K., Sharkey, J., and Hulme, S., 2010. Subseafloor seawater-basalt-microbe reactions: Continuous sampling of borehole fluids in a ridge flank environment. *Geochem. Geophy. Geosy.* **11**, 1-18.

Wheat, C. G., Jannasch, H. W., Kastner, M., Plant, J. N., DeCarlo, E. H., and Lebon, G., 2004. Venting formation fluids from deep-sea boreholes in a ridge flank setting: ODP Sites 1025 and 1026. *Geochem. Geophy. Geosy.* **5**, 1-12.

Wheat, C. G., McManus, J., Mottl, M. J., and Giambalvo, E., 2003. Oceanic phosphorus imbalance: Magnitude of the mid-ocean ridge flank hydrothermal sink. *Geophys. Res. Lett* **30**, 1895.

Whiticar, M. J., 1999. Carbon and hydrogen isotope systematics of bacterial formation and oxidation of methane. *Chem. Geol.* **161**, 291-314.

Wu, J., Sunda, W., Boyle, E. A., and Karl, D. M., 2000. Phosphate depletion in the western North Atlantic Ocean. *Science* **289**, 759-762

APPENDICES

Appendix A. Amino acid concentrations in basement fluids and sediment porewater.

2011 shipboard blank		**ASP**	**GLU**	**SER**	**HIS**	**GLY**	**THR**	**ARG**	**ALA**	**TYR**	**MET**	**VAL**	**PHE**	**ILE**	**LEU**	**LYS**	**GABA**	**BALA**
DFAA	Sample 1	0.1	1.4	1.2	0.0	0.3	0.1	0.0	0.9	0.0	0.0	0.2	0.0	0.0	0.0	0.0	0.0	0.0
DHAA	Sample 1	1	0	0	0	6	0	0	0	0	0	0	0	0	0	0	0	0

2009 CORK 1301A		**ASP**	**GLU**	**SER**	**HIS**	**GLY**	**THR**	**ARG**	**ALA**	**TYR**	**MET**	**VAL**	**PHE**	**ILE**	**LEU**	**LYS**	**GABA**	**BALA**
DFAA	Sample 1	1.2	0	4.3	0.0	1.3	0.0	0.0	1.6	0.0	0	1.1	0	0.6	0	N/A	N/A	N/A
	Sample 2	1.6	0	6.3	0.0	10.1	0.0	0.0	2.9	0.4	0	2.1	0	0.5	0	N/A	N/A	N/A
	Sample 3	1.8	0	7.8	0.0	1.2	0.8	0.0	3.4	0.4	0	0.4	0	0.9	0	N/A	N/A	N/A
	Sample 4	1.2	0	5.6	1.7	3.1	0.0	0.0	2.0	0.2	0	0.0	0	0.0	0	N/A	N/A	N/A
	Sample 5	1.4	0	6.0	2.2	3.8	0.2	0.2	2.0	0.0	0	0.0	0	0.6	0	N/A	N/A	N/A
	Average	*1.5*	*0.0*	*6.0*	*0.8*	*2.4*	*0.2*	*0.0*	*2.4*	*0.2*	*0.0*	*0.7*	*0.0*	*0.5*	*0.0*	*N/A*	*N/A*	*N/A*
	SD	*0.2*	*0.0*	*1.3*	*1.1*	*1.3*	*0.3*	*0.1*	*0.7*	*0.2*	*0.0*	*0.9*	*0.0*	*0.3*	*0.0*	*N/A*	*N/A*	*N/A*
DHAA	Sample 1	14	13	16	1	19	5	3	5	2	0	4	2	0	8	0	0	0

2010 CORK 1301A		**ASP**	**GLU**	**SER**	**HIS**	**GLY**	**THR**	**ARG**	**ALA**	**TYR**	**MET**	**VAL**	**PHE**	**ILE**	**LEU**	**LYS**	**GABA**	**BALA**
DFAA	Sample 1	0	2	2	0	1	0	2	3	0	1	0	N/A	0	0	N/A	N/A	N/A
	Sample 2	0	0	2	0	0	1	2	3	0	0	0	N/A	1	0	N/A	N/A	N/A
	Sample 3	0	0	3	0	1	1	3	0	0	2	0	N/A	0	0	N/A	N/A	N/A
	Sample 4	0	0	0	0	0	3	0	0	0	8	0	N/A	0	0	N/A	N/A	N/A
	Sample 5	0	3	2	0	0	1	0	0	0	0	0	N/A	0	0	N/A	N/A	N/A
		0	0	2	0	1	1	0	0	0	0	0	N/A	0	0	N/A	N/A	N/A
	Average	*0.0*	*0.9*	*1.7*	*0.0*	*0.5*	*1.2*	*1.3*	*0.9*	*0.0*	*1.9*	*0.0*	*N/A*	*0.2*	*0.0*	*N/A*	*N/A*	*N/A*
	SD	*0.0*	*1.5*	*1.1*	*0.0*	*0.5*	*0.8*	*1.5*	*1.3*	*0.0*	*3.2*	*0.0*	*N/A*	*0.4*	*0.0*	*N/A*	*N/A*	*N/A*
DHAA	Sample 1	15	16	12	1	14	7	2	2	3	0	3	1	0	13	0	0	0
	Sample 2	15	13	13	1	20	7	4	1	1	0	5	2	0	3	0	0	0
	Average	*15.2*	*14.7*	*12.9*	*0.8*	*17.3*	*7.0*	*3.4*	*1.7*	*1.9*	*0.1*	*3.8*	*1.7*	*0.0*	*7.7*	*0*	*0*	*0*
	SD	*0.0*	*2.2*	*0.7*	*0.0*	*4.2*	*0.6*	*1.3*	*0.9*	*0.9*	*0.2*	*1.8*	*0.9*	*3.2*	*6.7*	*0*	*0*	*0*

Appendix A. Amino acid concentrations in basement fluids and sediment porewater (continue).

2011 CORK 1301A		**ASP**	**GLU**	**SER**	**HIS**	**GLY**	**THR**	**ARG**	**ALA**	**TYR**	**MET**	**VAL**	**PHE**	**ILE**	**LEU**	**LYS**	**GABA**	**BALA**
DFAA	Sample 1	0.7	1.3	0.4	3.0	0.6	0.0	1.8	0.0	0.1	0.2	0.0	0.0	0.0	0.0	N/A	0.0	0.0
	Sample 2	0.5	3.1	0.7	1.6	2.4	0.0	0.1	0.5	0.0	0.4	0.0	0.0	0.0	0.0	N/A	0.0	0.0
	Sample 3	0.6	0	0.2	2.3	2.8	0.0	0.4	0.1	0.1	0.3	0.0	0.0	0.0	0.0	N/A	0.0	0.0
	Sample 4	0.5	1.8	0.5	1.3	1.8	0.0	0.3	0.1	0.1	0.2	0.0	0.0	0.0	0.0	N/A	0.0	0.0
	Average	*1*	*1.5*	*0.5*	*2.1*	*1.9*	*0.0*	*0.7*	*0.2*	*0.1*	*0.3*	*0.0*	*0.0*	*0.0*	*0.0*	*N/A*	*0.0*	*0.0*
	SD	*0.1*	*1.4*	*0.2*	*0.8*	*1.0*	*0.1*	*0.8*	*0.2*	*0.0*	*0.1*	*0.0*	*0.0*	*0.0*	*0.0*	*N/A*	*0.1*	*0.1*
DHAA	Sample 1	10	7	1	3	9	0	0	1	0	1	1	N/A	N/A	2	1	6	2
	Sample 2	8	6	0	4	0	0	0	1	0	2	1	N/A	N/A	2	0	4	1
	Sample 3	13	12	0	7	3	0	0	4	1	4	2	N/A	N/A	6	0	8	1
	Average	*10*	*8.4*	*0.1*	*4.5*	*4.2*	*0.0*	*0.0*	*2.1*	*0.5*	*2.3*	*0.9*	*N/A*	*N/A*	*3.5*	*0.4*	*5.8*	*1.1*
	SD	*2.3*	*3.3*	*1.3*	*2.1*	*4.6*	*0.0*	*0.0*	*1.9*	*0.5*	*1.3*	*0.5*	*N/A*	*N/A*	*2.4*	*0.7*	*2.3*	*0.5*
2011 CORK 1362B		**ASP**	**GLU**	**SER**	**HIS**	**GLY**	**THR**	**ARG**	**ALA**	**TYR**	**MET**	**VAL**	**PHE**	**ILE**	**LEU**	**LYS**	**GABA**	**BALA**
DFAA	Sample 1	0	0	0	0	1	0	0	0	0	0	0	0	0	0	0	0	0
	Sample 2	0	0	0	0	0	0	0	0	0	0	0	0	0	0	0	0	0
	Sample 3	0	0	0	0	0	0	0	0	0	0	0	0	0	0	0	0	0
	Sample 4	0	0	0	0	2	0	0	0	0	0	0	0	0	0	0	0	0
	Average	*0.0*	*0.0*	*0.0*	*0.0*	*1.0*	*0.0*	*0.0*	*0.3*	*0.0*	*0.1*	*0.0*	*0.0*	*0.0*	*0.0*	*0*	*0.0*	*0.0*
	SD	*0.1*	*0.1*	*0.1*	*0.0*	*0.7*	*0.0*	*0.0*	*0.1*	*0.0*	*0.1*	*0.1*	*0.0*	*0.0*	*0.0*	*0*	*0.0*	*0.0*
DHAA	Sample 1	12	13	13	1	14	1	3	5	1	0	2	0	1	0	0	0	2
	Sample 2	6	10	13	0	16	0	2	1	1	0	1	0	1	1	0	2	0
	Sample 3	10	12	14	2	13	3	3	7	1	0	3	0	1	2	0	0	0
	Average	*9.4*	*11.7*	*13.2*	*1.2*	*14.2*	*1.4*	*2.5*	*4.4*	*1.1*	*0.3*	*1.7*	*0.2*	*1.1*	*1.0*	*0*	*0.6*	*0.6*
	SD	*3.1*	*1.7*	*0.6*	*0.8*	*1.5*	*1.2*	*0.8*	*3.0*	*0.4*	*0.3*	*1.1*	*0.3*	*0.3*	*1.0*	*0*	*1.1*	*0.8*

Appendix A. Amino acid concentrations in basement fluids and sediment porewater (continue).

2011 CORK 1362A		**ASP**	**GLU**	**SER**	**HIS**	**GLY**	**THR**	**ARG**	**ALA**	**TYR**	**MET**	**VAL**	**PHE**	**ILE**	**LEU**	**LYS**	**GABA**	**BALA**
DFAA	Sample 1	0	0	0	0	0	0	0	1	0	0	0	0	0	0	0	0	0
	Sample 2	0	0	0	0	0	0	0	1	0	0	0	0	0	0	0	0	0
	Average	*0*	*0*	*0*	*0*	*0*	*0*	*0.3*	*0.5*	*0*	*0*	*0*	*0*	*0*	*0*	*0*	*0*	*0*
	SD	*0*	*0*	*0*	*0*	*0*	*0*	*0.1*	*0.0*	*0*	*0*	*0*	*0*	*0*	*0*	*0*	*0*	*0*
DHAA	Sample 1	1	6	7	3	13	2	0	3	0	2	0	0	0	0	0	18	0
	Sample 2	2	4	8	3	20	1	0	3	1	2	1	0	0	0	0	18	0
	Average	*1.9*	*4.7*	*7.4*	*2.9*	*16.5*	*1.7*	*0.2*	*3.1*	*0.4*	*2.0*	*0.8*	*0.1*	*0.1*	*0.0*	*0*	*18.0*	*0*
	SD	*0.7*	*1.4*	*1.1*	*0.4*	*4.9*	*0.6*	*0.4*	*0.5*	*0.4*	*0.2*	*0.6*	*0.1*	*0.1*	*0.3*	*0*	*0.4*	*0*

1363D 5X1 (222m)		**ASP**	**GLU**	**SER**	**HIS**	**GLY**	**THR**	**ARG**	**ALA**	**TYR**	**MET**	**VAL**	**PHE**	**ILE**	**LEU**	**LYS**	**GABA**	**BALA**
DFAA	Sample 1	38	18	56	4	39	15	3	32	3	0	17	4	9	13	10	0	1
	Sample 2	41	23	64	9	68	14	3	34	1	0	16	3	9	13	2	0	0
	Average	*40*	*20*	*60*	*7*	*54*	*15*	*3*	*33*	*2*	*0*	*17*	*3*	*9*	*13*	*6*	*0.4*	*0.7*
	SD	*2*	*4*	*6*	*3*	*21*	*0*	*0*	*1*	*1*	*0*	*1*	*0*	*0*	*0*	*6*	*0*	*1*
DHAA	Sample 1	62	86	101	22	349	23	6	42	5	0	16	6	14	15	0	48	195
	Sample 2	59	83	90	22	207	22	6	53	7	2	21	8	19	14	0	66	111
	Sample 3	63	88	96	20	247	23	5	52	5	27	24	4	3	14	0	63	104
	Sample 4	56	77	85	21	278	19	8	45	5	8	18	15	18	18	0	72	116
	Sample 5	64	89	94	41	223	20	8	46	7	11	19	8	22	19	0	52	55
	Average	*61*	*85*	*93*	*21*	*261*	*22*	*7*	*48*	*6*	*5*	*20*	*8*	*15*	*16*	*0*	*60*	*116*
	SD	*3*	*5*	*6*	*1*	*56*	*2*	*1*	*5*	*1*	*5*	*3*	*4*	*7*	*2*	*0*	*10*	*50*

Appendix A. Amino acid concentrations in basement fluids and sediment porewater (continue).

1363D 3X3 (207m)		**ASP**	**GLU**	**SER**	**HIS**	**GLY**	**THR**	**ARG**	**ALA**	**TYR**	**MET**	**VAL**	**PHE**	**ILE**	**LEU**	**LYS**	**GABA**	**BALA**
DFAA	Sample 1	181	58	396	171	138	98	22	129	48	1	84	0	47	48	0	0	0
	Sample 2	208	84	518	399	331	201	43	139	48	0	84	0	53	50	0	0	0
	Average	*195*	*71*	*457*	*285*	*235*	*150*	*33*	*134*	*48*	*1*	*84*	*0*	*50*	*49*	*0*	*0*	*0*
	SD	*19*	*19*	*86*	*161*	*137*	*73*	*15*	*7*	*1*	*1*	*0*	*0*	*4*	*2*	*0*	*0*	*0*
DHAA	Sample 1	184	357	525	352	609	234	38	162	47	5	75	22	45	55	56	39	17
	Sample 2	182	369	532	344	573	225	39	154	33	0	76	23	44	54	94	21	7
	Sample 3	208	401	500	306	296	108	16	162	48	0	79	2	47	60	88	61	18
	Sample 4	227	413	574	297	476	113	15	175	48	3	78	5	45	59	120	36	27
	Sample 5	208	385	606	343	N/A	217	35	179	43	0	61	12	41	51	N/A	N/A	N/A
	Sample 6	218	385	634	265	N/A	187	37	179	43	0	51	13	40	55	N/A	N/A	N/A
	Average	*205*	*385*	*562*	*318*	*489*	*181*	*30*	*168*	*44*	*1*	*70*	*13*	*44*	*56*	*89*	*39*	*17*
	SD	*18*	*20*	*52*	*34*	*140*	*57*	*11*	*10*	*6*	*2*	*11*	*8*	*2*	*3*	*27*	*17*	*8*
1363D 4X1 (213m)		**ASP**	**GLU**	**SER**	**HIS**	**GLY**	**THR**	**ARG**	**ALA**	**TYR**	**MET**	**VAL**	**PHE**	**ILE**	**LEU**	**LYS**	**GABA**	**BALA**
DFAA	Sample 1	71	26	118	28	137	11	27	79	9	7	30	12	20	27	0	2	2
	Sample 2	63	25	110	29	330	13	20	34	6	N/A	N/A	N/A	N/A	N/A	0	1	3
	Average	*67*	*26*	*114*	*28*	*234*	*12*	*23*	*57*	*7*	*7*	*30*	*12*	*20*	*27*	*0*	*1*	*3*
	SD	*5*	*1*	*5*	*1*	*136*	*1*	*5*	*32*	*2*	*N/A*	*N/A*	*N/A*	*N/A*	*N/A*	*0*	*1*	*1*
DHAA	Sample 1	92	110	182	57	386	50	43	110	17	9	37	18	26	39	25	36	8
	Sample 2	87	108	158	76	331	45	36	100	14	6	36	18	26	36	9	31	6
	Average	*90*	*109*	*170*	*66*	*358*	*47*	*40*	*105*	*15*	*7*	*36*	*18*	*26*	*37*	*17*	*33*	*7*
	SD	*4*	*1*	*17*	*13*	*39*	*3*	*5*	*7*	*2*	*2*	*1*	*0*	*0*	*2*	*11*	*4*	*2*

Appendix A. Amino acid concentrations in basement fluids and sediment porewater (continue).

1363D 4X2 (215m)		**ASP**	**GLU**	**SER**	**HIS**	**GLY**	**THR**	**ARG**	**ALA**	**TYR**	**MET**	**VAL**	**PHE**	**ILE**	**LEU**	**LYS**	**GABA**	**BALA**
DFAA	Sample 1	151	32	524	113	357	23	102	144	35	16	37	30	30	82	0	1	1
	Sample 2	139	28	536	108	N/A	22	104	104	30	N/A	N/A	N/A	N/A	N/A	0	1	5
	Average	*145*	*30*	*530*	*111*	*357*	*23*	*103*	*124*	*33*	*16*	*37*	*30*	*30*	*82*	*0*	*1*	*3*
	SD	*8*	*2*	*8*	*3*	*N/A*	*0*	*2*	*28*	*3*	*N/A*	*N/A*	*N/A*	*N/A*	*N/A*	*0*	*0*	*3*
DHAA	Sample 1	196	274	675	120	1144	51	118	186	42	16	45	40	33	85	112	61	11
	Sample 2	196	278	672	116	1024	49	118	189	43	16	56	43	39	88	140	47	8
	Average	*196*	*276*	*673*	*118*	*1084*	*50*	*118*	*187*	*43*	*16*	*50*	*42*	*36*	*87*	*126*	*54*	*10*
	SD	*0*	*3*	*3*	*3*	*85*	*1*	*0*	*2*	*0*	*0*	*8*	*2*	*4*	*2*	*20*	*10*	*2*

Appendix B. Summary of CORK 1301A basment fluid properties.

CORK 1301A

Temperature = 65.0 C Pressure = 1.013 bars
pH = 7.400
Ionic strength = 0.622833
Activity of water = 0.982099
Solvent mass = 1.000000 kg
Solution mass = 1.035743 kg
Solution density = 1.001 g/cm3
Chlorinity = 0.569887 molal
Dissolved solids = 34509 mg/kg sol'n
Hardness = 5707.00 mg/kg sol'n as CaCO3
carbonate = 21.89 mg/kg sol'n as CaCO3
non-carbonate = 5685.11 mg/kg sol'n as CaCO3
Rock mass = 0.000000 kg
Carbonate alkalinity= 21.89 mg/kg sol'n as CaCO3
Water type = Na-Cl

Appendix C. Activity coefficient of aqueous species in basment fluids from CORK 1301A.

Aqueous species	Molality	mg/kg solution	Activity coefficient	Log activity
Cl-	0.5496	1.88E+04	0.6119	-0.4733
Na+	0.4723	1.05E+04	0.6574	-0.508
Ca++	0.03857	1493	0.2274	-2.0569
CaCl+	0.01414	1031	0.6574	-2.0319
SO4--	0.009463	877.6	0.1527	-2.84
K+	0.006174	233.1	0.6119	-2.4228
NaCl	0.005834	329.2	1	-2.2341
CaSO4	0.004306	565.9	1	-2.366
NaSO4-	0.004291	493.2	0.6574	-2.5496
Mg++	0.001536	36.04	0.2958	-3.3427
SiO2(aq)	0.001126	65.32	1.1369	-2.8927
HCO3-	0.0003282	19.33	0.677	-3.6533
MgCl+	0.0002597	14.98	0.6574	-3.7677
MgSO4	0.0001667	19.37	1	-3.7782
NH4+	9.84E-05	1.713	0.5853	-4.2398
KSO4-	8.01E-05	10.45	0.6574	-4.2784
CaHCO3+	6.71E-05	6.551	0.7016	-4.3271
KCl	5.51E-05	3.969	1	-4.2585
NaHCO3	4.68E-05	3.793	1	-4.3301
NaH3SiO4	4.49E-05	5.125	1	-4.3473
CO2(aq)	1.91E-05	0.8108	1	-4.7194
H3SiO4-	1.85E-05	1.7	0.6574	-4.9147
CaCO3	1.01E-05	0.9772	1	-4.9951
NH3	9.20E-06	0.1512	1	-5.0364
OH-	4.87E-06	0.07998	0.6358	-5.5091
Mn++	4.23E-06	0.2241	0.2274	-6.0173
MgHCO3+	2.09E-06	0.172	0.6574	-5.8625
CO3--	2.01E-06	0.1166	0.1718	-6.4614
CH4(aq)	1.55E-06	0.02403	1.1369	-5.7535
CaOH+	1.44E-06	0.07943	0.6574	-6.0235
H2(aq)	1.14E-06	0.002214	1.1369	-5.8882

Apendix C. Activity coefficient of aqueous species in basment fluids from CORK 1301A. (continue)

Aqueous species	Molality	mg/kg solution	Activity coefficient	Log activity
MgOH+	6.64E-07	0.02647	0.6574	-6.3602
MnSO4	6.15E-07	0.08959	1	-6.2115
NaOH	5.81E-07	0.02242	1	-6.2362
FeCl+	5.07E-07	0.04473	0.6574	-6.4768
Fe++	3.46E-07	0.01866	0.2274	-7.1041
MgCO3	2.29E-07	0.01863	1	-6.6405
NaCO3-	1.85E-07	0.01481	0.6574	-6.9155
HS-	1.59E-07	0.005086	0.6358	-6.9945
NaHPO4-	8.25E-08	0.009471	0.6574	-7.266
FeCl2	5.32E-08	0.00651	1	-7.2741
H+	5.01E-08	4.87E-05	0.7952	-7.4
HSO4-	3.47E-08	0.003249	0.6574	-7.6423
FeSO4	2.25E-08	0.003295	1	-7.6484
H2S(aq)	1.65E-08	0.0005436	1	-7.7819
CaHPO4	1.62E-08	0.002127	1	-7.7907
MnOH+	1.31E-08	0.0009084	0.6574	-8.0656
HPO4--	9.90E-09	0.000917	0.1527	-8.8206
MnHCO3+	7.68E-09	0.0008593	0.6574	-8.2971
CaPO4-	1.89E-09	0.0002467	0.6574	-8.9053
H2PO4-	1.53E-09	0.0001433	0.6574	-8.9974
FeOH+	1.42E-09	1.00E-04	0.6574	-9.0295
H2SiO4--	1.42E-09	0.0001286	0.1527	-9.665
MgHPO4	1.14E-09	0.0001325	1	-8.9428
KHPO4-	5.28E-10	6.88E-05	0.6574	-9.4598
FeHCO3+	2.64E-10	2.98E-05	0.6574	-9.7602
MgPO4-	8.33E-11	9.59E-06	0.6574	-10.2615
MgH2PO4+	4.20E-11	4.92E-06	0.6574	-10.5588
FeCO3	1.69E-11	1.89E-06	1	-10.7729
MnHPO4	9.38E-12	1.37E-06	1	-11.0276
Fe(OH)2	5.92E-12	5.14E-07	1	-11.2274
PO4---	2.11E-12	1.94E-07	0.0134	-13.5482
S--	2.06E-12	6.37E-08	0.1906	-12.4066

Apendix C. Activity coefficient of aqueous species in basment fluids from CORK 1301A. (continue)

Aqueous species	Molality	mg/kg solution	Activity coefficient	Log activity
FeHPO4	1.09E-12	1.60E-07	1	-11.9623
HCl	6.53E-13	2.30E-08	1	-12.1851
FePO4-	1.62E-13	2.36E-08	0.6574	-12.9721
FeH2PO4+	1.26E-13	1.85E-08	0.6574	-13.083
H3PO4	8.48E-15	8.03E-10	1	-14.0715
Mg4(OH)4++++	1.70E-15	2.71E-10	0.0178	-16.5199
Fe(OH)3-	2.57E-16	2.65E-11	0.6574	-15.7724
S2--	7.56E-17	4.68E-12	0.1527	-16.9376
HP2O7---	9.80E-18	1.66E-12	0.0134	-18.8815
H2SO4	3.09E-18	2.93E-13	1	-17.5102
P2O7----	2.19E-18	3.68E-13	0.0004	-21.011
H2P2O7--	2.11E-19	3.58E-14	0.1527	-19.4921
S3--	4.27E-22	3.97E-17	0.1527	-22.1856
S4--	1.05E-24	1.30E-19	0.1527	-24.796
H3P2O7-	3.73E-25	6.38E-20	0.6574	-24.61
S5--	3.74E-30	5.78E-25	0.1527	-30.2438
H4P2O7	5.56E-32	9.56E-27	1	-31.2547
S6--	6.70E-36	1.24E-30	0.1527	-35.9901

Appendix D. Mineral saturation states in basment fluids from CORK 1301A.

Mineral	Log(Q/K)	Mineral	Log(Q/K)
Antigorite	20.1579s/sat	MHSH(Mg1.5)	-6.9159
Hydroxyapatite	7.6526s/sat	Ca(OH)2(c)	-7.2042
Tremolite	7.2109s/sat	Portlandite	-7.2042
Talc	4.7611s/sat	Antarcticite	-7.2241
Whitlockite	2.8569s/sat	Kalicinite	-7.5936
Chrysotile	1.7248s/sat	CaCl2^4H2O	-7.63
Sepiolite	1.2759s/sat	Melanterite	-7.821
Dolomite-ord	0.9058s/sat	Akermanite	-7.8876
Dolomite	0.9056s/sat	Pirssonite	-8.1608
Pyrite	0.7458s/sat	Bischofite	-8.477
Quartz	0.5473s/sat	Kainite	-8.5645
Calcite	0.5412s/sat	Na2Si2O5	-8.8886
Tridymite	0.4141s/sat	MgSO4(c)	-9.1765
Diopside	0.4123s/sat	Gaylussite	-9.4276
Aragonite	0.3801s/sat	MnCl2^4H2O	-9.5261
Chalcedony	0.3081s/sat	Na2SiO3	-9.5925
Minnesotaite	0.2250s/sat	Mg2Cl(OH)3^4H2O	-9.8773
Anthophyllite	0.1797s/sat	MgOHCl	-9.9496
Cristobalite	0.0748s/sat	CaCl2^H2O	-10.0148
Anhydrite	-0.1091	Ca2SiO4^7/6H2O	-10.0361
Gypsum	-0.3161	MnSO4(c)	-10.0536
Dolomite-dis	-0.3846	CaCl2^2H2O	-10.065
Amrph^silica	-0.493	MnCl2^2H2O	-10.2251
Monohydrocalcite	-0.6093	Ca2SiO4(gamma)	-10.2854
Bassanite	-0.7436	MgCl2^4H2O	-10.779
CaSO4^1/2H2O(be	-0.867	FeSO4(c)	-10.9343
Magnesite	-1.0517	MnCl2^H2O	-11.398
Enstatite	-1.0776	Vivianite	-11.4358
Ferrosilite	-1.3146	Larnite	-11.5285
Rhodochrosite	-1.5553	Carnallite	-11.7243
Greenalite	-1.7049	Mercallite	-12.1011
FeO(c)	-1.7398	Hydromagnesite	-12.3588
Hedenbergite	-2.0196	Ca5Si6O17^21/2H2	-12.485
Wollastonite	-2.1012	KNaCO3^6H2O	-12.7121
Rhodonite	-2.4042	Hydrophilite	-13.0094
Pseudowollastoni	-2.412	Rankinite	-13.0608
Siderite	-2.4177	Ca5Si6O17^11/2H2	-13.0655
CaSi2O5^2H2O	-2.4826	Scacchite	-14.1042
Halite	-2.6064	Ca2Cl2(OH)2^H2O	-14.8043
Troilite	-2.6757	Ca4Si3O10^3/2H2O	-14.9659
Brucite	-2.7062	Na3H(SO4)2	-15.0856
Fayalite	-3.3212	MgCl2^2H2O	-15.1847
Fe(OH)2(ppd)	-3.336	Lawrencite	-15.2204

Apendix D. Mineral saturation states in basment fluids from CORK 1301A (continue).

Mineral	Log(Q/K)	Mineral	Log(Q/K)
Thenardite	-3.4551	Merwinite	-15.3085
Forsterite	-3.7612	K2CO3^3/2H2O	-15.5411
Huntite	-4.0809	Ca5Si6O17^3H2O	-15.8123
Sylvite	-4.1498	Lime	-15.95
Monticellite	-4.2942	Burkeite	-16.4087
Graphite	-4.3118	Mn3(PO4)2(c)	-17.922
Nesquehonite	-4.3916	MgCl2^H2O	-17.9514
Ca2Si3O8^5/2H2O	-4.4642	KMgCl3^2H2O	-19.583
Hexahydrite	-4.4964	Ca3Si2O7^3H2O	-21.0826
Mn(OH)2(am)	-4.5882	Ca6Si6O18^H2O	-22.4812
Alabandite	-4.5994	Chloromagnesite	-22.8679
Mirabilite	-4.7154	KMgCl3	-25.6877
Epsomite	-4.7432	Tachyhydrite	-27.1111
Leonhardtite	-4.9137	Ca3SiO5	-29.5178
Kieserite	-4.9442	Ca4Cl2(OH)6^13H2	-33.2329
Tephroite	-5.0107	Na4SiO4	-35.5309
Artinite	-5.4032	Na6Si2O7	-56.2608
Sulfur-Rhmb	-5.5131	K8H4(CO3)6^3H2O	-61.2963
Arcanite	-6.346	Misenite	-79.5227
Manganosite	-6.7568		

Appendix E. Fugacity of dissolved gases in basment fluids from CORK 1301A.

Gases	Fugacity	Log fugacity
Steam	0.2423	-0.616
H2(g)	0.001793	-2.746
CH4(g)	0.001535	-2.814
CO2(g)	0.001134	-2.946
H2S(g)	4.35E-07	-6.361
S2(g)	5.43E-23	-22.265